THE USE OF UPPER MANTLE DERIVED ILMENITE TO PREDICT PRESERVATION OF DIAMOND PARCELS IN KIMBERLITE

STEVEN J HORWOOD

Thesis Submitted in Fulfilment of the Requirements for the degree of Master of Science

University of Cape Town

April 1998

Supervisor: Dr JJ Gurney


100µ
ELECTRON MICROSCOPE UNIT UCT Detector= SE1 15-Oct-1994

DECLARATION

I hereby declare that the work presented in this thesis is my own, except where otherwise stated in the text.

Steven J. Horwood
April, 1998

DEDICATION

I dedicate this thesis to the memory of Reg and Perianne

INSIDE COVER

Highly resorbed diamond which has ceased to display any form. The resorbtion mechanism has progressed from a edge and face dominated process to a rut dominated process. Although a resorbtion category of 6 is allocated, the true resorbtion may be nearer to a category 8 or 9 (Mag=42X, R_c=6)

ABSTRACT

Fe_2O_3: FeO ratios for nine upper mantle derived megacryst ilmenites have been measured using liquid ion chromatography. Good precision was obtained for ilmenites, and ratios obtained for international standards: W-2, BHVO-1, BIR-1, PCC-1 and STM-1 are in close agreement with recommended ratios. Good correlation was observed between Fe_2O_3/FeO determined using ion chromatography and Fe_2O_3/FeO calculated stoichiometrically from electron microprobe analyses for megacrystic ilmenite. This study justifies the use of electron microprobe analyses to predict Fe_2O_3 and FeO using stoichiometric calculations in megacryst ilmenites.

Six diamond parcels have been described, particularly with respect to resorbtion derived morphologies. A method has been devised to quantify the degree of preservation of a parcel of diamond from a particular locality and an attempt has been made to estimate the initial mass of the parcel and the initial grade of the kimberlite. Diamond parcels from group I kimberlites have been distinguished from diamond parcels from group II kimberlites in the Barkly West and Welkom-Theunissen areas, with group II kimberlites displaying better preservation than geographically associated group I kimberlites. Initial grade estimates for group I kimberlites are significantly lower than for their group II counterparts and it has been deduced that a major diamond corrosion event has occurred within the time period between eruption of the group I and group II kimberlites.

A large database, containing ilmenite analyses from different upper mantle derived parageneses, has been considered in an attempt to establish major element compositional criteria in order to distinguish between them. It has been shown that different ilmenite parageneses can be distinguished using a combination of six different plots, incorporating: TiO_2, FeO, Fe_2O_3, MgO, Cr_2O_3, MnO and the ilmenite-hematite-geikielite ternary. Significant overlap between fields from the different parageneses prevent allocation on the basis of any single parameter. Parageneses can only be assigned with confidence if trends are established for a large sample of ilmenite analyses.

The compositions of mainly macrocryst ilmenites from Tshibua, Premier, Palmietfontein and Iron Mountain have been used to establish criteria for assessing diamond preservation using ilmenite composition. The best criteria appear to be Fe_2O_3 and MgO, which represent oxidation conditions and the degree of fractionation respectively. Divisions have been created to qualitatively separate good, intermediate, poor, marginal and non-existent preservation, and a strict set of criteria established to assess ilmenite compositions from other kimberlites. These criteria have been applied to 13 southern African localities and diamond preservation predicted.

It is postulated that most corrosion of diamonds occurred during residence in the mantle lithosphere, prior to entrainment by the kimberlitic magma, and the starting composition, end composition and trend, if any, of ilmenite Fe_2O_3 and MgO compositions relates to the initial corrosiveness, amount of differentiation, intensity and the pervasiveness of the corrosion event.

...ooOoo...

TABLE OF CONTENTS

CHAPTER 1

INTRODUCTION

A number of methods are used by companies to search for economically viable diamond deposits. Although each exploration program is designed specifically to best suit the geological and geographical conditions, programs designed around the use of diamond indicator minerals to locate individual kimberlites or clusters are usually the most cost effective, and have successfully located a number of existing targets and allowed prioritization of targets within a cluster of kimberlites. The method uses the compositions of indicator minerals, derived from kimberlite pipes, to "track" and prioritise deposits (Gurney et al, 1978; Gurney, 1984; Fipke et. al., 1989; Gurney and Moore, 1991; Gurney et al, 1993; Gurney and Zweistra, 1995; Griffin et al, 1995) The method of Gurney and Moore (1991), is particularly attractive, because it identifies minerals that have compositions known to be directly associated with diamonds. These compositions have been obtained from extensive diamond inclusion studies, and evidence from diamondiferous xenoliths.

Although these systems can point towards the presence, and to some extent the grade of a body, one of the fundamental problems that still proves to be an obstacle to assessing the viability of a deposit is the degree to which a diamond population has been destroyed due to corrosion (resorbtion). Resorbtion has occurred extensively in diamonds from southern Africa and occurs when diamonds are exposed to conditions outside of their stability envelope (Robinson, 1989). A progressive change in diamond morphologies from sharp-edged octahedrons to rounded tetrahexahedrons occur during the resorbtion process, and Robinson (1989) has estimated the loss in mass of a diamond at five different stages during this process. No attempt has ever been made, however to use the degree of resorbtion to distinguish between diamond populations from different primary sources. Resorbtion has been believed to be caused by interaction of diamonds with a corrosive transporting magma (Robinson, 1986). This conclusion has been based on a number of observations of morphology and surface textures on diamonds, the most convincing of which is the occurrence of hemimorphic diamonds. These diamonds often protrude from the surface of xenoliths and exhibit pristine octahedral surfaces where protected by the xenolith and highly resorbed surfaces where exposed to the kimberlitic magma. Contrasting evidence of multiple growth and resorbtion events

in some diamonds have been reported, however (Bulanova, 1995; Chinn, 1995), showing that at least some resorbtion must have occurred in the mantle prior to entrainment in the kimberlitic magma. An idea of the loss of mass of diamonds due to resorbtion can be a useful indicator of destruction of diamonds even though other exploration indicators indicate otherwise.

Kimberlitic ilmenite compositions reflect ambient oxidation conditions at the time of crystallisation (Haggerty and Tompkins, 1983), and have been postulated to be a possible indicator of diamond preservation (Gurney et al, 1978). This is feasible, provided the ilmenites crystallised under similar conditions, or in some way reflect the conditions under which the diamonds were destroyed. Diamonds are believed to be resorbed under conditions where the oxygen activity is sufficient to allow conversion of C is to CO_2. The connection between oxygen fugacity and diamond resorbtion has been suggested by Haggerty (1986).

Ilmenites, in the size range >1mm, from group I kimberlites in southern Africa are dominantly derived from the Cr-poor megacrystic suite (Eggler, 1989; Haggerty, 1991), although locally other origins may be prevalent eg. kimberlitic ilmenite phenocrysts at Wesselton (Shee, 1985). Fe_2O_3:FeO ratios of upper mantle derived ilmenites vary as a function of ambient redox conditions (Haggerty and Tompkins, 1983) and consequently reliable, routine analysis of Fe_2O_3 and FeO in ilmenite is essential. The electron microprobe (E.M.P) is the most popular analytical tool used to analyse the compositions of ilmenite concentrate from exploration samples. This method cannot determine Fe_2O_3 and FeO directly and as a result the concentrations of these oxides are calculated stoichiometrically. In this study Fe_2O_3:FeO ratios in megacryst ilmenite, which are calculated from electron microprobe analyses are compared to direct analysis of Fe_2O_3:FeO ratios in the same samples using high pressure liquid ion chromatography (HPLC).

The resorbtion of parcels of diamonds from selected localities on the Kalahari craton have been described and quantified by establishing a diamond preservation index, and an attempt has been made to estimate the loss of diamond grade as a result of resorbtion. Preservation indexes are compared to other kimberlites in southern Africa for which diamond data has been collected. Ilmenite analyses from a number of kimberlites have been used to attempt to differentiate between different upper mantle parageneses of ilmenite. Ilmenite bearing kimberlites, with a range in observed diamond preservation have been studied to establish a set of criteria for routine forecasting of diamond preservation during exploration. These criteria have been applied to 13 southern African kimberlites.

...ooOoo...

CHAPTER 2

THE USE OF ION CHROMATOGRAPHY TO DETERMINE Fe_2O_3/FeO RATIOS IN ILMENITES

Used to assess the accuracy of Stoichiometric Calculations

This chapter provides results and discussion of a method for the direct determination of Fe_2O_3/FeO ratios in ilmenite megacrysts derived from kimberlites using ion chromatography. Results are compared to Fe_2O_3/FeO ratios calculated, using stoichiometric principles, from electron microprobe data. It is concluded that these calculations correctly estimate Fe_2O_3/FeO ratios in megacrystic ilmenites. International standards have been analysed and their ratios compared to recommended values and those derived from other studies.

2.1 INTRODUCTION

2.1.1 BACKGROUND

This study was undertaken to assess the viability of using ion chromatography as an alternative to traditional methods for the determination of Fe_2O_3/FeO in ilmenites and to assess the accuracy of using stoichiometric calculation to determine Fe_2O_3/FeO from electron microprobe analyses.

Reliable Fe_2O_3 and FeO values are often required for studies concerning the oxidation state of mantle minerals. Although easily obtained, results derived by stoichiometric calculation of major element analyses using total iron as FeO from electron microprobe analyses, contain a degree of uncertainty. This uncertainty results from a need to assume site allocations and element substitution, the multiple valency states of certain elements (Mn, Fe, Cr? etc), and the absence of accurate oxygen concentrations. Megacrystic ilmenites derived from kimberlites commonly have low concentrations of manganese, and have most Chromium present as Cr^{3+} (Haggerty 1975). Iron, therefore is the only abundant cation with a multivalent potential, thus allowing the assumption that any excess cations, after correction, are attributable to Fe^{3+}. Few routine techniques exist for the direct determination of FeO and Fe_2O_3 in rocks and minerals. Mössbauer spectroscopy, the most widely used amongst mantle petrologists, and wet chemical techniques are the most common.

Ion chromatography (Salman and Hale, 1959) is able to distinguish between different valence states of the same element. In the case of Fe^{2+} and Fe^{3+} it is possible to determine both simultaneously. Le Roex and Watkins (1995) established the usefulness of the technique to analyse whole rock sample powders for Fe_2O_3/FeO. In this study, additional analyses of international rock standards were assessed, and nine ilmenite megacrysts were selected to cover a range in Fe_2O_3/FeO ratios. These megacrysts were selected using calculated Fe_2O_3/FeO from microprobe analyses.

These ilmenites were analysed a number of times using ion chromatography, in several different batches. Factors such as dissolution techniques, other element interferences, Fe^{3+} complexing, crushing and other preparation procedures were addressed. Errors were estimated for both ion chromatography and electron microprobe determinations of Fe_2O_3/FeO.

2.1.2 AVAILABLE METHODS FOR THE DETERMINATION OF Fe_2O_3 AND FeO IN ROCKS AND MINERALS

Iron, the fourth most abundant element on earth, has always been an important element to mineralogists, petrologists and in mining and industry. However, given that in nature, iron exists in at least three different valence states (Fe^0, Fe^{2+} and Fe^{3+}), and that this information is critical to many studies in the above disciplines, there are very few techniques available to enable the quantitative analysis of these valency states. None of the more common methods used in the routine analysis of major elements (XRF-Spectrometry, electron microprobe analysis, atomic absorption, etc) can distinguish between the different oxidation states of iron. The electron microprobe has been used to determine Fe^{3+} and Fe^{2+} directly using Fe Lα and Lβ lines (Albee and Chodos, 1969), however this requires different setup parameters which have not been used to date in the routine analysis of major elements for exploration purposes.

2.1.2.1 Chemical Methods

All wet chemical methods require the dissolution of the sample to enable the determination of Fe^{3+} or Fe^{2+}, and procedures available can be subdivided into two broad categories.

i) The first, based on the method of Pratt (1884), involves the dissolution of the sample in HF (hydrofluoric acid) and H_2SO_4 (sulphuric acid) in the presence of water and the subsequent direct determination of ferrous iron using a number of methods.

These include colorimetric (Riley and Williams, 1959; Graves, 1951; Johnson and Maxwell, 1989), potentiometric (Helman, 1974; Shapiro and Brannack, 1962; Schafer, 1966; Johnson and Maxwell, 1989) and photometric methods (Mikhalova et al, 1965; Bien and Goldberg, 1956; Beyer et al, 1975). Even more variations exist in the method of dissolution than the method of analysis. These include dissolution in a sealed de-oxygenated bomb (Riley and Williams, 1959; Ito, 1962), various sealed vessels (Schafer, 1966; French and Adams, 1972; Fahey, 1961; Shapiro, 1960; Lo-Sun Jen, 1973; and others), fusion prior to dissolution (Groves, 1951; Jurinen, 1956; Mikhailova et al, 1965) and in a platinum crucible with a tight-fitting lid (Pratt, 1884; Johnson and Maxwell, 1989; Jeffries and Hutchison, 1983).

Special procedures for refractory minerals such as staurolite, tourmaline, chromite, ilmenite and magnetite have been described by Ito (1962), Whitehead and Malik (1975) and French and Adams (1972). Special mention is made of ilmenite and other Fe-Ti oxides and the difficulty of dissolving them by Fahey (1961) and Vincent and Phillips (1954). Johnson and Maxwell (1989) report that ilmenite is very refractory and seldom dissolved and they warn against overboiling and overgrinding. Over the years much work has gone into the exclusion of air from the decomposition vessel to avoid possible oxidation. Clemency and Hagner (1961) and Kiss (1977) report after experimentation, that the presence of air has little effect on the results.

ii) The second category is based on volumetric and colorimetric titrations, described by Wilson (1955, 1960, 1964) in which the sample is purposefully oxidised during dissolution with a known excess of oxidant (ammonium vanadate solution) and the product (sample in solution) titrated to determine the aliquot of oxidant used to oxidise the available Fe^{2+}. Whipple (1974) modified this method to avoid the complexing of Fe^{3+} with fluorides. Wilson (1960) reported good results with sample weights as low as 3mg using this technique.

Wet chemical methods, however routinely require large amounts of sample (up to 500mg), although sample sizes as low as 2mg have been reported by using non standard techniques, have much higher limits of detection, much less sensitivity and require the destruction of the sample.

2.1.2.2 Physical Methods

Many spectroscopic techniques are available for the determination of FeO and Fe_2O_3 in minerals. The most well known of these methods, is that of Mössbauer spectroscopy. It is a nuclear technique utilising the process known as resonant absorption as explained by G Wertheim (1964). Many studies of mantle minerals have used this technique eg. Wood et. al. (1989), Ballhaus (1993), Virgo et. al. (1988). Samples as small as 500μm have been analysed by using specially designed sample holders and a different source. (McCammon, 1991). Mössbauer spectroscopy has an advantage which none of the other techniques have, which is very useful to the mineralogist. Mössbauer produces information, which with careful interpretation, can indicate the Fe^{3+} and Fe^{2+} site positions within the crystal structure (eg. Virgo et al, 1985). Mössbauer spectroscopy requires experience to interpret and routinely requires large samples for analysis (10mm across) and is relatively slow. Furthermore, in order to attain bulk rock Fe_2O_3 and FeO contents, useful for studies of mantle petrology (Canil et al 1990), each individual mineral phase must be analysed and corrected using a modal mineral count.

The facilities necessary for the determination of Fe_2O_3/FeO in ilmenites using Mossbauer spectroscopy or wet chemistry were not available to this study. Research into the determination of Fe_2O_3/FeO in international rock standard powders using ion chromatography (le Roex and Watkins, 1995), was advanced. This presented an ideal opportunity to attempt to apply the technique to ilmenite and use the results to assess stoichiometrically calculated Fe_2O_3 and FeO concentrations from electron microprobe analyses.

2.1.3 PREVIOUS WORK DETERMINING FeO AND Fe_2O_3 USING ION CHROMATOGRAPHY

The principle of chromatic separation has been known for many years (Salmon and Hale, 1959), but with recent advances in the production of highly sensitive, high resolution resins, ion chromatography has become a routine analytical tool. Dionex (1987) has described a method for analysing transition metals in solutions and this has been applied by Moses et al (1988) to the analysis of water samples. Kanai (1990) used the technique to analyse for FeO and Fe_2O_3 in rock samples directly and quantitatively using a variation on classical dissolution techniques described before. Le Roex and Watkins (1995) have described a method similar to that of Kanai (1990),

where instead of analysing for absolute concentrations of Fe^{2+} and Fe^{3+}, the ratio of Fe_2O_3/FeO is determined. Should absolute concentrations be needed, then the ratio can be applied to total iron determined using XRF-Spectrometry or electron microprobe analysis. This approach saves time and reduces the errors associated with the preparation and storing of Fe^{3+} and Fe^{2+} standard stock solutions.

Johnson and Maxwell (1989) report that fluoride affects the Fe^{3+} peak due to the formation of ferric fluoride complexes, thus producing more reduced results. They state that H_2SO_4 prevents this complexing and that H_2O prevents the oxidation of Fe^{2+} by H_2SO_4. Kanai (1990) undertook detailed investigation into sources of error during the dissolution process and reported that fluoride has no effect on the Fe^{3+} peak. When present in high concentrations however, fluorides can result in a reduction in the Fe^{2+} peak area (oxidised ratio). High concentrations of H_2SO_4 stabilised Fe^{2+} in the presence of fluoride. Le Roex and Watkins (1995) adopted the approach outlined by Johnson and Maxwell (1989) using HF^-, H_2SO_4 and water during their dissolution process, whilst Kanai (1990) utilised only HF^- and H_2SO_4. In the method of Kanai (1990) the sample is mixed with boric acid after dissolution, which is also believed to prevent ferric fluoride complexing in the dissolved sample (Johnson and Maxwell, 1989). Le Roex and Watkins (1995) used sample sizes of 50mg and report good results down to 5mg whilst Kanai (1990) utilised 100mg samples.

2.1.4 GEOLOGICAL REFERENCE STANDARDS

The method used in this study makes heavy use of reference materials in the analysis of Fe_2O_3/FeO. USGS international standard W-2, a diabase, is used as the primary reference instead of the preparation of standard stock solutions. Other standards (BHV0-1, PCC-1, BIR-1, STM-1) were used to verify results. The quality of this work is directly dependent on the quality of the reported values for W-2 and also the other standards. A critical appraisal of the international rock standards is beyond the scope of this study, and the following quote from Roelandts (1981) is deemed sufficient to justify the use of these standards. "A chemist who obtains results for the international reference materials that are in good agreement with the recommended values for the major and minor constituents can apply his method with some confidence to the analysis of rocks of the same composition." In most cases FeO determinations for the standards are based on classical volumetric methods and Fe_2O_3 is calculated by difference from total iron as Fe_2O_3 (Roelandts, 1981).

"Working" values used in this study were derived from Govindaraju (1994). All values are

recommended except for Fe_2O_3 in peridotite PCC-1. A list of source areas for standards can be obtained in the same issue.

2.1.5 OBJECTIVES OF THE STUDY

Objectives of this study are to:

i) Further evaluate the use of ion chromatography to analyse Fe_2O_3/FeO ratios in rocks and minerals using the procedure proposed by le Roex and Watkins (1995).

ii) Apply the technique to megacrystic ilmenite, a refractory oxide mineral.

iii) Compare Fe_2O_3/FeO ratios obtained for megacrystic ilmenite using ion chromatography with those calculated using stoichiometric principles from electron microprobe analyses.

2.2 SAMPLE PREPARATION AND DISSOLUTION

Many analytical techniques require the crushing and dissolution of mineral and rock samples prior to analysis (viz. atomic absorption spectrometry, ICP and standard analysis using ion chromatography), and hence there are many described methods to achieve this. It is critical, however, in any technique designed to measure Fe_2O_3 or FeO, or any other elements with varying valency states, that no change occurs in the oxidation state or apparent oxidation state during sample preparation.

2.2.1 INSTRUMENTAL CONDITIONS, PREPARATION AND ANALYSIS

The instrument utilised in this study was a Dionex 4000i Ion Chromatograph with guard and separator columns. At no stage of analysis (ie. during sample injection, in the piston pump, column, liquid flow path or detector) is the sample in contact with any form of metal. The sample loop used is varied according to the overall concentration of the element analysed, the lower the concentration the greater the volume of the sample loop. Analysis of Fe_2O_3 and FeO is achieved by following the standard run for transition metals described by Dionex (1987), using PDCA (pyridine 2,6-dicarboxilic acid, appendix 2.1) as the transporting medium (eluent), which complexes with the sample. The eluent was sparged with helium before analysis. Sparging involves the flushing of the

liquid with an inert gas, in this case helium, in order to displace any dissolved oxygen from the system. A 0.2mM solution of PAR (4-(2-pyridylaze) resorsinol monosodium salt, appendix 2.1) reacts with the sample-eluent complexes formed and the resultant colour intensity detected photometrically by a Dionex UV/VIS variable wavelength detector set to a wavelength of 520nm. An eluent flow rate of 2ml/minute was used with a corresponding PAR flow rate of 0.5ml/minute. Some of the preliminary work was done at a flow rate of 1ml/min.

Although Dionex (1987) prescribes an eluent flow rate of 1ml/min (15min), it has been found to be possible to increase the flow rate to 2ml/min which reduces the analysis time to 8 minutes. This is achievable due to the good peak separation between the Fe^{3+} and the Fe^{2+} peaks. The sensitivity of detection for the Fe^{3+}-bearing complex is approximately 1.4x that for the Fe^{2+}-bearing complex (le Roex and Watkins, 1995). In most rock and many mineral samples, especially in mantle geochemistry, the Fe_2O_3 content is significantly less than the FeO content. This allows for the simultaneous determination of both Fe^{3+} and Fe^{2+} in the same analysis while both peaks are still within the same order of sensitivity, measured in absorption units.

Due to these differences in sensitivities and the susceptibility of the instrument to changes in analytical and environmental conditions (chemicals, temperature etc.), it is necessary to calibrate even though the determination of a ratio would not ordinarily require the use of a standard. Calibration was performed using USGS international rock standard W-2, a diabase from Centerville, USA (figure 2.2). The use of a rock powder avoids difficulties in the accurate preparation of Fe^{3+}/Fe^{2+} standard solutions which, once prepared, oxidise with time in storage. A further advantage of using a rock powder as a standard is that all conditions and processes (dissolution, sample injection, etc.) are exactly duplicated with both sample and standard. The final Fe_2O_3/FeO ratio of a sample is calculated by dividing the peak area (integrated intensity) of Fe^{3+} (sample) by the peak area of Fe^{2+} (sample) and multiplying by a factor derived by comparing the ratio of peak intensities determined for W-2 on the day and the recommended standard Fe_2O_3/FeO ratio for W-2 of 0.18 (Govindaraju, 1994). Absolute values for Fe_2O_3 and FeO can be established by first analysing total iron using electron microprobe analysis or X-Ray fluorescence spectrometry. The detection limits and errors during analysis of any sample are dependent on the detection limits, precision and error of the original analyses performed on international rock standard W-2 to obtain reference Fe_2O_3/FeO ratios. If absolute concentrations of Fe_2O_3 and FeO are required, the errors on electron microprobe or XRF analyses should be considered as well. Each analysis is repeated a minimum of three times to verify the result. If all three ratios are within error of one another, the average of the three is calculated.

2.2.2 SAMPLE PREPARATION

Excessive grinding of a sample results in the oxidation of a major portion of the ferrous iron (Johnson and Maxwell, 1981). Hildebrand et al (1953) report that the reason for oxidation is the heat build-up due to friction in the grinding vessel. Disc mills etc. crush in a very short time and build up considerable heat, and thus must not be used with Ferric iron determinations (Filton and Gill, 1970). If international standard powders are prepared in this way it becomes necessary to question the applicability of their use for Fe^{3+} determinations. In this study, one ilmenite sample was accidentally oxidised due to over-crushing and produced a consistently oxidised result when analysed. After re-crushing of the sample more reduced results with greater precision were obtained. The most reliable and reproducible results, especially with rock samples, are achieved when the sample is fully dissolved. This is often difficult to achieve due to the presence of minor amounts of highly refractory minerals such as chromite which are hard to dissolve and, which have the potential to severely affect the overall ferric to ferrous ratio of the rock or mineral sample powder. To encourage the full dissolution of all minerals in the sample, the sample must be crushed as finely as possible without causing oxidation. Some minerals, being more refractory, may have to be crushed finer than others. Ilmenite, for example, is a refractory mineral and consequently hard to dissolve during the above process and hence requires longer crushing effectively achieving a greater surface area to facilitate dissolution.

The ilmenite samples analysed during this study were all obtained from the mantle megacryst suite. Initial preparation involved the cutting of the megacryst using an ordinary diamond studded cutting wheel lubricated with water. One half was mounted in epoxy and polished for analysis using the electron microprobe. The remaining sample was crushed using a steel "piston mortar" and the powder created during this process screened out and further crushed using a corundum mortar and pestle. Crushing in the piston mortar was restricted to one or two blows to reduce the possibility of contamination. Sufficient fine material of less than two millimetres was produced after one blow that further crushing in the piston mortar was usually unnecessary. Crushing in the mortar and pestal was performed by hand initially and when fine enough using a mechanical mortar and pestle. The mortar was filled with acetone to prevent oxidation during the crushing process.

Samples were left to dry, screened to 300μm, and then transferred to a sealed glass vial using a wooden spatula to avoid preferential removal of magnetic grains.

2.2.3 SAMPLE DISSOLUTION

The method used in this study is based on that described by le Roex and Watkins (1995).

50mg of sample was measured into a platinum crucible with 3 drops of water to prevent bumping (minor explosion due to the release of gases from beneath the sample) and caking of the sample, both of which cause severe problems during dissolution. A mixture of 0.5ml 18M sulphuric acid, 0.5ml 28M hydrofluoric acid and 1ml of deionised, deoxygenated water was added to the dampened sample and heated for one minute using a Bunsen burner, gently boiling the mixture. Excessive, vigorous boiling causes partial oxidation of the sample whilst insufficient boiling often results in incomplete dissolution. One minute dissolution is an optimum time period for small sample sizes and samples with low total iron concentrations (less dilution possible). A longer dissolution period would require increased aliquots of acids which would result in too much acidity after dilution. The result is an acid peak which interferes with the Fe^{3+} peak during analysis. Due to the high total iron content of ilmenites, extreme dilutions are necessary to avoid overloading the column with iron and hence no acid peak interference occurs. One minute dissolution times were used for the ilmenite samples to replicate conditions exactly for the ilmenites and W-2. When dealing with such small quantities of acids, the 1 minute optimum time period should not be exceeded. If the H_2O evaporates completely, it is not available to prevent H_2SO_4 oxidising Fe^{2+} (Johnson and Maxwell, 1987). Disappearance of the H_2SO_4 results in the inability of the system to prevent the formation of ferric fluoride complexes which could result in an apparently reduced ratio.

After dissolution the dissolved sample is placed in a plastic beaker containing 50ml of refrigerated, deionised, deoxygenated water and further diluted according to the expected iron content of the analysed sample. This water was prepared by boiling vigorously for a number of minutes and sparging with helium to displace any free oxygen. The water was then sealed in sterile, plastic bottles and refrigerated until used. To prevent too high Fe^{3+} and Fe^{2+} concentrations in the sample solutions, which would overload the column, the dissolved ilmenite samples were diluted 2000 times, as opposed to W-2 which was diluted 300 times, resulting in the total absence of an acid peak. Utmost care was exercised to prevent contamination as small contaminations with such large dilutions could result in unwanted errors.

Smaller samples, down to 5mg, can be run using this dissolution technique with a corresponding loss in precision. It is essential that full dissolution is achieved, especially with samples containing

more than one mineral, as it is the only way of ensuring no preferential dissolution of Fe^{3+} over Fe^{2+} iron or vice versa.

2.2.4 LIST OF SAMPLES ANALYSED

Four international standards were analysed in addition to the Diabase W-2. These included basalt BHVO-1, basalt BIR-1, peridotite PCC-1 and syenite STM-1. During testing, ferric oxide, marine quartz, titanium oxide, ammonium ferrous sulphate, a transition metal standard solution (Figure 2.1 i), deoxygenated water, PDCA and a number of blanks were analysed. A synthetic diopside (EMMS-1, figure 2.1 ii), supplied by Emms (1993) was analysed.

Ilmenites that were analysed include NROB-1, a sample from Samada (also known as New Robinson and Kaalvallei) in the Free State, MON-1, MON-4, MON-5 all from Monastery Mine, again in the Free State, JJG1611 AND JJG1619 from Premier Mine in Mpumalanga, DTP17-2 and DTP18-3 from Du Toitspan in the Kimberley district, LKF-2 from Lekkerfontein and finally SJHIL-2 from Frank Smith Mine in the Barkly West district.

2.3 RESULTS

The results for the nine ilmenite megacrysts analysed are tabulated in table 2.1. The ratios of Fe_2O_3/FeO for these ilmenites range from 0.14 to 0.70 (figure 2.3) and the two sigma errors range from 0.02 to 0.04. All analyses except for MON-5, DTP18-3 and DTP17-2 were replicated on different occasions. Ratios derived from electron microprobe analyses for the same samples were calculated using stoichiometric principles (appendix 2.2 for method), errors determined (Two standard deviations from the mean, table 2.1, figure 2.3) by analysing the same spot 10 times, and results compared with the equivalent samples analysed using ion chromatography (I.C.). A range in Fe_2O_3/FeO ratios is evident from the more oxidised DTP18-3 to the more reduced JJG1611, in figure 2.3. Except for Mon-5, the analyses determined using ion chromatography are the same, within error, as those calculated from microprobe analyses. In all samples, except DTP18-3 and DTP17-2, both from the DuToitspan kimberlite, I.C. produces slightly more reduced results. Although the ilmenite samples were initially selected on the basis of the electron microprobe calculated Fe_2O_3/FeO ratio, these analyses, shown in figure 2.3 as open circles, differ markedly from the mean of multiple electron microprobe analyses determined later, and the I.C. data. This is attributable either to poor analytical conditions during the single analyses, or variability caused by

the overlap of the beam spot with an inclusion or imperfection. Figure 2.4 is a plot of Fe_2O_3/FeO determined by E.M.P analysis vs Fe_2O_3/FeO determined by I.C. The plotted correlation line has a gradient of 1. All samples except DTP17-2, from DuToitspan, plot slightly above the correlation line, indicating that the ratios derived from I.C. are slightly more reduced that the equivalent ratios determined using stoichiometric calculation from E.M.P analyses, but that the correlation is nevertheless a good one.

International standards BHVO-1, BIR-1, PCC-1 and STM-1 were analysed to evaluate the technique and repeat the precision and accuracy of le Roex and Watkins (1995). International rock standards were chosen to include as big a range of ratios as possible, and range from peridotite BIR-1 ($Fe_2O_3/FeO = 0.25$) to syenite STM-1 ($Fe_2O_3/FeO = 1.37$, table 2.2). Determinations of Fe_2O_3/FeO ratios for samples BIR-1, BHVO-1 and STM-1 agree, within error, to those obtained by le Roex and Watkins (1995) and the recommended values (Govindaraju, 1994), although BIR-1 has a more reduced ratio than the reported standard (Govindaraju, 1994). PCC-1 has been determined at 0.06 ± 0.02 which is significantly less than the published value of 0.54 (Govindaraju, 1994). Even though the exact mineralogy of PCC-1 is not known, the minerals present in an average peridotite are not likely to accommodate large concentrations of Fe^{3+} in their structure. Therefore a value of $Fe_2O_3/FeO = 0.06$ (this study) is far more consistent with peridotite mineralogy than 0.54 (Govindaraju, 1994). Accessory, refractory oxide minerals in PCC-1, left behind during dissolution could account for a more reduced ratio using I.C. To produce such good precision, however would require an equal degree of non-dissolution in each analysis, which is very unlikely. A minimum of six analyses were performed to obtain the ratios. BHVO-1 was analysed 26 times, in a number of different batches.

Potential problems may arise in certain samples where Fe^{3+} is present in greater concentrations than Fe^{2+} due to a greater sensitivity of the instrument to the Fe^{3+}-bearing complex than the Fe^{2+}-bearing complex at a detection wavelength of 520nm (le Roex and Watkins, 1995). EMMS-1, a synthetic diopside, was analysed for ceramic research purposes and yielded very high Fe_2O_3/FeO ratios. Reproducible results were obtained even though Fe^{3+} was far in excess of Fe^{2+} (Figure 2.1, table 2.2).

Where the total iron content is low, due to the nature of the sample or small sample sizes, and consequently small dilutions are applied, the more acidic solution contains ions which activate the photometric detector. These ions exit the column just prior to the Fe^{3+} complexes, producing an acid peak, fig 2.6(ii), which can potentially interfere with the Fe^{3+} peak. With ilmenites, the large dilutions (2000X) required to bring the total iron content to within the limits of the instrument reduce the acidity and no acid peak is detected.

An additional peak was discovered that was not reported by Dionex (1987) in their transition metal determinations. This peak has been identified as a titanium peak, probably Ti^{4+}, by analysing pure analytical grade TiO_2. Although not as prominent as in ilmenite (~55% TiO), the peak is perceptible in W-2 (1.06% TiO_2) and BHVO-1 (2.71% TiO_2, figure 2.6) and the change in size of the peak follows the increase in TiO_2 content. Even with the high concentrations of TiO_2 in ilmenites, the Ti^{4+} peak is small when compared to Fe^{3+} peak, indicating a decreased sensitivity of detection of Ti^{4+}. The tail of the Ti^{4+} peak does not overlap significantly with the Fe^{3+} peak, and with careful integration does not affect the precision of the analyses (figure 2.5 i- iii). The Ti^{4+} peak is much smaller than both the Fe^{3+} and Fe^{2+} peaks. This is possibly attributable to a lower sensitivity of the Ti^{4+} complex.

Sample weights less than 50mg were tested using BHVO-1. Very good precision, and agreement with both previous and subsequent BHVO-1 values, was recorded down to a sample weight of 20mg. Below 20mg the errors became greater, even though the mean value for Fe_2O_3/FeO remained the same (table 2.3, figure 2.6). The 2-sigma error increased from 0.02 to 0.06. Ilmenite is more conducive to analysis using small sample sizes due to its high iron content and this was utilised in the analysis of single whole grains. Multiple analyses on a single whole ilmenite grain showed good reproducibility, however care should be taken in selecting a sample that is monomineralic, with a clean and smooth outer surface and with no alteration along fractures in the sample. This has implications for the bulk analysis of kimberlitic macrocryst minerals, as long as single grains are cleaned and analysed using this method.

Peak area was used throughout this study rather than peak height, which proved to be unreliable (table 2.3). Using peak height produced much more oxidised ratios and greater errors. This may be a result of the very sharp non-Gaussian chromatogram peaks. Combinations of height and area were tried, but proved less successful than peak area alone. As long as area integration on the Fe^{3+} peak is both consistent and reproducible, especially between standard W-2 and sample, the precision reported in this study is attainable. The present method of selection of the baseline for integration is subjective, and precision and accuracy could be increased by developing a more tightly constrained integration procedure. This is however, beyond the scope of this study.

It was established early on that by doubling the eluent flow rate from 1ml/min (Dionex, 1987) to 2ml/minute the analysis time could be reduced from 15 minutes to 8 minutes without peak overlap or altering peak shape (figure 3.2). Although good precision was obtained using the faster flow rate, the precision on the 15 minute runs was marginally better, possibly due to more accurate integration,

using the present method, on the wider peaks.

2.4 DISCUSSION

Ion chromatography is a method which is relatively quick (ten minutes per analysis), utilises small sample amounts (50mg or less), has low detection limits (<1ppm) and high sensitivity, good precision (2σ = 0.02), is a relatively cheap method and instrument by modern standards, and furthermore has the ability to do both bulk rock Fe_2O_3/FeO, individual minerals, and the potential, with creative sample preparation, to analyse zoned minerals, whole rocks and large inclusions.

The dissolution stage of this technique is the most critical. Samples must be dissolved in such a way that the true Fe_2O_3/FeO ratio of the sample prior to treatment does not change either through oxidation during dissolution or the preferential complexing of either Fe^{3+} or Fe^{2+} with fluoride derived from the hydrofluoric acid. Fluoride preferentially complexes with silicon over other elements and hence the presence of sufficient silica will ensure that the excess fluorine complexes with silicon and not with Fe^{3+} or Fe^{2+}. If silica were absent, or only present in insufficient concentrations, the potential exists for the partial complexing of Fe^{3+} with fluoride. This would effectively remove Fe^{3+} from the analyte and result in a more reduced ratio. Furthermore, it could be expected that this more reduced ratio would remain consistent in different analyses of the same sample (buffering mechanism) and different between samples with differing amounts of silica. Addition of both quartz and colloidal silica (analysed beforehand for any applicable impurities) in various proportions to the ilmenite sample powder before dissolution had no detectable effect on the Fe_2O_3/FeO ratio. It was concluded that Fe^{3+} was not complexing with fluorides during dissolution of 50mg samples, and it is therefore likely that H_2SO_4 does indeed prevent fluoride complexes from forming, as suggested by Johnson and Maxwell (1989) and Kanai (1990). Kanai (1990) suggested that fluorides could result in a reduction in the Fe^{2+} peak if present in high concentrations. No such correlation was found in this study.

Another possible error, which could result in consistently reduced ratios is the micro-exsolution of spinel within ilmenite (Danchin and d'Orey, 1972). Ion chromatography averages Fe_2O_3/FeO for the entire sample, thus it would include the influence of the more reduced spinel exsolution.

Experimentation showed that the technique has potential to analyse samples down to 5mg and single ilmenite grains. With such small samples it was found that the addition of analytical grade quartz

powder to make up 50mg improved the precision, possibly due the effective reduction of the fluoride concentrations in the system.

The use of W-2 as the standard for the analysis of Fe_2O_3/FeO ratio in ilmenites is not ideal. There is no guarantee that the recommended ratio is accurate and the total iron levels in the ilmenites are much higher than in a diabase. In the absence of a suitable ilmenite standard, however, W-2 is preferable to the use of prepared standard stock solutions, as discussed previously.

Ion chromatography has succeeded in this study to achieve precise Fe_2O_3/FeO ratios for nine selected ilmenite megacrysts, which agree closely with the predicted ratio calculated using stoichiometric principles. It is concluded therefore that Fe_2O_3/FeO ratios calculated from electron microprobe analyses closely predict the true Fe_2O_3/FeO ratio in megacrystic ilmenites. The stoichiometric calculation should, however be based on a statistical number of analyses on the same ilmenite sample.

...ooOoo...

CHAPTER 3

A SEMI-QUANTITATIVE ASSESSMENT OF PRESERVATION IN DIAMOND PARCELS FROM SELECTED SOUTHERN AFRICAN KIMBERLITES.

Effects on Diamond Grade

Diamonds from Star, Messina, Ardo, Frank Smith, Samada and Leicester have been described, particularly with respect to resorbtion. A method has been devised to quantify the degree of preservation of a parcel of diamonds and has been applied to studied parcels and published descriptions. An attempt has been made to estimate the initial mass of the diamond parcel and the initial grade of the kimberlite. It has been established that diamonds from the group II kimberlites (Star, Messina and Ardo) are better preserved than diamonds from the geographically associated group I kimberlites (Samada and Leicester). The isotopically intermediate Frank Smith kimberlite is also intermediate in age and diamond preservation. It is postulated that a major diamond corrosive episode has occurred in the mantle lithosphere between 124 Myr and 94 Myr, within a period of 25-30 Myrs.

3.1 INTRODUCTION

Diamonds originate in the cool upper mantle lithosphere at pressures of between 50 kbars and 60 kbars with temperatures ranging from 900°C to 1400°C. These temperatures and pressures are calculated using diamond inclusion assemblages (Boyd et al, 1985), and are sampled by kimberlitic magmas intruding the continental lithosphere, migrating upwards and ultimately erupting at surface. The xenocrystic origin of diamonds is indicated by the inclusion of euhedral diamond crystals in peridotite and eclogite xenoliths recovered from kimberlite diatremes and age determinations of diamonds using inclusions (Kramers, 1977; Richardson, 1984, 1986, 1993, 1997) and nitrogen aggregation rates (Harris et. al., 1987). Richardson (1993) has identified three generations of diamonds from the Premier kimberlite attributable to an archaean (>3000 Myr) metasomatic event which resulted in the crystallisation of peridotitic diamonds, a 1930 Myr lherzolitic diamond crystallisation event and finally an eclogitic diamond crystallisation event (≈1150 Myr) just prior

to the eruption of the Premier kimberlite. Previously Richardson (1984, 1986) has dated peridotitic inclusions (3200 Myr) and eclogitic inclusions (1580 Myr) from Finsch mine using Rb-Sr and Sm-Nd systematics. Recent studies have provided much younger ages for diamonds (Shimizu and Sobolev, 1995). The age of diamonds has major implications for the residence time and consequent growth histories of diamonds in the lithosphere, confirmed by the complex growth and resorbtion histories recorded in some diamonds (Bulanova, 1995; Chinn 1995). For example, diamonds resident in the continental lithosphere since the Archaean will have had more opportunity to be subjected to a destructive event/s than younger diamonds which have crystallised in the late proterozoic, or closer to the kimberlitic sampling event.

Euhedral diamonds commonly display a consistent range in primary and secondary shapes, which allows useful observation of morphology, surface features and internal structure. Primary morphologies include the octahedron and other volumetrically less abundant morphologies such as cubes (occasionally prominent e.g. Mbuji Mayi), twinned varieties (macles, cubo-octahedrons, simple twins), aggregates, rare irregular shapes and rare tetrahedrons (figure 3.1). Secondary morphologies result mainly from the resorbtion of primary shapes of diamond and include rounded forms. Terminology of these rounded forms depend on the author, however the term tetrahexahedroid, introduced by Robinson (1978) to describe the resorbed form of the octahedral diamond has been adopted for this study. Although this term strictly applies to a 24 sided form derived from a cube or hexahedron (Klein and Hurlbut, 1985), the naturally resorbed product of an octahedron also commonly exhibits 24 faces (eg. figure 3.6e), and resembles the tetrahexahedron in shape (figure 3.1h), but displays a different orientation of the crystallographic axes, and a subtle difference in the shape of the faces. This occurs because edge dominated resorbtion on an octahedron results in three new tetrahexahedral faces for every original octahedral face ("8x3" resorbtion), whilst for a cubic diamond, every original cubic face is resorbed to become four new tetrahexahedral faces ("6x4" resorbtion).

Other terminology has been used to describe the secondary forms of diamond. Whitelock (1973) and Harris et. al. (1975, 1979) refer to a rounded dodecahedron and Sunagawa (1984) refers to a hexoctahedral form becoming a dodecahedroid with progressive resorbtion. Klein and Hurlbut (1985) assign a hexoctahedron form to multifaceted octahedral diamond (figure 3.1d). A diamond which has attained a rounded shape through progressive growth layering resembles a trisoctahedron (figure 3.1b), whilst stepped octahedrons exhibit a combination of both the octahedral and trisoctahedral forms (figure 3.1c). The natural product of resorbtion of these might be a dodecahedroid (figure 3.1i). The hexoctahedral form (eg. figure 3.4e), is common in many diamond

parcels, but appears to be less common than the tetrahexahedroid.

The tetrahexahedroid (Robinson, 1979) is a secondary morphology derived from the resorbtion of primary octahedra (Harris et. al., 1979; Robinson, 1979; Sunagawa, 1984; Robinson et.al., 1989). Although some tetrahexahedroids may be a product of fine growth layering on the faces of octahedrons (Varma, 1967; Yamaoka et al, 1977), etching experiments (Seal, 1965) and X-Ray topographic studies (Moore and Lang, 1974), where original growth layering can be seen truncated by resorbtion surfaces, suggest that most tetrahexahedroids are a product of successive resorbtion at corners and along edges of octahedrons. Further evidence of resorbtion includes: Rare examples of sharp-edged octahedrons, which have been observed in rounded diamond hosts (Sunagawa, 1984); etching experiments on diamonds using destructive reagents (ie. by dissolution) have produced surface textures that are commonly observed on natural diamonds (Phaal, 1965; Harris and Vance, 1974; Evans, 1976; Kennedy and Kennedy, 1976; Arima and Inoue, 1995) and trigonal etch pits on pristine octahedral faces are frequently linearly arranged and often correspond to lamination lines exposed on resorbed edges. Robinson (1979), ascribed this to the outcropping of dislocations. This suggests that dislocations (or any other planar weaknesses) in the diamond provide zones along which preferential dissolution can occur. Robinson (1979) has, in fact, interpreted only 2 out of the observed 41 surface textures on natural diamond crystals, as products of growth processes (Gurney, 1989). Finally, broken stones, cleavage fragments and edges of ruts are often rounded, which can only be a result of dissolution. Corners and edges of crystals have the highest area of exposed surface per unit volume and hence are preferentially resorbed (Robinson, 1979). This process naturally decreases the surface area of the crystal faces while the original edge grows into a new resorbed face, finally producing a rounded morphology. A full range in the degree of rounding from the octahedron to the tetrahexahedroid can be observed in many parcels of natural diamonds (e.g. Robinson et.al., 1989).

The natural change in shape from octahedron to tetrahexahedroid has been divided into 5 resorbtion categories by Robinson (1979). Each category displays the effects of successive dissolution starting at the edges of the 8 faced octahedron and progressively removing the remnant octahedral faces until a 24 face tetrahexahedroid remains. During this process, Robinson (1979) estimated a 45% loss in mass from a pristine equidimensional octahedron to its related tetrahexahedroid and devised transitional estimated preservation percentages based on observable changes in morphology of the diamond. Otter (1989, 1993) applied a numeric sequence to these resorbtion induced shapes (figure 3.2) and allocated a value of 1 to a tetrahexahedroid and 5 to a stone with resorbed edges (5% reduction in mass).

The ratio of primary to secondary forms of diamonds extracted from kimberlite differs between diamond parcels (Harris et. al., 1979; Robinson, 1989). However in many instances, especially in southern Africa, secondary (resorbed) forms may predominate (Gurney, 1989). Diamonds liberated from xenoliths are generally well preserved, sharp-edged octahedrons. Furthermore, hemimorphic diamonds exposed on the surface of xenoliths are well preserved where bound by the xenolith and resorbed where exposed on the surface. This suggests that the diamonds were resorbed where exposed to t he corrosive medium, widely believed to be the kimberlitic magma (eg. Robinson, 1989). Resorbtion of diamonds in the kimberlite is a fairly recent event in the history of most diamonds. Studies of the internal structure of diamonds (eg. Chinn, 1995) has revealed "old" resorbtion events and sometimes multiple growth and resorbtion events. This indicates that the resorbtion of some diamonds occurs during residence in the mantle in addition to any resorbtion that may occur in the kimberlitic magma.

The phase transition from diamond to graphite has been well established (Bundy, 1963; Kennedy and Kennedy, 1976). However, diamond can exist metastably outside the diamond stability field and, under conducive conditions, the rate of conversion from diamond to graphite is very slow (Evans, 1976). With the addition of reactive gases, reaction rates are substantially increased and the temperatures at which conversion will proceed decreases. Therefore, changes in chemical environment, temperature or pressure can adversely affect the growth and preservation of diamonds.

Oxygen fugacities in the upper mantle are variable. Partial melting of fertile asthenospheric garnet lherzolite and the localised extraction of komatiitic and other melts has resulted in depleted subcontinental lithosphere reaching depths of 150 to 200 km (Boyd et. al., 1985). During this process volatiles, specifically CO_2 and H_2O were removed, and a lithosphere with fO_2 s between those corresponding to oxygen fugacities defined by the Fayalite-magnetite-quartz (FMQ) and magnetite-wüstite (MW) buffers remained (Daniels and Gurney, 1991). Calculated fugacities derived from diamond inclusions and diamondiferous source rocks, define a range of fO_2 values, which fall between the iron-wüstite (IW) and magnetite-wüstite (MW) buffers (Haggerty and Tompkins, 1983; Haggerty, 1986; Haggerty and Erlank, 1987; O'Neill and Wall, 1987, Daniels and Gurney, 1991 and Eggler, 1991). Although local heterogeneities and stratification with respect to fO_2 do occur in the subcontinental lithosphere (Daniels and Gurney, 1991), the deep subcontinental lithosphere is nevertheless an ideal storage reservoir for diamonds, in which ambient oxidation conditions are conducive to the growth and preservation of diamonds. The growth of diamonds under reducing conditions is corroborated by the presence of certain minerals in diamonds (

Haggerty, 1986). These include: Metallic iron (Sobolev et. al., 1981), sulphides (Harris and Gurney, 1979), magnesiowüstite (Scott-Smith et. al., 1984), Cr^{2+} bearing olivine (Burns, 1975 ; Meyer, 1975) and methane (Melton and Giardini, 1972). In contrast, the discovery of CO_2 bearing diamonds by Schrauder and Navon (1993) and also Chinn (1995) suggests that more oxidising conditions have existed during the growth of some diamonds. Asthenospheric, and upper lithospheric spinel peridotite are more oxidised relative to lower lithospheric harzburgites, with fO_2's close to QFM (Eggler and Lorand, 1994). Evidence of diamond growth in the asthenosphere is suggested by high pressure pyroxene and ferro-periclase inclusions in diamond reported by Moore and Gurney (1985), Moore et. al. (1986), Rickard et. al. (1989) and Otter et. al. (1989), as well as in alluvial diamonds found in Brazil (Wilding et al, 1994). Local incursions of oxidising metasomatic fluids could, however, disrupt the balance of redox conditions in an area of the subcontinental lithosphere, and lead to conditions which are unfavourable for the preservation of diamonds.

In this study, diamond parcels from selected group I and group II kimberlites in southern Africa were observed, and individual diamond morphology and resorbtion characteristics were recorded. Localities where diamonds were made available for study included the Leicester, Frank Smith, Ardo and Messina kimberlites, located in the Barkly West district, and the Samada and Star kimberlites in the Welkom-Theunissen area. Further localities for which diamond resorption data are available include: Kao (Whitelock, 1973); Premier, Palmietgat, Bultfontein, De Beers, Dutoitspan, Kamfersdam, Wesselton, Jwaneng (Robinson et. al., 1989); Koffiefontein and Premier (Harris et. al., 1975); and Loxtonsdal, Letseng La Terae, Orapa, Lethlakane, and Mir (Robinson, 1979). An attempt is made to quantify resorbtion, (degree of preservation) of a diamond parcel and predict the effect this may have had on the grade of a kimberlite.

3.1.1 THE EFFECT OF RESORBTION ON DIAMOND GRADE:

The diamond grade of a particular kimberlite is expressed as the total number of carats per metric tonne or per 100 tonnes. Grade can be applied to a pipe, dyke, individual phase, demarcated zone or even to individual samples. The grade at a particular locality is commonly variable and the reported average grade is only calculated after a statistically representative amount of ore body has been effectively and strictly processed. This requires an assessment of variability within or between ore bodies. In addition, a distinction must be made between the diluted (run-of-mine) grade and the undiluted grade of the ore body, especially when mining dykes where mining of a percentage of wall-rock is inevitable. The efficiency of the extraction process also affects grade determinations.

Examples of this can be seen where tailings dumps can be processed economically, for example at Bellsbank dyke system, west of Kimberley, South Africa. To establish a representative "average grade", therefore, is not always feasible, possible or even meaningful.

Although the grade of the ore body can be determined, subject to the restrictions just mentioned, the concentration, distribution and variability of diamonds within the source rocks of the subcontinental lithosphere, which was subsequently sampled by the ascending kimberlitic magma, remains unknown. Furthermore, the efficiency of the magma to assimilate the diamondiferous wallrock, and the quantities that were sampled are also unknown. Notwithstanding these factors, however, it is acceptable to envisage that a diamond population exhibiting visual evidence of resorbtion represents a significant loss in mass of diamond, and that an unresorbed parcel has not suffered the same loss of mass. Resorbtion, therefore, lowers the ultimate grade of an ore body, whether due to corrosion of diamonds taking place during residence in the source rock/s, or while exposed to the transporting magma en route to the surface. To further complicate matters, the resorbtion morphology seen on diamonds may not represent a single resorbtion event caused by a particular destructive process, but the morphology may be a result of multiple related, or unrelated resorbtion events or multiple growth and resorbtion events.

The "average grade" of an ore body is therefore affected by a number of criteria. Firstly, determination of the "average grade" is subject to errors caused by the practicalities of processing. Secondly, the history and concentration of diamonds in the lithospheric rocks through which the magma travelled, and the proportions of diamondiferous mantle and other non-diamondiferous rocks sampled are unknown.

An attempt has been made here to express diamond resorbtion morphology in a semi-quantitative manner and to establish an initial mass of diamonds had no resorbtion of that particular population of diamonds occurred.

3.2 METHOD

A number of diamond parcels, representing the "run-of-mine" production, were described particularly with respect to their resorbtion characteristics. The size of the parcel was determined by the length of time over which production occurred, and was contingent on the on the security procedures at the respective mine. Results were collated and a preservation index was calculated

to represent the degree to which diamonds were preserved.

3.2.1 DESCRIPTION AND DATA RECORDING

A number of parameters were described in each parcel of diamonds, including general parameters such as weight, form, colour, colour intensity, and impurities as well as parameters relating to the outward appearance of the diamond which included: breakage, shape, habit, morphology and degree of resorbtion. An example of the form used to collect data during diamond parcel descriptions is included in appendix 3.1. In some instances, descriptions were used to evaluate the diamond parcels, hence the first half of the form includes parameters used by TERRAC (Rombouts, 1992). All descriptions have been entered into a relational database to allow easy data manipulation.

The parcel of diamonds from each locality was weighed and screened into convenient size categories shown in table 3.1 with corresponding metric equivalents. Each sieve category was split until a practical number of stones was obtained and all the diamonds from the split were individually described. Descriptions were made for all diamonds greater than Pierre size 24, irrespective of the number of stones. All parcels described represent run of mine production. Security arrangements precluded long periods of time being available to describe parcels, which constrained the possible number of stones described. The descriptive parameters are set out in table 3.2 along with the various descriptors. An explanation of all descriptors, except for the parameters: Form, colour, colour intensity, and impurities taken from Rombouts (1992) follow.

3.2.1.1 Breakage:

Broken stones were subdivided into 3 categories according to an estimate of the percentage of the original stone remaining. A diamond is termed *chipped* if greater than 80% of the original stone remains, *broken* if 40% to 80% remains and a *fragment,* if less than 40% remains. No entry is made if the diamond is still whole.

3.2.1.2 Shape:

This descriptive parameter describes the outward shape of a stone, without inferring any origin for this shape. Descriptors include terms such as elongate, flat or lopsided. Elongate refers to the lengthening of one dimension with respect to the other two, whilst flat refers to the shortening of one dimension with respect to the other two. Although for primary crystallised stones this is

synonymous with the crystallographic axes, it need not necessarily be so for secondary resorbed forms and hence any such correlation should be avoided. A diamond is skew when it has a distorted appearance (eg. a rhombohedron is a skew cube). However, the term "distorted" implies deformation which is only one way of achieving this effect. A skew shape is often caused by unusual crystallization. No entry is made for a a perfectly shaped, equidimensional diamond.

3.2.1.3 Intergrowths:

Intergrowth alludes to all stones where the shape is governed by twinning, aggregation and hemimorphism. Descriptors include: Twin (all simple twins made up of a small number of individual crystals), polycrystalline aggregates and hemimorphic stones. A twin or an aggregate of stones is normally made up of crystals with identifiable morphologies. These morphologies are referred to the following parameter.

3.2.1.4 Morphology:

Crystal morphology describes angular relationships, size and shape of faces on a crystal. It is dependent on influences such as temperature, pressure, nature of solution, direction of movement of the solution and the availability of open space for free growth (Klein and Hurlbut, 1985). Primary morphologies (figure 3.1) of diamond include the octahedron (Octa), cube, macle, cubo-octahedron (CuOc), trisoctahedrons (Tris), rare tetrahedrons (Thn) and diamonds crystallised with irregular symmetry (Irre). A macle is a specific term used for a contact twin of two octahedrons and is included under morphology due to its consistently reproducible shape which produces a unique resorbed form. Resorbed, or secondary morphologies (figure 3.1) of diamond include the tetrahexahedroid (Thd), dodecahedron (Dodec) and resorbed irregulars (Irre). The term irregular should be restricted to a crystal with forms other than the usual forms, probably resulting from spacial restriction during crystal growth. This differs from a stone in which no form can be identified, particularly the case with fragments and highly resorbed diamonds, which should be classed as undetermined (Und).

3.2.1.5 Resorbtion:

Resorbtion categories as determined by Robinson (1979) along with their numeric allocations (Otter, 1985) have been discussed previously. For the purposes of this study, the numeric sequence has been reversed and two further categories added. A pristine octahedron therefore is allocated the number 0, whilst a tetrahexahedroid representing 45% loss in mass is allocated a 5. Any stone which is obviously more resorbed than 45% is allocated to a further category 6 (figure 3.3). Category 6 stones are identified by severe rounding in which no visible crystal faces remain, and resorbtion along planar and point defects which produce deep pits and canyon rutting. These effectively create new edges along which further resorbtion occurs.

In cases where the faces of the primary octahedron are heavily layered (stepped, laminated) and more specifically the edges are topographically sunken (trisoctahedron), the rate of resorbtion would be faster due to the multitude of edges available to resorbtion. Such stones may attain a higher degree of rounding relative to flat faced octahedrons and are easily miss-assigned to inflated resorbtion categories.

Morphologies other than the octahedron are subjected to similar resorbtion processes. Cubes for example have 6 faces and 8 coigns as opposed to the 8 faces and 6 coigns of the octahedron, but both have 12 edges. It can be expected therefore that with edge dominated resorbtion, the modified shape of a cube will be a tetrahexahedroid closely resembled by that derived from an octahedron. A macle has a flat triangular shape with a central twin plane and when resorbed, loses most of its triangular shape resembling a disk-shaped flattened tetrahexahedroid. For ease of identification, all morphologies other than the octahedron have resorbtion values determined, as with the octahedron, by the proportion of the remnant primary faces remaining.

Hemimorphic diamonds are diamonds which have undergone differential resorbtion, probably as a result of armouring of the less resorbed half in a xenolith (Robinson, 1989). Maximum and minimum resorbtion values are recorded.

Polycrystalline diamonds are an aggregate of individual crystals which are often individually resorbed, for example, an aggregate of octahedrons, tetrahexahedroids or cubes. Resorbtion values for polycrystalline aggregates are therefore determined by the resorbtion values of the individual stones. For situations where individual grains, each with differing degrees of resorbtion, make up the aggregate, the aggregate is treated the same way as a hemimorphic diamond and two representative values given. Such aggregates are quite common and have potentially interesting implications for their formation.

3.2.2 PRESERVATION INDEX:

The degree of preservation of a parcel of diamonds from a particular kimberlite, comprising different populations each with potentially differing degrees of preservation, is deduced by the amount of resorbtion displayed by individual stones within that parcel. Differentiating between different populations of diamond in a single suite is not normally possible by mere observation and as a result preservation indexes are calculated for the entire parcel. To calculate a preservation index the proportion of diamonds in each resorbtion category for each size category was established. Fragments were excluded to avoid the possible duplication of diamonds.

The preservation index (PI) is determined by dividing the sum of the lesser resorbed categories (0 to 3) by the total number of eligible stones from both the resorbed and un resorbed categories.

$$Preservation\ Index\ (PI) = \frac{N_{\in+\cap+\|+\sum+}}{N_{\in+\cap+\|+\sum+} + N_{\infty+\neg+}}$$

This equation yields values between 0 and 1. 0 represents a resorbed parcel where all diamonds have lost more than 25% of their original mass, whilst 1 represents a well preserved parcel.

Categories of resorbtion are relatively easily observed in diamonds which belong to the octahedron-tetrahexahedroid transition and where loss in mass as a result of resorbtion has already been estimated (Robinson, pers. comm. in Otter, 1989). Cubic morphologies , when resorbed, also produce secondary morphologies, for which weight loss should be classified differently. However, apart from Tshibua, where resorption is minimal, no such localities are considered in this study and the issue is not dealt with further here.

Although a further category 6 was included during description to describe stones with obviously greater than 45% loss in mass (eg. severely rutted stones), for the purposes of calculating a preservation index, these diamonds were classified into category 5.

3.2.3 ESTIMATION OF PRE-RESORBTION MASS:

The pre-resorbtion mass of a parcel of diamonds is established by dividing the parcel into the various resorbtion categories and applying a correction for the loss of mass to each category. The total percentage by which the mass of the diamonds increases is then applied to the reported grade for the mine to obtain the initial grade. A major shortcoming is only being able to quantify a resorbed stone that has lost up to 45% of its mass. However, an attempt is made to predict mass lost from higher resorbtion categories and the mass of diamond which has been totally resorbed. The method is outlined below and the mathematical solution to the equation is set out in appendix 3.2(i). Data, calculations and graphs plotted as per step (iii) in the calculations in appendix 3.2 for the individual localities are shown in table 3.3 (a-f).

i) Diamonds are described and the number of diamonds in each resorbtion category (N) recorded. Fragments are excluded to avoid any duplication of diamonds.

ii) The mass of the diamonds, in carats, is used in order to derive an initial grade. A single large stone in the parcel, however will contribute greatly to the overall mass of the parcel and distort any correction for loss of mass of the whole parcel. For this reason, the average mass per stone is used to normalise out the effect of any individual diamond on the overall resorbtion of the parcel. The number of stones for each resorbtion category (N) is multiplied by the average mass per stone for the whole parcel, thus producing the present normalised mass (pm). The average mass per stone is determined by dividing the total mass of the parcel (PM_T) by the total number of stones (N_T).

iii) Values of pm are plotted against the resorbtion category (percentage of mass lost due to resorbtion)

iv) Diamonds described initially as category 5 resorbtion include all diamonds which have lost greater than 35% of their pre-resorbtion mass (ie. all diamonds in

categories 5 and 6). In the majority of cases the category 5 stones are inflated relative to the curve defined by the other resorbtion categories and are therefore deduced to contain diamonds with more than 45% loss in mass. The area under the curve between 35% and 45% loss in mass provides a constraint on the number of stones restricted to the most resorbed category, by the trend defined by other resorbtion categories in the parcel. Therefore, as long as the area under the curve is maintained the final category can be adjusted to fit the curve, thereby correcting for stones which may have greater than 45% loss in mass. An example is shown in appendix 3.2(ii).

v) The new extrapolated resorbtion curve, which includes estimated resorbtion for categories above 35% loss in mass, is used to estimate normalised present mass for diamonds with greater than 35% loss in mass (step ii). These values are then included with the existing normalised masses for resorbtion categories with less than 35% loss in mass.

vi) An initial (pre-resorbtion) mass (normalised; *im*) for each resorbtion category is determined by adding the percentage mass lost by the stones (R) in the respective resorbtion categories (r_c).

vii) The initial mass, ie. before resorbtion, for each category (IM) is calculated by dividing the actual (present) mass of diamonds in each resorbtion category (PM) by the normalised present mass (pm) for the parcel (step ii) and then multiplying by the normalised initial mass (im) determined in the previous step (in effect, the ratio of normalised initial to present mass). This true initial mass in carats represents the mass of diamonds that might have been were it not for resorbtion. Initial masses (IM) are plotted against the resorbtion categories in which they ended up after resorbtion, and represent the initial mass of diamonds that were affected by equal amounts of resorbtion, and consequently were grouped together by morphology. The curve of initial masses is extrapolated to resorbtion category 10 which, in terms of initial mass, represents the mass of diamond which was completely resorbed (100% loss in mass). This attempts to predict the mass of diamonds which experienced total destruction and are no longer represented in the parcel. The overall initial mass (IM_T) is calculated by adding all individually determined initial masses (IM) from the 10 resorbtion categories and represents the estimated total initial mass of the parcel.

viii) The final step involves applying the ratio determined by dividing the total initial mass (IM_T) of the parcel by the present mass (PM), and multiplying this by the present grade (PG) to calculate the initial grade.

The calculation of initial grade using the this method is thus represented by the equation:

$$Initial\ Grade\ (IG) = \frac{PG}{PM_{\text{[illegible]}}} \sum_{\text{[illegible]}} \left(\frac{100(N)(PM_{\text{[illegible]}})}{(100-R)(N_{\text{[illegible]}})} \right)$$

A number of factors affect the determination of initial grade:

i) The manner in which resorbtion is categorised is dependent on the interpretation and consistency of whomever performs the assessment.

ii) The assessment and the estimation of the percentage loss of mass in the different resorbtion categories is only semi-quantitative and applies to ideally shaped, equidimensional octahedrons. In addition, many stones exhibit distorted growth, are structurally deformed, have thick growth laminations or are of an entirely different morphology, and therefore require individual assessments of loss in mass which are empirical and imprecise.

iii) The diamonds showing shapes correlating to category 5 include not only diamonds which have lost 45% mass, but all diamonds which have lost greater than 45%. The lack of identifiable and quantifiable resorbtion for categories greater than 45% complicates the application of a correction factor to establish initial mass.

iv) Diamonds which have obviously lost greater than 45% of their mass are rare. This could be due to an inability to recognise such stones or a function of an increased rate of resorbtion. It is possible that the resorbtion proceeds so quickly after the diamond becomes a tetrahexahedroid that few of these diamonds survive, particularly when extreme rutting is present. In addition the rate of resorbtion is affected by the original size of the diamond and hence the smaller size categories are likely to have had the most quantity of diamonds completely destroyed.

Although an attempt is made to determine the diamonds which have lost greater than 45% of their mass, it has been achieved by extrapolating using diamonds that were described. An increased rate of corrosion in the more resorbed categories would result in the complete resorbtion of some

diamonds. This, combined with a large number of resorbed, small diamonds not recovered due to the minimum cut-off size during extraction by the plant, and which would have had pre-resorbtion diameters large enough for recovery, would effectively deflate the mass of the parcel, and hence the factor applied to calculate pre-resorbtion mass. Furthermore, the greater the resorbtion capacity of the resorbing medium, the more this effect would occur, and consequently a highly resorbed locality could have proportionately less increase in mass during the correction for initial mass, than a moderately resorbed locality due to the destruction of a large percentage of the original population. As a result, therefore, the calculations in this study produce an effective minimum pre-resorbtion or initial mass.

3.3 RESULTS

Resorbtion data and the calculation of preservation indexes and initial grades from the description of diamond parcels from the localities: Leicester, Samada, Frank Smith, Ardo, Messina Investments and Star are presented in table 3.3 (a-f), with a summary in table 3.4. The individual parcels range from 158.6 carats (Ardo) to 1027.8 carats (Messina). The number of diamonds described from each parcel varied from 313 (Ardo) to 777 (Leicester). Other parcel sizes were: Star (322), Frank Smith (396), Samada (481) and Messina (712).

Size distribution histograms of diamonds from the various kimberlites, with the exception of Samada (figure 3.7), indicate an exponential increase in the number of diamonds with decreasing diamond size. Samada shows a reduction in the number of stones in the +6-9 category caused by routine loss of small diamonds during the extraction process. The weight of diamonds in the individual size categories increases with decreasing diamond size suggesting that either the growth of smaller diamonds is favoured over larger ones, or that the growth period was insufficient for the routine growth of larger diamonds. With the exception of the Messina, Samada and Leicester parcels, the curve of weight distribution is less smooth than the curve which represents the number of diamonds. The Leicester distribution is undulatory, probably due to a greater than average number of large (up to 22ct) diamonds found in the Leicester kimberlite. Distributions in the larger size categories probably do not contain sufficient diamonds to be representative. The Messina, Samada and Leicester weight distributions are smooth in comparison to the equivalent Frank Smith, Star and Ardo curves, suggesting that the larger Messina, Samada and Leicester parcels contain a more representative sample of diamonds. The distribution curves, based on the number of diamonds are smooth, and therefore the quantity of stones in the respective diamond parcels, is considered to be

representative for the purposes of this study.

Preservation indexes were calculated using diamond parcels from: Star, Messina, Ardo, Frank Smith, Samada and Leicester and are presented in table 3.5. The effect of variations in diamond size on the preservation ratio was tested by calculating a separate preservation ratio for each size category. This enabled direct comparison with the data of Robinson (1979, 1989), Whitelock (1973) and Harris et. al. (1975, 1979). These studies only report proportions of octahedrons, tetrahexahedroids/dodecahedrons and cubes whilst they omit other morphologies. Robinson (1989) defines the transition from octahedron to tetrahexahedroid as being when the last remnants of any original octahedral faces remain. In the studies of Whitelock (1973) and Harris et. al. (1975, 1979) the morphological transition is not addressed and consequently the assumption has been made that the transition occurs at a similar stage to that described by Robinson (1989).

All parcels are dominated by diamonds exhibiting octahedral and tetrahexahedral morphologies (table 3.6), while the proportion of other less abundant morphologies varies according to the locality. At Frank Smith and Leicester, for example, the parcels contain a significant proportion of cubic diamonds (Frank Smith ≈ 12%; Leicester ≈ 17%), and the Star parcel contains 12% macles. The calculated preservation index increased from 0.34 to 0.38 for the Frank Smith parcel, and from 0.64 to 0.68 for the Messina parcel, when resorbtion data for cubes, macles, irregulars and other morphologies were included (table 2.5). These morphologies, which possibly represent different populations with different degrees of preservation, can increase the value of the preservation index if they are less resorbed and report to the numerator of the index. In contrast, the preservation index of the Leicester parcel (0.22 vs 0.23) remained almost the same, despite the inclusion of other morphologies (mainly cubes and irregulars) which constitute 27% of the entire parcel. This occurs because the degree of preservation for these morphologies is low and therefore report to the denominator.

The size of the diamond has a significant effect on the preservation index (figure 3.8a). In all six parcels the preservation index decreases with decreasing size (sieve category), supporting the conclusion of Robinson (1979) that the larger surface area per unit mass promotes resorbtion in the smaller size categories. The better preserved parcels exhibit a smaller range in preservation index, whilst the more resorbed localities exhibit not only a greater range of indexes, but also greater variability. It is therefore not accurate to use a single size category or even an average of all size categories when calculating preservation indexes. The different diamond parcels maintain the same

order of preservation index for sieve categories smaller than 12, but become variable in the size categories represented by large diamonds. This could be a result of a less representative number of diamonds in the larger size categories or, more likely due to a difference in the rate of resorbtion between smaller and larger diamonds, coupled with a greater variation between the size distributions of the larger size categories in the different parcels. This explanation is supported by a poor correlation between the average weight per stone for different parcels in the larger sieve categories when compared with the smaller sieve categories (figure 3.8b).

A full range of preservation indexes are represented by the different diamond parcels (table 3.4, table 3.5), ranging from Star: the most preserved (PI=0.91) to Leicester, the least preserved (PI=0.22). The Messina (PI=0.68), Ardo (PI=0.49), Frank Smith (PI=0.38) and Samada (PI=0.30) parcels define a trend from well preserved to poorly preserved and are intermediate in preservation between Star and Leicester. Frank Smith, Samada and Leicester all have preservation indexes significantly less than 0.5, representing parcels where greater than 50% of the diamonds have lost more than 25% of their original mass. Preservation Indexes for parcels from other southern African localities (table 2.5) show a range of preservation values between 0.56 (Loxton, "-11+9" fraction only; Robinson, 1979) and 0.08 (Kao; Octas and "dodecs" only; Whitelock, 1973). Mir, a Siberian kimberlite, known for its large proportion of pristine octahedrons, has been included to test the preservation index. The preservation index is high (PI=0.96), as expected, even though the parcel contains only 92 diamonds in the "-11+9" sieve category. Group II kimberlites appear to be better preserved than group I kimberlites, particularly for parcels described in this study.

Table 3.3(a-f) includes all parcel and resorbtion data for the various localities. The individual pages can be divided into a number of blocks and are numbered clockwise 1 to 6. Block 1 contains all parcel information including the weight, number of stones, average weight per stone and the preservation index for each size category. Block 2 includes all resorbtion data individually recorded for each sieve category, the calculation of the preservation indexes and data for the total parcel including preservation index and the calculations of the initial mass. Blocks 3 and 4 contain the calculation of initial grade and details of any hemimorphic diamonds. The graph in block 5 shows the distribution of diamonds in various resorbtion categories (0-5), and block 6 is the legend.

The calculation of the initial weight of the parcel follows the procedure outlined in section 4.2.3 (i - viii). "N*Wt/st" is the normalised weight determined by multiplying the number of stones in each resorbtion class (N) by the average weight per stone. "$Graph_{(Corr)}$" lists the same values, but uses the

graph to extrapolate the area under the curve and includes the prediction of the normalised weight of diamonds which may have experienced greater than 45% loss in mass. In "$L.O.M_{(corr)}$" the "$Graph_{(corr)}$" values are adjusted to include the mass lost due to resorbtion in that class. The initial weight, "Init. Weight", distinct from the normalised weight, for each resorbtion class is then calculated by taking the normalised weight and recasting it as a proportion of the total normalised weight (sum of "$Graph_{(corr)}$" for all resorbtion classes), and applying it to the total parcel weight allocated to each resorbtion category ($WT_{(total)}$). The total of the sum of all "Init. Weight" values equals the total initial weight for the parcel. Finally, initial grade is calculated by taking the total initial weight (491.61) and dividing it by the present total parcel weight (418.34) and multiplying by the present grade.

The plotted normalised weights for the individual resorbtion classes (figure 3.9) display curves which are similar in shape for all parcels, with a steep peak and long tail on the more resorbed side. The lesser resorbed parcels show a more flattened peak, whilst diamonds from the more resorbed localities produce sharper peaks. Furthermore, the position of the peaks is displaced towards categories with higher resorbtion for parcels with lower preservation (table 3.4). The peak for normalised weight of diamonds in the parcel from Star plots between 5% and 15% loss in mass, whilst the peak for Leicester falls at a loss of mass >45%. Integration of the area under the curve of described resorbtion categories is assumed to reflect the weight of stones. Inflated weights of diamonds in the most resorbed category (35% - 45%) reflects the inclusion of diamonds which have undergone greater resorbtion than 45%, but are allocated to resorbtion category 5. Consequently, the curve is extended such that the area beneath the curve between the 35% and 45% resorbtion categories is maintained. Resorbtion values for unrecognisable categories greater than 45% loss in mass can then be estimated from the curve and the appropriate corrections for loss in mass applied (figure 3.10). This is more suitable than applying a 45% loss in mass correction to all stones which report to resorbtion category 5. A further advantage is that once the correction for loss in mass has been applied, the new curve can be extended to intersect the right hand y-axis. This intercept represents the initial weight of diamonds that were completely destroyed.

The percentage increase from actual grade to initial grade (table 3.4) increases as the overall preservation of the parcel decreases. This is to be expected due to the greater destruction of diamond. However, the initial grade of the less preserved parcels is still significantly lower than the better preserved parcels. This suggests that the kimberlites from which the parcels with greater preservation were derived were inherently of significantly higher grade. Conversely, and more

likely, the diamonds remaining in the lesser preserved parcels, possibly do not fully represent the unresorbed original parcel, and a large complement of the original diamonds have been completely destroyed. The procedure presented here calculates initial grade by utilising only the remainder of the original complement of diamonds. Hence, a well preserved parcel, such as the parcel from Star, with the majority of diamonds displaying little to moderate, and identifiable, levels of resorbtion is less likely to have had many diamonds completely resorbed, and the estimated initial mass and grade is probably fairly accurate. In contrast, however, the badly preserved parcel from Leicester, in which the majority of diamonds probably experienced greater than 50% loss in mass, is likely to have experienced complete resorbtion of a significant amount of diamonds. With the complete absence of these diamonds, it is impossible to extrapolate back to a realistic starting mass of the parcel and hence in these instances, the estimation of initial weight and initial grade will be an absolute minimum.

3.4 DISCUSSION

Resorbtion begins at the coigns of diamonds and progresses to the edges due to the higher surface area per unit of mass. As resorbtion of the edges proceeds, the area exposed to resorbtion increases and the area of the less reactive remnant octahedral face decreases. As the resorbtion surface truncates the original octahedral growth layering, a multitude of microscopic edges are exposed to the resorbing fluid. It is therefore probable that the more the diamond is resorbed, the faster the rate of resorbtion becomes. Furthermore, once a diamond changes morphology to a tetrahexahedron, the surface is rough and the form is bounded by a number of faces and edges. At this stage resorbtion may occur at a high rate, with corrosive fluids exploiting deep "canyon" ruts and cracks in the crystal. The unrealistically low initial grade of the poorly preserved parcels, when compared to the initial grade of well preserved parcels, indicates that less preserved parcels are under-represented in the higher resorbtion categories. This is supported by the parcel from Leicester mine ,in which the curve representing the change in the normalised weight of diamond with resorbtion category (figure 3.9f), does not reach a peak before category 5. In this category, described diamonds have lost 45% or more of their original mass. The under-representation of diamonds in category 5 may be explained by a rapid increase in the rate of resorbtion as resorbtion proceeds. By the time the diamond has lost 50% of its original mass any weakness in the crystal, (eg. Planar dislocations, internal fractures etc.) have been exploited, which may result in deep canyon ruts and eventual breakage of the diamond. The mechanism of resorbtion may therefore change from being edge dominated, to being weakness dominated. An increased rate of resorbtion along new edges,

combined with resorbtion of new rough faces, and the exploitation of planer and other weakness probably results in the quick destruction of the diamond.

The group II kimberlites in this study have higher preservation indexes than the associated group I kimberlites. These differences in diamond preservation exist despite close geographical proximity, and are consistent with relative isotopic and age differences. Samada and Star, for example, are geographically closely associated and have contrasting preservation indexes and ages. Star has a K-Ar age of 124 Myr (MacIntyre and Dawson, 1976), and is 30 Myr older than Samada, with a Rb-Sr age of 84 Myr (Viljoen, 1994). In the Barkly West area, the Messina and Ardo diamond parcels are better preserved than the Frank Smith and Leicester parcels. All are again geographically closely associated, falling on a SE-NW trend, with Leicester, the south-eastern most kimberlite, followed approximately 20km to the north-west by Frank Smith, Ardo (Sover) dyke and the Messina (Bobbejaan) dyke. The increase in the preservation of the diamond parcels and in the ages of the kimberlites follow the same geographical trend. Messina on the Bobbejaan dyke is associated with the Bellsbank dyke dated at 119 Myr (Smith et. al., 1985). Frank Smith, although petrographically a group I kimberlite is intermediate in isotopic signature and age (114 Myr, Smith et. al., 1985) between Leicester dated at 93.6 Myr (Davis, 1977), a typical group I kimberlite and the group IIs, Messina and Ardo. It also has intermediate diamond preservation.

The grade of group I kimberlites in the Barkly West and Welkom districts is low with respect to their geographically associated group II kimberlites. Leicester has an approximate grade of 8cts/100tonnes and Messina: 45-60cts/100tons (Gurney and Kirkley, 1996), while Samada has a grade of 10cts/100tonnes and Star: 40cts/100tonnes (Gurney and Kirkley, 1996). After correction for parcel resorbtion, the percentage increase in grade is greater for group I kimberlites than for the better preserved group II kimberlites. Even with this correction, the initial grade is very different between geographically associated group I and group II kimberlites. This may be explained by an extremely heterogeneous mantle lithosphere with respect to diamond content, but this is unlikely given that diamonds from the group I kimberlites in this study are consistently less preserved than diamonds from the group II kimberlite. An alternative is that the lithosphere was reasonably homogeneous with respect to diamond content and some process has destroyed a significant proportion of diamonds that were resident in the lithosphere at the time of eruption of the group II kimberlites. This would have occurred within a time interval of 25 to 30 Myrs. This is either attributable to changing conditions within the subcontinental lithosphere, or due to a group I kimberlite magma which was dramatically more corrosive than the group II magma. The Mir

kimberlite on the Siberian craton, however, is a group I kimberlite with a well preserved diamond population (table 3.5), which suggests that high corrosive capability is not an inherent characteristic of group I kimberlites.

Poorly constrained preservation indexes calculated from data from other studies of diamond parcels from southern African localities (table 3.5), show that nearly all the reported parcels, except Loxtonsdal, appear to be poorly preserved. Both group I and group II kimberlites from a range of different ages are represented, although many are younger than 100 Myr. Further work is necessary, in order to confirm whether the relationship between preservation and age displayed by kimberlites from the Barkly West and Welkom areas is reflected by other kimberlites in southern Africa. Although, an effort has been made to choose a preservation index which is compatible with data from the literature, it is clear that there is insufficient consistency in data from the literature and the use, in most cases, of a single size category has resulted in poorly preserved indexes for all localities.

Destruction of diamonds in the continental lithosphere in the 25 Myr period between eruption of the group I and group II kimberlites, in the Barkly West and Welkom districts, may have been caused by the widespread infiltration of metasomatic fluids derived from the group II kimberlites (Sweeney et al, 1993; Konzett et al, in press.), or the migration of megacryst magmas (Moore, 1986; Wyatt, 1989) and associated metasomatic fluids (Kinny and Dawson, 1992) into the lithosphere just prior to the eruption of the group I kimberlites. Therefore, corrosive fluids derived from magmatic activity at the base of the subcontinental lithosphere (eg Wyatt, 1989), which penetrate the diamond bearing lithosphere may resorb diamonds. This combined with evidence to support the resorbtion of diamond in the kimberlite magma (Robinson, 1979) provides ample opportunity for the significant destruction of diamonds, observed in the younger group I kimberlites.

...ooOoo...

CHAPTER 4

COMPOSITIONS OF ILMENITES FROM KIMBERLITE

Trends, Stoichiometric Behaviour and Paragenesis

5300 electron microprobe analyses of ilmenites from kimberlite have been evaluated and trends identified. Cation plots are used to corroborate the theoretical stoichiometric behaviour of kimberlitic ilmenite. Ilmenites from different parageneses are considered and an attempt made to separate parageneses using major element compositions. New trends are discussed, particularly with respect to Fe_2O_3:FeO ratios and inferred oxidation state.

4.1 INTRODUCTION

Ilmenite is an abundant accessory phase in most group I kimberlites in southern Africa and due to its distinctive composition it is useful in locating new kimberlite occurrences. The composition of ilmenite is controlled by conditions in the crystallising liquid, post-crystallisation reactions and external conditions of temperature, pressure and oxygen fugacity (Haggerty and Tompkins, 1984). As a result, ilmenite compositions reflect environmental conditions during crystallisation, during residence in the mantle, in the kimberlite magma and during metasomatism. The Fe^{3+}/Fe^{2+} ratio in particular is used to determine oxygen fugacity (fO_2) conditions in the upper mantle (Moats, 1989; Haggerty and Tompkins, 1983). The study of ilmenites from kimberlites, however, is hampered by non-stoichiometry (Haggerty 1991), and a number of different ilmenite parageneses. Consequently a knowledge of the crystallographic and stoichiometric behaviour and compositional tendencies in ilmenites is essential.

4.1.1 CRYSTALLOGRAPHY, STOICHIOMETRY AND COMPOSITION

Ilmenite ($FeTiO_3$) belongs to the rhombohedral crystal system, and has a structure similar to that of hematite in which the cations are distributed in [0001] crystallographic planes. The unit cell comprises six repetitions of these crystallographic planes. In ilmenite, however, Fe^{2+} and Ti^{4+}

occupy the cation sites rather than Fe^{3+}, resulting in non-equivalent cation sites across the structure, and reducing the symmetry from R3C (hematite) to R3. Variations in the electric and atomic structure of ilmenite crystals therefore have a fundamental effect on the physical properties and chemical reactivity of the mineral (Waychunas, 1991). These include properties such as conductivity, magnetism and elemental substitution. In order to conserve charge and atomic radii throughout the structure, the Fe^{2+} and Ti^{4+} cations are paired vertically between layers throughout the structure, with every layer containing at least one unoccupied site. Substitution into the structure, can either be simple (eg. $Fe^{2+} \leftrightarrows Mg^{2+}$), or coupled (eg. $Fe^{2+}+Ti^{4+} \leftrightarrows 2Fe^{3+}$). In order to accommodate charge-coupled substitutions the charge and size of the substituting cations must be balanced across the structure, either statistically throughout the crystal or locally (Waychunas, 1991).

A stoichiometricaly balanced ilmenite contains two cations for every three oxygens, but non-ideal cation/oxygen ratios can occur due to the filling of usually unoccupied sites in the crystal structure. This may be caused by extraneous physical factors such as temperature, pressure and fO_2 (Ghiorso and Sack, 1991). These, and other forms of crystal defects, cause non-stoichiometry, which may result in non-standard cation abundances.

The compositions of upper-mantle derived (UMD) ilmenite reflects the ultramafic source rocks from which it was derived (Haggerty, 1991). It contains moderate to high MgO, variable, but often high Cr_2O_3 contents with respect to most crustal derived ilmenites, and is generally reduced, but can also contain high Fe_2O_3, indicative of oxidising conditions.

A number of solid solutions between ideal end-member compositions reflect the range in compositions observed in UMD ilmenite. Some of these include: ilmenite-geikielite *($MgTiO_3$)*, ilmenite-hematite *(Fe_2O_3)* and ilm-pyrophanite *($MnTiO_3$)*. Cr and Al, other common constituents of UMD ilmenite, only exist in minor concentrations and therefore do not attain end-member compositions (Haggerty, 1976). The phase diagram for the system *FeO-TiO_2-Fe_2O_3* at 1300°C (figure 4.1(a): Lindsley, 1976 after Taylor, 1964) at 1atm total pressure and under different partial pressures of oxygen, exhibits a number of these solid solutions. The *FeO-TiO_2* join includes the minerals ulvöspinel (Usp), ilmenite (Ilm) and ferropseudobrookite (Fpb). Pure end member Ferropsuedobrookite is unstable at temperatures below approximately 1140°C, and breaks down to ilm-rutile. Pure end-member pseudobrookite, part of the *Fe_2O_3-TiO_2* join, is unstable at temperatures below 585°C, breaking down to rutile and hematite (Lindsley, 1965). The

orthorhombic (Fpb-Psb), rhombic (Ilm-Hem) and the Cubic (Usp-Mt) solid solutions are complete at high temperatures. The instability of ferropseudobrookite and pseudobrookite obviously affects the nature of the Fpb-Psb solid solution at lower temperatures with solid solution occurring between the break-down components rather than Fpb and Psb. Both the Ilm-Hem and Usp-Mt solid solutions are interrupted by immiscibility gaps at temperatures below about 640°C (Haggerty, 1991a) and 600°C (Lindsley, 1965) respectively, which results in exsolution textures under equilibrium conditions. Oxygen fugacity increases from left to right in the diagram as the phases lose FeO and gain Fe_2O_3 (Lindsley, 1991). Oxygen fugacity is also affected by temperature and composition. Figure 4.1b (Lindsley, 1976) shows that a decrease in temperature is accompanied by a decrease in fO_2 and that the gradient of the Hem-Ilm contours decreases with increasing Hem mol%. This supports the observation that the hematite content of UMD ilmenites increases with increasing fO_2 at a given temperature. Furthermore this increase in hematite content will be proportionately greater at lower temperatures than at higher temperatures.

Two other solid solutions which are important to UMD ilmenite, are $FeTiO_3$-$MgTiO_3$ and $FeTiO_3$-$MnTiO_3$. These are represented in the ternary diagrams figure 4.1(c) (Woerman, 1969 in Haggerty, 1991) and figure 4.1(d) (Haggerty, 1991). In both diagrams the base of the ternary reflects the substitution of Mg^{2+} for Fe^{2+}. In figure 4.1(c) the vertical axis (Fe_2O_3) represents conditions of increasing oxidation, which is evident by the increase in the value of the fO_2 isobars towards Fe_2O_3. The manganese content of UMD ilmenite from kimberlite is usually low and is mainly subject to the availability of manganese in the crystallising liquid.

Interaction of ilmenite with the kimberlitic magma can result in the exchange of CaO for FeO forming rims of perovskite($CaTiO_3$) by the reaction $(Mg,Fe)TiO_3+CaCO_3 \rightarrow CaTiO_{3(perovskite)}+(Mg,Fe)Fe_2O_4+CO_2$ (Frick, 1973). Many other minor and trace elements commonly encountered in the ilmenite structure have not been mentioned above, including: Nb, Zr, Ta, Co and Ni (Mitchell, 1977; Moore et al, 1992)

4.1.2 ILMENITE PARAGENESIS

Ilmenite recovered from rocks of kimberlitic affinity can either be of xenocrystic origin or paragenetically related to the kimberlitic magma. In both instances there are different ilmenite populations derived from different conditions of crystallisation, post-crystallisation reaction and secondary alteration. Ilmenite can be divided into paragenetic groups based on whether the primary

environment in which the ilmenite crystallised was xenocrystic or autolithic with respect to the kimberlite, and further subdivided by post-crystallisation reactions in response to changing conditions.

Ilmenite parageneses which can be ascribed to a ***Xenocrystic*** origin include:

i) Ilmenite in coarse peridotite xenoliths (Sobolev, 1977).
ii) Ilmenite in mantle eclogite xenoliths (Tompkins, 1983; Tollo, 1982).
iii) Rare ilmenite diamond inclusions (Meyer and Svisero, 1975; Chinn, 1995).
iv) Ilmenite from granulites and other crustal fragments (Nixon and Boyd, 1973; Sutherland et al, 1983)
v) Discrete ilmenite nodules of variable size (0.5-15cm), rounded, and belonging to the megacryst suite of minerals (Wagner, 1914; Jakob, 1977; Moore, 1986; Moore et al, 1992).
vi) Ilmenite intergrown with megacrystic silicates (Gurney et al, 1973; Frick, 1973; Jacob, 1977, Harte and Gurney, 1981; Moore et al, 1992).
vii) Ilmenite of metasomatic origin in peridotitic harzburgites, lherzolites, websterites, dunites, pyroxenites and polymict peridotites (Harte and Gurney, 1975; Erlank et al, 1985; Shee, 1985; Wyatt and Lawless, 1984).
viii) Ilmenite intergrown with diopsides and phlogopites of the Granny Smith suite of nodules (Boyd et. al., 1984).
ix) Ilmenite intergrown with silicates belonging to the MARID and glimmerite suites (Smith and Dawson, 1975; Erlank et al, 1985; Waters, 1987).
x) Ilmenite in high pressure deformed peridotites (Hops, 1989; Hops et al, 1986).

Kimberlite Magma ilmenite parageneses include:

i) Primary groundmass ilmenite (Haggerty, 1975; Shee, 1985; Wyatt et al, 1995)
ii) Rims and along fractures in ilmenite macrocrysts (Mitchell, 1973, 1977; Haggerty, 1973; Pasteris, 1980; Agee et al, 1982; Garanin, 1978)
iii) As phenocrysts in the kimberlitic magma (Pasteris, 1989; Shee, 1985)
iv) As inclusions in euhedral olivine crystals (Pasteris, 1980; Shee, 1985)

Other ilmenite parageneses:

i) Subsolidus reactions in which ilmenite exsolves from a host mineral eg. titanomagnetite (Haggerty, 1975)
ii) Ilmenite, which has undergone post-crystallisation reaction.
iii) Ilmenite intergrown with diamond (Sobolev, 1977).
iv) Secondary alteration products due to near surface weathering (Wyatt et al, 1979).

4.1.2.1 Xenocrystic Ilmenite Parageneses

Xenocrystic ilmenite is derived from stratigraphic levels between the source of the kimberlite and the surface, and is sampled by the rising kimberlitic magma. It occurs as rare primary accessory constituents of subcontinental lithospheric peridotites and eclogites, as a result of metasomatism and as a member of the megacryst suite of minerals. In addition, crustal granulites, basement, and country-rock may also contribute variable quantities of ilmenite with compositions representative of that source. Paragenetic identification is relatively straight forward, while the ilmenite is still associated with the rock of origin, however, identification becomes difficult once the host xenolith has disaggregated.

Ilmenite bearing peridotite and eclogite xenoliths have rarely been reported, and ilmenite inclusions in diamonds are even more unusual. Metasomatic infiltration and diffusion can result in the introduction of ilmenite (and other metasomatic minerals) into existing mantle rocks, altering their compositions. Metasomatic fluids are derived from magmatic events and occur under a wide variety of P, T and fO_2 regimes (Erlank et. al., 1987). Metasomatised peridotite, the most common source of metasomatic ilmenite, contains metasomatic minerals disseminated throughout a matrix of deformed and recrystallised nodules or as veinlets (Gurney and Harte, 1980). Further sources include: MARID xenoliths, which have crystallised from a relatively oxidising magma (Dawson and Smith, 1977), and calcic diopside "Granny Smith" megacrysts with frequent lenticules of ilmenite, deformation textures and with similar compositions to MARIDs (Boyd et al, 1984). Polymict peridotites (Lawless et al, 1977), breccias of primary mantle material cemented by metasomatic minerals, and high temperature deformed peridotites (Hops et al, 1986) provide evidence of pervasive and sometimes disruptive fluid migration, the latter associated with the passage of Cr-poor megacryst magmas (Gurney and Harte, 1980; Hops et al, 1986; Hops,

1989).

The Cr-poor megacryst suite is found in most group I kimberlites in southern Africa (Smith, 1984) and includes ilmenite as discrete ovoid nodules or intergrown with clinopyroxene, orthopyroxene, garnet, zircon, Fe-rich olivine and phlogopite (Moore et al, 1992). Eggler et. al. (1979) has described 2 separate suites of megacryst minerals: The Cr-poor suite (olivine, orthopyroxene, clinopyroxene and ilmenite), contains high TiO_2 and lower and more variable Mg#. The Cr-rich suite (olivine, orthopyroxene, clinopyroxene and garnet) is comparable to the "Granny Smith" suite.

The Cr-poor megacryst assemblages define a magma fractionation trend commencing at 1400°C (Gurney et al, 1979) with ilmenite joining the crystallising sequence at a temperature of about 1150°C (Lindsley and Dixon, 1976). The Cr-poor megacryst suite has been argued as originating as phenocrysts in the kimberlitic magma or alternatively as a megacryst magma body. Proponents of the phenocryst source (Mitchell, 1973, 1977; Eggler and Wendlandt 1979; Garrison and Taylor, 1980) advocate crystallisation in a kimberlitic magma chamber, crystal settling and the formation of a cumulate layer which is then subjected to shear forces and reincorporated into the magma during eruption. Haggerty and Boyd (1975), Gurney et al (1979) and Wyllie (1989), have suggested that megacryst magmas are proto-kimberlitic magmas and that megacrysts are phenocrysts in the proto-kimberlite. In contrast, Boyd and Nixon (1973) and Pasteris et al (1979) proposed a xenocrystic origin for megacryst suite minerals, crystallising from a separate megacryst magma of intricate form and limited vertical extent (Harte and Gurney, 1981) which cooled rapidly during eruption and was entrained by the kimberlite within hours of crystallisation (McCallister and Noord, 1981).

Trace element and REE patterns of clinopyroxene megacrysts, are suggestive of a magma with a composition similar to basanite (Harte, 1983; Jones, 1987). Wyllie (1987) has suggested that the "change in rheology at the lithosphere-asthenosphere boundary is sufficient to stall mantle plumes or diapirs with the formation of magma chambers and the transition from a mechanism of diapiric uprise to crack propagation." Any asthenosphere derived megacryst magmas intruding the subcontinental lithosphere will cause crack propagation, deformation and metasomatism (Harte and Gurney, 1975; Wyllie, 1989)

4.1.2.2 Kimberlite Magma Ilmenite Parageneses

Ilmenite parageneses which crystallise directly from the kimberlitic magma can be phenocrystic, or late crystallising groundmass ilmenite. Groundmass ilmenite is usually small (<0.3mm; Shee, 1985; 0.02-0.05mm; Dawson, 1980) and has been reported to contain high MgO and Cr_2O_3, average MnO and low FeO and Fe_2O_3 relative to megacryst ilmenite (Shee, 1985; Wyatt et al, 1995; McCallum, 1989). Ilmenite, with similar composition, often forms rims around ilmenite macrocrysts (Mitchell, 1977; Haggerty, 1991; Pasteris, 1980; Wyatt et al, 1995). Phenocryst ilmenite is represented by ilmenite inclusions in olivine phenocrysts (Pasteris, 1980; Shee, 1985) and phenocryst ilmenite macrocrysts (Wyatt et al, 1995).

4.1.2.3 Other Parageneses

Ilmenites undergo post-crystallisation, subsolidus reduction and oxidation reactions as a response to changing conditions of P,T and fO_2 (Haggerty, 1975). The compositions of these ilmenites are unlikely to reflect primary compositions during crystallisation and will therefore have lost their primary paragenetic signature, adopting a new secondary one. Ilmenite intergrown with diamond (Sobolev, 1977) and epigenetic ilmenite diamond inclusions may reflect a paragenesis removed from that in which the diamond originally crystallised. Finally, Wyatt et al (1979) have reported the replacement of MgO with MnO in ilmenites from the Premier mine as a result of groundwater alteration.

Group I diamondiferous kimberlites in Southern Africa are usually abundant in ilmenite macrocrysts. The ilmenite macrocryst population in these kimberlites is predominantly derived from disaggregated ilmenite megacrysts (Gurney and Moore, 1991), and consequently, other ilmenite parageneses are heavily diluted. Since the use of ilmenite as an indicator of diamond preservation is only applicable to group I kimberlites, it stands to reason that the majority of ilmenite macrocrysts recovered from exploration samples are likely to be megacrystic in paragenesis. Furthermore, the medium to large size categories of ilmenite commonly used in exploration programs, usually excludes any significant contribution from the kimberlitic groundmass ilmenite paragenesis, which, if present, normally resides in the smallest size categories.

Even though the assumption that most kimberlitic derived ilmenite macrocrysts are megacrystic

holds true under most conditions, it is nevertheless still beneficial to attempt to identify and distinguish between the different parageneses of ilmenite, using compositional criteria. In this chapter, the stoichiometric behaviour of megacrystic ilmenite is assessed and major element compositions of ilmenites from different parageneses compared. The data has been derived from the Kimberlite Research Group database at the University of Cape Town. This database has been compiled from analyses reported in the literature, unpublished theses and from unpublished probe data.

4.2 GRAPHICAL REPRESENTATION OF MAJOR ELEMENT CATION SUBSTITUTIONS IN MANTLE DERIVED ILMENITES.

The following section evaluates major element cation substitutions. In ilmenite, major element trends are dominated by the substitutions of 7 major cations, as discussed in section 4.1.1. In figure 4.2 (a-d) common divalent and trivalent cations are plotted against Ti^{4+} for 920 ilmenite megacrysts from the Kimberlite Research Group database. This has been done to test the common substitutional criteria used to calculate ferric iron calculations for electron microprobe data in the absence of analysed oxygen concentrations. Figure 4.2 (e-f) includes cation data from four kimberlites, all of which have been used to define a diamond preservation curve in the following chapter and have been selected by virtue of the fact that they each represent differing degrees of diamond preservation.

The graph of trivalent Fe^{3+} plotted against tetravalent Ti^{4+} (Figure 4.2(a)) exhibits a negative correlation between Fe^{3+} and Ti^{4+} with a gradient of -1.85. This is close to the expected stoichiometric correlation where two Fe^{3+} cations should substitute for a single Fe^{2+} and Ti^{4+} couple (gradient -2). Even though the correlation is good, the data is slightly diffuse and defines a trend which is slightly deficient in trivalent cations, particularly at low values of trivalent cations. The divalent cations, Fe^{2+} and Mg^{2+}, exhibit a positive correlation (0.95) when plotted against Ti^{4+}(figure 4.2(b)). 15 analyses plot away from the general trend, and are deficient in divalent cations with respect to Ti^{4+}.

The shortage of both divalent and trivalent cations with respect to Ti^{4+} has been addressed by including Al, Cr and Mn, while assuming that Cr and Al are present in the trivalent state and that

Mn is present in the divalent state. The revised plots (figure 4.2(c-d) demonstrate the resulting improved correlations, with the exception of the most Ti^{4+} rich analysis (Farmington meteorite), which may either contain divalent Cr, or may include other divalent cations not included in the analysis, and not usually present in significant quantities in megacrystic ilmenites.

Analyses of ilmenite from four different kimberlites have been plotted in figure 4.2(e,f). The four localities (Tshibua, Premier, Palmietfontein and Iron Mountain) have been chosen on the basis of the diamond preservation exhibited at each locality and display a range in Cr_2O_3 and MgO contents in their ilmenites. Tshibua ilmenites exhibit relatively high Cr_2O_3 and MgO and Iron Mountain ilmenites, intermediate Cr_2O_3 and low MgO. The remaining localities both have low to intermediate Cr_2O_3 and intermediate MgO. Together these localities define a parabolic curve with respect to Cr_2O_3 and MgO (figure 5.1(c)), similar to that described by Haggerty (1975). Variations in Cr_2O_3, however, are not well understood although Moore et al (1992) have suggested that the compositional variation on the high MgO limb is consistent with trends to be expected from differentiation of a megacryst magma and the compositions on the low MgO limb are in accordance with the introduction of Cr_2O_3 from wallrock assimilation or magma mixing.

Figure 4.2(e) reveals two different trends, both negative correlations, of Cr^{3+} with respect to Ti^{4+}. The steeper (Tshibua) trend has a gradient of -1.36 (see insert). The addition of Fe^{3+} and Al^{3+} to Cr^{3+} results in the required gradient of -2 for trivalent cations vs Ti^{4+}. Effectively, the relationship between trivalent cations and Ti^{4+} can therefore be expressed as $1-0.5(Fe^{3+}+Cr^{3+}+Al^{3+})=Ti^{4+}$; and consequently, a decrease in Ti^{4+} accompanied by a severe increase in Cr^{3+} must result in a relative decrease in $(Fe^{3+}+Al^{3+})$. If the assumption is made that Al^{3+} is present in insignificant concentrations, decreasing Cr^{3+} and increasing Ti^{4+} would be accompanied by an increase in Fe^{3+}/Fe^{2+} which indicates an increase in oxidation state. The shallower trend (Iron Mountain) indicates conditions where either Cr^{3+} was less available, or the environment favoured other trivalent cations, eg. Fe^{3+}. The steeper trend intersects the x-axis at $Ti^{4+}\approx 0.94$, whilst the shallower trend intersects at $Ti^{4+}\approx 1$. For the steeper trend, Fe^{3+} is present throughout the range in Cr^{3+} values (figure 4.2(f)) and increases very slightly with increasing Cr^{3+} up to $Cr^{3+}=0.07$ and then decreases with increasing Cr^{3+} thereafter. This suggests that the absence of Fe^{3+} from the y-axis has resulted a Ti^{4+} intercept of 0.94 instead of 1 in figure 4.2(e). Ilmenites from the shallow trend show a positive correlation between Fe^{3+} and Cr^{3+} and hence the Ti^{4+} intercept for these ilmenites in figure 4.2(e) is 1.

The stoichiometric validity of megacrystic ilmenite has been assumed, in the absence of oxygen analyses, and is supported by correlations between commonly substituted cations. The assumptions are based on the valency states of the most common cations found in megacrystic ilmenite. Al^{3+} and Mn^{2+} are usually only present in low concentrations and always in their respective 3+ and 2+ valence states. Cr is most commonly found in the trivalent state, particularly in ilmenites where the presence of Fe^{3+} indicates varying degrees of oxidation, and Mg is only present in the Mg^{2+} state.

4.3 COMPOSITIONS OF ILMENITES FROM DIFFERENT PARAGENESES

Ilmenite compositions are affected by conditions at the time of crystallisation and sometimes may be modified by subsequent re-equilibration and alteration. Although ilmenite macrocryst suites at most localities are dominated by ilmenites of megacrystic paragenesis (Wagner, 1914; Gurney and Zweistra, 1995), specific localities can deviate from this rule with significant contributions from groundmass parageneses (eg. Cleve Kimberlite; Wyatt et al, 1995 and Wesselton; Shee, 1985). It is important to attempt to separate ilmenite parageneses.

It has been mentioned before that calculation of Fe_2O_3 from electron microprobe analyses of major oxides in ilmenite is acceptable for UMD megacrystic ilmenites. This calculation is contingent however on the quality of the analysis and the stoichiometric validity of the ilmenite. The stoichiometry of megacrystic ilmenite has already been ratified, but ilmenites from other parageneses, particularly ilmenites introduced or affected by metasomatic infiltration or diffusion, have not and may be subject to conditions of non-stoichiometry. Furthermore, when dealing with ilmenites recovered from large databases, as in this study, or with an unknown batch of ilmenites from an exploration sample, it is essential to authenticate ilmenite analyses.

The system FeO-TiO_2-Fe_2O_3 (figure 4.1a) includes a number of oxide minerals commonly found in association with or exsolved in ilmenite. An adjustment has been made to the diagram to include all divalent and trivalent cations commonly substituted in ilmenite (figure 4.2), therefore altering the system to $(Fe,Mg,Mn)O_3$-TiO_2-$(Fe,Al,Cr)_2O_3$ with ilmenite representing a combination of pure ilmenite, geikielite and pyrophanite, and ferropseudobrookite a combination of pure ferropseudobrookite and Karooite ($MgTi_2O_5$) etc. Under the assumption mentioned in the previous

section that all excess cations are attributable to Fe^{3+}, any reasonable ilmenite analysis should plot on the ilmenite-hematite solid solution and that under these constraints, any deviation from this would suggest that the analysis may not be an ilmenite, includes a component of another mineral, or is possibly non-stoichiometric. It should be noted, however, due to constraints in the allocation of end-member compositions, that rare instances may occur where non-ilmenites can plot along the ilmenite-hematite join.

Analyses of megacrystic, groundmass, peridotitic, eclogitic and metasomatic ilmenite and ilmenite inclusions in diamond and olivine from the kimberlite research group database have been verified using the above system (figure 4.3 a-f). The majority of analyses plot along the ilmenite-hematite solid solution join, with ilmenite from the megacrystic suite exhibiting the greatest range in hematite and the most oxidised compositions. Two analyses in both the peridotitic and metasomatic suites plot below the ilm-hem_{ss} suggesting a component of ulvöspinel in the analyses. This may be due to the microprobe spot overlapping with a small spinel exsolution. Likewise, 2 metasomatic ilmenites plot above the ilm-hem_{ss} possibly suggesting an influence of rutile, or in the case of samples quenched at high temperatures, ferropseudobrookite. Deviations from the ilm-hem_{ss} occur for reduced compositions along the TiO_2-Fe(Mg,Mn)O join in figures 4.3(a & c) in the direction of TiO_2. In figure 4.3(a) the high TiO_2 analysis is from the Farmington meteorite and was mentioned in the previous section. The same argument may be applied to the deviant metasomatic ilmenite. Figure 4.3 shows that nearly all analyses used for the purposes of this study plot along the ilmenite-hematite join, which conforms to the criteria defining an ilmenite, supports the assumptions used in the calculation of Fe_2O_3 , and consequently justifies the use of Fe_2O_3 as a discriminatory tool.

4.3.1 MEGACRYSTIC ILMENITE

920 megacrystic ilmenite analyses from kimberlites in southern, central and west Africa are plotted in figure 4.4(a-f). Plots of TiO_2 and Fe_2O_3 vs MgO (figures 4.4a,b) as well as Fe_2O_3 vs TiO_2 (figure 4.4c) exhibit possible trends, as marked. TiO_2 decreases with MgO, defining a gentle curve which steepens as MgO decreases. The scattered points above the trend contain analyses from Koidu and Liberia, whilst analyses on the trend with TiO_2<38wt% are exclusively from Koidu. Fe_2O_3 increases with decreasing MgO following a hyperbolic curve, with the scatter of points below the curve corresponding to analyses of ilmenites from west Africa. Analyses define a straight line when Fe_2O_3 is plotted against TiO_2, and once again data falling outside of the trend is mostly from West Africa with a few analyses from

Monastery.

In the plot of Cr_2O_3 vs MgO the parabolic relationship defined by Haggerty (1975) is not clear. Ilmenite analyses from Jagersfontein, Bultfontein, Klipfontein, Kamfersdam, Monastery, Leicester and Koidu (MgO rich limb) and Koidu (MgO poor limb) do conform to the parabolic relationship. The two pronounced concentrations are due to 2 populations of ilmenite from Monastery, as identified by Moore (1986) on the basis of Cr_2O_3 content. The Kimberlite Research Group database, used here, is dominated by analyses of ilmenites from Monastery, which contrives to obscure any parabolic or other trend which may be present. High MgO, low Cr_2O_3 ilmenites to the right of the trend mainly include analyses from Liberia, and a few from Frank Smith and Monastery. Analyses plotting above the parabolic trend (ie. Cr_2O_3>1.5wt% and 5%<MgO<12%) mainly include ilmenites from Koidu, but also some from Kalkput, Jagtfontein, Liberia, Leicester, Nouzees, Frank Smith and Monastery.

Megacryst ilmenites appear to cluster around a mean MnO of 0.24wt% and MgO of 11wt% in figure 4.4(e). The majority of megacryst analyses plot between 50 and 60mol% ilmenite, 8-17mol% hematite and 25-60mol% geikielite on the Ilm-Hem-Geik ternary, extending towards geikielite, with analyses from Jagersfontein, Bultfontein and one from De Beers at geikielite values >55mol% (figure 4.4f). A high ilmenite, high hematite cluster exists containing analyses exclusively from Koidu, whilst analyses plotting at Hem<20mol% and Ilm>65mol% are exclusively from west Africa. A number of analyses, especially from Monastery plot within the ternary solvus or decomposition loop described by Haggerty (1991).

4.3.2 KIMBERLITIC MAGMA DERIVED ILMENITE

141 analyses of ilmenite from southern, central and west Africa, believed to have crystallised from kimberlite magma are plotted in figure 4.5(a-f). The plots of TiO_2 and Fe_2O_3 vs MgO and Fe_2O_3 vs TiO_2 exhibit well defined trends. Two discernable populations of ilmenite are evident in the plot of TiO_2 vs MgO (figure 4.5a). The first is a trend in which TiO_2 decreases as MgO decreases, defining a gentle curve which steepens as MgO decreases. This trend corresponds to that displayed by the megacryst data. A separate population occurs at low MgO (<5wt%) and intermediate TiO_2 (47-53wt%) and consists of ilmenites from De Beers(2), East Griqualand(1), Koidu(34), Premier(8) and Wesselton(3). The majority of ilmenites with values of MgO>15wt% are from Wesselton and were used by Shee (1985)

to define the field for groundmass ilmenite from this locality. Many of these analyses plot in the extension of the "megacryst" trend and the remainder, with the exception of 6 analyses, define a separate field with very high MgO (20-25wt%). Most groundmass ilmenite contains low Fe_2O_3 (<10wt%; figure 4.5b) and those with greater than 10wt% are either outliers or correspond to a trend similar to the equivalent megacryst trend, but broadening at lower Fe_2O_3. The population of ilmenite with Fe_2O_3<10wt% and MgO<5wt% corresponds to the low MgO population in 4.5(a), and the high MgO Wesselton population from figure 4.5(a) forms a separate cluster. Ilmenite analyses with low Fe_2O_3 contain high concentrations of TiO_2 (figure 4.5c), and three subparallel trends can be distinguished, agreeing with separations in previous plots. The linear trend which extends to high values of Fe_2O_3 corresponds almost exactly to the equivalent megacryst trend. In figure 4.5(d) the high MgO and low MgO populations can be distinguished. A possible third cluster may exist around 15wt% MgO, although overall, distribution of ilmenite analyses with respect to Cr_2O_3 and MgO is fairly scattered. A hyperbolic relationship exists between MnO and MgO, with MnO contents reaching 20.4wt% at the expense of MgO (figure 4.5e). Groupings are strongly governed by locality, with the highest MnO grouping only containing analyses of ilmenites from the Premier kimberlite. High MgO ilmenites have MnO<1wt%, and the inserted graph contains MnO vs MgO for all analyses where MnO<2wt%. Three populations are identified: firstly is a high MnO (1-2wt%), low MgO vertical trend, secondly a trend of decreasing MnO with decreasing MgO for ilmenites where MgO >13%, and a third potential population between 5 and 10wt% MgO and <0.5wt% MnO. In the Ilm-Geik-Hem ternary (figure 4.5f), three distinct populations are identified. the first is a low MgO population which plots close to ilmenite. The second defines a range in compositions characterised by a decrease in the geikielite component and an increase in the Fe_2O_3 component, with a concentration of analyses at the high geikielite end, and the third population has a high geikielite component and includes the high MgO Wesselton ilmenite population.

4.3.3 ECLOGITIC ILMENITES

11 ilmenite grains in eclogite xenoliths from worldwide kimberlite occurrences have been plotted in figure 4.6(a-e). Eclogitic ilmenite compositions are tightly constrained with respect to Cr_2O_3, MgO and TiO_2 (figure 4.6a,d), with Cr_2O_3<0.2wt%, MgO from 8 to 12wt% and TiO_2 from 52 to 56wt%, and they define a range in Fe_2O_3 from 0 to 12.5wt% (figure

4.6b). Although a small dataset, analyses can be divided into two groups on the basis of TiO_2, with the divide at approximately 54.5wt%. This separation is consistent in other plots. MnO ranges from 0.22 to 0.54wt% (figure 4.6e), with a mean of 0.36wt%, which is higher than that for megacrystic ilmenite (x=0.24wt%, excluding analyses where MnO >1 to avoid any influence of secondary alteration affects). A roughly linear correlation exists between Fe_2O_3 and TiO_2 (figure 4.6c). Eclogitic ilmenites form a well defined field on the Ilm-Hem-Geik ternary, plotting at Hem<15mol% and Ilm between 55 and 70mol%.

4.3.4 PERIDOTITIC ILMENITES

37 ilmenite analyses from peridotite xenoliths are presented. TiO_2 decreases with decreasing MgO (figure 4.7a) and fits a trend similar to megacrystic ilmenite. Three analyses plot above the trend, two from Jagersfontein (with high MnO and SiO_2) and one from Mir. The majority of the ilmenites plot with MgO contents ranging between 7 and 16wt% and Fe_2O_3 from 0 to 13wt%. One ilmenite from Kao has a very high Fe_2O_3 content (figure 4.7b). The linear correlation between Fe_2O_3 and TiO_2 mimics the megacryst trend, but extends down to very low Fe_2O_3 and high TiO_2 contents (figure 4.6c). Cr_2O_3 concentrations range from 0 to 6.5wt%, but the majority of analyses plot below 2.8wt% Cr_2O_3 (figure 4.7d). No obvious correlation exists between MnO and MgO (figure 4.7e), and the mean value for MnO is 0.26wt% (for analyses where MnO <1). Peridotitic ilmenites define a broad field on the Ilm-Hem-Geik ternary with values of hematite<15mol%, ilmenite from 25 to 70 mol% and geikielite from 30 to 70mol%.

4.3.5 DIAMOND INCLUSION ILMENITES

12 analyses of ilmenite in diamond have been obtained from worldwide occurrences. Where TiO_2 is plotted against MgO (figure 4.8a), three populations are identified: low MgO; MgO≈5wt% (George Creek), Chinn, 1985, and high MgO (10-15wt%). In figure 4.8(b) the same three populations are evident, with the lower MgO populations displaying low Fe_2O_3, whilst the high MgO inclusions define a differentiation trend of Fe_2O_3, increasing with decreasing MgO. Cr_2O_3 concentrations (figure 4.8d) are low for most inclusions, especially those with low MgO, but two of the high MgO population contain ≈2wt% Cr_2O_3. The three populations define two trends with respect to Fe_2O_3 in figure 4.8(c) (the two George Creek analyses are included with the low Fe_2O_3 trend). In figure 4.8(e), the low MgO population

can be differentiated from the intermediate and high MgO populations using MnO; the former having MnO contents between 0.6wt% and 0.8wt% and the latter defining a trend of decreasing MnO with decreasing MgO. The George Creek inclusions plot on the continuation of this high MgO inclusion trend. The low MgO population plots close to pure ilmenite on the Ilm-Hem-Geik ternary (figure 4.8f) and the high MgO population defines a trend between 45 and 55mol% ilmenite, 30-50mol% geikielite and 5-15mol% hematite. The two George Creek ilmenites plot at ≈80mol% Ilm and <5mol% Hem and are intermediate in composition between the low and higher geikielite populations.

4.3.6 METASOMATIC ILMENITE

Figure 4.9(a-f) utilises analyses of 42 ilmenites in xenolith samples, which display metasomatic characteristics, from worldwide occurrences (particularly from the Kimberley pool, RSA and Lesotho). The majority of these ilmenites plot between 10 and 16wt% MgO (figure 4.9a), have low Fe_2O_3 (2-7wt%), intermediate to high TiO_2 (51-57wt%; figure 4.9b), and low to intermediate MnO (0.2-0.65wt%; figure 4.9d). Seven metasomatic ilmenites from Wesselton (Shee, 1985) plot outside of these compositional ranges, five of which define a trend of increasing Fe_2O_3 with decreasing MgO, and the remaining two (ilmenites in metasomatised harzburgite) contain almost no Fe_2O_3 or MgO (figures 4.9d,e), but have MnO and Cr_2O_3 concentrations of ≈14wt% and 6-7wt% respectively. Ilmenites with different metasomatic origins are partially discriminated using Cr_2O_3 and MgO (figure 4.9d). Ilmenites from lherzolitic xenoliths plot in a restricted field with MgO contents between 11 and 14wt% and low Cr_2O_3 (0.5-1.5wt%). Two glimmerite analyses plot with slightly lower average MgO (10.5wt%) and higher Cr_2O_3 (1.5-2wt%). Harzburgitic and polymict peridotitic ilmenite analyses along with a few peridotitic ilmenites of unknown metasomatic affinity, plot as a vertical trend with constant MgO and variable Cr_2O_3. This trend appears to become more MgO rich at low concentrations of Cr_2O_3, while interestingly, all polymict peridotite analyses used in this study (Wyatt and Lawless, 1984) fall within a restricted range of MgO (14-15wt%). In the Ilm-Hem-Geik ternary, the two Wesselton low MgO harzburgitic ilmenites plot near pure ilmenite, which is misleading because both these analyses have significant pyrophanite and eskoliate components. The majority of metasomatic ilmenites, however define a restricted field with <10mol% Hem and between 40 and 60mol% Ilm. Four out of the five Wesselton ilmenites from the high Fe_2O_3 trend plot within the ternary solvus (1300°C, 1atm) defined by the assemblage Sp-Psb-Ilm.

4.3.7 ILMENITE INCLUSIONS IN OLIVINE PHENOCRYSTS

26 analyses of ilmenite inclusions in olivine phenocrysts from the Wesselton kimberlite have been plotted in figures 4.10(a-f). Most ilmenite inclusions contain intermediate to high TiO_2 (51.5-57.5wt%), high MgO (13.5-15.5wt%; figure 4.10a), low to intermediate Fe_2O_3 (<10wt%; figure 4.10b) and intermediate Cr_2O_3 (2-6wt%; figure 4.10d) and plot within a tightly constrained group. Three outliers exist, the first with TiO_2=52.5wt%, the second with MgO=19.9wt% contains elevated calculated Fe_2O_3 (17.79wt%; $Total_{(calculated)}$=107wt%), and the last with 49% TiO_2 and elevated Cr_2O_3 (8.26wt%). A trend of increasing Fe_2O_3 with decreasing TiO_2(figure 4.10c) and decreasing MnO with decreasing MgO (figure 4.10e), is discernable. One analysis contains 0.21wt% MnO and 15.86wt% MgO and plots off the trend, but is however an unusual sample containing 0.21wt% SiO_2. The Wesselton ilmenite olivine inclusions plot in a restricted field in the Ilm-Hem-Geik ternary with hematite<10mol% and ilmenite plotting between 30 and 50mol%.

Plots of megacrystic ilmenites (figure 4.4) support fractionation trends with less differentiated ilmenites containing high MgO, high TiO_2 and low Fe_2O_3. Analyses tend to be scattered with respect to Cr_2O_3 and MgO and the parabolic relationship described by Haggerty (1975) is not immediately obvious using this data. Furthermore, the high Cr_2O_3 (>4wt%) and MgO limb of the parabola contains analyses of ilmenites from Jagersfontein, Bultfontein and Klipfontein, and these analyses plot within the trend described for metasomatic ilmenites (figure 4.9d). If high Cr_2O_3 "megacrystic" ilmenites from southern Africa are in fact metasomatic this makes the parabolic relationship even less obvious. The precision of the trends in figures 4.4(a-c) for southern African megacrysts is supported by the fact that nearly all analyses plotting outside of these trends are derived from west African localities. The fractionation trend is shown on the ilm-hem-geik ternary by a trend of decreasing geikielite and increasing hematite. The majority of analyses, however plot towards the hematite rich end of the trend, with many plotting within the spinel-pseudobrookite-ilmenite solvus under conditions slightly more oxidising than the less differentiated high geikielite compositions.

Ilmenites which have crystallised from the kimberlite magma are either of phenocrystic (crystallised slowly during the early stages of magma evolution) or groundmass (late stage crystallates in the kimberlite) origin. For the purposes of this discussion the term magmatic is used for these ilmenites unless specific paragenesis is implied.

In the plot of TiO_2 vs MgO (figure 4.11a), trends for magmatic and metasomatic ilmenites correspond closely to the trend for megacrystic ilmenites. The peridotitic trend follows the megacryst trend but is displaced towards slightly higher values of TiO_2. The larger of the three diamond inclusion fields plots halfway along this trend while ilmenites included in olivine phenocrysts (olivine inclusions) plot towards the higher MgO end of the trend. High TiO_2 eclogitic ilmenites plot above the megacryst trend while the low TiO_2 eclogitic ilmenites overlap with medium to high MgO ilmenites of the megacrystic and magmatic trends. George Creek eclogitic diamond inclusions plot separately while low-Mg diamond inclusions plot within the field defined by low-Mg magmatic ilmenites.

Magmatic ilmenites produce a trend on the Fe_2O_3 vs MgO plot (figure 4.11b) which tapers towards higher values of Fe_2O_3, but nevertheless falls mostly within the hyperbolic megacryst trend. Peridotitic ilmenites define a wide field which overlaps with the Fe_2O_3-poor end of the megacryst trend. The main diamond inclusion field, eclogitic field and metasomatic field (low Fe_2O_3) plots within the peridotitic field. The high Mg magmatic population plots just above the low Fe_2O_3 extension of the megacryst trend. Low MgO diamond inclusions once again plot within the field for low-Mg magmatic ilmenites, whilst the George Creek diamond inclusions plot at the edge of this field.

The relationship between Fe_2O_3 and TiO_2 in upper mantle derived ilmenites is represented in figure 4.11(c). The megacryst and main magmatic trends coincide while the peridotitic, eclogitic, main diamond inclusion and olivine inclusion fields plot within these trends and roughly define the same gradient. Although the metasomatic field plots within this trend, a line drawn through the data presented here defines a shallower gradient. All low MgO diamond inclusions plot within the low-Mg magmatic field which trends roughly parallel to the main trend, but with lower x and y intercepts. George Creek ilmenites define the extension of the low MgO diamond inclusion field towards low Fe_2O_3 and high TiO_2 and plot on the edge of the eclogitic trend. The high-Mg Wesselton groundmass field plots immediately above the main trend.

On the plot of Cr_2O_3 vs MgO (figure 4.11d), the magmatic ilmenites separate into three restricted fields, the second of which contains ilmenites from the main trend and overlaps with the high MgO limb of the megacryst parabola. Metasomatic ilmenites define a trend with overlaps the high-Mg limb of the parabola and extends to high levels of Cr_2O_3. Eclogitic and the main diamond inclusion field plot within the broad peridotite field which overlaps considerably with the majority of

megacrystic analyses. Very low Cr_2O_3 is an apparent characteristic of eclogitic ilmenites. The Low-Mg magmatic ilmenite field again includes the field for low-Mg diamond inclusions while George Creek inclusions plot on the edge. Except for the low and high-Mg magmatic ilmenites, the Cr_2O_3:MgO plot is not very useful for discriminating ilmenite parageneses especially since the largest concentration of analyses from each paragenesis are in roughly the same region of the plot.

MnO is a minor oxide in UMD ilmenites. It is sometimes concentrated in rims of macrocryst ilmenites and sometimes in groundmass ilmenites (Haggerty et al, 1979). In addition, MgO is believed to be replaced by MnO over long periods of time during alteration of ilmenites due to near surface weathering (Wyatt, 1979). Although most ilmenite parageneses overlap in the plot of MnO vs MgO (figure 4.11e) the well constrained megacryst field, the main magmatic trend and the field for olivine inclusions are interesting. Considering the vast number of analyses of megacrystic ilmenites the field is well constrained with the highest concentration of analyses plotting at the Mg-poor half of the field. Olivine inclusions define a trend of increasing MnO with MgO in figure 4.11(e), and overlap with the main magmatic trend. George Creek eclogitic diamond inclusions plot on the extension of the field for the main diamond inclusion trend indicating a possible relationship between the these two populations, rather than a relationship to the low MgO inclusion population as suggested by figure 4.11(c).

The ilmenite-hematite-geikielite ternary diagram (figure 4.12) reflects both fractionation (MgO vs FeO) and oxidation state (Fe_2O_3 vs FeO), however the positions of the fugacity isobars and the ternary solvus are only valid for temperatures of 1300°C and pressures of 1atm. This should be considered when interpreting trends. Analyses of ilmenites from the main diamond inclusion trend plot within the field for peridotitic ilmenite and overlap with the field for eclogitic ilmenites. The field for eclogitic ilmenites plots within the highest density region of the peridotitic trend, and hence cannot be distinguished using this plot. All metasomatic ilmenite analyses plot towards the high geikielite, low hematite end of the peridotite trend. The magmatic trend of increasing hematite with decreasing geikielite overlaps with the similar megacrystic trend. Wesselton olivine inclusions correspond to the high geikielite end of the magmatic trend, the end with the highest density of magmatic ilmenites. The highest density of megacrystic ilmenite analyses plot at the hematite rich end of the megacryst trend. High-Mg, Wesselton groundmass ilmenites define a separate field off the geikielite rich end of the magmatic trend while low-Mg magmatic ilmenites plot close to the ilmenite end-member and within the kimberlite reduction trend described by Haggerty et al (1979). A separate field containing ilmenite analyses from the Koidu kimberlite in west Africa has a high

hematite component and plots above the inflection of the ternary solvus.

4.4 OXYGEN FUGACITY - IMPLICATIONS FROM IHG TERNARY SYSTEM

Care should be taken when interpreting data with respect to oxidation. The oxygen fugacity isobars in figure 4.12 are strongly temperature and pressure dependent and have been experimentally estimated using a temperature of 1300°C and a pressure of 1atm (Woerman, 1969). This immediately constrains the fugacity isobars in this diagram to ilmenites which crystallised under these conditions. Furthermore, the ternary solvii retreat with decreasing temperature, disappearing at temperatures of approximately 700°C (Haggerty, 1991) and therefore, in the absence of textural information to the contrary, any ilmenite, plotting within this field, should have crystallised at lower temperatures. Different ilmenite parageneses crystallise at differing temperatures and pressures making the direct comparison of the fugacity of one population with that of another impossible. In addition, the temperature and pressure of crystallisation of ilmenites within one population can vary dramatically and hence any relationship of population trend to fugacity isobars in this plot must be interpreted carefully. It is known for example that the megacryst suite represents a fractionation trend which spans temperatures of approximately 450°C and a relatively small range in pressures (Gurney et al, 1979). An evolving megacryst magma, migrating through a process of crack propagation, essentially representing a closed system, may be expected to increase in oxygen fugacity. The field representing this megacryst trend in figure 4.12 barely changes fugacity at all which is unlikely considering the above argument. In contrast the field for high MgO groundmass ilmenites from Wesselton (Shee, 1985), which represents final crystallisation of a kimberlite magma traverses 3 fugacity log units. This is more likely to be a result of a sudden decrease in both temperature and pressure rather than a significant change in fO_2. It is concluded therefore, that the usefulness of the IHG ternary to imply oxygen fugacity of ilmenites, is limited and the only reliable method of determining fO_2 is by applying various oxybarometers to rare ilmenite - silicate assemblages. The direct determination and use of fO_2 for the purposes of predicting diamond preservation is therefore impractical.

4.5 DISCUSSION AND CONCLUSIONS

The distribution of Cr in megacrystic ilmenites exhibits two distinct trends. In the steeper trend, Fe^{3+} increases with decreasing Cr^{3+} at atomic proportions of Cr^{3+} above 0.06, consistent with crystallisation from an evolving magma. In the more shallow trend, however, Fe^{3+} increases as Cr^{3+} increases. This is consistent with Cr^{3+} being introduced as the magma continues to evolve, either due to magma mixing or magma reaction with the wallrock (Moore, 1992), and with conditions becoming more oxidising. The continuous nature of the Cr^{3+} distribution suggests that Cr^{3+} was introduced into the system continuously rather than sporadically supporting assimilation of country rock as the most likely source of Cr^{3+} .

Stoichiometric trends in UMD megacrystic ilmenites confirm that Mg^{2+} and Mn^{2+} commonly substitute for Fe^{2+} and that two trivalent cations substitute for a coupled pair of Fe^{2+} and Ti^{4+} producing a mineral formula resembling: $(Fe,Cr,Al)^{3+}_{2x}\ (Fe,Mg,Mn)^{2+}_{1-x}\ (Ti)^{4+}_{1-x}\ O_3$.

The majority of ilmenite analyses from parageneses other than the megacrystic suite, when plotted in the system (Fe,Mg,Mn)O-TiO_2-$(Fe,Al,Cr)_2O_3$, are well constrained and plot along the ilmenite-hematite solid solution with only a few exceptions.

Upper mantle derived ilmenites can be obtained from a diversity of different parageneses which can be primary, metasomatic, megacrystic or crystallised from the kimberlitic magma. While they are still in association with their host assemblage they are easily classified, however when xenoliths and xenocrysts are disaggregated the ilmenites are liberated and become part of the macrocryst suite. The objective therefore is to broadly classify ilmenites in the macrocryst suite on the basis of major element compositions to enable more reliable forcasting of diamond preservation. Ilmenite in peridotite and eclogite nodules and as diamond inclusions are rare and are therefore not expected to contribute significantly to the macrocryst ilmenite populations at any given locality. Metasomatised nodules, including: Metasomatised peridotites, polymict peridotites, Granny Smith megacrysts, marids and glimmerites, are rare inclusions in kimberlites, but can contain significant modal proportions of ilmenite, when present. The rarity of the samples implies that the contribution of metasomatic derived ilmenites to the macrocryst population is not significant, however this could also be a function of preferential disaggregation of metasomatised xenoliths. Under these circumstances, certain localities may have macrocryst populations with a significant proportion of

ilmenites contributed from the metasomatic suite. Groundmass ilmenites are common at many localities, but apart from compositional characteristics discussed later, usually report to the smallest size categories. Larger macrocryst grains (>1mm) found in group I kimberlites where ilmenite megacryst nodules are widespread (eg. Frank Smite, Monastery and Samada), are widely believed to have been derived from disaggregated megacryst nodules. Course kimberlitic groundmass, or phenocryst ilmenites have been reported by Wyatt et al (1995), in the macrocryst population from the Cleve kimberlite in southern Australia, but this appears to be the exception.

Ilmenites which have crystallised directly from the kimberlitic magma fall within three categories (figure 4.5). The low-Mg population is dominated by analyses of ilmenites from west Africa with an additional 8 ilmenites from Premier and 3 from Wesselton. These Premier ilmenites have very high MnO concentrations which suggests that they may have been subjected to secondary alteration (Wyatt, 1979) and may have contained significantly higher initial MgO values. These low-Mg compositions are not only restricted to west Africa, however as similar compositions have been reported for groundmass ilmenites from the Chicken Park kimberlite, USA (McCallum, 1989).

The high-Mg field consists of groundmass ilmenites from Wesselton (Shee, 1985). Evidence for the existence of this separate field is supported by apparent differences to the main trend with respect to major element relationships (figure 4.11a-d) and end-member compositions (figure 4.12). In contrast, these high-Mg ilmenites appear to plot on the high MgO extension of the main trend with respect to MnO and MgO, and would hence appear genetically related. Similar high-Mg compositions of ilmenite have been reported as rims on macrocryst ilmenites in kimberlite (Haggerty et al, 1979; Apter et al, 1984; Shee, 1985).

The main magmatic trend corresponds to the megacryst trend on most plots, with the exception that the highest density of analyses plot at the MgO rich end of the trend. Ilmenite inclusions in olivine phenocrysts coincide with the MgO rich end of the magmatic trend, and since olivine phenocrysts must represent an early crystallising phase in the kimberlite the main magmatic trend is probably a kimberlite phenocryst trend. Two scenarios can be presented to explain the data. The first is that the phenocryst trend commenced with the crystallisation of lower-Mg ilmenites, including ilmenite inclusions in olivine, and the MgO content increased with MnO and eventually culminated in the crystallisation of high-Mg, late-stage groundmass ilmenite in a process where Mg is scavenged in order to permit further crystallisation of ilmenite in a magma where the Fe^{2+}:Fe^{3+} ratio is decreasing due to an increasing oxidation state (Shee, 1985; Wyatt et al, 1995). This is supported by the trend

of MnO with respect to MgO (insert, figure 4.5e), but is undermined by incontinuity between the high-Mg groundmass field and the phenocryst trend when plotted on the Cr_2O_3 vs MgO and ilm-hem-geik diagrams. Furthermore the high-Mg groundmass does not plot as an extension to the linear Fe_2O_3:TiO_2 correlation, but plots immediately above it. The second scenario is that ilmenites plotting within the phenocryst trend may represent an early crystallising ilmenite phenocryst phase which crystallised concurrently with the olivine phenocryst phase, and followed a more regular fractionation trend indicated by decreasing MgO. Ilmenite phenocrysts and ilmenite inclusions in olivine phenocrysts commenced crystallisation with MgO concentrations of approximately 18wt%, and continued crystallising until MgO concentrations of 13wt%, at which stage a hiatus occurred in ilmenite crystallisation. Ilmenites with MgO contents less than 13wt%, which plot within the TiO_2-MgO and Fe_2O_3-TiO_2 megacryst trends, plot separately on the Cr_2O_3 and MnO vs MgO plots suggesting that they may in fact be misassigned small fragments of ilmenites from the megacryst suite. The high-Mg Wesselton groundmass ilmenites may represent a late stage renewal of ilmenite crystallisation as a result of the reconcentration of TiO_2 in the magma after crystallisation of TiO_2 free minerals in the kimberlite, or from the partial resorbtion of existing ilmenite macrocrysts and megacrysts.

Based on current data, no distinction can be made between eclogitic and peridotitic derived ilmenite except that high-Ti eclogitic ilmenites plot above the peridotitic TiO_2-MgO trend (figures 4.6a and 4.7a), Cr_2O_3 is characteristically almost absent in eclogitic ilmenites, and eclogitic ilmenites tend to plot in small well constrained fields, based on a small number of analyses.

Ilmenites in diamond fall into two main fields on all graphs (figure 4.11). The primary field plots within the field for peridotitic ilmenites, and the secondary (low-Mg) field, corresponds to the field for low-Mg west African groundmass ilmenites. It is therefore concluded that the low-Mg diamond inclusions have been introduced into the diamond after growth, and may be epigenetic. Diamond inclusions used to define the main inclusion trend are separated into high and low Cr_2O_3 varieties, with the three low Cr analyses plotting close to or overlapping with the field for eclogitic ilmenites on all plots (figures 4.6, 4.8 and 4.11). It is therefore likely that these three inclusions are eclogitic and the remaining two peridotitic. The eclogitic diamond inclusions can be further subdivided into high- and low-Ti groups on all plots with the high Fe_2O_3- low TiO_2 inclusion corresponding to the high Fe_2O_3 outlier in the eclogitic plots. The two George Creek ilmenite inclusions are syngenetic and coexist with eclogitic garnet in their diamond host (Chinn pers comm). These two analyses are well separated from the other eclogitic ilmenite analyses, except for the Fe_2O_3-TiO_2 and MnO-MgO

relationships where they plot relatively closely. The George Creek diamond inclusions, therefore have either different or unusual compositions, or require a major expansion of the eclogitic fields in this study.

Metasomatic ilmenites are not easily distinguishable from other parageneses of ilmenite. This is further complicated by metasomatic ilmenites themselves being derived from a number of different origins. Ilmenites from metasomatised lherzolites, for example, define a well constrained field which is indistinguishable from most parageneses of ilmenite. High-Cr, high-Mg harzburgitic and polymict ilmenites on the other hand are distinguishable from all parageneses except the equivalent high-Cr megacrysts. High Cr_2O_3 (>4wt%) megacrystic ilmenites used in this study (figure 4.4d), coincide with high Cr_2O_3 metasomatic ilmenites and originate in kimberlites well known for metasomatic suite minerals these megacrystic ilmenites may potentially be derived from metasomatised peridotites or polymict peridotites (figure 4.4d)

Oxygen fugacity is a major factor which affects the composition of UMD ilmenite. Attempts to establish the fO_2 of the environments in which ilmenites crystallised requires well constrained pressure and temperature estimates which will also determine the positions of fO_2 isobars in the ilmenite-hematite-geikielite ternary phase diagram. Knowledge of the displacement of these isobars is necessary before inferences about the fO_2 of the environments in which ilmenites crystallised, can be assessed.

Based on trends observed in a comprehensive set of data extracted from other studies, it is concluded that no individual ilmenite analysis can be assigned to a paragenesis using major element compositions alone, but the observation of trends in ilmenite populations may allow identification of paragenesis. In practice, however kimberlitic ilmenite suites from any one locality often include ilmenites from a number of different parageneses, but in the majority of cases, and in size categories greater than 1mm, the macrocryst suites are dominated by megacrystic ilmenite. If any locality deviates from this tendency and is dominated by ilmenite from a different paragenesis, it should be possible to identify this deviation and allocate these populations, to a paragenesis, using criteria presented here.

...ooOoo...

CHAPTER 5

THE USE OF ILMENITE COMPOSITIONS TO PREDICT THE PRESERVATION OF DIAMOND PARCELS

-Applied to southern African Kimberlites-

Analyses of Ilmenite concentrate from Tshibua, Premier, Palmietfontein and Iron Mountain, where the degree of preservation of diamonds is known, has been used to establish compositional criteria for the prediction of diamond preservation. These criteria have been applied to 13 southern African kimberlites and diamond preservation predicted. Prediction categories include: Good preservation, intermediate preservation, poor preservation, marginal preservation and no preservation (barren). Correlation has been obtained between predicted preservation and the observed preservation of diamond parcels from the localities. It is postulated that most diamond corrosion occurs in the mantle lithosphere prior to entrainment in the kimberlite.

5.1 INTRODUCTION

Ilmenite is a very common mineral in many kimberlites and even dominates the macrocryst population at some kimberlite localities. Due to the durability of ilmenite in the secondary environment, grains may travel large distances from their source and as a result has been used since the late 1800's to locate and identify primary kimberlite deposits (Wagner, 1914). More recently, it has been noted that ilmenite may play a greater role in diamond prospecting than only the tracking of kimberlites. Fesq et al (1976) observed empirically that the average chromium content in a small number of kimberlitic ilmenites from southern African kimberlites may reflect their diamond content. Ilmenite macrocrysts, however are derived from sources which are not directly related to diamond genesis. Dominant parageneses include ilmenites derived from the Cr-poor megacryst suite, the metasomatic suite, as ilmenite phenocrysts in kimberlite, and kimberlitic groundmass. In contrast, diamonds are derived from disaggregated peridotite and eclogite xenoliths. Unlike other diamond indicator minerals, which are useful due to their association with diamond, (eg. garnet and chromite, Gurney and Switzer, 1973),either as inclusions in diamond or in xenoliths which host diamond, no such direct association exists for ilmenite. Ilmenite, in fact only rarely occurs in diamondiferous eclogite and peridotite.

Even though ilmenite parageneses have no known relationship to diamond genesis (Gurney, 1989), relationships have been noted between diamond content of some kimberlites and ilmenite composition (Fesq et al, 1976; Gurney et al, 1978), more specifically the MgO, Fe_2O_3 and Cr_2O_3 contents. Since ilmenites have no obvious genetic relationship to diamond content, ilmenite compositions may reflect a secondary process that affected the diamonds, and which ultimately resulted in lower diamond contents in the kimberlite.

Diamond parcels from many kimberlite localities exhibit a wide range of diamond morphologies which can be attributed to resorbtion (chapter 3). This process occurs as a result of conditions outside of those under which diamonds are stable, the most notable of which is oxygen fugacity (Haggerty, 1986). It has been observed that diamonds which are armoured by intact xenoliths are relatively unresorbed in comparison to those exposed to kimberlite magmas, and it has been concluded that resorbtion occurs as a result of diamond been in contact with the kimberlitic magma en route to the surface (Robinson, 1979, 1989). If the kimberlitic magma is responsible, then conditions within the magma either inside or outside of the diamond stability field, would result in the conversion of diamond to graphite, or more frequently CO_2, and the rate at which this occurs may depend on the O_2 activity in the magma (Eggler, 1989; Gurney et al, 1993). The range in resorbtion observed in diamonds from within a particular kimberlite is, therefore most likely to be a result of the length of time the diamond was in contact with the kimberlitic melt which is, in turn, governed by how late the xenoliths containing the diamonds disaggregated and liberated the diamonds.

Ilmenite compositions are dependent on P, T and fO_2, and have been used to estimate redox conditions of the upper mantle (Haggerty and Tompkins, 1983; Moats, 1989). Haggerty and Tompkins (1983) have suggested that ilmenites may reflect redox conditions in the mantle at, or close to the time of emplacement, and in the proximity of the transporting magma, and as a result may reflect the potential for diamond resorbtion to occur. Ilmenites that contain high MgO and low Fe_2O_3 concentrations are more likely to be associated with kimberlites with higher average grade, and ilmenites with low MgO and higher Fe_2O_3 indicate more oxidising conditions during crystallisation and are often associated with kimberlites with poor grade (Gurney et al, 1978, 1993; Fipke et al, 1995).

The grade of a kimberlite is a measure of the diamond content of the kimberlite. Grade is affected by fundamental factors such as the amount or peridotite and eclogite sampled by the kimberlite, their

average grade and the efficiency of the kimberlite in bringing the diamond to the surface (Gurney et al, 1993). If the kimberlite sampled barren rocks on the way to the surface, or had low carrying capacity (Gurney and Zweistra, 1995), the fO_2 of the magma possibly reflected by the ilmenite composition will have no bearing on the assessment of economic viability of a deposit. The prediction of diamond preservation therefore will never improve a forecast which has been based on other indicator minerals, but may serve to detract from it. Positive ilmenite compositions, for example, will not increase the forecast of diamond potential of a deposit. On the other hand, ilmenite compositions which indicate oxidising conditions will reduce any forecast of diamond potential.

To confirm and quantify a relationship between diamond preservation and ilmenite composition, a group of ilmenite bearing kimberlites, preferably from the same geological terrain, which define a range in diamond preservation, are required. Ilmenites are, however only present in group I kimberlite, and most group I kimberlites in southern Africa have diamond parcels which are highly resorbed. Well preserved diamond parcels are generally restricted to group II kimberlites which are devoid of any meaningful ilmenite. In addition, a diamond parcel from a particular locality may conceivably comprise a number of different populations of diamond each displaying unique resorbtion characteristics, and furthermore each locality may contain vastly different proportions of these different populations.

An attempt is made here to assess the use of ilmenite to forecast the degree of preservation displayed by some diamond parcels. Compositions of ilmenite, in the heavy mineral concentrate from different localities, is assessed in terms of diamond preservation trends.

5.2 ILMENITE COMPOSITION AND DIAMOND PRESERVATION

Ilmenite compositions have traditionally been represented on Cr_2O_3 - MgO and ilmenite-hematite-geikielite plots. Some authors have alluded to a possible correlation between ilmenite, MgO and Cr_2O_3 compositions and degrees of diamond preservation (Haggerty, 1975; Gurney et al, 1978; Gurney and Moore, 1991; Gurney et al, 1993, Gurney and Zweistra, 1995 and Schultz et al, 1995). More specifically, it has been suggested that ilmenites which plot along the high MgO limb of the Cr_2O_3 - MgO parabolic relationship (Haggerty, 1975) have been associated with good preservation,

whilst ilmenites on the lower MgO limb are associated with poor preservation. In reality, however this plot often contains ambiguous compositional trends and undefinable scatter, possibly due to variations in the Cr_2O_3 content, due to wall rock assimilation by the megacryst magma. This restricts the value of this plot for making preservation predictions. The ilm-hem-geik ternary plot has often been cited because it offers an insight into fO_2 conditions represented by the ilmenite compositions. This, however is spurious because the fO_2 isobars and the ternary solvii are only valid for temperatures of 1300°C at pressures of 1 atm. Since many megacryst ilmenites crystallise at temperatures closer to 1150°C (Harte and Gurney, 1981), and possibly even crystallise under conditions of decreasing temperature, interpretation of the fO_2 of ilmenite compositions must be viewed with caution.

Ilmenites from four localities have been chosen to represent as large a range in diamond preservation as possible. These analyses are plotted on various graphs (figure 5.1 a-h) to establish the most useful relationship between ilmenite composition and diamond preservation. In southern Africa, few localities with well preserved diamonds occur and those that do are usually group II kimberlites, which usually do not contain significant megacrystic ilmenites. As a result, localities outside of southern Africa have been chosen to represent both the high and very low preservation diamond parcels. Quantitative diamond morphology data is not available for 3 of these localities, namely Tshibua, Palmietfontein and Iron Mountain and consequently it has not been possible to predict preservation indices.

Tshibua, in central Africa, is a high grade kimberlite with diamonds that frequently display fibrous coatings. Fibrous coats represent late-stage growth on diamonds and in some cases may possibly even bear a relationship to the kimberlitic magma (Akagi and Masuda, 1988). Late stage growth implies redox conditions under which diamond is stable, and consequently represents the ultimate in preservation state ie. regrowth. Premier is a kimberlite with intermediate grade (26-33 carats/100 tonnes) and a parcel of diamonds, which have been extensively resorbed with 92% of all surviving diamonds in the -11+9 sieve category having lost between 35% and 45% of their original mass (Robinson, 1989). Palmietfontein, the third locality, has a very low grade (≈1carat/100 tonnes) and the diamonds are extensively resorbed (Gurney, pers comm). This locality is included as a kimberlite exhibiting marginal preservation. The last locality, Iron Mountain is barren, even though the indicator minerals point to the presence of diamonds, and other geographically associated kimberlites in the State Line District do contain diamonds (McCallum and Vos, 1993).

Figure 5.1 contains a number of plots depicting analyses of ilmenites from these four localities. In all plots a line has been drawn to represent the most Fe_2O_3 rich and MgO poor analysis for each locality. These boundaries are identified by a number enclosed in a circle. The ilmenite analyses depicted in figures 5.1(a) and (b), conform to those one would expect from Cr-poor megacryst ilmenites (chapter 4). Although all trends in figure 5.1 exhibit a range in MgO, the analyses tend to concentrate at intermediate MgO, making discrimination between the 4 localities for the purposes of predicting diamond preservation almost impossible. The relationship of Cr_2O_3 to MgO (figure 5.1c) is characterised by a distorted "parabolic" relationship with Tshibua ilmenite containing unusually high levels of Cr_2O_3 and high MgO. Premier ilmenite analyses plot on the lower Cr_2O_3 section of the high MgO limb of the parabola and extend towards lower concentrations of MgO with constant Cr_2O_3. Iron Mountain ilmenite concentrate defines a trend of increasing Cr_2O_3 with decreasing MgO at intermediate to low levels of MgO (<10wt%). Ilmenite from Palmietfontein does not conform to the parabola with Cr_2O_3 concentrations remaining constant with decreasing MgO (9-4wt% MgO).

The ilmenite-geikielite-hematite ternary in figure 5.1(d) shows an overall trend from high geikielite, less differentiated compositions, away from geikielite and curving up towards the hematite end-member. Ilmenite concentrate from Iron Mountain intersects the Sp+Psb+Ilm solvus indicating that the ilmenites probably crystallised at temperatures lower than 1300°C (decomposition loop retracts with decreasing temperature). All analyses from Tshibua, Premier and Palmietfontein, plot between the fO_2 isobars of -7 and -6 log units. Therefore, either fO_2 ranges are within one log unit, or the trend represents a drop in temperature which will result in a shift of oxygen isobars with respect to the ilmenite trend. Iron Mountain ilmenites ranges over 3 log units. The Palmietfontein ilmenites define a trend which spans one log unit.

The hyperbolic trend in figure 5.1(e) and the parallel trends in figure 5.1(h) appear to discriminate best between ilmenites from the 4 localities. If the assumption that diamond resorbtion is linked to oxygen activity in the resorbing medium is true then it might be expected that a plot containing Fe_2O_3 and MgO may be the most applicable. Fe_2O_3 represents a very crude indicator of redox conditions and MgO is a simplified fractionation index which is used instead of the more traditional Mg#. In figure 5.1, the trend of increasing oxidation with increasing differentiation is accompanied by decreasing preservation. Important features of this plot are that the better preserved parcels are characterised by ilmenites with higher MgO and lower Fe_2O_3 than their less preserved counterparts, and the linear spread, starting compositions and width of the fields are different for the different

localities. Iron Mountain, which has probably experienced complete destruction of the diamond parcel, commences at ilmenite compositions which are high in MgO (12wt%) and low in Fe_2O_3 (6wt%), but increase rapidly in Fe_2O_3 with decreasing MgO. Furthermore, the trend is the longest of all the trends, is well constrained in terms of width and has overall Fe_2O_3 greater than that for Palmietfontein ilmenite. Tshibua, in contrast, plots within a tightly constrained group with high MgO and low Fe_2O_3 and defines a marginal increase in Fe_2O_3 with decreasing MgO. Palmietfontein ilmenite analyses define a trend of increasing Fe_2O_3 with decreasing MgO, but commence with intermediate Fe_2O_3 (9.5wt%) and MgO (10.5 wt%). Premier ilmenite analyses are spread with respect to both Fe_2O_3 and MgO.

The criteria to be utilised when predicting diamond preservation from ilmenite compositions, using the plot represented in figure 5.1 would therefore appear to involve:

i) The starting (least differentiated) composition.
ii) The length of the trend, if a trend is present.
iii) Final compositions of ilmenites in the trend
iv) The vertical position or the trend along the 'y'- axis, (relative to the main fractionation trend represented here).

Ferrous iron concentrations define two distinct trends with respect to MgO (figure 5.1f). The first trend (A) is a fractionation trend with Fe^{2+} substituting for Mg^{2+} with increasing differentiation. The flattening out of the trend is a result of increasing Fe_2O_3. The second trend (B) is defined by Iron Mountain ilmenites, and defines a trend which conforms to an inverted parabola. The decrease in FeO with MgO at MgO concentrations less than 8wt% is a result of increasing Cr_2O_3 and rapidly increasing Fe_2O_3. The increase in Cr_2O_3 is probably a result of wallrock assimilation (Moore et al, 1992; section 4.2, this study). Figure 5.1 (g) serves to illustrate that the results of plotting Fe_2O_3 versus MgO are similar to those obtained from plotting the oxidation ratio Fe# (FeO/Fe_2O_3+FeO) versus Mg# (MgO/MgO+FeO). Discrimination between ilmenite from the four localities is not noticeably better using the more complicated Fe# and Mg#, and therefore Fe_2O_3 and MgO will be used for further data interpretation. The plot of Al_2O_3 vs MgO appears to be a useful discriminator of ilmenites from the four localities, however, as with the Cr_2O_3 - MgO plot, more work is required to establish the mechanism which relates Al_2O_3 and MgO to diamond preservation. As In addition, the accurate determination of low concentrations of Al_2O_3 in ilmenite make routine microprobe analysis for exploration purposes, more difficult.

For the purposes of this study, the relationship between Fe_2O_3 and MgO in concentrate ilmenite is considered to be the most likely to discriminate between compositions of ilmenites which adversely affect diamond preservation and compositions which do not. Trends observed in ilmenite concentrate from Tshibua, Premier, Palmietfontein and Iron Mountain correlate with the observed degree of preservation, or lack thereof, of diamond parcels from these localities.

5.3 SELECTED SOUTHERN AFRICAN LOCALITIES

Ilmenite concentrate analyses from 14 southern African kimberlite localities have been selected. These localities have been selected because they represent a range in different ilmenite compositional trends. Furthermore, the diamond parcels range in preservation from intermediate to marginal. A summary of interpretations and approximate locations is presented in table 5.1.

5.3.1 KAMFERSDAM

The majority of the ilmenite analyses form a tight, well constrained cluster, which commences at high MgO and low Fe_2O_3. A second poorly constrained cluster of 4 analyses exists within the division representing intermediate preservation. The first cluster is probably of metasomatic origin or a phenocryst phase in the kimberlite (figure 5.3 a-f), and falls within the zone representing good preservation. Consequently, these ilmenites may not relate to the event which corroded the diamonds, and may even have been part of a metasomatic injection which resulted in a diamond growth event. The ilmenites in the unconstrained, second cluster are probably megacrystic in origin and have analyses which are more likely to relate to a diamond corrosion event. However, due to the few analyses in this cluster, it is not possible to ascertain whether the corrosive megacryst event was less pervasive, and consequently less diamonds were resorbed, or the lack of analyses is a function of skew sampling. Kamfersdam diamonds from the -11+9 sieve category display a poorly constrained preservation index of 0.11 (table 3.5). This index is low due to the use of a single small size category (-11+9), and the true preservation index is probably higher. In the absence of any descriptions or diamond quantities from other size categories, it is not feasible to attempt to extrapolate the degree of resorbtion of other size categories.

5.3.2 ORAPA

Two populations of ilmenite are present here, the first of which plots between 8 and 10wt% MgO and contains no Fe_2O_3. This population probably represents eclogitic ilmenite. This is not unlikely, since eclogitic diamonds make up a significant proportion of the total diamond parcel, and they plot within the field for high TiO_2 eclogitic ilmenites defined in figure 4.6(b). The field has been defined using 11 ilmenites, 7 of which were derived from Orapa eclogites (Tollo, 1984) The second population defines a trend which is megacrystic (figure 4.4b), long, commences at very high MgO and low Fe_2O_3 and terminates at compositions representing intermediate preservation. A preservation index of 0.11 has been calculated for Orapa diamonds (table 3.5). Once again, this index is low due to the use of a single small size category (-11+9), and the true preservation index is probably higher.

5.3.3 JWANENG

Jwaneng ilmenites display a long trend, but with a dominant cluster which commences at high MgO and low Fe_2O_3 and extends to just inside the intermediate preservation field. These ilmenites may indicate a population of diamonds which show good preservation. Cubic diamonds and fibrous overcoats on diamonds from Jwaneng support this. The rest of the ilmenite analyses plot in the poor to marginal preservation category. The overall scarcity of these ilmenites means these poor compositions should not override the preservation forecast, unless the scarcity is a result of a sample which is skewed towards the ilmenites with higher MgO. Jwaneng diamonds have an underestimated preservation index of 0.21 (table 3.5).

5.3.4 BULTFONTEIN

Two populations of ilmenite are represented at Bultfontein. The first is a well defined, short trend which commences at very high MgO and low Fe_2O_3 ,and plots in the high preservation field. The second trend, is long and narrows as Fe_2O_3 increases. This trend commences at intermediate compositions and terminates at marginal compositions. Most ilmenites in this trend, however plot in the intermediate field. A preservation index of 0.22 (table 3.5) has been calculated using descriptions reported in Robinson (1989).

5.3.5 WESSELTON

The majority of ilmenites plot in a tight cluster which commences at very high MgO and low Fe_2O_3. This concentrate is probably derived from an kimberlitic ilmenite phenocryst population. A scatter of ilmenites surrounds this cluster and extends through to compositions plotting within the marginal preservation field, although only two ilmenites plot here. This scatter combined with a large range in Fe_2O_3 amongst ilmenites scattered in the field for good compositions reduces the preservation forecast from good to intermediate. The calculated preservation index for Wesselton is 0.04 (table 3.5).

5.3.6 FRANK SMITH

Ilmenite concentrate from Frank Smith defines a long, well constrained trend which commences at high MgO and higher than usual Fe_2O_3. The trend terminates at intermediate to poor compositions. Diamonds from Frank Smith have been described in this study, and an "intermediate"overall preservation index of 0.38 determined.

5.3.7 SAMADA

Ilmenite compositions from Samada, (previously known as Kaalvallei and New Robinson) define a short trend which commences at intermediate compositions. The trend terminates at poor to marginal preservation. Diamonds from Samada have been described in this study, and an "intermediate"overall preservation index of 0.30 determined.

5.3.8 LEICESTER AND BALMORAL

The Leicester and Balmoral kimberlites are geographically closely associated and are represented by ilmenites which define similar trends. The ilmenites define a trend which is extended, well constrained and commences at high MgO and low Fe_2O_3 compositions. The trend extends to very marginal compositions. Three ilmenites plot separately in the barren field. The majority of ilmenites plot in the field of good compositions. The length and continuous nature of the trend would suggest that diamond preservation would be poor to marginal, with many diamonds completely destroyed. The high concentration of ilmenites with compositions plotting in the well preserved field, and the reduction in the density of plotted analyses as differentiation proceeds may

suggest that not all diamonds were subjected to marginal preservation. Diamonds from Leicester have been described in this study, and an "intermediate to low" overall preservation index of 0.22 determined.

5.3.9 KAO

Ilmenites from the Kao kimberlite in Lesotho define compositions with intermediate MgO and intermediate to high Fe_2O_3, and plot across the boundary between the intermediate and marginal preservation fields. The calculated preservation index, from the descriptions of Whitelock (1973, table 3.5), is 0.2.

5.3.10 GOOD HOPE

Two clusters are evident in the plot of ilmenite analyses from the Good Hope kimberlite. The first, is a well constrained cluster with compositions which plot at the transition between the intermediate to good preservation fields. The second cluster defines a trend, which plots within the marginal field and extends towards the first cluster. No preservation data is available for the diamonds, however the deposit has a very low grade and is sub-economic, which may be a result of a corrosion episode. It is not possible to determine, however whether the kimberlite in fact sampled a significant quantity of diamondiferous mantle material. The low grade could therefore merely be an indication that no diamonds were sampled by the kimberlite, and consequently the composition of the ilmenites becomes irrelevant.

5.3.11 ANDRIES

Ilmenites analyses from the Andries kimberlite are defined by an interrupted, narrow, long trend which commences with compositions inside the field for intermediate preservation. The low initial MgO combined with the long differentiation trend indicates marginal preservation of diamonds. Once again, no preservation data is available for the diamonds, however the deposit has a very low grade and is sub-economic, which may have been a result of a corrosion episode.

5.3.12 LAST HOPE

Ilmenite analyses define a long, narrow trend which commences at intermediate MgO and low Fe_2O_3

and terminates at high Fe_2O_3 and low MgO. The trend begins around the boundary which separates the intermediate and marginal preservation field, and extends to well within the marginal field. No preservation data is available for the diamonds, however the deposit has a very low grade and is sub-economic.

5.3.13 VICTORIA

The majority of ilmenites define a medium length trend which commences at low MgO and high Fe_2O_3. A scatter of isolated analyses plot to the high MgO side of this trend. The trends extends to the boundary between marginal and barren. The Victoria kimberlite has a very low grade and no information is available about the diamonds.

The Fe_2O_3 and MgO contents of concentrate ilmenite from 13 southern African kimberlites have been assessed in order to predict the preservation of diamonds at these localities. Results are presented in table 5.1 along with actual preservation, and actual grade. No attempt has been made to estimate grade from ilmenite compositions because this is of little value without knowing the quantity of diamonds present before resorbtion occurred and the quantity of diamonds entrained by the kimberlite. Ilmenite compositions have been assessed following a set procedure which establishes the following parameters:

i) Paragenesis of the ilmenite and any different ilmenite populations
ii) Length of the fractionation trend
iii) Commencement composition of the trend
iv) Termination composition of the trend
v) Continuity of the trend
vi) Presence of any clustering

Results in table 5.1 show a poor correlation between observed preservation and predicted preservation. This may be a result of two factors. The first is that group I kimberlites in southern Africa all exhibit similar preservation, and the kimberlites with more preserved diamonds are generally group II kimberlites, which do not contain megacrystic ilmenites. Secondly, the available diamond data available in the literature has been collected by different researchers, and using different schemes. Harris et. al. (1979), for example produced data for diamonds from the Premier Mine, for all size categories which results in a calculated preservation index of 0.37. Robinson et. al. (1986), however have recorded diamond data, which when calculated produces

an index of between 0.04 and 0.11 using only diamonds in the -11+9 sieve class from three different phases of kimberlite.

5.4 DISCUSSION

The relationship between ilmenite compositions and diamond preservation and consequently grade, has been postulated since 1978 (Gurney et al, 1978). This prompted the supposition that ilmenite composition and diamond preservation were linked by a common factor - fO_2. Since then, exploration programs, in which ilmenite concentrations have been analysed and used to assess diamond preservation by utilising the Cr_2O_3 vs MgO plot of Haggerty (1975), have frequently had to contend with ambiguous results. The problem is that no direct evidence exists to connect ilmenite compositions with the diamond corrosive event. Clearly, if ilmenite is to reflect preservation, ilmenite must have crystallised from liquids which caused the diamond corrosive event, or the crystallising ilmenites were constrained by the same conditions which were concurrently resorbing diamonds.

Most diamonds which are resorbed have been purported to have had this done by an oxidising kimberlitic magma (Robinson, 1989), and the range in secondary morphologies is a result of the stage at which xenoliths disaggregated and released diamonds into the magma. On the other hand, most concentrate ilmenites are derived from disaggregated megacryst suite nodules. The origin of the megacryst suite of minerals has been linked to the kimberlitic event in some way or another since 1973 (Mitchell, 1973; Gurney et al, 1979) and as a result ilmenites may reflect the oxidising potential of the kimberlitic magma. Moore et al (1992), have shown however that the kimberlitic magmas are unlikely to be late stage differentiates of a megacrystic magma and in addition, ages of megacrystic zircons place the crystallisation of the megacrystic magma just prior to of the kimberlite eruption (Kinny et. al., 1987). This creates a dilemma, because if anything the fractionating megacryst suite may represent failed kimberlite intrusions into the mantle lithosphere and hence the fO_2 of this fractionated megacryst magma may have changed from the original fO_2 of the original kimberlitic magma.

Observations of ilmenite compositions from kimberlites, which are characterised by poorly preserved diamond populations, allow an association to be made between ilmenite that displays a range of ilmenite compositions (extending to compositions with high hematite), and poorly preserved diamond parcels. This suggests that either the kimberlite is directly related to the

megacrystic suite and an equivalent fO_2 is displayed by both, or the majority of diamonds are resorbed while resident in the mantle lithosphere.

A hyperbolic relationship exists between Fe_2O_3 and MgO in megacrystic ilmenites. The nature of this fractionation (Moore et al, 1992) is that the first ilmenites crystallised with more primitive high $Mg^{\#}$ ilmenites and as fractionation proceeded, MgO decreased and FeO and Fe_2O_3 increased. Initially, with decreasing MgO (15 wt% - 10 wt%), Fe_2O_3 remains constant. This suggests that if Fe_2O_3 is a measure of redox conditions, initial loss in preservation occurs irrespective of fO_2 conditions. Perhaps the initial differentiation trend is a measure of the pervasiveness of the megacryst magma.

Interpretation of the ilmenite differentiation trend is explained by the following argument. A range in ilmenites, which defines a short differentiation trend represents a shortened cooling time and consequently shorter distance travelled within the mantle lithosphere. High degrees of differentiation defined by a long fractionation trend suggest slower cooling and a more pervasive magmatic event. Long fractionation trends which extend to high levels of Fe_2O_3 may imply a more pervasive event combined with an increase in fO_2 as a result of differentiation. The assimilation trend (figure 5.1f) implies large amounts of fractionation, a pervasive event, a severe increase in fO_2 and slow cooling with stationary periods in which time significant wallrock assimilation may occur.

Certainly, the distances travelled and the fO_2 of the megacryst magma may then be responsible for a significant proportion of diamond corrosion, via a mechanism of crack propagation (Wyllie ,1989). Therefore, greater fractionation indicates greater pervasiveness and consequently greater resorbtion than a small amount of fractionation. Also of importance, is the initial (commencing) composition of the ilmenite trend. Ilmenite trends commencing with high Fe_2O_3 compositions (eg. Samada and Andries) indicate that the initial magma was more oxidising, and that even with a short fractionation significantly more resorbtion will occur, even if only over a small volume of lithosphere. Lower Fe_2O_3 compositions would indicate a less corrosive magma and slower rates of resorbtion.

This process is probably not unique to megacryst events, but may apply to any resorption event recorded during the history of the diamond. Consequently, ilmenite Fe_2O_3 and MgO compositions will only be useful if the ilmenite crystallisation is directly related to the resorbtion of diamonds. Consequently, the fact that megacryst ilmenite is the most dominant paragenesis in most group I kimberlites and that megacrystic ilmenites reflect diamond preservation, fortuitously makes

ilmenites a useful indicator of diamond preservation. This also explains why group I diamond parcels from kimberlites in the Barkly West area and the Welkom-Theunissen district are significantly less preserved than diamond parcels from geographically associated group II kimberlites.

Ilmenites which are believed to be in a phenocryst phase in the kimberlite (eg. Kamfersdam and Wesselton) display very high MgO (≥15 wt%), very low Fe_2O_3 (6 wt%) and have very short trends. This suggests that the kimberlitic magma in these cases was in fact less oxidising and consequently less corrosive than previously believed. If true, this is fortunate as slower corrosion rates in the kimberlite means that resorption in the kimberlite is less significant and survival of transport to the surface is more likely. It is also possible that localities where initial ilmenite compositions have high Fe_2O_3 represent more corrosive kimberlites. The most primitive ilmenite analyses from the megacryst suite trend, is the closest approximation of the oxidation state of the kimberlitic magma from which the megacryst magma was potentially derived.

Ranges in secondary diamond morphology therefore are not only dependent on the point at which the host xenolith is disaggregated within the kimberlite, but more significantly the abundance, per unit volume, and pervasiveness of the lithosphere intrusion event.

Many problems exist which hinder the quantitative application of ilmenite to diamond preservation. Firstly, a reliable prediction in loss of grade requires an accurate estimate of what the grade ought to be. This is unrealistic partly due to the difficulty of assessing the quantity of diamondiferous eclogites and peridotite which was sampled, and the diamond content of these source rocks, but also because many diamonds have experienced multiple growth and resorption events. Secondly, rates of resorbtion are dependant, not only on the fO_2 of the corrosive medium, but also on the type of diamond. Deformation, internal defects, nitrogen aggregation (Mendelsohn and Milledge, 1995), and indirectly the age of the diamond affect dissolution rates. This implies that older peridotitic diamonds with complicated internal structures caused by longer residence times in the lithosphere may resorb faster than younger eclogitic diamonds. If this is true, then a kimberlite which samples a greater proportion of older, peridotitic diamonds may inherit a lower degree of preservation than a kimberlite which has sampled a greater amount of younger, eclogitic diamonds.

Finally, prediction of diamond preservation requires a quantitative estimation of diamond preservation. This has been attempted in Chapter 3. The biggest problem is that a significant

proportion of diamonds have been lost altogether in less preserved parcels, and therefore the degree to which destruction of diamonds has occurred is drastically underestimated in these parcels. The result is that localities with intermediate preservation, eg. Premier, Frank Smith or Leicester report very low preservation indexes of 0.25, 0.37 and 0.22 respectively. In the "-11+9" size fraction at Premier (Robinson, 1989), 92% of all diamonds are tetrahexahedroids which have lost between 35% and 45% of their original mass. Using the present calculation of preservation index an index of 0.1 is calculated. On a preservation scale, with ranges between 0 and 1, 0.1 suggests almost no preservation, while in reality it may represent as high as 50% preservation. This cannot be overcome unless the amount of diamonds which have been resorbed more than 45%, or have been completely destroyed, can be estimated. An attempt has been made to do this in chapter 3 with diamond parcels described in this study. Applying this here, however would not have allowed comparison with data from the literature.

A number of important issues must be resolved before ilmenite compositions can be used to quantitatively predict the expected reduction in grade resulting from resorbtion of diamonds. Ilmenite compositions do, however, provide a qualitative indication of diamond preservation by applying a set of graphically based criteria.

...ooOoo...

CHAPTER 6

DISCUSSION AND CONCLUSIONS

Liquid ion chromatography has been used to directly determine Fe_2O_3:FeO ratios in international standards BHVO-1, BIR-1, STM-1 and PCC-1, and nine upper mantle derived megacryst ilmenites. Good precision has been obtained for ilmenite megacrysts, and ratios determined for international standards agree closely with recommended values (Govindaraju, 1994). Ratios for the ilmenite samples, calculated using stoichiometric principles from electron microprobe analyses, correlate well with ratios determined directly using ion chromatography. Ion chromatography is a quick, simple, relatively cheap method with good analytical precision and accuracy. Correlation curves suggest that determination of Fe^{3+} is accurate, but the determination of Fe^{2+} is slightly underestimated. This would have the effect of producing slightly oxidised results. Fe_2O_3/FeO determined for international standards are, however, more reduced than recommended values. The disadvantage of the technique is that the sample is destroyed.

Detailed descriptions of the morphology of diamonds in parcels from six southern African kimberlites have been used to establish the degree of preservation of each parcel, and to attempt to calculate the loss in grade due to resorbtion of diamonds. A sequence of increasing preservation is displayed by parcels from Leicester, Samada, Frank Smith, Ardo, Messina and Star. Preservation indexes for group II kimberlites (Messina and Ardo) are higher than for geographically associated group I kimberlites (Frank Smith and Leicester), in the Barkly West area. Similarly, the group II kimberlite, Star is significantly better preserved than the poorly preserved geographically associated group I kimberlite, Samada. The group II kimberlites are 25-30 Myr older than the group I kimberlites. Frank Smith (114Myr), is intermediate in age between Leicester and Messina/Ardo, and exhibits intermediate diamond preservation. The calculation of a preservation index provides a semi-quantitative representation of the extent of resorbtion in a parcel. This allows comparisons

to be drawn between different kimberlites and provides a frame of reference for the purposes of prediction during grade forecasting. The accuracy of the index is however dependent on the consistency of the descriptions, and is susceptible to errors in the estimation of loss of mass, particularly for diamonds with distorted shapes. A major disadvantage is that distinctive changes in morphology are only recognisable up to 45% loss in mass, after which the mechanism of resorbtion changes from edge and face dominated to defect dominated. Furthermore, diamonds which have been completely resorbed are not represented. The result is a preservation index where a hypothetical parcel in which every diamond has lost 45% of its original mass (ie. the parcel is truly intermediate) reports a preservation index of 0. There is, however, no foreseeable way to solve this situation.

Initial grade estimations, rely on how representative the diamonds are of the overall parcel. Parcels which have experienced large amounts of resorbtion may have lost a significant proportion of the original diamonds. Calculation of initial grades for the better preserved parcels become more accurate as the preservation improves, however, the less preserved localities suffer from gross underestimation of the original mass of diamonds. The percentage increase from present grade to initial grade was, nevertheless greater for the less preserved parcels, than for the better preserved parcels. The large discrepancy between the initial grade of geographically associated group I and group II kimberlites is concluded to be a result of total resorbtion of a significant proportion of the original diamonds in group I kimberlites. It is apparent therefore that a diamond corrosive event occurred in the geologically short (25Myr) time period between the eruption of group I and group II kimberlites. The intermediate preservation of Frank Smith, which erupted halfway through this period, suggests that the corrosion of diamonds was either a continuous process or was linked to the eruption of the kimberlite.

This observation is not only restricted to the kimberlites studied here. Other kimberlites with published diamond data exhibit similar trends. All diamond parcels from kimberlites younger than 100 Myr are dominated by resorbed morphologies. Some older kimberlites such as Premier (1080 Myr; Richardson, 1993) and Dokolwayo (200 Myr; Allsopp and Roddick, 1984) also contain poorly preserved diamond parcels (Robinson 1989). Kao, in Lesotho (84 Myr) is a further example of a kimberlite with a poorly preserved diamond population (Whitelock,1973). Destruction of diamonds has occurred to a greater or lesser extent at localities across the entire southern Africa (Robinson et al, 1989).

Analyses from a large database containing upper mantle derived (UMD) ilmenites from different parageneses have been assessed in an attempt to establish distinguishing criteria for their discrimination. It has been established that no single criterion can distinguish between all the parageneses. Six key plots have been used to show characteristic trends from seven different ilmenite parageneses. An adequate sample of ilmenite analyses should allow identification of paragenesis using a combination of these six plots.

Diamond preservation is a major grade reducing factor, which must be considered when forecasts using indicator minerals are made. Preservation intervals have been established on the plot of Fe_2O_3 versus MgO, using trends in concentrate ilmenites and known diamond preservation from Tshibua, Premier, Palmietfontein and Iron Mountain. This plot has been applied to other southern African localities to predict diamond preservation at these localities, using a set of strict criteria. Reasonably good correlations have been recorded between ilmenite compositions and diamond preservation from these localities. Exceptions include Wesselton and Kamfersdam, where the majority of the ilmenites are derived from either a phenocryst phase in the kimberlite, or a metasomatic source. Prediction based on a minority of scattered analyses from these localities does however correctly predict preservation. The most consistent predictions are obtained using ilmenite concentrate derived from the megacryst suite, which fortunately dominates ilmenite suites at most group I localities. Assessment of concentrate ilmenite from southern African kimberlites, allows a qualitative assessment of diamond preservation. A number of factors preclude the quantitative assessment of preservation. These include the inability to accurately quantify preservation of localities where complete resorbtion of some diamonds has occurred, and an uncertainty of the exact relationship of ilmenite megacrysts to the diamond resorbtion event. Ilmenite compositions may reflect the corrosiveness of the resorbing medium, and therefore may indirectly give a handle on the rate of resorbtion. The amount of time that the diamond is in contact with the resorbing medium, however also fundamentally affects the overall preservation of a parcel. Hypothetically, if 50% of diamonds were armoured against resorbtion and remained unresorbed, and the remaining 50% were exposed to the resorbing liquid and lost 50% or more of their original mass, then the preservation index will be 0.5, which is unrealistically high. This cannot be predicted by ilmenite compositions. The rate of resorbtion is affected by the type of diamond (Mendelssohn and Milledge, 1995). It is also conceivable that more complex internal structures are characteristic of older diamonds that have been subjected to multiple growth, resorbtion and deformation events. If true, older peridotitic diamond may be subjected to faster rates of resorbtion than younger eclogitic diamonds. Therefore, all other factors being equal, a locality such as Finsch, where the majority of diamond inclusions are

peridotitic (Richardson, 1984), may have a less preserved diamond parcel than Orapa, where the xenolith suite is dominated by eclogites (Tollo, 1982).

It is unclear whether resorbtion of diamonds occurs dominantly in the kimberlite, en route from the mantle to the surface, or whether corrosion occurs during residence in the subcontinental lithosphere. Evidence of multiple growth and resorbtion events in the internal structures of diamonds proves that at least some resorbtion does occur in the lithosphere, the extent of this however is unknown.
In contrast, hemimorphic diamonds, diamonds with resorbed faces protruding from intact xenoliths and resorbed breakage surfaces all support corrosion by the kimberlite magma (Robinson 1979).

An alternative hypothesis which explains the above features, involves a rapid igneous event beneath the lithosphere, resulting in the violent intrusion of fluids into the lithosphere by a mechanism of crack propagation (Wyllie, 1989). If rates of strain were fast enough to overcome ductile flow, brittle fracturing of the lithosphere could ensue, and may result in a set of conjugate stress fractures. If the energy release during crack propagation or fracturing was high, breakage of diamonds could occur. The fractures or cracks would permit the passage of fluids into the lithosphere and if sufficiently corrosive, the fluids may resorb diamonds along the fractures and metasomatise lithospheric rocks on either side. Alteration caused by this metasomatism may weaken the rock along the fractures and result in the formation of rounded corestones. These corestones when sampled by a kimberlite magma, will be "cleaned" by abrasion and reactions within the kimberlite may occur.

This scenario would adequately explain the resorbtion features and trends displayed by parcels of diamonds, and provides an alternative to the kimberlite magma being the dominant corrosive liquid. Furthermore, this would imply that any rapid igneous event beneath the diamondiferous mantle lithosphere could result in the widespread resorbtion of diamonds. Examples of this might be: megacryst events immediately preceding eruption of group I kimberlites, metasomatic infiltration during and after group II emplacement (Sweeney et al, 1993; Konzett et al, in press) or fluids resulting from metasomatic events triggered by the Karoo continental basalt event (Matsoku; Harte and Gurney, 1975). The Proterozoic Premier kimberlite was preceded by a megacryst event and the group II Dokolwayo kimberlite, Swaziland (200Myr) was preceded by the Stormberg volcanics (Daniels, 1989). The extent of diamond resorbtion will be governed by the extent of the fluid migrations and the intensity of the event. Small scale infiltration may result in localised

metasomatism, however an intense event may result in large scale fracturing and metasomatism or even in the destruction of the entire mantle root (Helmstaedt and Gurney, 1995).

.....ooOoo.....

CHAPTER 7

REFERENCES

AGEE I.J., GARRISON J.R. AND TAYLOR L.A. (1982) Petrogenesis of oxide minerals in kimberlite, Elliot County, Kentucky. *Amer. Mineral.*, **67**, 28-42

AKAGI T. & MASUDA A. (1988) Isotopic and elemental evidence for a relationship between kimberlite and Zaire cubic diamonds. *Nature*, **336**, 665 - 667.

APTER D.B., HARPER F.J., WYATT B.A. AND SMITH B.H.S. (1984) The geology of the Mayeng kimberlite sill complex, South Africa. In: Kornprost J.(Ed) *Kimberlites and Related Rocks*, Proc.Third International Kimberlite Conference,**1**, 43-57

ARIMA M. & INOUE M. (1995) High Pressure experimental study on growth and resorbtion in kimberlite melts. Extended Abstracts, *Sixth International Kimberlite Conference*, Pg 8-10

BALLHAUS C. (1993) Redox states of lithospheric and asthenospheric upper mantle. *Contrib. Mineral. Petrol.*,**114**, 331 - 348

BEYER M.E. BOND A.M. AND MCLAUGHLIN R.J.M (1975) Simultaneous polargraphic determination of ferrous, ferric, and total iron in standard rocks. *Anal. Chem.*, **47**, 479

BIEN G.S. AND GOLDBERG E.G. (1956) Polarographic determination of ferrous and ferric iron in refractory minerals. *Anal. Chem.*, **28**, 97

BOYD F.R. & NIXON H. (1973) Origin of the ilmenite-silicate nodules in kimberlites from Lesotho and South Africa. In: Nixon PH (Ed) *Lesotho Kimberites*, Lesotho Natl. Dev. Corp.,Maseru, 254-268

BOYD F.R., GURNEY J.J. AND RICHARDSON S.H. (1985) Evidence for a 150-200 km thick Archaean lithosphere from diamond inclusion thermobarometry. Nature, **315**, 387-389

BOYD F.R., DAWSON J.B. AND SMITH J.V. (1984) Granny Smith diopside megacrysts from the kimberlites

of the Kimberley area and Jagersfontein, South Africa, *Geochim. Cosmochim. Acta*, **48**, 381-384

BULANOVA G.P. (1995) The Formation of diamond. In: Griffin WL (Ed), Diamond Exporation : Into the 21st Century, *J. Geochem Expl*, **53** : 1-23

BUNDY F.P. (1963) Direct conversion of graphite to diamonds in static pressure apparatus, *J. Chem. Phys.*, **38(3)**, 631- 643

BURNS R.G. (1975) On the occurrence and stability of divalent chromium in olivines included in diamonds. *Contrib. Mineral. Petrol.*, **51**, 213-221

CANIL D., VIRGO D. AND SCARFE C.M. (1990) Oxidation state of mantle xenoliths from British Columbia, Canada. *Contrib. Mineral. Petrol.*, **104**, 453-462

CHINN I.L. (1995) A Study of unusual diamonds from the George Creek K1 Kimberlite Dyke, Colorado. *Unpubl.. PhD thesis, Univ. Cape Town*

CLEMENGY C.V. AND HAGNER A.F. (1961) Titrimetric determination of ferrous and ferric iron in silicate rocks & minerals. *Anal. Chem.*, **33**, 888

CLIFFORD T.N. (1966) Tectono-metallogenic units and metallogenic provinces of Africa. *Earth Plan. Sci. Lett.*, **1**, 421-434

DANCHIN R.V. AND D'OREY F. (1972) Chromium spinel exsolution in ilmenite from the Premier Mine, Transvaal, South Africa. *Contrib. Mineral. Petrol.*, **35**, 43-49

DANIELS L.R.M. AND GURNEY J.J. (1989) The chemistry of the garnets, chromites and diamond inclusions from the Dokolwayo kimberlite, Kingdom of Swaziland. In: Ross (Ed), *Kimberlites and Related Rocks*, II, Forth International Kimberlite Conference, 759-770

DAVIS G.L. (1977) The ages and uranium contents of zircons from kimberlites and associated rocks. *Extended Abstracts*, Second International Kimberlite Conference, Sante Fe, (unpaged)

DAWSON J.B. & SMITH J.V. (1977) The MARID (mica - amphibole - rutile - ilmenite - diopside) suite of xenoliths in kimberlite. *Geochim Cosmochim Acta* **41**: 589-607

DIONEX (1987) Determination of transition metals. Dionex Corporation, Sunnyvale, California,

Technical Note, **23**, 4

EGGLER D.H., MCCALLUM M.E. & SMITH C.B. (1979) Megacryst assemblages in kimberlites from Northern Colorado and Southern Wyoming : petrology, geothermometry, barometry and areal distribution. In Boyd FR, Meyer HOA (Eds) *The Mantle Sample: inclusions in kimberlites and other volcanics*. AGU, Washington, 213-216

EGGLER D.H. & WENDLANDT R.F. (1979) Experimental Studies on the relationship between kimberlite magmas and partial melting of peridotite. In : Boyd FR, Meyer HOA (Eds) *Kimberlites, diatremes and diamonds : their geology , petrology and geochemistry*. AGU Washington, 308-338

EGGLER D.H. (1989) Kimberlites : How do they form? In *Kimberlites and Related Rocks*, In: J Ross (Ed) Geological Society of Australia, Special Publication, **14** , 323-342

EGGLER D.H. AND LORAND J.P. (1994) Sulfides, diamonds and mantle fO_2. In: Meyer HOA and Leonardos OH (Eds), *Diamonds: characterization, genesis and exploration*, **2**, Fifth International Kimberlite Conference

EMMS S. (1993) Crystalisation of PFA glasses. Unpublished Msc Thesis, University of Cape Town

ERLANK A.J., WATERS F.G., HAWKSWORTH C.J., HAGGERTY S.E., ALLSOPP H.L., RICKARD R.S. AND MENZIES M.A.(1987) Evidence for mantle metasomatism in peridotite nodules from the Kimberley pipes, South Africa. In: *Mantle Metasomatism*, Menzies MA and Hawkesworth CJ (Eds), Academic Press, 221-309

EVANS T. (1976) Diamonds. *Contemp. Physics* **17**, 45-70

FAHEY J.J. (1961) Determination of ferrous iron in magnetite and ilmenite in the presence of amphiboles and pyroxenes. *U.S.Geol. Surv. Prof. Paper*, **424**, C386

FESQ H.W. , KABLE E.J.D. AND GURNEY J.J. (1976) The geochemistry of some selected South African kimberlites and associated heavy metals. *Natl. Inst. Metallurgy*, South Africa, Rep **1703**

FIPKE C.E., GURNEY J.J. , MOORE R.O., AND NASSICHUK W.W. (1989) The development of advanced technology to distinguish between productive diamondiferous and barren diatremes. *Geological Survey of Canada, Open File 2124*, **1-3**, 1-621

FIPKE C.E., GURNEY J.J. & MOORE R.O. (1995) Diamond Exploration techniques emphasising indicator mineral geochemistry and Canadian Examples. *Geological Survey of Canada,* **Bulletin no 423.**

FITTON J.G. & GILL R.C.O. (1970) The oxidation of ferrous iron in rocks during mechanical grinding. *Geochim. Cosmochim. Acta.* , **34**, 518-523

FRENCH W.J. AND ADAMS S.J. (1972) A Rapid method for the determination of iron (II) in silicate rocks & minerals. *Analyst*, **97**, 828

FRICK C. (1973) Intergrowths of orthopyroxene and ilmenite from Frank Smith mine, near Barkly West, South Africa. *Trans. Geol. Soc. S. Africa*, **76**, 195-200

GARANIN V.K., KUDRYAVTSEVA G.P. AND LAPIN A.V. (1978) Typical features of ilmenite from kimberlites, alkali-ultrabasic intrusions, and carbonatites. *International Geology Rev.*, **22**, N9, 1025-1050

GARRISON J.R. & TAYLOR L.A. (1980) Megacrysts and xenoliths in kimberlite, Eliot county, Kentucky: A mantle sample from beneath the Permian Appalachian plateau. *Contrib. Mineral. Petrol.*, **75**, 27-42

GHIORSO M.S. AND SACK R.O. (1991) Thermochemistry of oxide minerals. In: Oxide Minerals: Petrologic and Magnetic Significance, Lindsley DH (Ed). *Reviews in Mineralogy*, **25**, 221-264

GOLD D.P. (1984) A diamond exploration philosophy for the 1980's. *Earth and Mineral Sciences,* **53,** 37-42.

GOVINDARAJU K. (1994) Compilation of working values and sample description for 383 geostandards. *Geostandards Newsletter Special Issue*, **18**, 1-158

GRIFFIN W.L., MOORE R.O., RYAN C.G., GURNEY J.J. AND WIN T.T. (1995) Geochemistry of magnesian ilmenite megacrysts from Southern African kimberlites., Extended Absracts, *Sixth International Kimberlite Conference*, Novosibirsk, Russia

GRIFFIN W.L. & RYAN C.G. (1995) Trace elements in indicator minerals: area selection and target evaluation in diamond exploration, *J. Geochem. Expl.*, **53**, 311-337

GROVES A.W. (1951) Silicate Analysis. 2nd Ed., Allen and Unwin

GURNEY J.J. & SWITZER G.S. (1973) The discovery of garnets closely related to diamonds in the Finsch

pipe, South Africa. *Contrib. Mineral. Petrol.*, **39**, 103-116.

GURNEY J.J., FESQ H.W., KABLE E.J.D. (1973) Clinopyroxene - ilmenite intergrowths from kimberlite : a re-appraisel. In: Nixon PH (Ed) *Lesotho Kimberlites*. Lesotho National Development Corporation, Maseru, 238-253

GURNEY J.J., BRISTOW J.W. & MOORE A.E. (1978) Orientation study on the use of indicator mineral compositions in prospecting for diamondiferous kimberlites. *Report by Mineral Dienste, Cape Town to Falconbridge Explorations, Johannesburg*

GURNEY J.J., JAKOB W.R.O. & DAWSON J.B. (1979) Megacrysts from the Monastery kimberlite , South Africa. In : Boyd FR and Meyer HOA (Eds) *The mantle sample : inclusions in kimberlites and other volcanics*, American Geophysical Union, Washington, 249-256

GURNEY J.J. (1984) A correlation between garnets and diamonds in Kimberlites. *In:* Glover JE and Harris PG (Eds) *Kimberlite occurrence and origin: A basis for conceptual models in exploration*, Geology Department and University Extension , University of Western Australia, **Publication no 8**, 143-144

GURNEY J.J. (1989) Diamonds. In: Ross J and Danchin RV (Eds) Kimberlites and Related rocks, *Geol. Soc. Australia Spec. Publ.*, **14**, 2, Fourth International Kimberlite Conference, 935-965

GURNEY J.J. & MOORE R.O. (1991) Kimberlite garnet , chromite and ilmenite compositions : applications to exploration. In: *Proceedings of the International Congress Applied Mineral.* (ICAM 91), Pretoria, **1**, Paper 21

GURNEY J.J., HELMSTAEDT H. & MOORE R.O. (1993) A review of the use and application of mantle mineral geochemistry in diamond exploration. *Pure and Applied Chem.*, **65**, 12, 2423-2442.

GURNEY J.J. & ZWEISTRA P. (1995) The interpretation of the major element compositions of mantle minerals in diamond exploration. J. Geochem. Expl., **53**, 293-309.

GURNEY J.J. & KIRKLEY M.B. (1996) Kimberlite dyke mining in South Africa. *Africa Geoscience Review*, **3**, 2 , 191-201

HAGGERTY S.E. (1973) Spinels of unique composition associated with ilmenite reactions in the Liquobong kimberlite pipe, Lesotho. In: Nixon PH (Ed.) *Lesotho Kimberlites*, Lesotho National Development Corporation, Maseru, 149-159

HAGGERTY S.E. (1975) Chemistry and genesis of opaque minerals in kimberlites. *Phys. Chem. Earth*, **9**, 295-307

HAGGERTY S.E. (1976) Opaque mineral oxides in terrestrial igneous rocks. In: Rumble D (Ed.) Oxide Minerals, *Reviews in Mineralogy*, **3**, Hg101-Hg277

HAGGERTY S.E. (1986) Diamond genesis in a multiply-constrained model. *Nature*, **320**, 34-38

HAGGERTY S.E. (1991) Oxide mineralogy of the upper mantle. In: Lindsley DH (Ed.) Oxide Minerals: Petrologic and Magnetic Significance, *Reviews in Mineralogy*, **25**, 355-416

HAGGERTY S.E. & BOYD F.R. (1975) Kimberlite inclusions in an olivine megacryst from Monastery. Extended Abstracts, *Kimberlite Symposium, Cambridge,* unpaged

HAGGERTY S.E. AND TOMPKINS L.A. (1983) Redox state of earth's upper mantle from kimberlitic ilmenites. *Nature*, **303**, 295-300

HAGGERTY S.E. AND TOMPKINS L.A. (1984) Subsolidus reactions in kimberlitic ilmenites: Exsolution, reduction and the redox state of the mantle. *In:* Kornprobst J (Ed.) *Kimberlites and Related Rocks*, **I**, Second International Kimberlite Conference, 335-357

HAGGERTY S.E., HARDIE R.B., MCMAHON R.M. (1979) The mineral chemistry of the ilmenite nodule associations from the Monastery diatreme. In Boyd, FR and Meyer HOA (Eds), *The Mantle Sample: Inclusions in Kimberlites and other volcanics*, Second International Kimberlite Conference, **2**, 249-256.

HARRIS J.W., HAWTHORNE J.B. AND OOSTERVELD M.M. (1979) Regional and local variations in the characteristics of diamonds from some Southern African kimberlites In: Boyd FR and Meyer HOA (Eds.) *Kimberlites, Diatremes and Diamonds: Their Geology, Petrology and Geochemistry.* American Geophysical Union, Washington, 27-41.

HARRIS J.W. (1987) Recent physical, chemical and isotopic research of diamond. In: Nixon PH (Ed.) Mantle Xenoliths, 477-500, John Wiley and Sons, Chichester, England.

HARRIS J.W. AND GURNEY J.J. (1979). A study of the mineralogy and chemistry of sulphide inclusions in diamonds. Extended Abstracts, *Kimberlite Symposium*, **II**, Cambridge, England

HARRIS J.W. & VANCE E.R. (1974) Studies of the reaction between diamond and heated kimberlite. *Contrib. Mineral. Petrol.*, **47**, 237-244.

HARRIS J.W., HAWTHORNE J.B., OOSTERVELD M.M. AND WEHMEYER E. (1975) A classifiation scheme for diamond and a comparative study of South African diamond characteristics, *Physics and Chemistry of the earth*, **9**, 765-783, Pergamon Press, Oxford, England

HARTE B. AND GURNEY J.J. (1975) Ore mineral and phlogopite mineralisation within ultramafic nodules from the Matsoku kimberlite pipes, Lesotho. *Carnegie Inst. Washington Yearbook*, **74**, 528-535

HARTE B. AND GURNEY J.J. (1981) The mode of formation of chromium-poor megacryst suites from kimberlites. *J. Geol.*, **89**, 749-753

HARTE B. (1983)Mantle peridotites and processes - the kimberlite sample. In: Hawkesworth CJ and Norry MJ (Eds.), *Continental basalts and mantle xenoliths*, 46-99, Shiva, Nantwich

HELMSTAEDT H.H. AND GURNEY J.J. (1995) Geotectonic controls of primary diamond deposits: implications for area selection *J. Geochem. Expl.*, **53**, 125-144

HELMSTAEDT H.H. & GURNEY J.J. (1989) Geotectonic controls on the formation of diamonds and their kimberlitic and lamproitic host rocks: applications to diamond exploration , *Fifth International Kimberlite Conference*, 236 - 250

HELMAN J.S. (1974) Potentiometric determination of ferrous iron in silicate rocks and minerals. *Bull. Centre Reserches u* - SNPA, **8**, 153-157

HILDEBRAND W.F. , LUNDELL G.E.F. ,BRIGHT H.A. AND HOFFMAN J.I. (1953) Applied Inorganic Analysis, **2nd Ed.** ,Wiley, New York

HOPS J.J. (1989) Some aspects of the geochemistry of high-temperature peridotites and megacrysts from the Jagersfontein kimberlite pipe, South Africa. *Unpubl.PhD thesis*, Univ. Cape Town

HOPS J.J., GURNEY J.J., HARTE B. AND WINTERBURN P. (1986) Megacryst and high temperature nodules from the Jagersfontein kimberlite pipe. In: *Kimberlites and Related Rocks*, Ross (Ed.), **II**, Fourth International Kimberlite Conference, 759-770

HURLBUT C.S. AND KLEIN C. (1985) Manual of Mineralogy. **19th edition,** John Wiley and Sons, Chichester, England

ITO J. (1962) Special techniques for the determination of ferrous and ferric concentrations in refractory minerals. *Bull. of Chem. Soc. of Japan*, **35,** 225

JAKOB W.R.O. (1977) Geochemical aspects of the megacryst suite from the Monastery kimberlite pipe. *Unpubl. MSc thesis*, Univ. Cape Town

JANSE A.J.A. (1989) Is Clifford's rule still valid ? Affirmative examples from around the world, *Fifth International Kimberlite Conference,* 215-235

JEFFREY P.G. AND HUTCHINSON D. (1983) Iron. In: *Chemical Methods of Rock Analysis*, 3rd Ed., chap **25**, 192-212, Pergamon Press

JOHNSON W.A AND MAXWELL I.A. (1981)The determination of iron, uranium, thorium, flourine, chlorine and tungsten. In: *Rock and Mineral Analysis*, **2nd Ed.**, chap **6**, 183-235, Krieger

JONES R.A. (1987) Stronium and Neodymium isotopic and rare earth element evidence for the genesis of megacrysts in kimberlites of Southern Africa. In : Nixon PH (Ed.) *Mantle Xenoliths*, 711-724, John Wiley and Sons, Chichester, England

KANAI Y. (1990) Simultaneous determination of iron (II) and iron (III) oxides in geological materials by ion chromatography. *Analyst* **115**, 809-812

KENNEDY C.S. AND KENNEDY G.C. (1976) The equilibrium boundary between graphite and diamond. *J. of Geophys. Res.*, **81**, 2467-2470

KINNEY P.D. & DAWSON J.B. (1992) A Mantle metasomatic injection event linked to late Cretaceous kimberlite magmatism , *Nature,* **360** , 726-728

KISS E. (1977)Rapid potentiometric determination of the iron oxidation state in silicates *Anal. Chimica Acta*, **89,** 303

KONZETT J., ARMSTRONG R.A., SWEENEY R.J. AND COMPSTON W. (1998) The timing of MARID metasomatism in the Kaapvaal mantle: An ion probe study of zircons from MARID xenoliths. *Earth Planet. Sci. Lett.*, **160(1-2),** 133-145

KRAMERS J.D. (1977) Lead and strontium isotopes in inclusions in diamonds and in mantle-derived xenoliths from southern Africa. Extended Abstracts, *Second International Kimberlite Conference*, Sante Fe, New Mexico, A.G.U., Washington (unpaged)

LAWLESS P.J., GURNEY J.J. AND DAWSON J.B. (1979) Polymict peridotites from the Bultfontein and De Beers Mines, Kimberley, South Africa. In: Boyd FR and Meyer HOA (Eds.) *The Mantle Sample*, A.G.U., Washington, Second International Kimberlite Conference, 145-155

LE ROEX A.P. AND WATKINS R.T. (1995) A rapid ion chromatographic method for the determination of the Fe^{3+}/Fe^{2+} ratio in silicate rocks and minerals. *Geochem. J.*, **29**, 35-39

LINDSLEY D.H. (1965) Iron-titanium oxides. *Carnegie Inst. Washington Yearbook*, **62**, 144-148

LINDSLEY D.H. (1991) Experimental studies of oxide minerals. In: Lindsley DH (Ed.) Oxide minerals: petrologic and magnetic significance, *Reviews in Mineralogy*, **25**, 69-106

LINDSLEY D.H. (1976) Experimental studies of oxide minerals. In: Rumble D (Ed.) Oxide Minerals, *Reviews in Mineralogy*, **3**, L61-L84

LINDSLEY D.H. & DIXON S.A. (1977) Diopside - enstatite equilibria at 850 ^{0} to 1400 ^{0} C, 5 to 35 kb, *Am. J. Sci.* **276,** 1285 - 1301

LO-SUN JEN (1973)The determination of iron (II) in silicate rocks and minerals *Anal. Chimica Acta.*, **66**, 315

MACINTYRE R.M. AND DAWSON J.B. (1976) Age and significance of some South African kimberlites, *4th Eur. Colloq. Geochron. Cosmochron. Isotope Geol. Amsterdam*, **Abstr 66**

MCCALLISTER R.H. & NORD G.L. (JNR) (1981) Subcalcic diopsides from kimberlites : Chemistry, exsolution microstructures and thermal history. *Contrib. Mineral. Pet*rol., **78,** 118-125

MCCALLUM M.E. (1989) Oxide minerals in Chicken Park kimberlite, Northern Colorado. In: Ross (Ed.) *Kimberlites and Related Rocks*, **II,** Fourth International Kimberlite Conference, 759-770

MCCAMMON C.A., CHASKAR V. & RICHARDS G.G. (1991) A Technique for spatially resolved Mossbauer spectroscopy applied to quenched metallurgical slags, *Meas.Sci.Tech*, **2**, 657-662.

MELTON C.E. & GIARDINI A.A. (1974) The compostion and significance of gas released from natural diamonds from Africa and Brazil. *Am. Mineral.*, **59,** 775-782

MENDELSOHN M.J. AND MILLEDGE H.J. (1995) Morphological characteristics of diamond populations in relation to temperature-dependent growth and dissolution rates. *Internat. Geol. Rev.*, **37**, 285-312

MEYER H.O.A AND SVISERO D.P. (1975) Mineral inclusions in Brazilian diamonds. *Phys Chem Earth* **9**, 785-795, Pergamon Press, Oxford, England

MIKHAILOVA Z.M. YARUSHKINO A.A. MIRSKII R.V. AND SHIL'DKROT E.A. (1965)(Ref. Zh. Khim. 19GDE, Abstr. 4G122) through Brit. str., 12, 114

MITCHELL R.H. (1973) Magnesian ilmenite and its role in kimberlite petrogenesis. *J. of Geol.*, **81,** 301-311

MITCHELL R.H. (1977) Geochemistry of magnesian ilmenites from kimberlites in South Africa and Lesotho. *Lithos*, **10,** 29-37

MOATS M.A. (1989) Intrinsic oxygen fugacity (IOF) studies of kimberlitic, ilmenite-bearing megacrysts. Unpubl. MSc thesis, Temple Univ.

MOORE, M. AND LANG A.R. (1974) On the origin of the rounded dodecahedral habit of natural diamond *J. Crystal Growth*, **26**, 133-139

MOORE R.O. , OTTER M.L., RICKARD R.S., HARRIS J.W. AND GURNEY J.J. (1986) The occurence of moissanite and ferropericlase as inclusions in diamond . Extended Abstracts, *Fourth International Kimberlite Conference, Geological Society of Australia Abstracts* Series no **16**, 409-411.

MOORE R.O. (1986) A study of the kimberlites, diamonds and associated rocks and minerals from the Monastery mine, South Africa. *Unpubl. PhD thesis*, Univ. Cape Town

MOORE R.O., GRIFFEN W.L., GURNEY J.J., RYAN C.G., COUSENS D.R., SIE S.H. AND SUTER G.F. (1992) Trace element geochemistry of ilmenite megacrysts from the Monastery kimberlite, South Africa. *Lithos*, **29,** 1-18

MOORE R.O. AND GURNEY J.J. (1985) Pyroxene solid solution in garnets included in diamond. *Nature,* **318**, 553-555

MOSES C.O., HERLIHY A.I., HERMAN J.S. AND MILLS A.L. (1988) Ion chromatographic analysis of mixtures of ferrous and ferric iron. *Talanta*, **35**, 15-22

NIXON P.H. AND BOYD F.R. (1973) The geology of the Kao kimberlite pipes: Deep-seated nodules. In: Nixon PH (Ed.) *Lesotho Kimberlites*, Lesotho National Development Corporation, Maseru, 106-109

OTTER M.L. , GURNEY J.J. (1989a) Mineral inclusions in diamonds from the Sloan diatremes, Colorado - Wyoming State Line kimberlite district, North America. In: Ross (Ed.) *Kimberlites & Related Rocks, Fourth International Kimberlite Conference*, 1042-1054.

OTTER M.L., MCCALLUM M. AND GURNEY J.J. (1993) A physical characterisation of the Sloan (Colorado) diamonds using a revised diamond description scheme. In: Meyer HOA and Leonardos OH (Eds.) *Diamonds: Characterization, Genesis and Exploration, Fifth International Kimberlite Conference*, **2**, 15-31

PASTERIS J.D., BOYD F.R. , NIXON P.H. (1979) The ilmenite association at the Frank Smith mine, RSA. In: Boyd FR, Meyer HOA (Eds.) *The mantle sample : inclusions in kimberlites and other volcanics*, A.G.U., Washington, 257-264

PASTERIS J.D. (1980) The significance of groundmass ilmenite and megacryst ilmenite. *Contrib. Mineral. Petrol.*, **75**, 315-325

PHAAL C. (1965) Surface studies of diamond. *Industrial diamond Review*, **25**, 486-489, 591-595.

PRATT J.H. (1894) On the determination of ferrous iron in silicates. *Am. J. Sci.*, **CXLVIII**, 283-288

RICHARDSON S.H., GURNEY J.J., ERLANK A.J. AND HARRIS J.W. (1984) Origin of diamonds in old enriched mantle, *Nature*, **310** ,198-202

RICHARDSON S.H., HARRIS J.W. & GURNEY J.J. (1993) Three generations of diamonds from old continental mantle , *Nature*, **366**, 256-258

RICHARDSON S.H., (1986) Latter-day origin of diamonds of eclogitic paragenesis. *Nature*, **322** , 623-626

RICHARDSON S.H. AND HARRIS J.W. (1997) Antiquity of peridotitic diamonds from the Siberian craton , in Press

RICKARD R.S., HARRIS J.W., GURNEY J.J. AND CARDOSO P. (1989) Mineral inclusions in diamonds from Koffiefontein mine. In: Ross (Ed.) *Kimberlites and Related Rocks, Fourth International Kimberlite Conference, 2, Geological* Society of Australia Special Publication, **14**, 1054-1062

ROBINSON D.N. (1978) The characteristics of natural diamond and their interpretation. *Minerals Science and Engineering*, **10**, 55-72.

ROBINSON D.N., (1979) Surface textures and other features of diamonds. *Unpubl.PhD thesis,* Univ. Cape Town , South Africa, 221p

ROBINSON D.N., SCOTT J.A., VAN NIEKERK A. AND ANDERSON V.G. (1989) The Sequence of events reflected in the diamonds of some Southern African Kimberlites.In: Ross (Ed.) Kimberlites and related rocks, Fourth International Kimberlite Conference, **2**, Geological Society of Australia Special Publication, **14**, 980-990

ROELANDTS I. (1981) Weaknesses and strengths of geochemical reference materials. *Chem. Geol*, **32**, 155-165

ROMBOUTS L.(1992) TERRAC *Computer Program for the Commercial Evaluation of Alluvial Diamond Parcels*

SALMON J.E. AND HALE D.K. (1960) Ion exchange - A laboratory manual. Butterworths

SCHAFER H.N.S (1966) The determination of Iron (II) oxide in silicate and Refractory Materials. *Analyst,* **91**, 755-763

SCHRAUDER M. AND NAVON O. (1993) Solid carbon dioxide in a natural diamond, *Nature*, **365**, 42 - 44

SCHULZE D.J., ANDERSON P.F.N., HEARN B.C. AND HETMAN C.M. (1995) Origin and significance of ilmenite megacrysts and macrocrysts from kimberlite, *International Geology Review,* **37**, 780-812.

SCOTT SMITH B.H., DANCHIN R.V., HARRIS J.W. AND STRACKE K.J. (1984) Kimberlites near Orrorroo, South Australia. In: Kornprobst J (Ed.), Kimberlites 1: *Kimberlites and Related rocks, Third International Kimberlite Conference*, **1**, 121-142, Elseriver

SEAL M.(1965) Structure in diamond as revealed by etching. *Am. Mineral.*, **50**, 105-123

SHAPIRO L. (1960)A spectrophotometric method for the determination of FeO in rocks. *U.S.G.S. Prof. Papers*, **400B**, 496-497

SHEE S.R. (1985) The petrogenesis of the Wesselton mine kimberlites, Kimberley, Cape Province, R.S.A. Unpubl. PhD thesis, Univ. Cape Town

SMITH C.B. (1983) Isotopic evidence for sources of Southern African cretaceous kimberites, *Nature,* **304,** 51-54

SMITH J.V. AND DAWSON J.B. (1975) Chemistry of Ti-poor spinels, ilmenites and rutiles from peridotite and eclogite xenoliths. *Phys. Chem. Earth*, **9**, 309-322

SMITH C.B., GURNEY J.J., SKINNER E.M.W., CLEMENT R., AND EBRAHIM N. (1985) Geochemical character of Southern African kimberlites: A new approach based on isotopic constraints Trans. Geol. Soc. South Afrrica, **88**, 267-280

SOBOLEV N.V. (1977) Deep-Seated inclusions in kimberlites and the problems of the composition of the Upper Mantle. A.G.U., Washington.

SOBOLEV N.V., EFIMOVA E.S. AND POSPELOVA L.M. (1981) Natural iron in Yakutian diamonds, and its paragenesis: Geology and geophysics, *Dokl. Akad. Nauk SSSR*, **12**, 25-29, in Russian

SUNAGAWA I. (1984) Morphology of natural and synthetic diamond crystals. In: Sunagawa I (Ed.) *Materials Science of the Earth's Interior*, 303-330, Terra Scientific Publishing Co, Tokyo

SUTHERLAND S.L., HOLLIS J.D. & BARRON L.M. (1984) Garnet lherzolite and other inclusions from a basalt flow, Bow Hill, Tasmania , In: Kornprobst J, *Kimberlites and related rocks*, **1**, *Third International Kimberlite Conference,* 145-160, Elseriver

SWEENEY R.L., THOMPSON A.B., ULMER P. (1993) Phase relations of a natural MARID composition and implications for MARID genesis, lithospheric melting and mantle metasomatism *Contrib. Mineral. Petrol.,* **115**, 225-241

TAYLOR R.W. (1964) Phase equilibria in the system FeO-Fe_2O_3-TiO_2 at 1300°C. *Am. Mineral.*, **49**, 1016-1030

TOLLO R.P. (1982) Petrography and mineral chemistry of ultramafic and related inclusions from the Orapa A/K-1 kimberlite pipe, Botswana. **Contr. No. 39**, Univ. Massachusetts, Amherst

TOMPKINS L.A. AND HAGGERTY S.E. (1984) The Koidu kimberlite complex, Sierra Leone: Geological setting, petrology and mineral chemistry. In: Kornprobst J (Ed.) *Kimberlites and Related Rocks*, **I**, Second International Kimberlite Conference, 335-357

TOMPKINS L.A. (1983) The Koidu kimberlite complex, Sierra Leone, West Africa. Unpubl. MSc thesis, Univ. Massachusetts.

VARMA, C.K.R. (1967) Studies of natural diamonds of the dodecahedral form. *Phil. Mag.*, **16**, 621-634

VILJOEN (1994) The Petrology and geochemistry of a suite of mantle derived eclogite xenoliths from the Kaalvallei kimberlite, South Africa, Unpubl. PhD thesis, Univ. Witwatersrand, Johannesburg, South Africa

VINCENT E.A. AND PHILIPS R. (1954) Iron-titanium oxide minerals in layered gabbros of the Skaergaard intrusion, East Greenland, I: Chemistry and ore-microscopy. *Geochim. et. Cosmochem. Acta.*, **6**, 1-26

WAGNER P.A. (1914) The Diamond Fields of Southern Africa. Struik

WATERS F.G. (1987) A geochemical study of metasomatised peridotite and marid nodules from the kimberley pipes, South Africa. Unpubl. PhD thesis, Univ. Cape Town.

WAYCHUNAS G.A. (1991) Crystal chemistry of oxides and oxyhydroxides. In: Oxide Minerals: Petrologic and magnetic significance, Lindsley DH (Ed.), *Rev. in Mineral.*, **25**, 11-68

WERTHEIM G.K. (1964) Mossbauer effect: Principles and applications. Academic Press

WHIPPLE E.R. (1974) A Study of Wilson's determination of ferrous iron in silicates, *Chem. Geol.*, **14**, 223

WHITEHEAD D. AND MALIK S.A. (1975) Determination of ferrous and total iron in silicate rocks by automated colorimetry, *Anal. Chem.*, **47**, 554

WHITELOCK T.K. (1973) Morphology of the Kao diamonds In: Nixon PH (Ed.) *Lesotho Kimberlites*. Lesotho National Development Corporation, Maseru, 128-140

WILDING M.C., HARTE B. AND HARRIS J.W. (1989) Evidence of an asthenospheric source for diamonds from Brazil. Extended Abstracts, *28th International Geological Conference*, **3**, 359-360

WILSON A.D. (1960) The microdetermination of ferrous iron in silicate minerals by a volumetric and colorimetric method. *The Analyst*, **35**, 823-827

WILSON A.D. (1964) The titrimetric and spectrophotometric determination of the oxidising capacity of manganese compounds. *Analyst*, **89**, 571

WILSON A.D. (1955) A new method for the determination of ferrous iron in rocks and minerals. *Bull. of Geol. Surv. Great Britain*, **9**, 56

WOERMAN E, HIRSCHBERG A, LAMPRECHT A. (1970) Das system hematit-ilmenit-geikielith unter hohen temperatures und hohen druken. Extended Abstracts, *Fortschr. Mineral.*, **47**, 79-80

WYATT B. (1979) Manganoan ilmenite from the Premier kimberlite. Extended Abstracts, Kimberlite Symposium, **II**, Cambridge, United Kingdom

WYATT B.A., SHEE S.R., GRIFFEN W.L., ZWEISTRA P. AND ROBISON H.R. (1994) The Petrology of the Cleve kimberlite, Eyre peninsula, south Australia. In: Meyer HOA and Leonardos OH *Kimberlites, Related Rocks and Mantle Xenoliths*, **I**, CRPM Spec. Publ., **1A**, Fifth International Kimberlite Conference, 62-79

WYATT B. AND LAWLESS P.J. (1984) Ilmenite in polymict xenoliths from the Bultfontein and De Beers mines, South Africa. In: *The Mantle and Crust-Mantle Relationships*, Kornprobst J (Ed.), **II**, Third International Kimberlite Conference, 43-56

WYLLIE P.J. (1987) Metasomatism and fluid generation in mantle xenoliths: experimental. In: Nixon PH (Ed.), *Mantle Xenoliths*, 609-621, John Wiley and Sons, Chichester, England

WYLLIE P.J. (1989) The genesis of kimberlites and some low - SiO_2, high alkali magmas, In : *Kimberlites and Related rocks : Their Composition, occurrence origin and Emplacement*, Geological Soc. of Aus. Spec. Pub., **1**, Fourth International Kimberlite Conference, 603 - 615

YAMAOKA S., KOMATSU H., KANDA H. AND SETAKA N. (1977) Growth of diamond with rhombic dodecahedral faces, *J. Crystal Growth*, **37**, 349-352

...ooOoo...

ACKNOWLEDGEMENTS

I would like to thank my supervisor, John Gurney for his invaluable expertise and patience, as well as BHP Minerals and the Foundation for Scientific Research and Development for providing funds to make the research possible.

Special thanks must be extended to the management of River Ranch diamond mine, Leicester mine, Frank Smith mine, Samada mine and Ardo diamond mines and to Messina Investments Pty(Ltd), for permission to describe their diamond parcels.

I am grateful to Ron Watkins for inspiration and teaching me the art of Ion Chromatography; Gail Kiviets for help with diamond descriptions; Hartwig Frimmel, Anton Le Roex, Gavin Walton, Tansy Horwood and Sue Blake for reading drafts at various stages. Dane Gerneke and Trevor Sewell are thanked for SEM assistance; Mr Williams and Charlie Basson for photographic advice; Dick Rickard for EMP assistance; James Willis for advice on analytical related matters; Rory Moore for initiating the KRG database, and Dave Reid, Andy Duncan, Anton le Roex, Terry Heaney, Ted Mills and Dave Hill for help with computer related matters. I would like to acknowledge support by Isabelle, Shirley, Jackie, Anne, Neville, Ivan, Patrick, Peter and Anita.

Also due is acknowledgement and appreciation of useful discussions with Mal McCallum, Steve Haggerty, Jeff Harris, Melissa Kirkley, Judith Milledge, Dave Bell and Ingrid Chinn. I would like to extend heartfelt thanks to Marian Tredoux, Bruce Cairns and Eric Bryce are for much support and plenty of good advice, and for keeping me on the right track.

Help with formatting and final collation was provided by Sue, Tansy and Ingrid

Special mention is required for my family and close friends for day to day help and support.

...ooOoo...

TABLES

Table 2.1		DTP18-3	MON-5	MON-4	MON-1	LK F-2	NROB-1	DTP17-2	JJG1611	JJG1619
Fe_2O_3/FeO **Determined using Ion Chromatography**		0.68 0.71 0.72	0.51 0.52 0.53	0.49 0.48 0.48 0.48 0.49 0.46	0.44 0.43 0.45 0.43 0.44 0.45	0.43 0.42 0.44 0.43 0.45 0.46 0.46 0.44	0.33 0.32 0.31 0.30 0.35 0.35 0.34 0.35 0.30 0.30 0.32 0.31	0.23 0.23 0.24 0.25	0.17 0.16 0.17 0.17 0.17 0.17 0.16 0.16 0.18 0.19 0.19 0.17 0.17	0.14 0.13 0.14 0.16 0.18 0.18
MEAN	**X**	**0.70**	**0.52**	**0.48**	**0.44**	**0.44**	**0.32**	**0.24**	**0.17**	**0.16**
2x STANDARD DEV.	**2S**	**0.04**	**0.02**	**0.02**	**0.02**	**0.02**	**0.04**	**0.02**	**0.02**	**0.04**
No of Analyses	**N**	**3**	**3**	**6**	**6**	**8**	**12**	**4**	**13**	**6**
Fe_2O_3/FeO **Calculated Stoichiometrically from Electron Microprobe Results**		0.80 0.80 0.74 0.71	0.63 0.66 0.63 0.67 0.64 0.64 0.64 0.64 0.65 0.64 0.64 0.63 0.63 0.62 0.65	0.49 0.52 0.47 0.50 0.50 0.52 0.53 0.50 0.53 0.52 0.51 0.52 0.52 0.54 0.54	0.47 0.48 0.50 0.50 0.50 0.50 0.49 0.50 0.49 0.48 0.49 0.51 0.48 0.47	0.51 0.49 0.50 0.48 0.50 0.51 0.51 0.52 0.51 0.49 0.49 0.49 0.51 0.47 0.45	0.38	0.20 0.20 0.19 0.22 0.21 0.21 0.20 0.23 0.20 0.23 0.22 0.21 0.22 0.23 0.24	0.19 0.20 0.21 0.21 0.19 0.18 0.20 0.20 0.21 0.20	0.16 0.15 0.17 0.14 0.16 0.17 0.16 0.11 0.16 0.14 0.14 0.15 0.17 0.16 0.14
MEAN	**X**	**0.76**	**0.64**	**0.51**	**0.49**	**0.49**	**0.38**	**0.21**	**0.20**	**0.15**
2xSTANDARD DEV.	**2S**	**0.10**	**0.02**	**0.04**	**0.02**	**0.04**	**n/a**	**0.02**	**0.02**	**0.04**
No of Analyses	**N**	**4**	**15**	**15**	**15**	**15**	**1**	**15**	**10**	**15**

Table 2.1 Analyses of Fe_2O_3/FeO for nine ilmenite megacrysts using ion chromatography and stoichiometric calculation from electron microprobe analyses. Descriptive statistics, including 2-sigma errors, are included for each.

Table 2.2	Fe_2O_3/FeO This Study		No of Analyses	Fe_2O_3/FeO	Le Roex and Watkins
	(Mean)	*2S*	*N*	*USGS*	*(1995)*
PCC-1	0.06	0.02	6	0.54	
BIR-1	0.22	0.02	8	0.25	0.23±0.02
BHVO-1	0.31	0.04	26	0.33	0.30±0.02
STM-1	1.35	0.06	6	1.37	1.35±0.02
EMMS-1	4.05	0.03	3	n/a	n/a

Table 2.2 Measured Fe_2O_3/FeO, standard deviation, recommended USGS values and le Roex and Watkins (1995) results for selected international rock standards: PCC-1, BIR-1, BHVO-1, STM-1 and a synthetic diopside with an elevated Fe_2O_3/FeO ratio (EMMS-1).

BHVO-1				
Sample Mass (mg)	**Fe_2O_3/FeO (Area)**	**Statistics**	**Fe_2O_3/FeO (Height)**	**Statistics**
50	0.31		0.37	
40	0.31		0.36	
35	0.31	**X=0.32**	0.35	**X=0.39**
30	0.32	**2σ=0.02**	0.41	**2σ=0.06**
25	0.32		0.43	
20	0.32		0.41	
15	0.33		0.46	
10	0.34		0.39	
10	0.37	**X=0.32**	0.44	**X=0.38**
10	0.33	**2σ=0.06**	0.39	**2σ=0.14**
5	0.30		0.29	
5	0.27		0.29	
X	0.32		0.38	
S	0.02		0.05	

Table 2.3 Variation of sample mass with international standard BHVO-1 and a comparison of peak area integration and peak height. The ratios obtained using peak height are significantly more oxidised than those from peak area, and the errors are more than double.

Table 3.1

Pierres Sieve Sizes	Equivalent Metric Aperture Diameters (mm)	Sieve Categories used for Descriptions in this Study
20	4.5	"+18-21"
19	4.3	
18	4.1	"+15-18"
17	3.9	
16	3.7	
15	3.5	"+14-15"
14	3.3	"+12-14"
13	3.1	
12	2.9	"+11-12"
11	2.7	"+9-11"
10	2.5	
9	2.3	"+6-9"
8	2.1	
7	1.9	
6	1.7	"+3-6"
5	1.5	
4	1.4	
3	1.3	-3
2	1.2	
1	1.1	
0	1.0	

Table 3.1 Metric aperture diameters for Pierre circular diamond screens. Size ranges in the third column are categories used in this study. Once screened, diamonds in these categories were split into manageable parcels. Diamonds larger than Pierre size 24 were screened using every third larger screen (ie 27, 39, 33, 36, 39), and all diamonds were described.

Weight	- Form - Colour - Colour-Intensity - Impurities	Breakage	Shape	Habit	Morphology	Resorbtion
CARATS & GRAMS		CH =Chipped (>80%) BR =Broken (>60%) FR =Fragment (<40%)	EL= Elongated SK=Skew FL=Flat ST=Stepped	TWIN -simple -interpenetrant -dumbbell -clover POLY -polycrystalline-aggregate HEMI -hemimorphic	OCTA -Octahedron THD -Tetrahexahedron CUBE MACLE DODEC -Dodecahedron CuOc -Cubo-Octrahedron TRIS -Trisoctrahedron THN -Tetrahedron IRRE -Irregular UND -Undetermined	0 =pristine 1 2 3 4 5 6=>45% loss in mass

Table 3.2 Diamond description categories with appropriate descriptors. The description procedure and form (appendix 3.1), is designed to record comprehensive diamond shape and morphology data, whilst economising on description time. Time is a critical limiting factor when describing diamonds, due to strict security arrangements at most mines.. The Description categories in column two, are used by TERRAC, a computer program designed to evaluate alluvial diamond deposits (Rombouts, 1992). TERRAC has been used successfully on kimberlite derived diamond parcels as well.

Star Diamonds

Size	Carats	No. Stones	WT/Stone	Pres. Index
+39	0	0	ERR	n/c
+36	0	0	ERR	n/c
+33	2.11	1	2.11	n/c
+30	1.94	1	1.94	n/c
+27	14.53	9	1.61	n/c
+24	30.46	28	1.09	0.95
+21	39.53	49	0.81	0.98
+18	63.95	117	0.55	0.94
+15	53.33	155	0.34	0.94
+12	71.85	329	0.22	0.91
+9	75.96	621	0.12	0.86
+6	56.61	899	0.06	0.75
+3	7.22	258	0.03	ERR
-3	0.85	90	0.01	ERR
	418.34	2557		0.91

SIEVE	RES %	+24	+21-24	+18-21	+15-18	+12-15	+9-12	+6-9	+3-6	-3	Total Parcel							
		N	N	N	N	N	N	N	N	N	N	% N	WT(desc)	WT(total)	N*Wt/st	Graph (corr	L.O.M.(corr	Init. Weight
N(D+FR)		39	49	[illegible]	[illegible]	50	[illegible]	26	0	0	322							
N(D-FR)		39	43	50	48	44	44	24	0	0	792							
N (T)		39	49	117	155	329	621	899	258	90	2557							
Wt (T)		49.04	38.17	63.95	53.33	71.85	75.96	56.61	7.22	0.85	418.14							
WT/STONE		1.26	0.81	0.55	0.34	0.22	0.12	0.06	0.03	0.01	0.16							
R-0	0	11	12	[illegible]	[illegible]	3	5	1	[illegible]	0	[illegible]	17	[illegible]	[illegible]	[illegible]	[illegible]	[illegible]	[illegible]
R-1	5	8	13	20	16	9	9	5	0	0	80	27	41.96	115.01	13.09	13.09	13.78	131.06
R-2	15	10	12	11	17	22	12	1	0	0	46	30	40.06	123.63	14.07	14.07	16.55	145.45
R-3	25	4	5	7	6	6	12	11	0	0	51	18	20.06	73.32	8.34	8.34	11.13	97.76
R-4	35	2	0	3	2	4	4	6	0	0	21	7	5.94	30.19	3.44	3.44	5.29	46.45
R-5	45	0	1	0	1	0	1	0	0	0	4	1	1.81	5.75	0.65	0.55	1.00	10.46
R-6	50															0.00		
R-7	60																	
R-8	70																	
R-9	80																	
R-10	90																	
R-11	100																	
Sum		38	45	50	48	49	44	24	0		291	100	146.00	418.34	47.61	47.50	55.78	491.61
Pres Index		0.95	0.98	0.94	0.94	0.91	0.86	0.75	ERR	ERR	0.91							
Grade	40																	

Initial Grade (Carats/100ton)	47

Hemimorphic Diamonds		
N = 2		
CARATS	*UN-RESB*	*RESB*
0.21	5	3
0.08	5	3

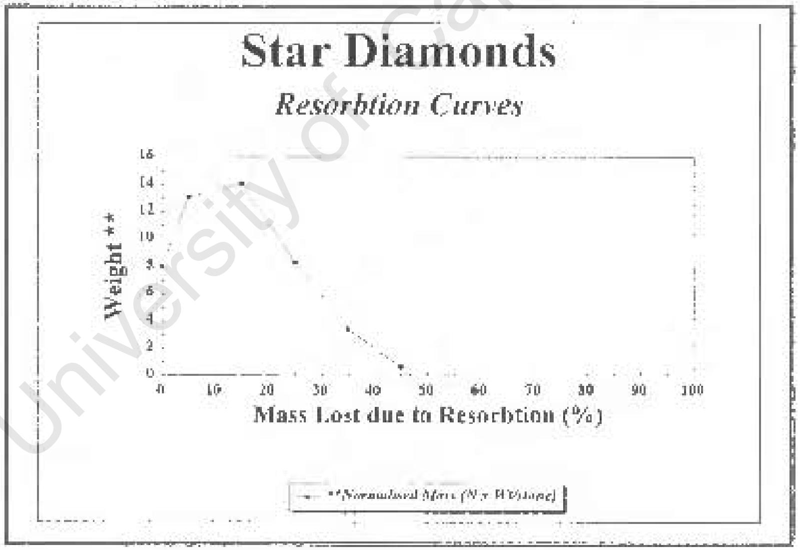

n/c	= Not Calculated.
%N	= Number of stones in each resorbtion category as a percentage.
N(D+FR)	= Number of stones described, including fragments.
N(D-FR)	= Number of stones described, excluding fragments
N(T)	= Total number of stones.
Wt(T)	= Total weight.
R-0..5	= Identified resorbtion categories, 1 to 5.
R-6..11	= Postulated resorbtion categories, 6 through 11, from graph.
L.O.M. (c	= Correction for the mass lost during resorbtion.
Init. Weig	= Initial Weight.
Grade	=Carats per 100 tonnes

Table 3.3(a) Resorbtion data, preservation indexes and calculation of initial mass and grade for the diamond parcel from Star Mine, near Welkom, Free State, RSA. The table is divided into 6 different blocks (clockwise): Block 1 contains all parcel information, including weight, No. Stones, average weight per stone and the preservation index for each size category and the total parcel. Block 2 includes all resorbtion data, individually recorded for each sieve category, the calculation of the preservation indexes and data for the total parcel including preservation index and the calculations of the initial mass. Blocks 3 and 4 contain the calculation of initial grade and details of any hemimorphic diamonds. The graph (block 5) shows the distribution of diamond in various resorbtion categories (0-5), and block 6 is a legend. This data is summarised in table 3.4.

Messina Diamonds

Size	Carats	No. Stones	WT/Stone	Pres. Index
+39	25.43	5	5.09	n/c
+36	7.09	2	3.55	n/c
+33	6.47	2	3.24	n/c
+30	10.08	5	2.01	n/c
+27	18.5	13	1.42	n/c
+24	32.44	33	0.98	0.92
+21	55.96	68	0.82	0.81
+18	94.10	159	0.59	0.74
+15	120.64	319	0.38	0.73
+12	175.62	768	0.21	0.79
+9	187.09	1650	0.11	0.66
+6	193.08	3643	0.05	0.56
+3	71.65	2756	0.03	0.38
+0	29.65	2281	0.01	0.24
	1027.77	11702		0.68

SIEVE	RES %	+24 N	+21-24 N	+18-21 N	+15-18 N	+12-15 N	+9-12 N	+6-9 N	+3-6 N	-3 N	Total Parcel N	% N	WT(desc)	WT(total)	N*Weig	Grade (corr)	L.O.M.(corr	Init. Weight
N(D+FR)		68	82	78	73	93	108	106	51	65	712							
N(D-FR)		58	64	69	63	91	82	84	32	47	582							
N(T)		68	68	159	319	766	1650	3643	2756	2281	11702							
Wt(T)		99.99	55.95	94.1	120.64	175.62	187.09	193.08	71.65	29.65	1027.77							
WT/STONE		1.67	0.82	0.59	0.38	0.23	0.11	0.05	0.03	0.01	0.09							
R-0	0	1	0	2	[illegible]	1	[illegible]	2	[illegible]	0	5	1	[illegible]	[illegible]	[illegible]	[illegible]	[illegible]	[illegible]
R-1	5	2	0	1	2	1	1	1	2	1	11	2	41.96	21.75	1.05	1.05	1.11	22.90
R-2	15	35	31	31	19	19	26	13	6	1	184	32	40.06	333.53	16.16	16.16	19.01	392.38
R-3	25	5	19	17	23	49	24	29	3	9	181	32	20.06	328.09	15.90	15.90	21.20	437.45
R-4	35	4	11	17	9	14	15	20	8	34	112	20	5.94	203.02	9.84	9.82	15.13	312.33
R-5	45	0	1	1	7	5	11	16	10	21	72	13	3.81	130.51	6.32	3.85	7.00	144.44
R-6	50															0.86	1.71	35.31
R-7	60															0.00		
R-8	70																	
R-9	80																	
R-10	90																	
R-11	100																	
Sum		50	62	63	68	59	77	82	29		567	100	146.09	1027.77	49.88	48.18	65.68	1355.69
Pres Index		0.92	0.81	0.74	0.73	0.79	0.66	0.56	0.38	0.24	0.68							
Grade	50																	

n/c	= Not Calculated.
%N	= Number of stones in each resorbtion category as a percentage.
N(D+FR)	Number of stones described, including fragments.
N(D-FR)	– Number of stones described, excluding fragments.
N(T)	= Total number of stones.
Wt(T)	= Total weight.
R-0 5	– Identified resorbtion categories, 1 to 5.
R-6 11	= Postulated resorbtion categories, 6 through 11, from graph.
L.O.M. (c	= Correction for the mass lost during resorbtion.
Init. Weig	= Initial Weight.
Grade	= Carats per 100 tonnes.

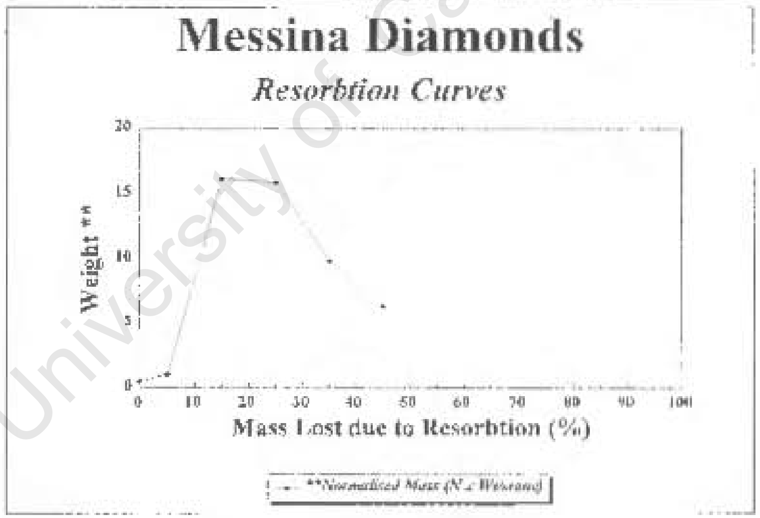

Initial Grade (Carats/100ton)	66

Hemimorphic Diamonds		
N = 2		
CARATS	UN-RESB	RESB
0.21	5	3
0.08	5	4

Table 3.3(b) Resorbtion data, preservation indexes and calculation of initial mass and grade for the diamond parcel from Messina Mine (Bobbejaan Fissure), Barkley West district, RSA. The table is divided into 6 different blocks (clockwise): Block 1 contains all parcel information, including weight, No. Stones, average weight per stone and the preservation index for each size category and the total parcel. Block 2 includes all resorbtion data, individually recorded for each sieve category, the calculation of the preservation indexes and data for the total parcel including preservation index and the calculations of the initial mass. Blocks 3 and 4 contain the calculation of initial grade and details of any hemimorphic diamonds. The graph (block 5) shows the distribution of diamond in various resorbtion categories (0-5), and block 6 is a legend. This data is summarised in table 3.4.

Ardo Diamonds

Size	Carats	No. Stones	WT/Stone	Pres. Index
+39	4.58	1	4.58	n/c
+36	8.08	2	4.04	n/c
+33	11.18	4	2.80	n/c
+30	0	0	ERR	n/c
+27	7.34	5	1.47	n/c
+24	3.24	4	0.81	0.83
+21	12.92	16	0.81	0.64
+18	12.16	24	0.51	0.55
+15	18.62	54	0.34	0.54
+12	16.74	86	0.19	0.49
+9	31.99	296	0.11	0.47
+6	29.73	583	0.05	0.35
+5	2.02	63	0.03	0.40
	158.60	1138		0.49

SIEVE	RES %	+21 N	+21-24 N	+18-21 N	+15-18 N	+12-15 N	+9-12 N	+6-9 N	+5-6 N	Total Parcel N	% N	WT(desc)	WT(total)	N*Wt/st	Graph(corr)	L.O.M.(corr)	Init. Weight
N(D+FR)		16	16	24	54	51	52	44	49	314							
N(D-FR)		14	14	20	37	35	35	44	36	225							
N(T)		16	16	24	54	86	296	583	63	1138							
Wt(T)		34.42	12.92	12.16	18.62	16.74	31.99	29.73	2.02	158.60							
WT/STONE		2.15	0.81	0.51	0.34	0.19	0.11	0.05	0.03	0.14							
R-0	0	[illegible]	1	1	0	2	3	[illegible]	[illegible]	7	3	[illegible]	5.02	[illegible]	[illegible]	[illegible]	5.02
R-1	5	5	1	1	5	1	2	3	1	15	7	8.09	10.76	2.09	2.09	2.20	11.33
R-2	15	7	5	6	6	5	6	3	5	43	19	30.65	30.86	5.99	5.99	7.05	36.30
R-3	25	3	2	3	9	9	4	6	8	44	20	15.77	31.58	6.11	6.13	8.18	42.10
R-4	35	2	3	4	12	10	12	6	9	58	26	16.86	41.62	8.08	4.87	7.49	38.54
R-5	45	1	2	5	5	8	5	16	12	54	24	12.00	38.75	7.53	3.61	6.56	33.80
R-6	50														2.98	5.96	30.69
R-7	60														1.72	4.30	22.13
R-8	70														0.46	1.53	7.87
R-9	80														0.00		
R-10	90																
R-11	100																
Sum		18	14	20	37	35	32	34	35	221	100	85.35	158.60	30.80	28.83	44.25	227.84
Pres Index		0.83	0.64	0.55	0.54	0.49	0.47	0.35	0.40	0.49							
Grade	50																

n/c	= Not Calculated
%N	= Number of stones in each resorbtion category as a percentage.
N(D+FR)	= Number of stones described, including fragments.
N(D-FR)	= Number of stones described, excluding fragments.
N(T)	= Total number of stones.
Wt(T)	= Total weight.
R-0..5	= Identified resorbtion categories, 1 to 5.
R-6..11	= Postulated resorbtion categories, 6 through 11, from graph.
L.O.M. (c	= Correction for the mass lost during resorbtion.
Init. Weig	= Initial Weight.
Grade	= Carats per 100 tonnes

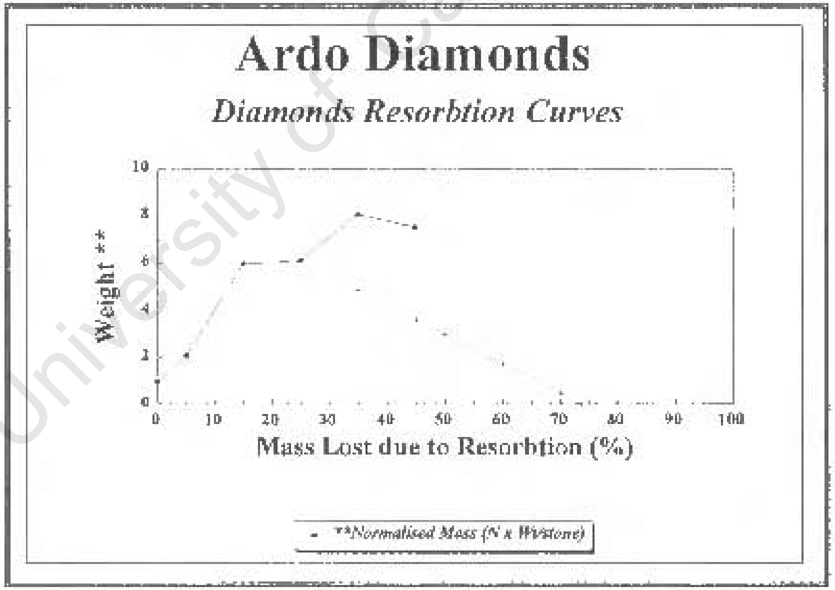

Initial Grade (Carats/100ton)	72

Hemimorphic Diamonds		
N = 3		
CARATS	UN-RESB	RESB
0.7	6	2
0.05	3	1
0.34	3	3

Table 3.3(e) Resorbtion data, preservation indexes and calculation of initial mass and grade for the diamond parcel from Ardo Mine, Barkley West district, RSA. The table is divided into 6 different blocks (clockwise): Block 1 contains all parcel information, including weight, No. Stones, average weight per stone and the preservation index for each size category and the total parcel. Block 2 includes all resorbtion data, individually recorded for each sieve category, the calculation of the preservation indexes and data for the total parcel including preservation index and the calculations of the initial mass. Blocks 3 and 4 contain the calculation of initial grade and details of any hemimorphic diamonds. The graph (block 5) shows the distribution of diamond in various resorbtion categories (0-5), and block 6 is a legend. This data is summarised in table 3.4.

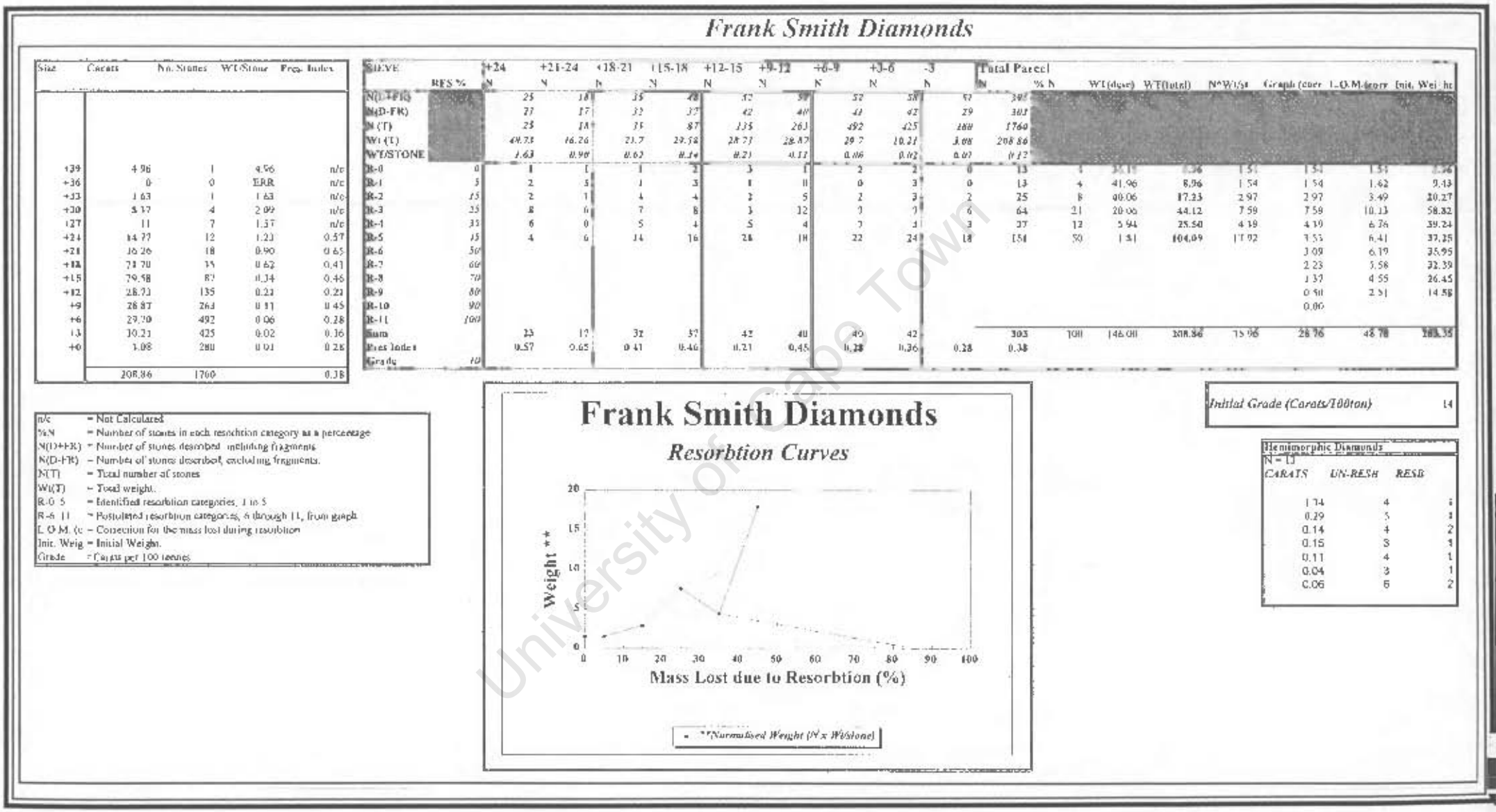

Table 3.3(d) Resorbtion data, preservation indexes and calculation of initial mass and grade for the diamond parcel from Frank Smith Mine, Barkley West district, RSA. The table is divided into 6 different blocks (clockwise): Block 1 contains all parcel information, including weight, No. Stones, average weight per stone and the preservation index for each size category and the total parcel. Block 2 includes all resorbtion data, individually recorded for each sieve category, the calculation of the preservation indexes and data for the total parcel including preservation index and the calculations of the initial mass. Blocks 3 and 4 contain the calculation of initial grade and details of any hemimorphic diamonds. The graph (block 5) shows the distribution of diamond in various resorbtion categories (0-5), and block 6 is a legend. This data is summarised in table 3.4.

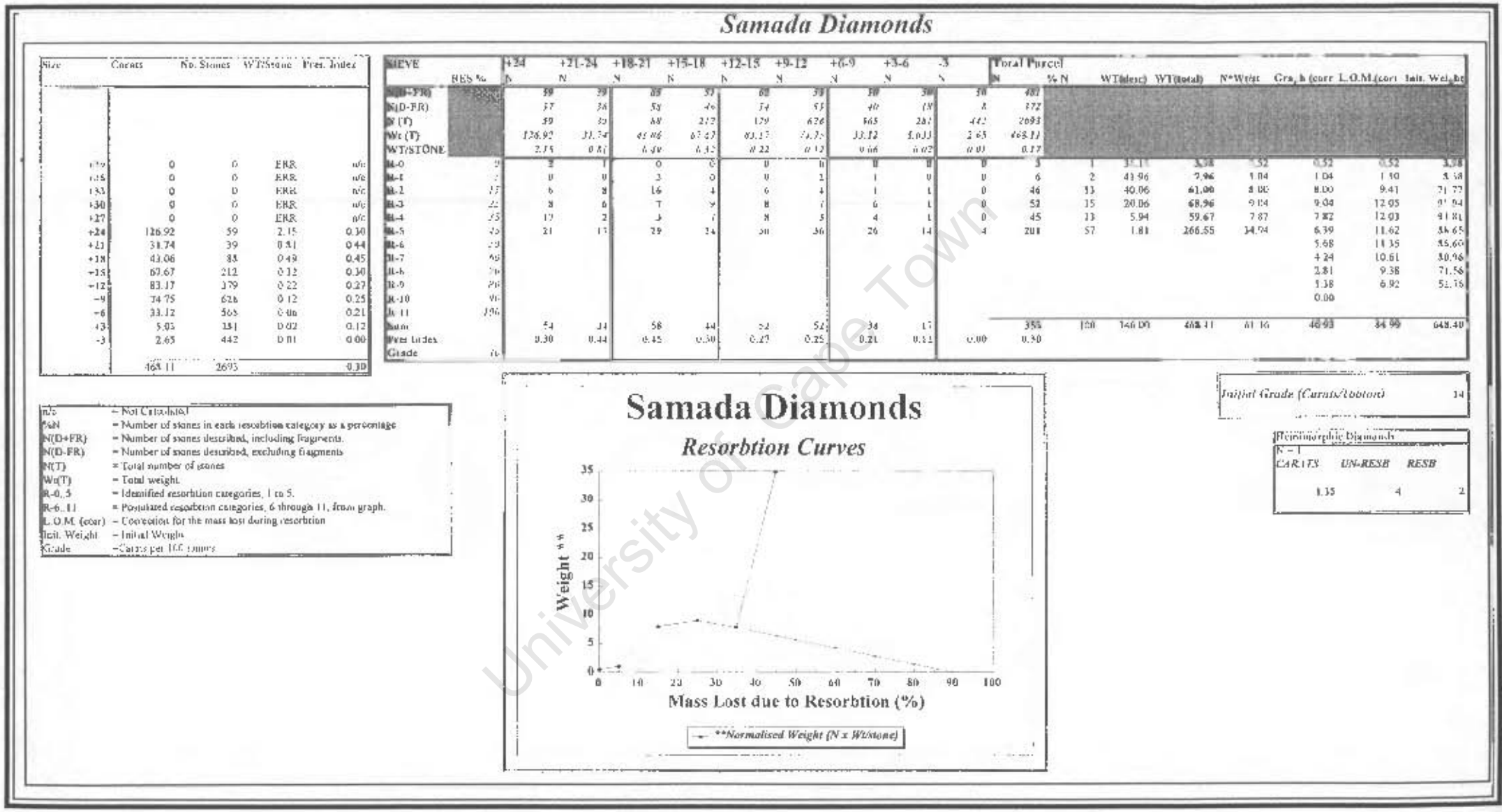

Table 3.3(e) Resorbtion data, preservation indexes and calculation of initial mass and grade for the diamond parcel from Samada Mine, near Welkom, Free State, RSA. The table is divided into 6 different blocks (clockwise): Block 1 contains all parcel information, including weight, No. Stones, average weight per stone and the preservation index for each size category and the total parcel. Block 2 includes all resorbtion data, individually recorded for each sieve category, the calculation of the preservation indexes and data for the total parcel including preservation index and the calculations of the initial mass. Blocks 3 and 4 contain the calculation of initial grade and details of any hemimorphic diamonds. The graph (block 5) shows the distribution of diamond in various resorbtion categories (0-5), and block 6 is a legend. This data is summarised in table 3.4.

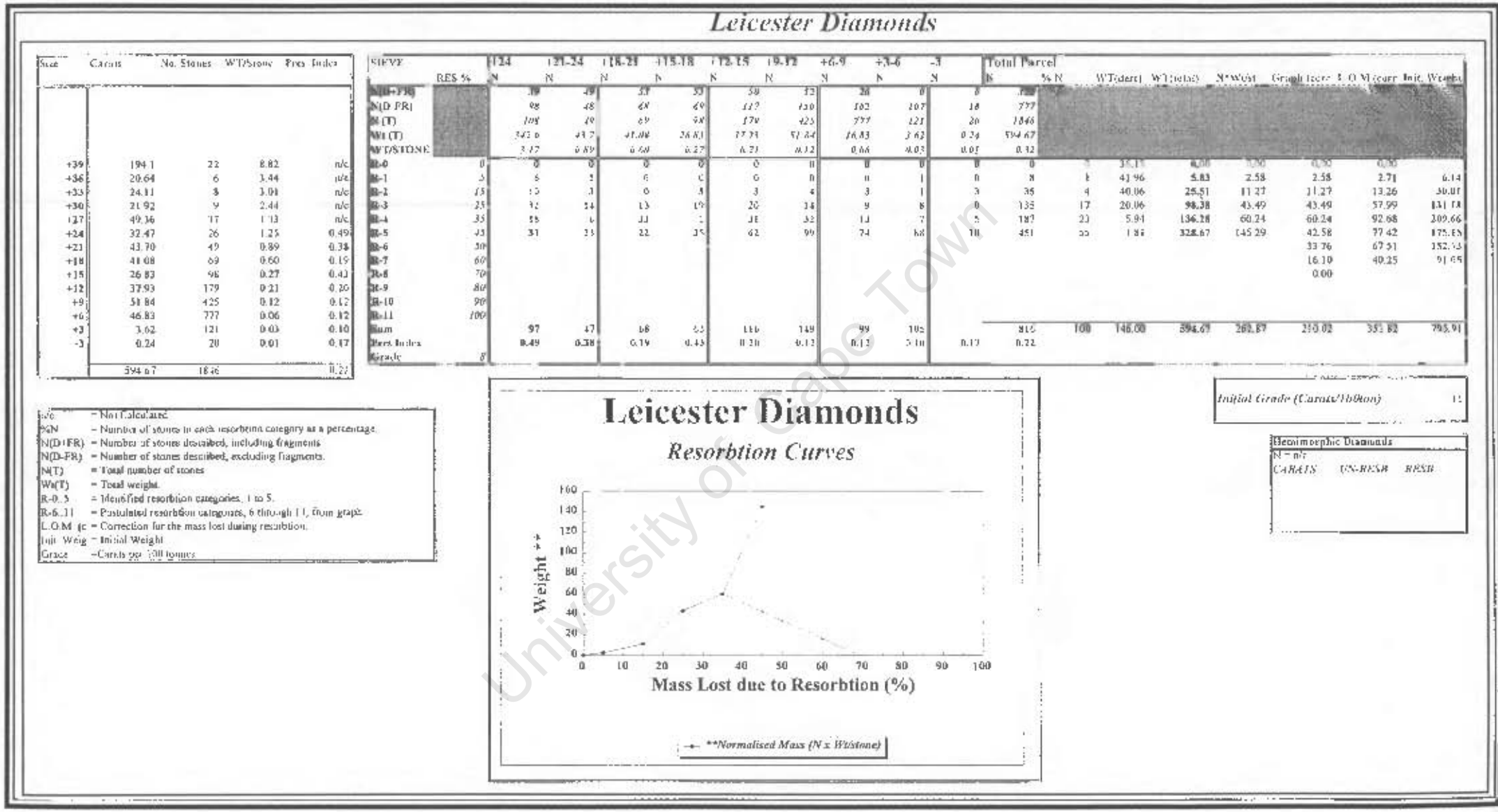

Table 3.3(f) Resorbtion data, preservation indexes and calculation of initial mass and grade for the diamond parcel from Leicester Mine, Barkley West district , RSA. The table is divided into 6 different blocks (clockwise): Block 1 contains all parcel information, including weight, No. Stones, average weight per stone and the preservation index for each size category and the total parcel. Block 2 includes all resorbtion data, individually recorded for each sieve category, the calculation of the preservation indexes and data for the total parcel including preservation index and the calculations of the initial mass. Blocks 3 and 4 contain the calculation of initial grade and details of any hemimorphic diamonds. The graph (block 5) shows the distribution of diamond in various resorbtion categories (0-5), and block 6 is a legend. This data is summarised in table 3.4.

Locality	*Preservation Index* (PI)	*Initial Mass* (IM_T)	*Run-of-mine Grade* (Cts/100tonnes)	*Initial Grade* (IG)	Grade Increase %
Star	0.91	492	60	71	18
Messina	0.68	1540	40	53	32
Ardo	0.49	213	45	61	44
Frank Smith	0.38	274	10	13	60
Samada	0.30	821	10	18	60
Leicester	0.22	792	8	11	63

Table 3.4 Results of calculations of preservation index (PI), initial mass (IM_T), Run-of-mine grade in carats per 100 tonnes, initial grade (IG) and the percentage increase in grade after correction for resorbtion . Localities include: Star, Messina, Ardo, Frank Smith, Samada and Leicester mines.

Locality	Group	Reference	N	Preservation Index (PI)													
				All Morphologies	Whole Parcel	Octahedron - Tetrahexahedron Transition Only											Mean P.I.**
						[illegible]	[illegible]	[illegible]	[illegible]	[illegible]	[illegible]	[illegible]	[illegible]	[illegible]	[illegible]	[illegible]	
This Study																	
											[illegible]						
Leicester	I		593	0.22	0.23	0.33	0.36	0.29	0.43		0.11	0.39	0.10	0.12	0.03	0.0?	0.20
Samada	I		305	0.30	0.18	0.30	0.44	0.33	0.28		0.28	0.33	0.39	0.10	0.07	0.00	[illegible]
Frans Smith	I		273	0.78	0.34	0.46	0.67	0.39	0.32	0.11	0.33	0.40	0.36	0.16	0.24	0.17	0.34
											[illegible]			[illegible]			
Ardo	II		215	0.49	0.49	0.83	0.64	0.23	0.38		0.54		0.43	0.22	0.41		[illegible]
Messina	II		521	0.65	0.64	0.90	0.76	0.72	0.71	0.73	0.81	0.64	2.61	0.45	0.37	0.23	[illegible]
													[illegible]				
Star	II		252	0.91	[illegible]	0.53	0.97	0.95	0.51	2.43	0.53		2.86	0.77			[illegible]
From Literature																	
Dokolwayo	II	Robinson et al. (1989)	301										0.06				
Dullstroom	II	Robinson et al. (1989)	72										0.04				
Helam	II	Robinson et al. (1989)	246										0.18				
Palmietgat	I	Robinson et al. (1989)	445										0.03				
Premier, Brown	I	Robinson et al. (1989)	300										0.04				
Premier, Grey	I		300										0.1?				
Premier, Black	I		300										0.07				
							[illegible]										
Premier	I	Harris et al. (1975)	219		0.25		0.23	0.24	0.20	[illegible]	0.11	0.11	[illegible]	0.2?	0.20		[illegible]
Kimberley Province																	
Bultfontein	I	Robinson et al. (1989)	300										0.22				
De Beers Mine	I	Robinson et al. (1989)	16?										0.07				
Dutoitspan	I	Robinson et al. (1989)	253										0.1?				
Kamfersdam	I	Robinson et al. (1989)	300										0.1?				
									[illegible]						[illegible]		
Loxtondal	II	Robinson (1979)	175						0.5?				0.36		0.3?		0.3?
Wesselton	I	Robinson et al. (1989)	844										0.24				
							[illegible]										
Koffiefontein	I	Harris et al. (1975)	307		0.13		0.49	0.54	0.4?	0.16	0.27	0.32	0.25	0.10	0.16		0.32
Postmasburg Province																	
Finsch Mine	II	Robinson et al. (1989)	400										0.30				
Makganyene	II	Robinson et al. (1989)	332										0.2?				
Peize?	II	Robinson et al. (1989)	108										0.36				
Lesotho																	
Letseng le Terae	I	Robinson (1979)	250										0.56				
							[illegible]										
Kao	I	Whitelock (1973)	963		0.06		0.33	0.56	0.37	0.31	0.12	0.13	0.18	0.04	0.32		0.26
Botswana																	
DK9	I	Robinson (1979)	600										0.07				
Orapa	I	Robinson (1979)	400										0.11				
Letlhakane	I	Robinson (1979)	600										0.08				
Jwaneng	I	Robinson et al. (1989)	300										0.27				
Pipe DK 7	I	Robinson et al. (1989)	299										0.33				
Siberia																	
															[illegible]		
Mir	n/a	Robinson (1979)	100										0.05	0.06	[illegible]		2.91

Note: Screen size changes within the table apply to the next line only.

** Average of P.I. for all sieve categories

Table 3.5 Results of the calculation of preservation index for parcels from various group I and II kimberlites described in this study, combined with calculation of preservation index for diamond data from the literature. Different researchers have used differing screen size categories and size changes within the table apply to the next line only. The effect of excluding cubes, macles and irregulars during the calculation of preservation index can be observed for diamonds from this study.

Table 3.6	Octa	Thd	Dodec	Cube	Macle	Irre	UND	N
Star	78	8	0	1	12	0	1	322
Messina	55	29	«1	2	4	8	«1	712
Ardo	40	39	«1	6	5	3	6	313
Frank Smith	29	44	«1	12	6	6	3	289
Samada	19	53	0	«1	3	5	19	481
Leicester	17	56	0	17	«1	10	«1	826

Table 3.6 The number of diamonds in each parcel with the percentages of each morphology present. Note the variations in the percentages of cubes and macles in the different parcels.

Predicted Diamond Preservation

Locality	Predict. Preserv.	Preservation Index (P.I.)	Approximate Location	Known Grade (carats/100 tons)
Tshibua	G	No Data	Zaire	?High?
Kamfersdam	I	0.11	Kimberley, RSA	?14?*1
Orapa	I	0.11	Botswana	67*3
Jwaneng	I	0.21	Botswana	70-80*3
Premier	I	0.37	Mpumalanga, RSA	30*3
Bultfontein	P/I	0.22	Kimberley, RSA	?55?*1
Wesselton	I	0.04	Kimberley, RSA	?41?*1
Frank Smith	I	0.38	Barkley West, RSA	5-10
Samada (Kaalvallei, New Robinson)	P/M	0.30	Welkom, RSA	7*2
Leicester/ Balmoral	I/P	0.22	Barkley West, RSA	8
Kao	I/P	0.20	Lesotho	?low?
Good Hope	P/M	No Data	Barkley West, RSA	?
Andries	M	No Data	Barkley West, RSA	?
Last Hope	P/M	No Data	Barkley West, RSA	?
Victoria	M	No Data	Barkley West, RSA	?

Table 5.1 Predicted diamond parcel preservations for selected southern African localities with known preservation index (P.I.) and grade. " Predicted Preservation" codes are: G = good, I = intermediate, P = poor, M = marginal.

*1 Wagner (1914)
*2 Gold (1984)
*3 Gurney and Zweistra (1995)

FIGURES

(i)

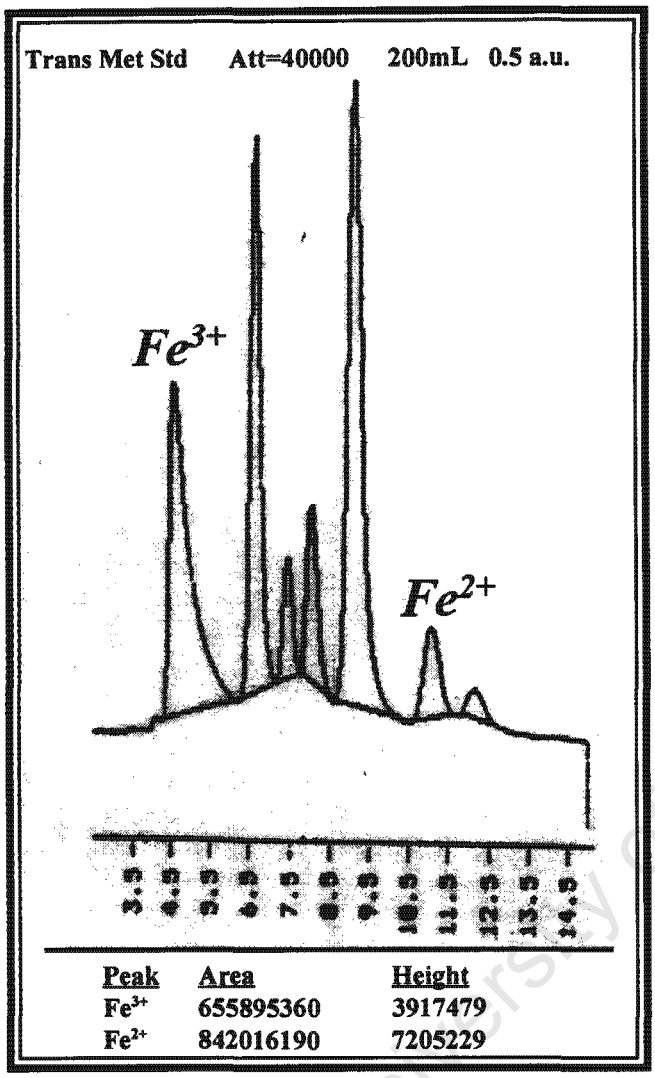

Peak	Area	Height
Fe^{3+}	655895360	3917479
Fe^{2+}	842016190	7205229

(ii)

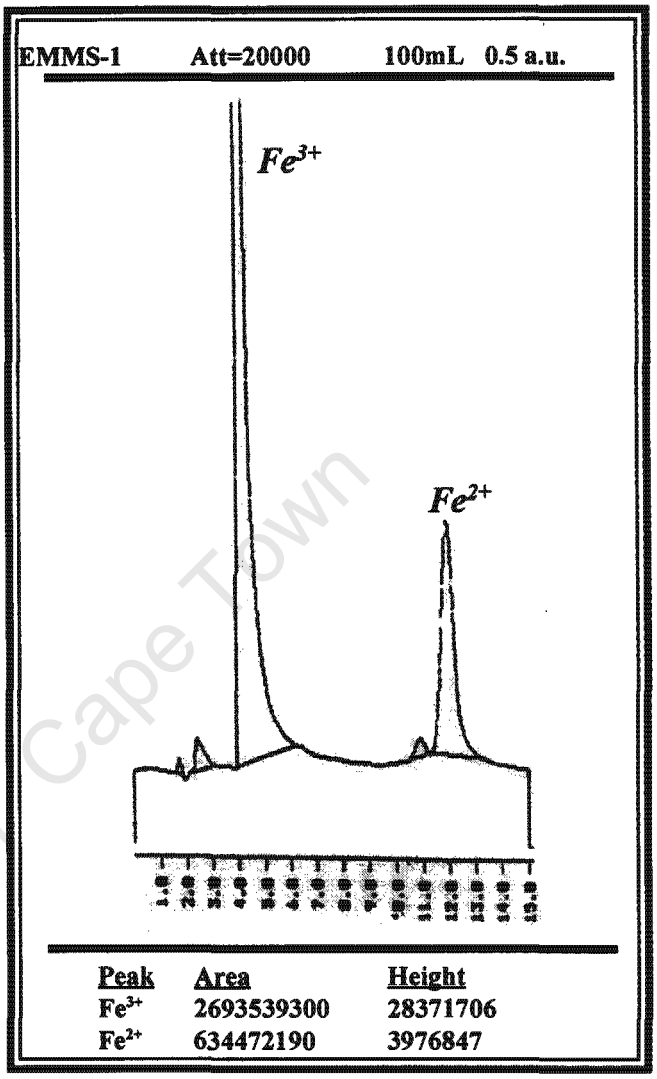

Peak	Area	Height
Fe^{3+}	2693539300	28371706
Fe^{2+}	634472190	3976847

Figure 2.1 (i) Transition metal standard stock solution, prepared prior to analysis, and used to confirm sensitivity and shape of peaks, and (ii) A synthetic diopside (EMMS-1), which has been prepared at high temperatures with no attempt to exclude oxygen. This sample has very high Fe_2O_3/FeO

(i)

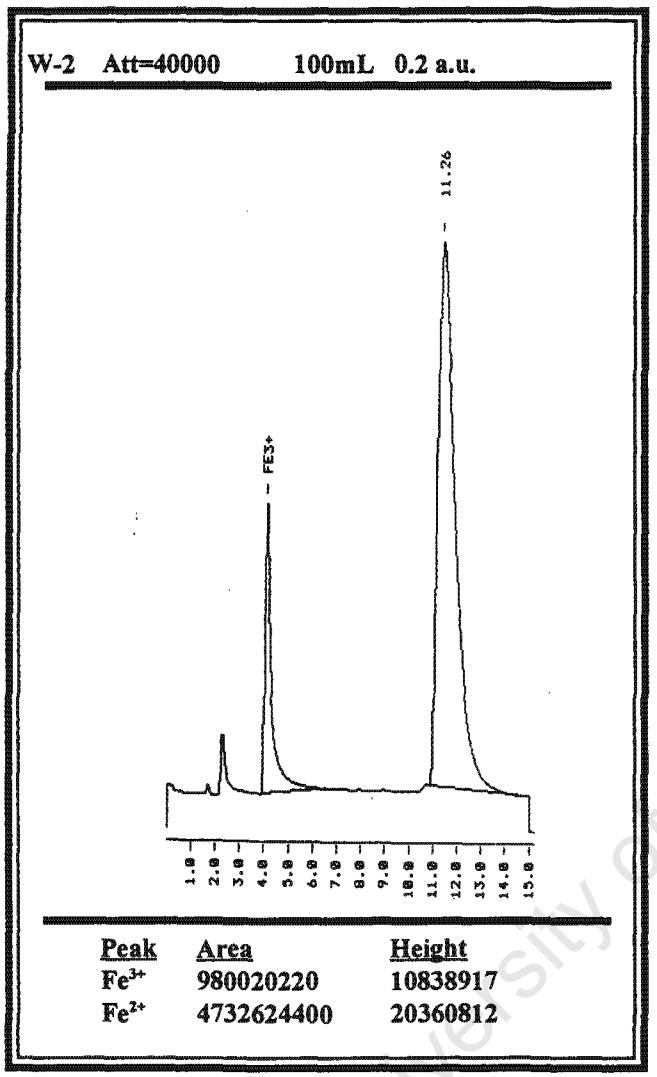

Peak	Area	Height
Fe^{3+}	980020220	10838917
Fe^{2+}	4732624400	20360812

(ii)

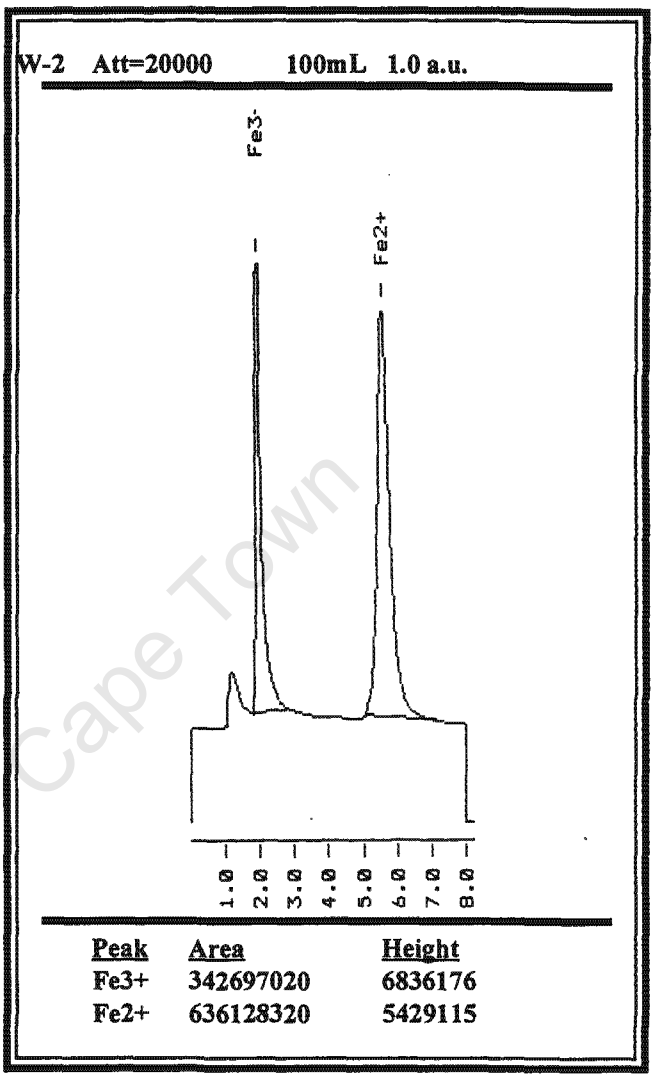

Peak	Area	Height
Fe3+	342697020	6836176
Fe2+	636128320	5429115

Figure 2.2 Ion chromatographic traces for international diabase standard W-2. (i) Standard 1ml/min eluent flow with 15 minute analysis time. (ii) Increased eluent flow rate (2ml/min) with consequent shortened analysis time of 8 minutes. Chromatograhic peaks are well separated and are sharp with tails. The first small peak represents titanium, present in W-2 at concentrations of 1.06% (Govindaraju, 1994).

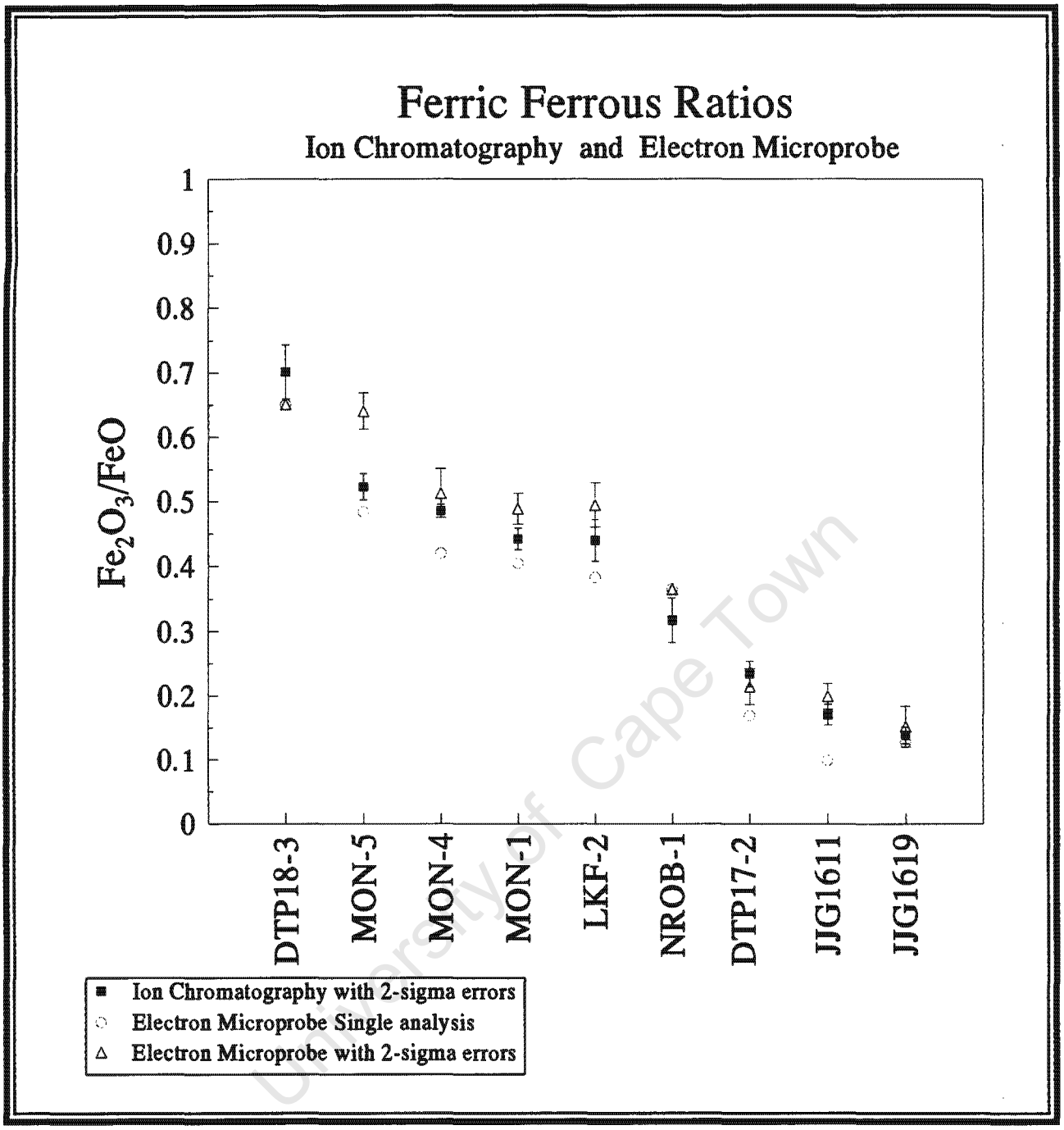

Figure 2.3 Fe_2O_3/FeO for nine ilmenite megacrysts in order of decreasing ratio. Errors are included for electron microprobe and ion chromatography (see table 2.3. Also included are individual analyses of megacryst chips using E.M.P Most samples show good correlation and are within error.

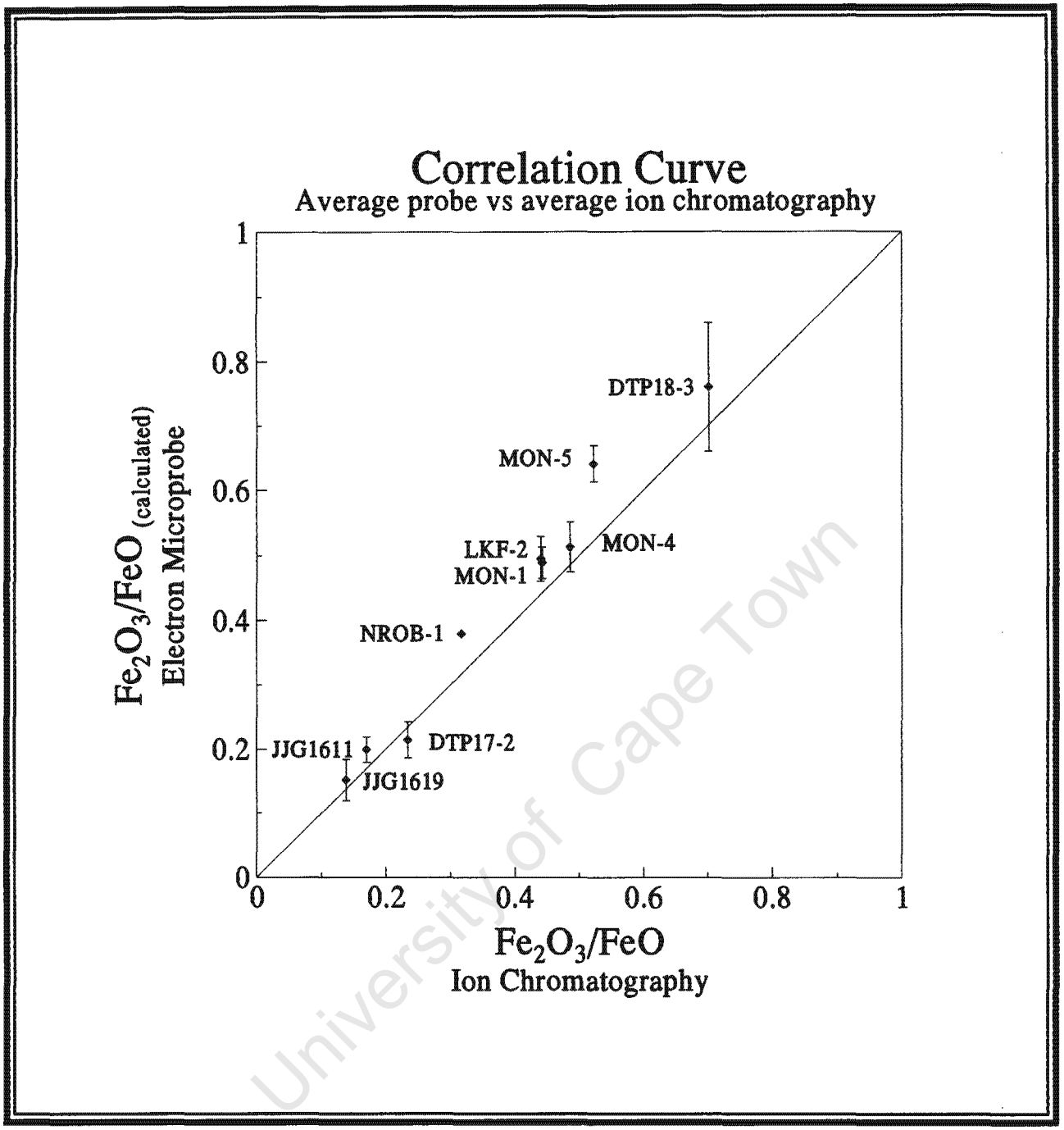

Figure 2.4 Correlation curve for electron microprobe vs ion chromatography for ilmenite megacrysts. A good correlation exists between stoichiometric calculation of Fe_2O_3/FeO from E.M.P analyses and direct determination using I.C.

(i)

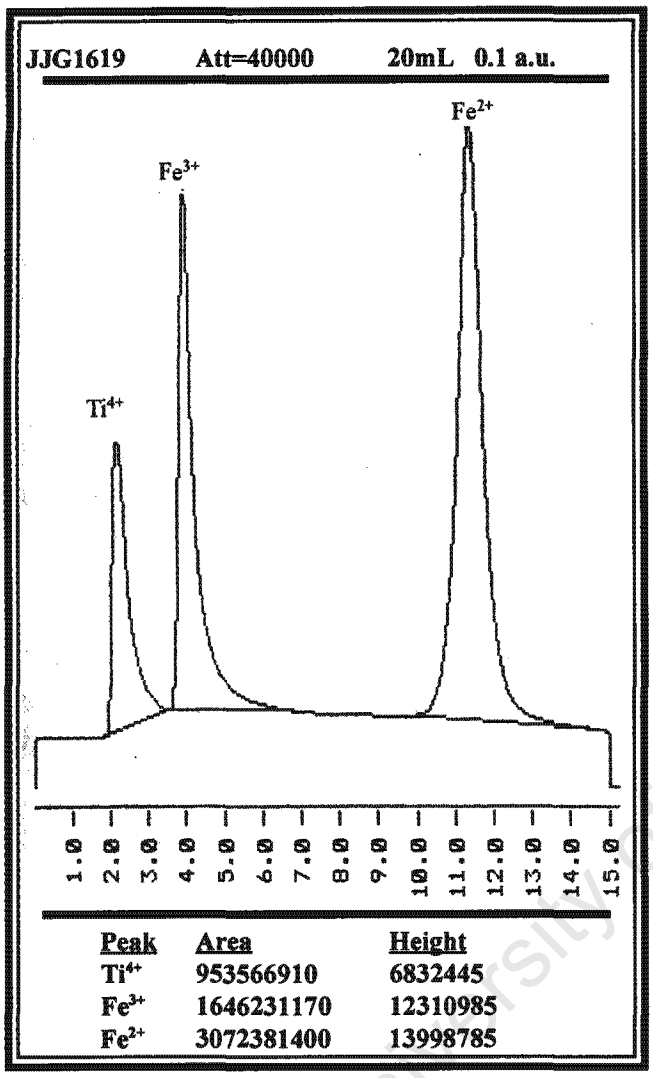

Peak	Area	Height
Ti^{4+}	953566910	6832445
Fe^{3+}	1646231170	12310985
Fe^{2+}	3072381400	13998785

(ii)

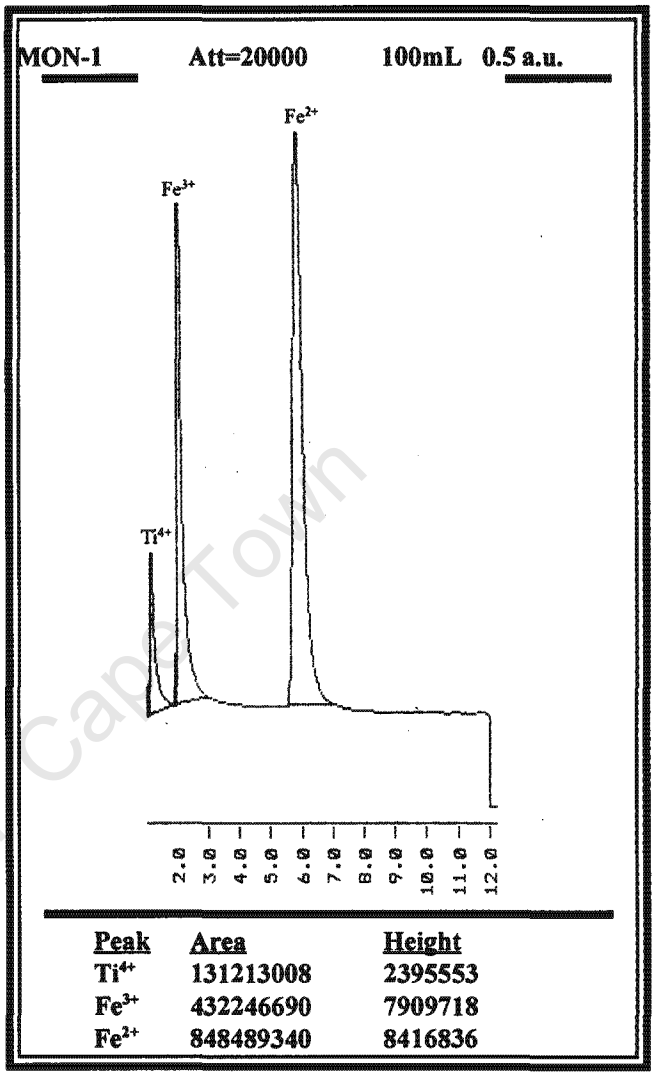

Peak	Area	Height
Ti^{4+}	131213008	2395553
Fe^{3+}	432246690	7909718
Fe^{2+}	848489340	8416836

Figure 2.5 Chromatograms of ilmenite megacrysts (i) JJG1619, (ii) MON-4 and (iii) NROB-1. Due to excessive dilutions to bring the iron values to within the linear calibration range of the instrument there is no acid peak. However the Ti^{4+} peak is large, but with careful integration of the Fe^{3+} peak, precision is maintained.

(iii)

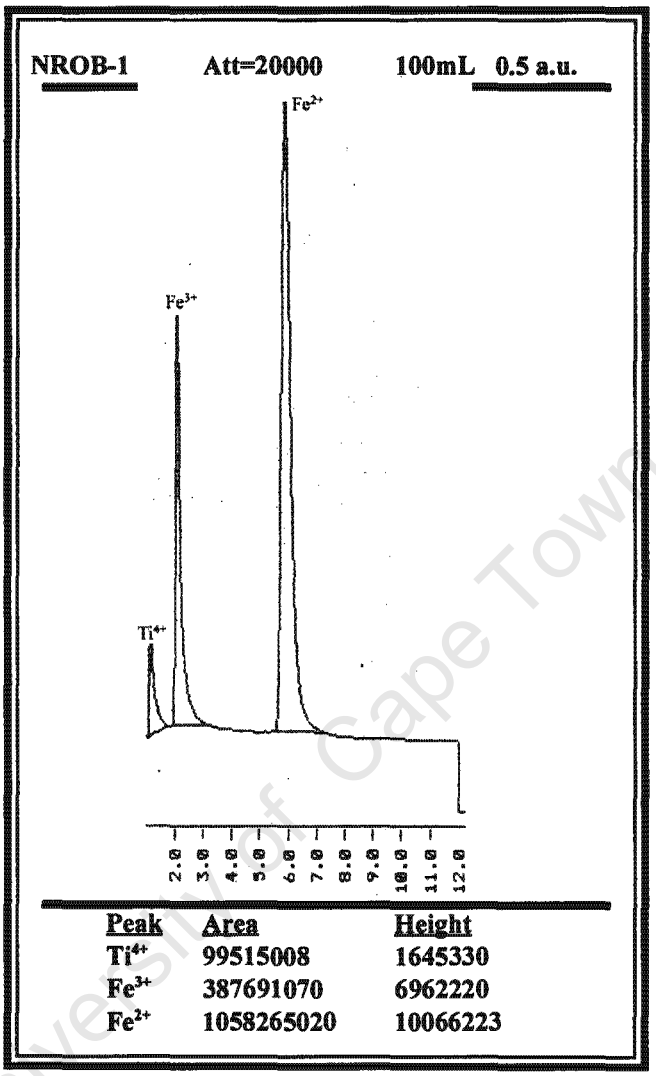

Peak	Area	Height
Ti^{4+}	99515008	1645330
Fe^{3+}	387691070	6962220
Fe^{2+}	1058265020	10066223

Figure 2.5 cont.....

(i)

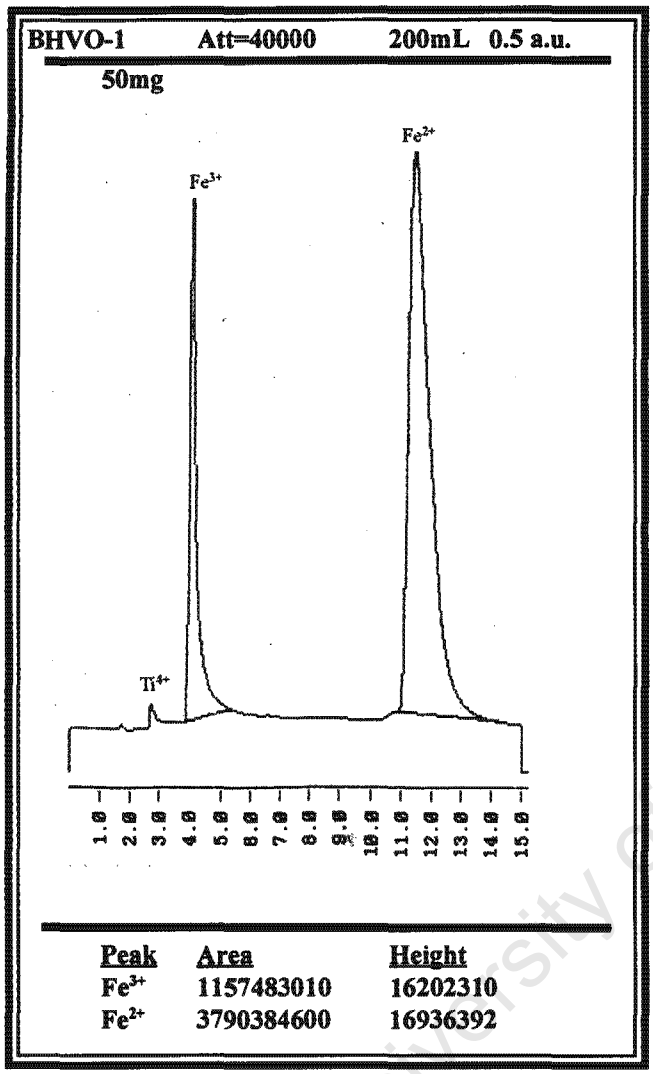

Peak	Area	Height
Fe^{3+}	1157483010	16202310
Fe^{2+}	3790384600	16936392

(ii)

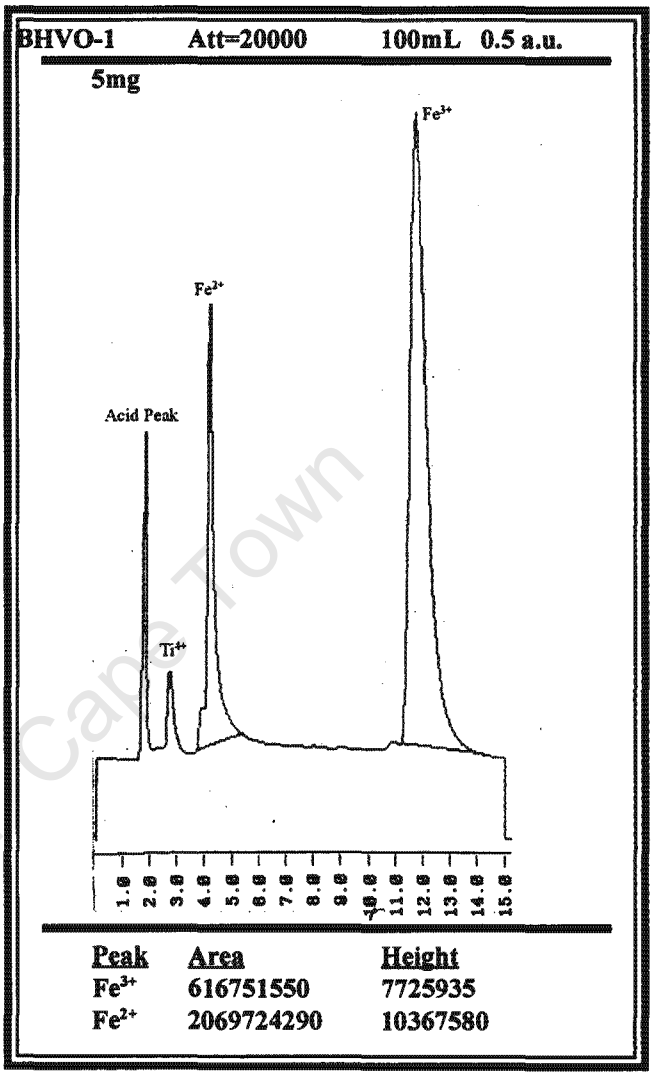

Peak	Area	Height
Fe^{3+}	616751550	7725935
Fe^{2+}	2069724290	10367580

Figure 2.6 Chromatograms for 50mg and 5mg samples of international standard basalt BHVO-1. The peak at 1.5 minutes in chromatogram (ii) is an acid peak resulting from much smaller dilutions. The second peak at 2.7 minutes, also visible, but very small in chromatogram (i), is Ti^{4+} (TiO_2=2.71% in BHVO-1 (Govindaraju, 1994)) and also is more pronounced in (ii) due to less dilution.

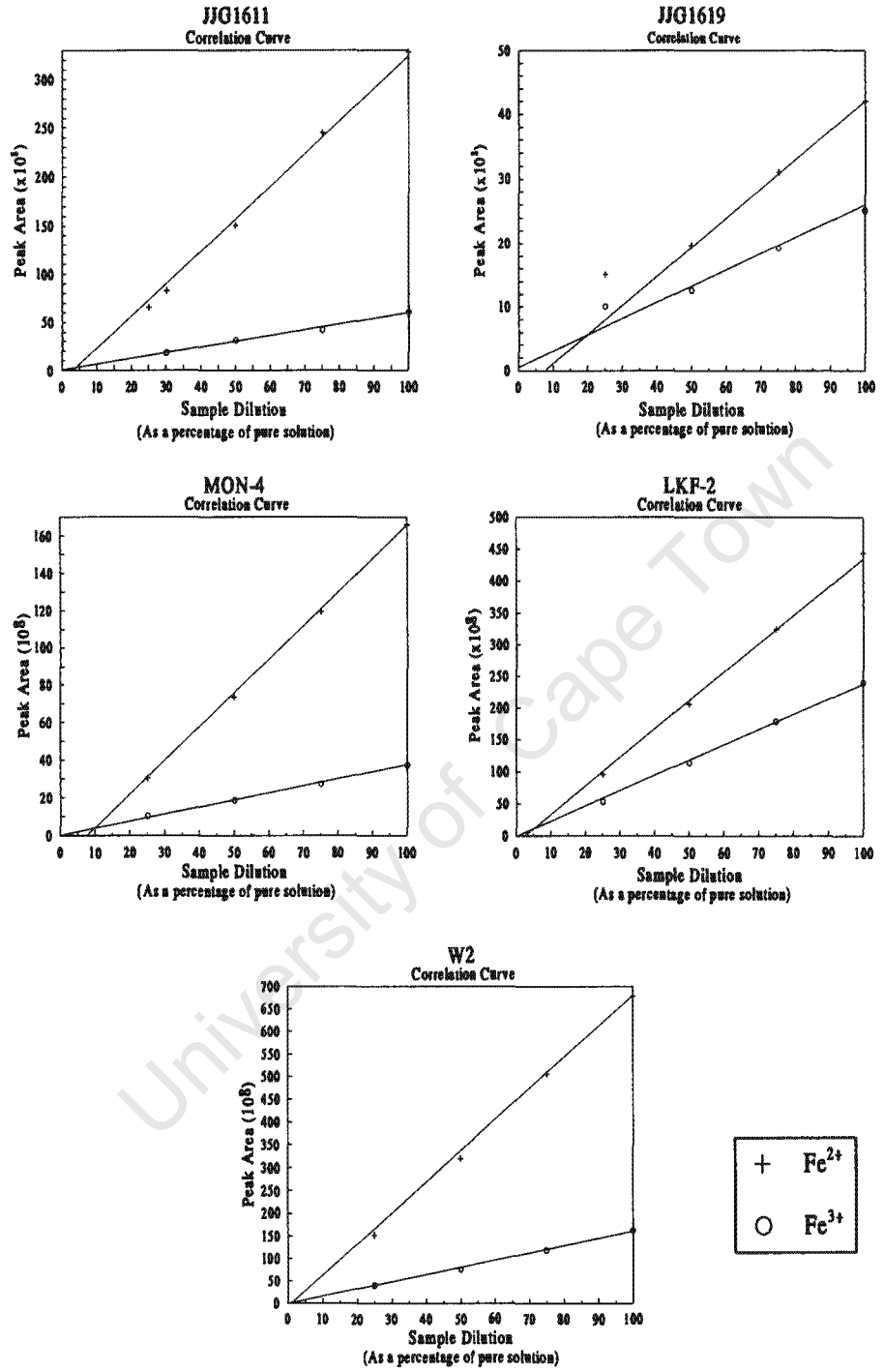

Figure 2.7 Correlation Curves for ilmenite samples JJG1611, JJG1619, MON-4, LKF-2 and international standard W-2. The integrated values for peak area for both Fe^{3+} and Fe^{2+} are plotted against varied dilutions (concentrations) of the same sample and show good correlations and intersect the axes close to the origin.

Common Forms of Diamond

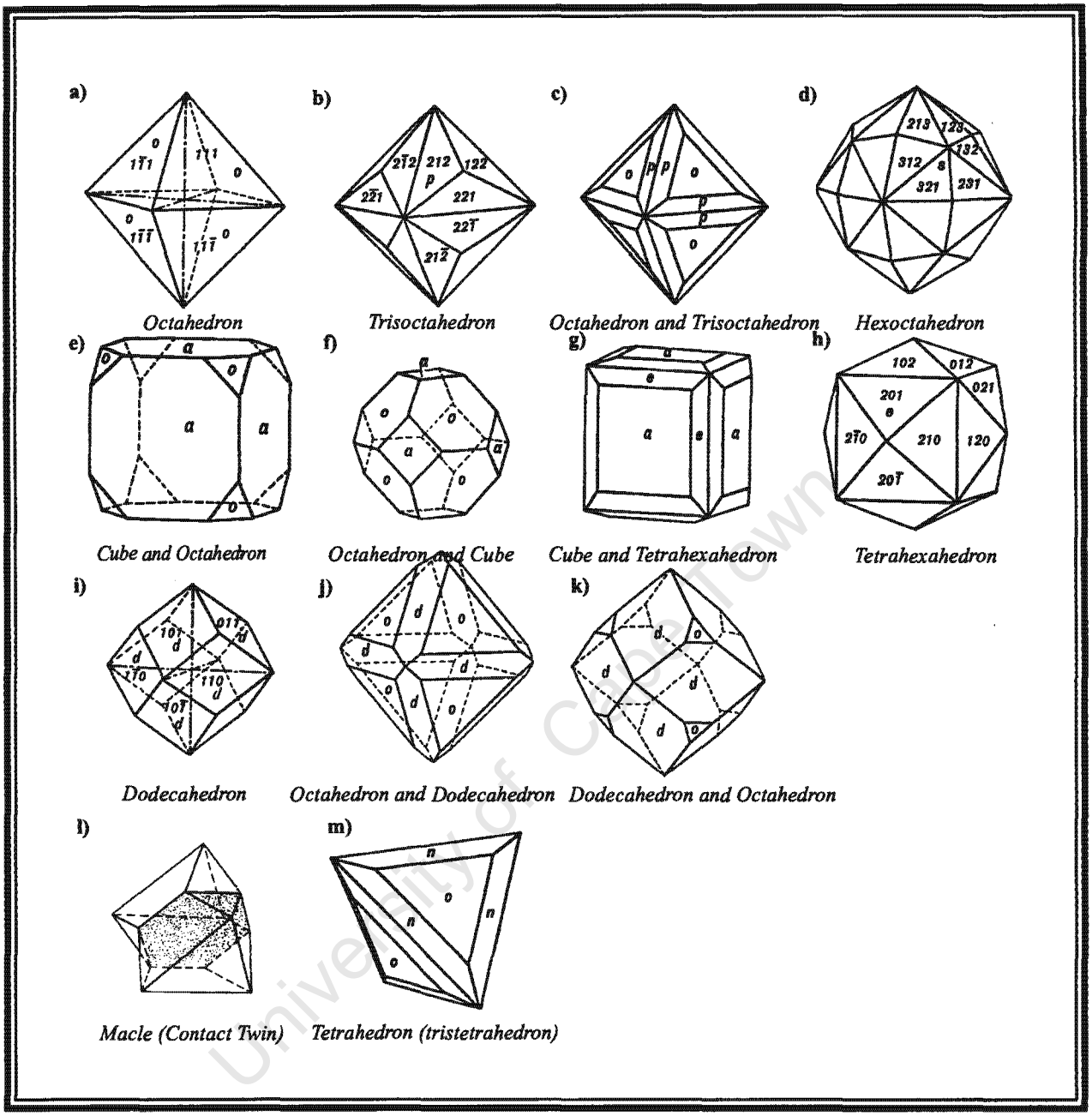

Figure 3.1 Common crystal forms and potential combinations of forms in diamond. (taken from Hurlbut and Klein, 1985).

Row 1: **a)** Octahedron, **b-c)** Trisoctahedron and octahedron combinations which produce laminated (stepped) octahedrons and **d)** Hexoctahedron -theoretical secondary resorbtion form of an octahedron (Sunagawa, 1984).

Row 2: **e-f)** Cube-octahedron combinations, **g)** Combination of cube and tetrahexahedron representing the first stages of resorbtion of a cube, **h)** Tetrahexahedron- resorbtion form of a cube(6x4: one original cube face produces 4 new tetrahexahedroid faces) and an octahedron (8x3: one original octahedron face produces 3 new tetrahexahedroid faces).

Row 3: **i)** Dodecahedron- potential resorbtion form of the trisoctahedron, **j-k)** combinations of dodecahedral and octahedral forms.

Row 4: **l)** Macle- contact twin of a octahedron, common to diamond and of variable thickness. **m)** Initial resorbtion form of a tetrahedron, rare primary diamond form.

Diamond Resorbtion Categories

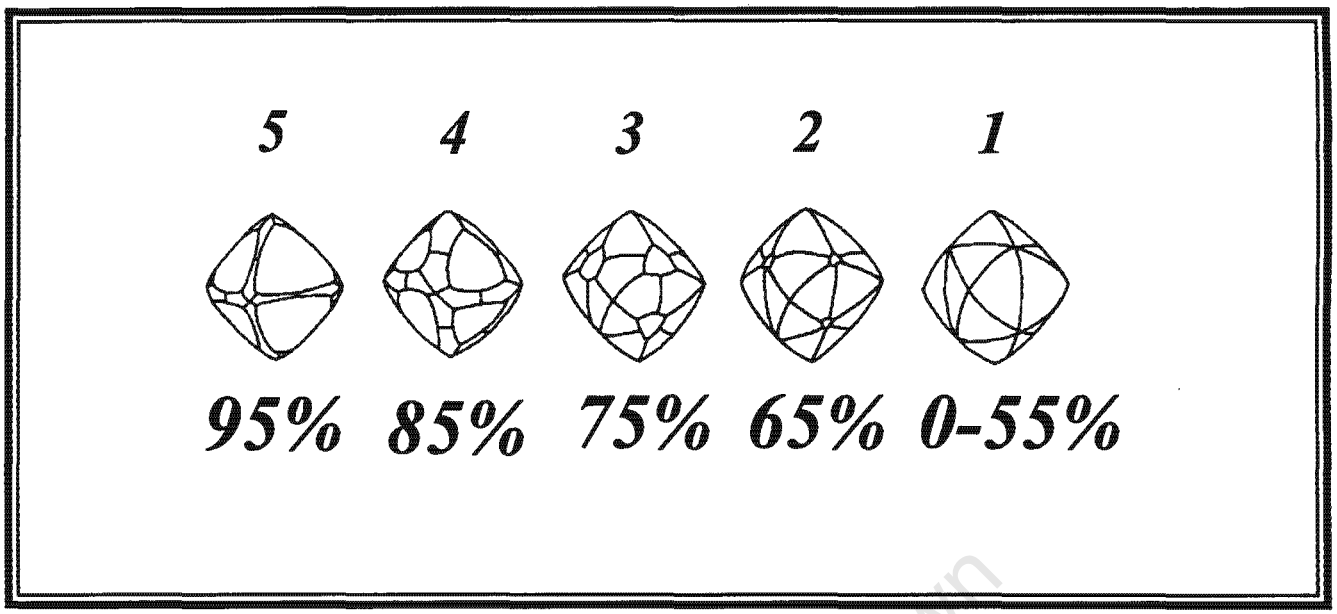

Figure 3.2 Resorbtion categories for the transition from octahedron to tetrahexahedroid (Otter, 1989) with estimates of the percentage of the original diamond remaining for each category (Robinson, 1979).

Octahedron- Tetrahexahedroid Transition

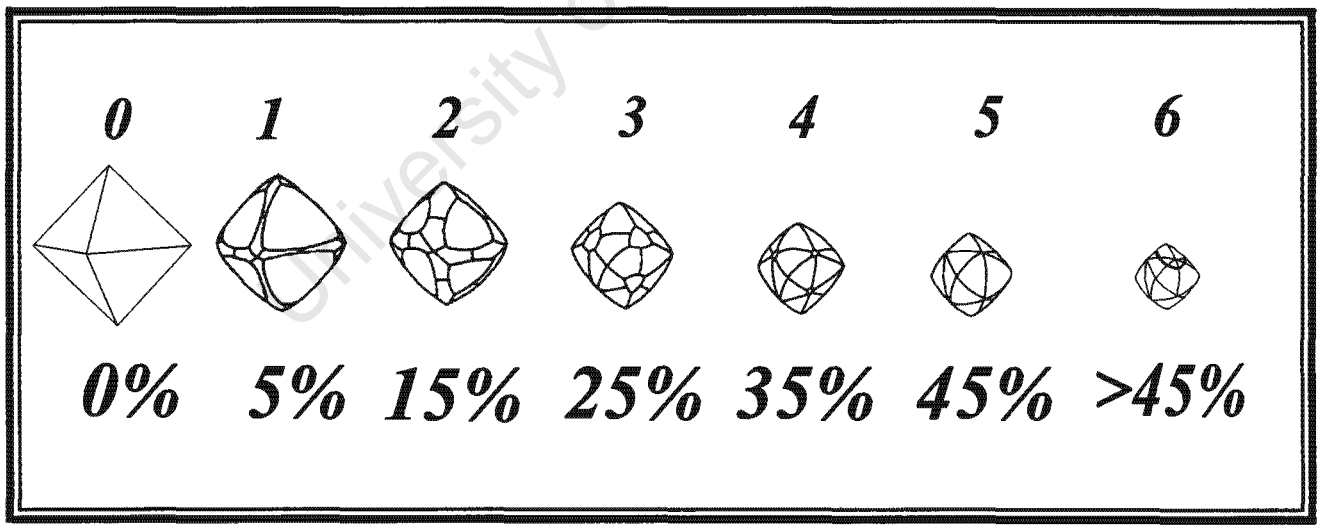

Figure 3.3 Categories representing the percentage loss of mass of diamonds during the transition from octahedron to tetrahexahedroid (after Robinson, 1979). Category 0 represents a pristine octahedron and category 6 a tetrahexahedroid which has lost greater than 45% of its original mass. It is not evident how or whether the form of a diamond changes with successive resorbtion after the diamond becomes a tetrahexahedroid. One obvious mechanism, however, is the formation of deep canyon ruts (figure 3.4 (f) and figure 3.6 (a)), represented in category 6 above.

Figure 3.4

a) Slightly resorbed cube (magnification = 33X), exhibiting smooth, resorbed edges and etched faces. A diagonal fine crack from top left to bottom right displays the begins of rut development in the centre of the face and on the upper corner. The linear depression along the crack consists of tetragonal etch pits, suggesting that in this case the formation of the rut is being caused by etching along the weakness caused by the crack. Resorbtion category (R_c) = 2.

b) Characteristic roughly etched faces and smooth resorbed edges of cubic diamond. Tetragonal etch pits form on faces perpendicular to the crystallographic axes. (Mag= 37X; R_c= 3).

c) Skew octahedron-trisoctahedron combination displaying different sizes of residual octahedral faces. The skew shape of the octahedron results in apparent differential resorbtion (hemimorphism). Growth laminations are observed at the resorbed edges of the faces. A deep rut can be seen at the top of the image. (Mag=106X; R_c=2)

d) Almost pristine octahedron with rounded corners and the beginnings of resorbtion along the edges. (Mag= 150X, R_c=0)

e) Combination of the octahedral and hexoctahedral forms on a partially resorbed octahedron. Heavy etching can be seen on the resorbtion surface. (Mag=170X; R_c=2)

f) Resorbed octahedron. Although there are no remnant octahedral faces, the original octahedral shape has been retained. This suggests the original diamond may have been a stepped (laminated) octahedron (ie. a combination of the octahedron and trisoctahedron). Under these circumstances the observed resorbtion (R_c=5), is probably inflated and should therefore be dropped a category (to Rc = 4). Two deep ruts are observed at the top of the image. (Mag =97X)

...ooOoo...

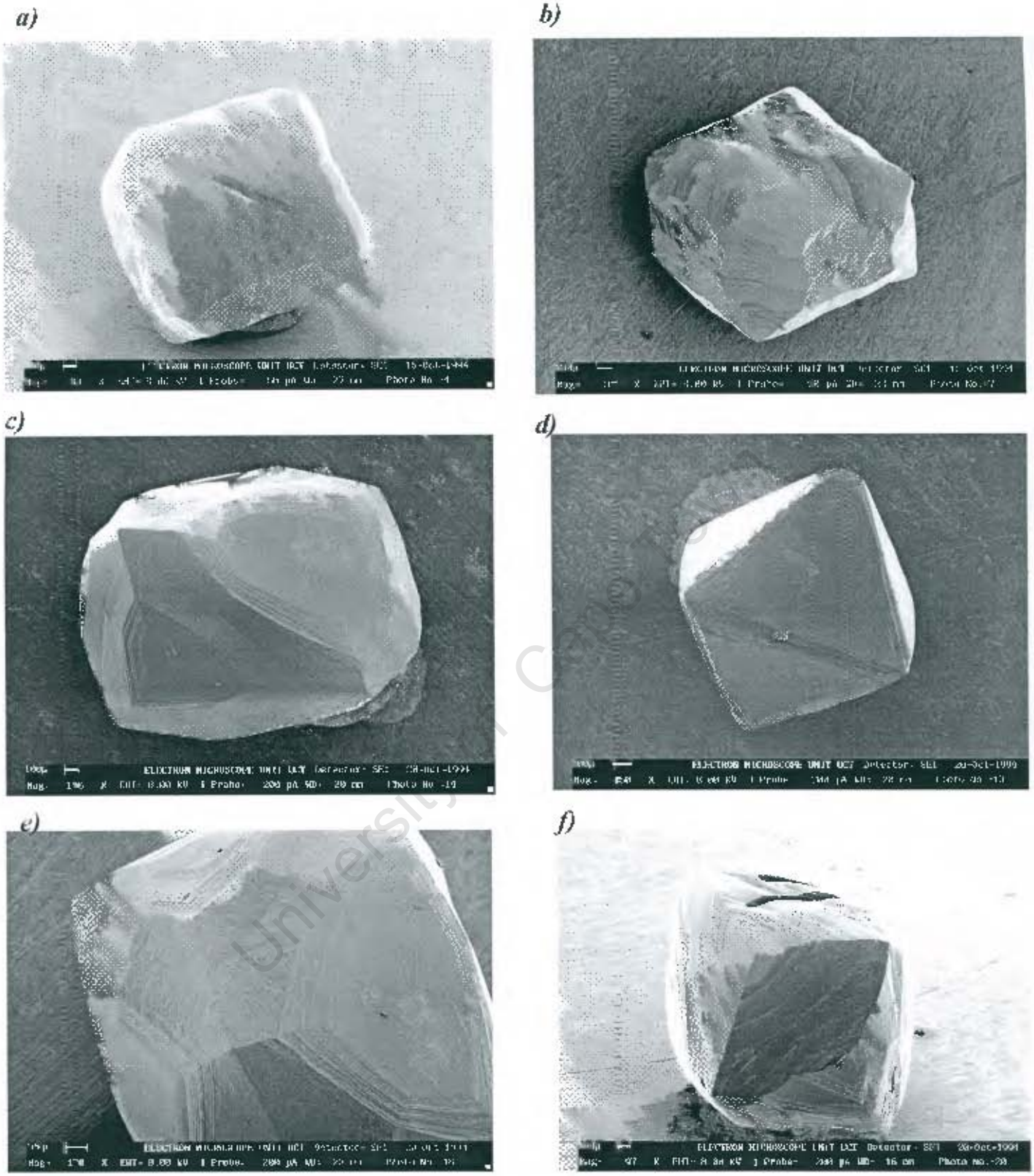

Figure 3.4

Figure 3.5

a) Slightly resorbed octahedron-trisoctahedron combination with a single thick growth step (lamination). In this instance the edges are sunken with respect to the overall shape. (Mag=120X, R_c=1)

b) Interpenetrate twinned pair of finely stepped octahedron-trisoctahedron combinations with uneven growth surfaces. This type of interpenetrate is referred to as a dumbbell twin (this study). (Mag=149X, R_c=0)

c) Pristine octahedron with polished (glassy) faces. The diamond is elongated with respect to the x-crystallographic axis and exhibits tetragonal etch pits normal to the z-crystallographic axis on the top coign. (Mag=80X, R_c=0)

d) Pristine octahedron-trisoctahedron combination with a single thick growth step. Negatively orientated triangular etch pits are obvious on the octahedral faces and sunken edges are well pronounced. (Mag=115X, R_c=0)

e) Rare resorbed tetrahedron. (Mag=80X, R_c=2)

f) Asymmetrical tetrahexahedroid caused by a previously chipped face on the left side of the diamond. Shadow on the resorbed chipped face is a deep rut. Once again, a resorbtion category should be dropped due to the probable original stepped shape of the diamond. (Mag=85, R_c=4)

...ooOoo...

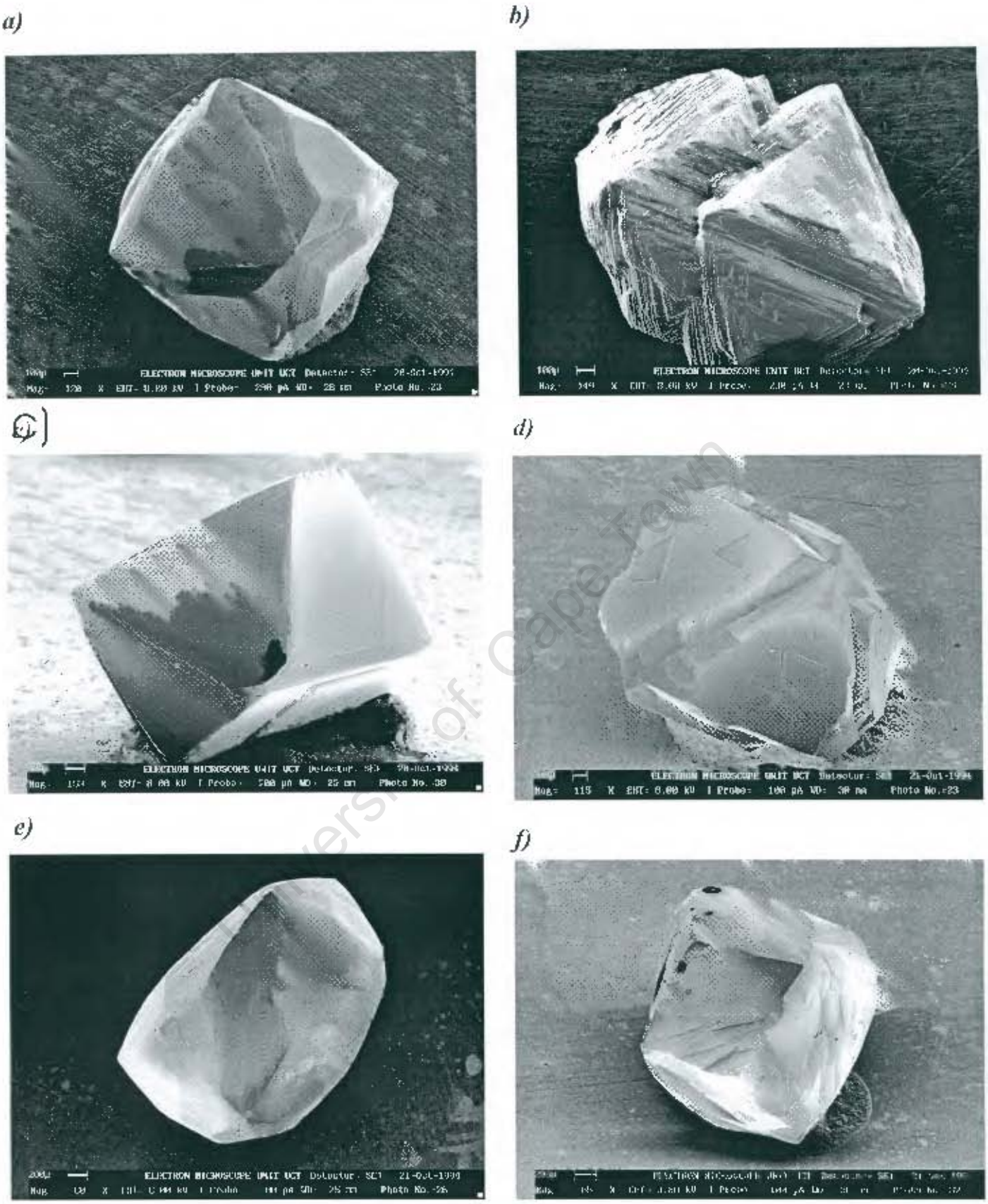

Figure 3.5

Figure 3.6

a) Resorbed contact twin (macle) displaying very deep rutting. (Mag=95X, R_c=6)

b) Flattened hexoctahedroid resulting from the resorbtion of a skew octahedron. (Mag=159X. R_c=5)

c) Equidimensional resorbed octahedron displaying combined octahedron-hexoctahedron forms. (Mag=83X, R_c=2)

d) Aggregate of intergrown finely stepped combined octahedron-trisoctahedron forms. Primary clefts along the grain boundaries would be exploited by resorbtion forming deep ruts. Tetragonal etch pits can be observed at the coigns, perpendicular to the crystallographic axes, and triangular growth features on the faces. (Mag=187X, R_c=0)

e) Resorbed diamond with a dodecahedral shape. Each dodecahedral face, however is subtly divided into two halves, thus making the true form a tetrahexahedroid. The overall shape suggests this diamond may have been derived from a cube. (Mag=163X, R_c=5)

f) Flattened hexoctahedroid or macle with deformation lines and slip scarps crossing growth laminations. Deep holes exist along the edge of the remnant octahedral face. (Mag=30X, R_c=4)

Inside Cover) Highly resorbed diamond which has ceased to display any form. The resorbtion mechanism has progressed from a edge and face dominated process to a rut dominated process. Although a resorbtion category of 6 is allocated, the true resorbtion may be nearer to a category 8 or 9 (Mag=42X, R_c=6)

...ooOoo...

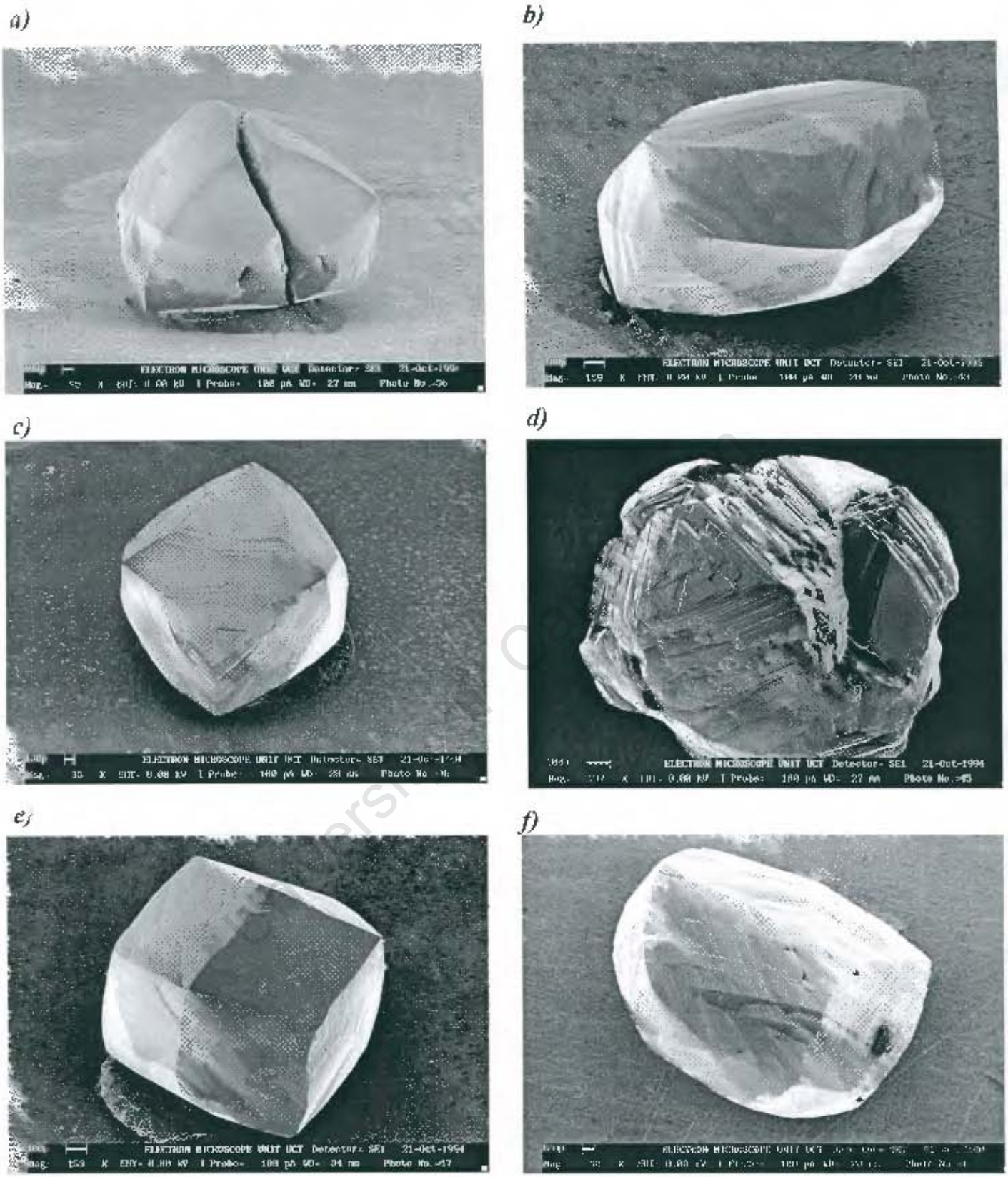

Figure 3.6

Parcel Size Distributions

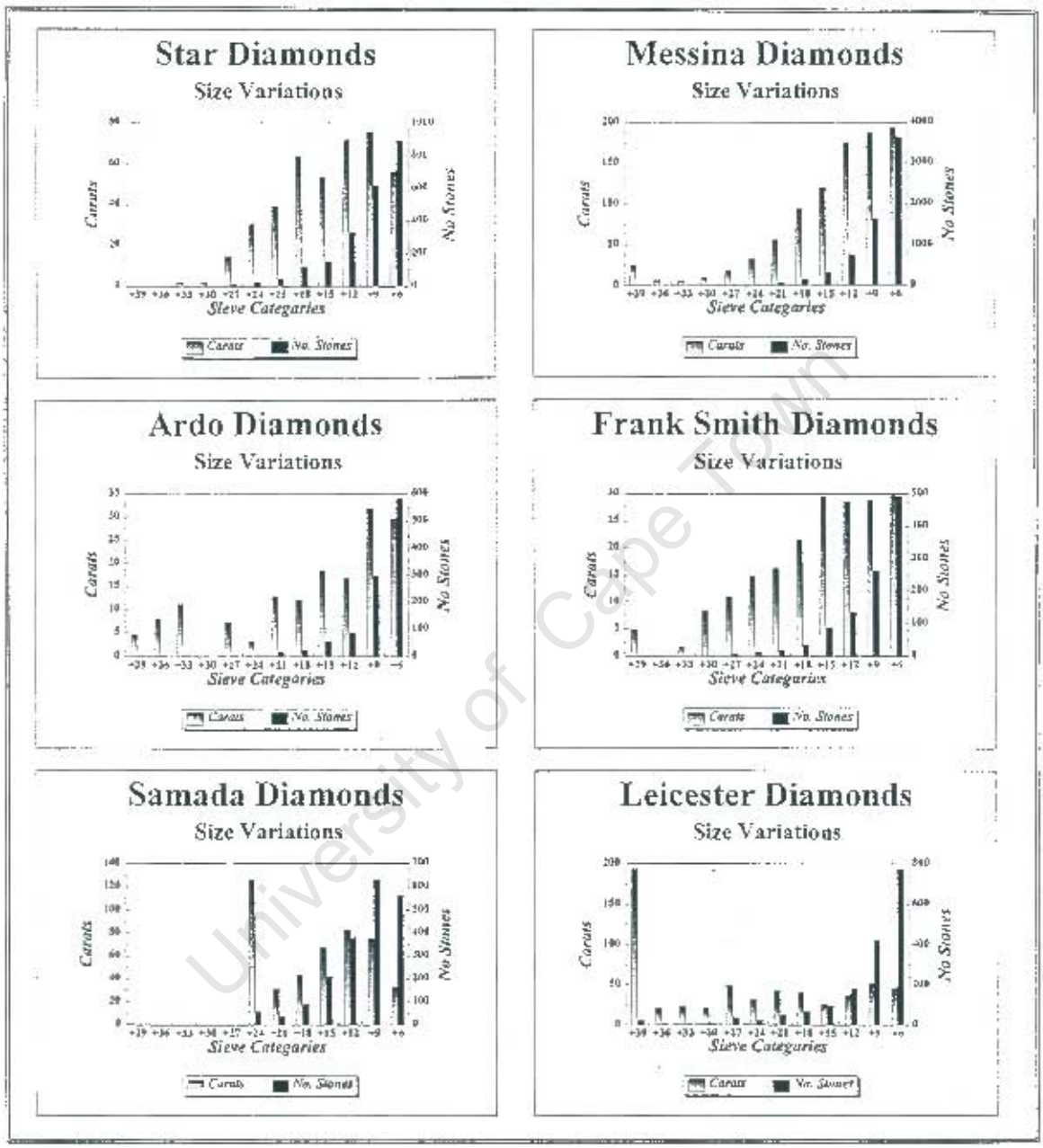

Figure 3.7 Variability of number of stones and weight with size for diamond parcels from Star, Messina Investments (Bobbejaan), Ardo (Exselsior), Frank Smith, Samada and Leicester.

Variations in Preservation Index and Weight per Stone

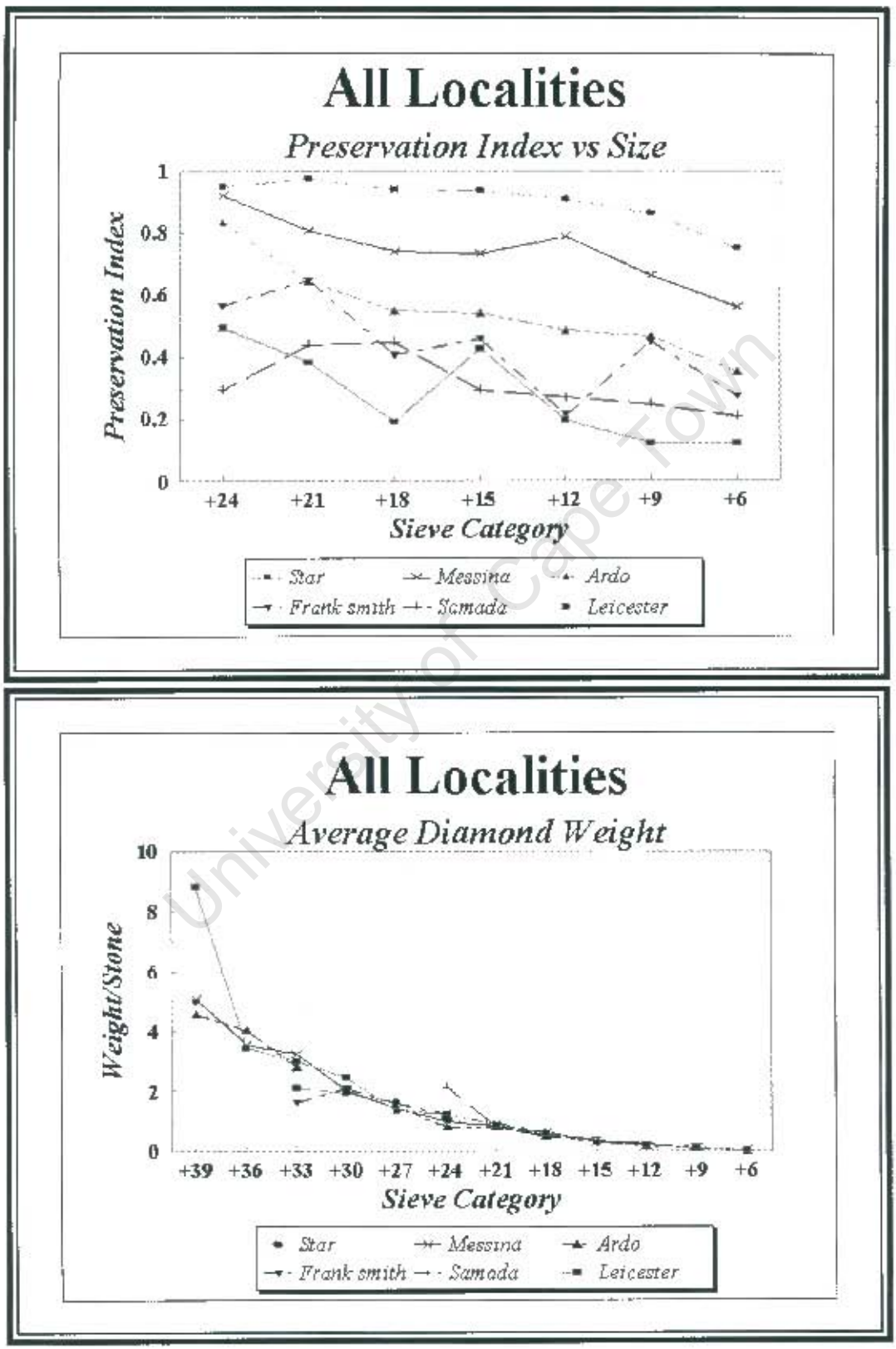

Figure 3.8 a) Variation of preservation index with size for parcels of diamond from Star, Messina, Ardo, Frank Smith, Samada and Leicester.
b) Variation of Average weight per diamond with size for parcels from Star, Messina, Ardo, Frank Smith, Samada and Leicester.

Parcel Resorbtion Curves

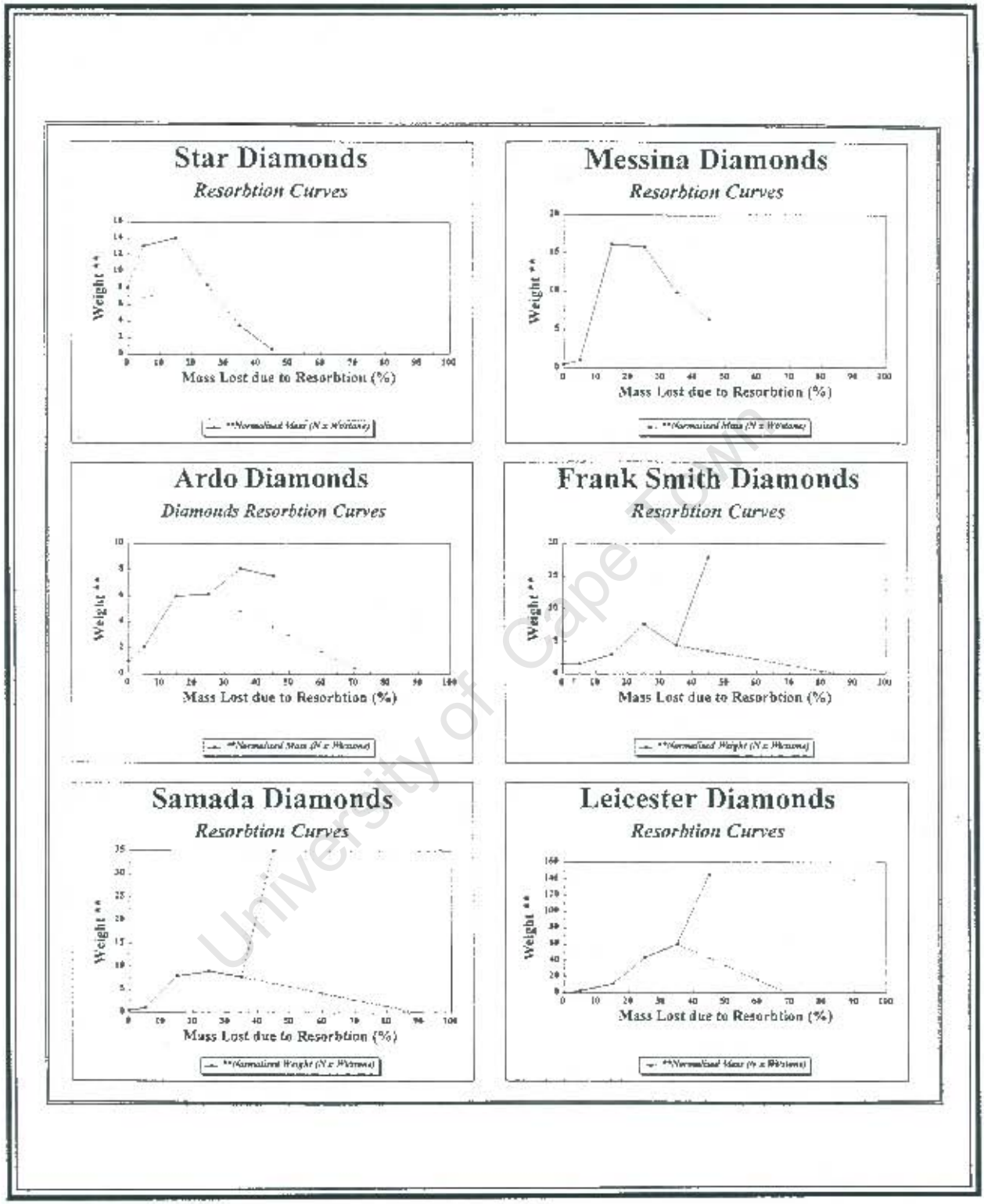

Figure 3.9 Resorbtion Curves for diamond parcels from various localities in the Barkly West and Welkom districts. The plot represent the curve for the normalised mass versus the percentage mass lost as a result of resorbtion. The dotted line represents the correction for resorbtion beyond 45% loss in mass after integration under the curve between 35% and 45%.

Estimation of Initial Mass

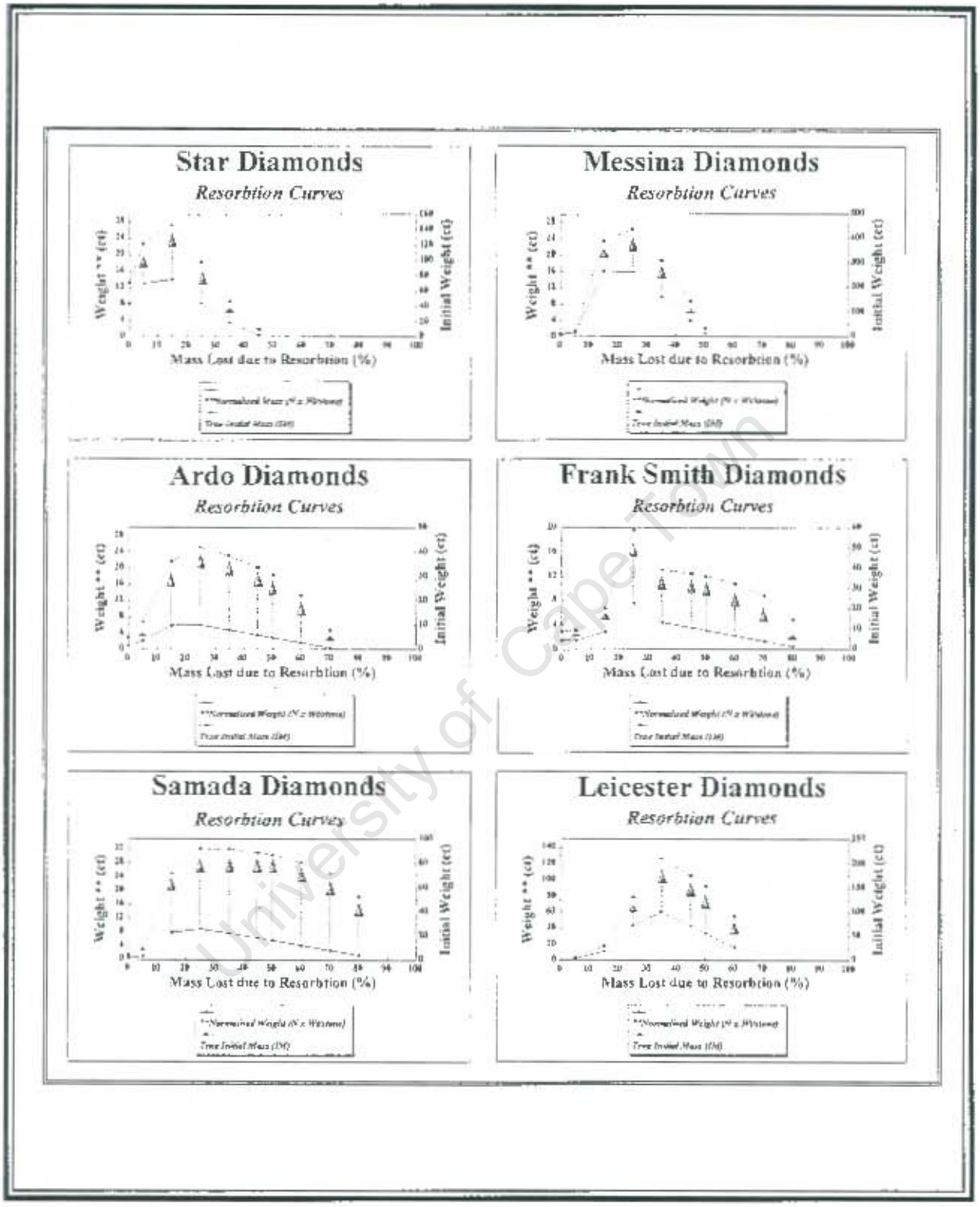

Figure 3.10 Curve of initial weight represents the adjustment of diamond parcels for the loss of mass due to resorbtion. The group II kimberlites, Star, Messina and Ardo, are less resorbed an hence exhibit the least correction. The remaining group I kimberlites extend further into the higher resorbtion categories, with Samada extending further than Frank Smith, consistent with their relative preservation indexes. Extension of the initial mass curve, for Samada, intersects the second y-axis allowing the minimum prediction of the weight of stones which were completely destroyed. Leicester, the least preserved parcel, exhibits the least correction for initial mass of the group I parcels. This is an indication that a large proportion of diamonds have been completely destroyed. The calculation of initial mass is based on existing diamonds and will be deficient if many of these stones have been removed.

Ilmenite Phase Relations

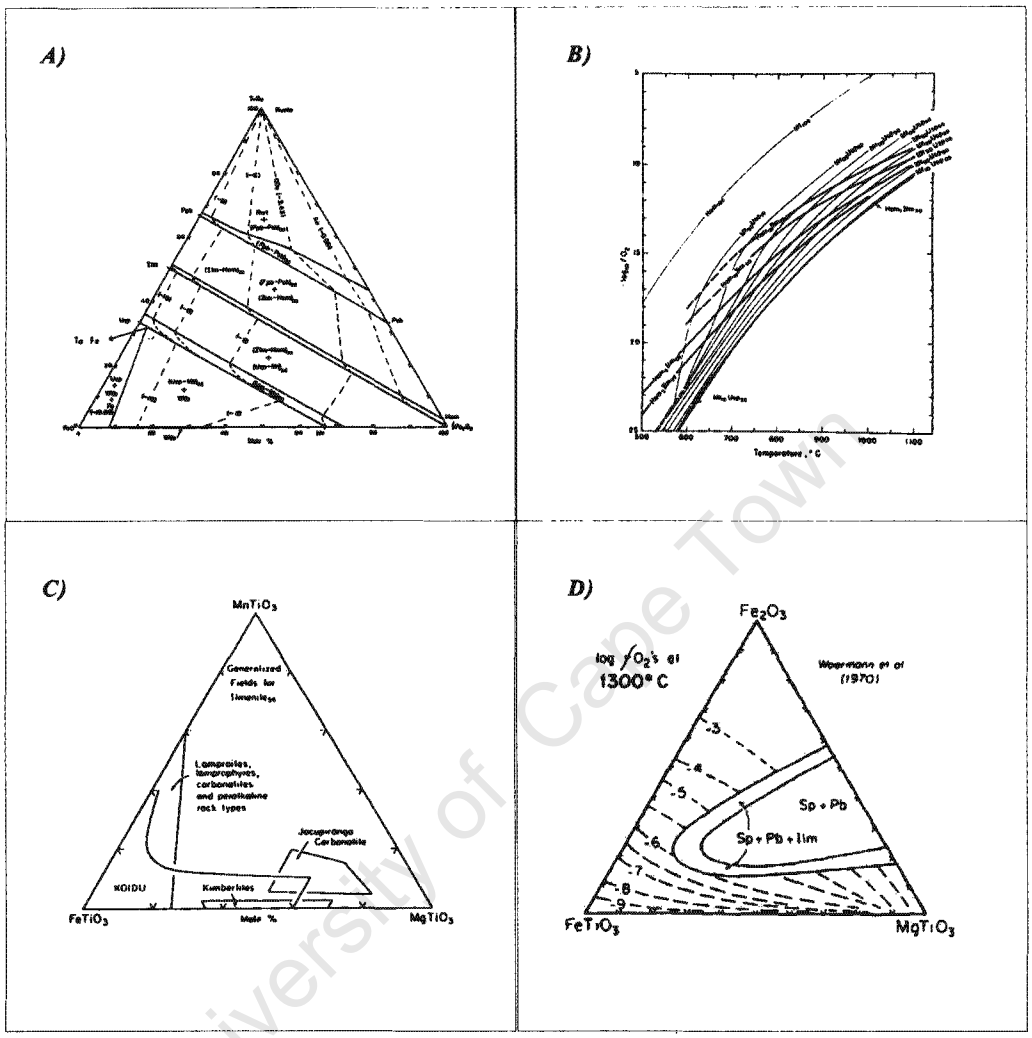

Figure 4.1 *A)* Ilmenite phase diagram for the system FeO-TiO_2-Fe_2O_3 at 1300°C, copied from Lindsley (1976; after Taylor, 1964). *B)* Diagram indicating variation of fO_2 with temperature for compositions of co-existing Ilm-hem solid solutions (Lindsley, 1976). *C)* Ilmenite-pyrophanite-geikielite phase diagram showing fields upper mantle derived ilmenites (Haggerty, 1991). *D)* Oxygen fugacity isobars in the system ilmenite-hematite-geikielite at 1300°C and 1 atm from Haggerty and Tompkins (1984; taken from Woermann et al, 1970). The sp-psb and sp-psb-ilm ternary solvii decreases with temperature and disappears at approximately 700°C.

Stoichiometric Trends in Megacrystic Ilmenites

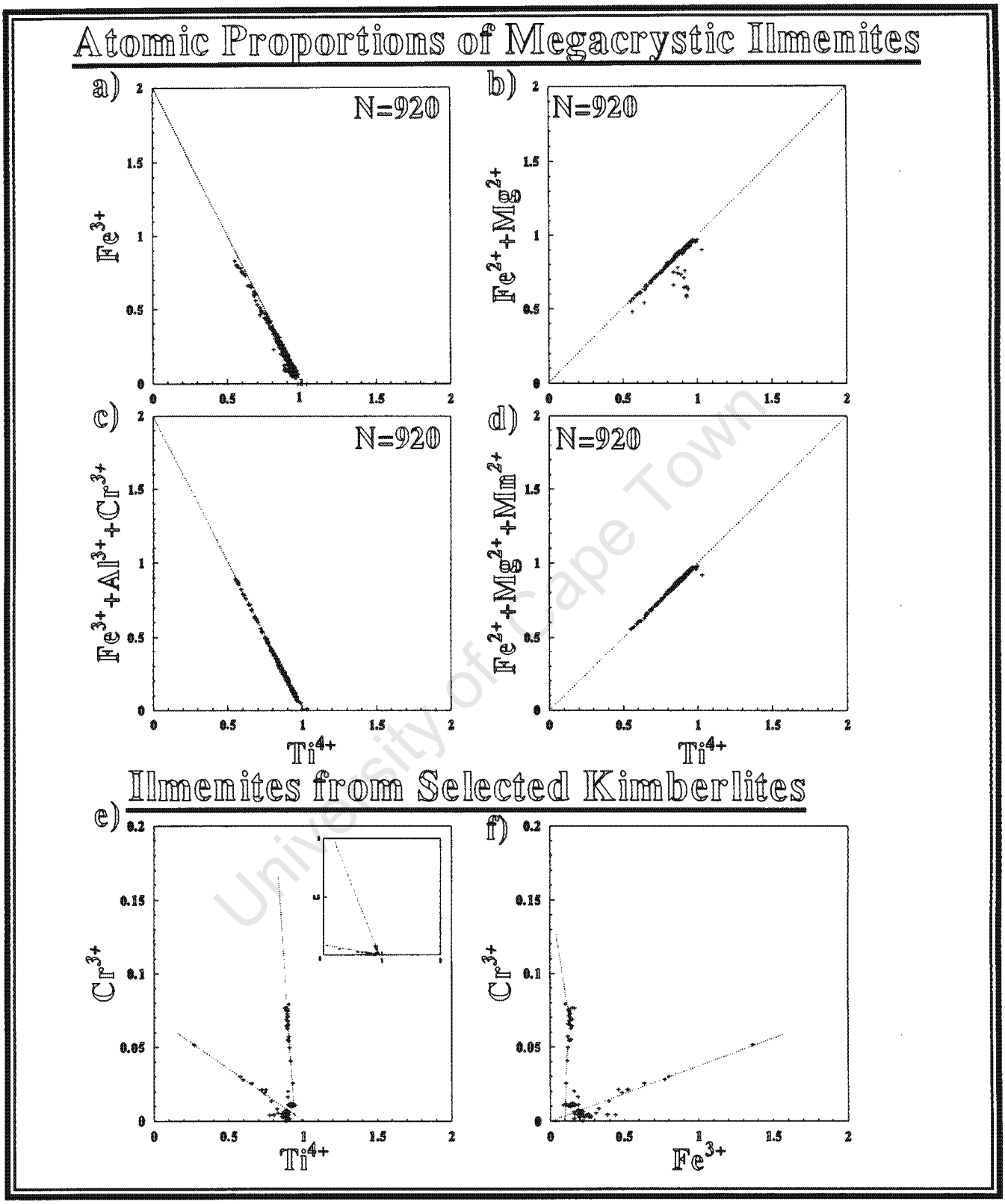

Figure 4.2 Observations of Cation trends: ***(a-d)*** For 920 ilmenite megacrysts from localities in southern, central and west Africa, and ***(e-f)*** Four selected localities: Tshibua (steep trend), Premier and Palmietfontein (inflection) and Iron Mountain (shallow trend), which together represent almost the complete megacrystic ilmenite fractionation trend with compositions from high-Mg, high-Cr to low-Mg, intermediate-Cr.

$(Fe,Mg,Mn)0\text{-}TiO_2\text{-}(Fe,Cr,Al)_2O_3$ Ternary

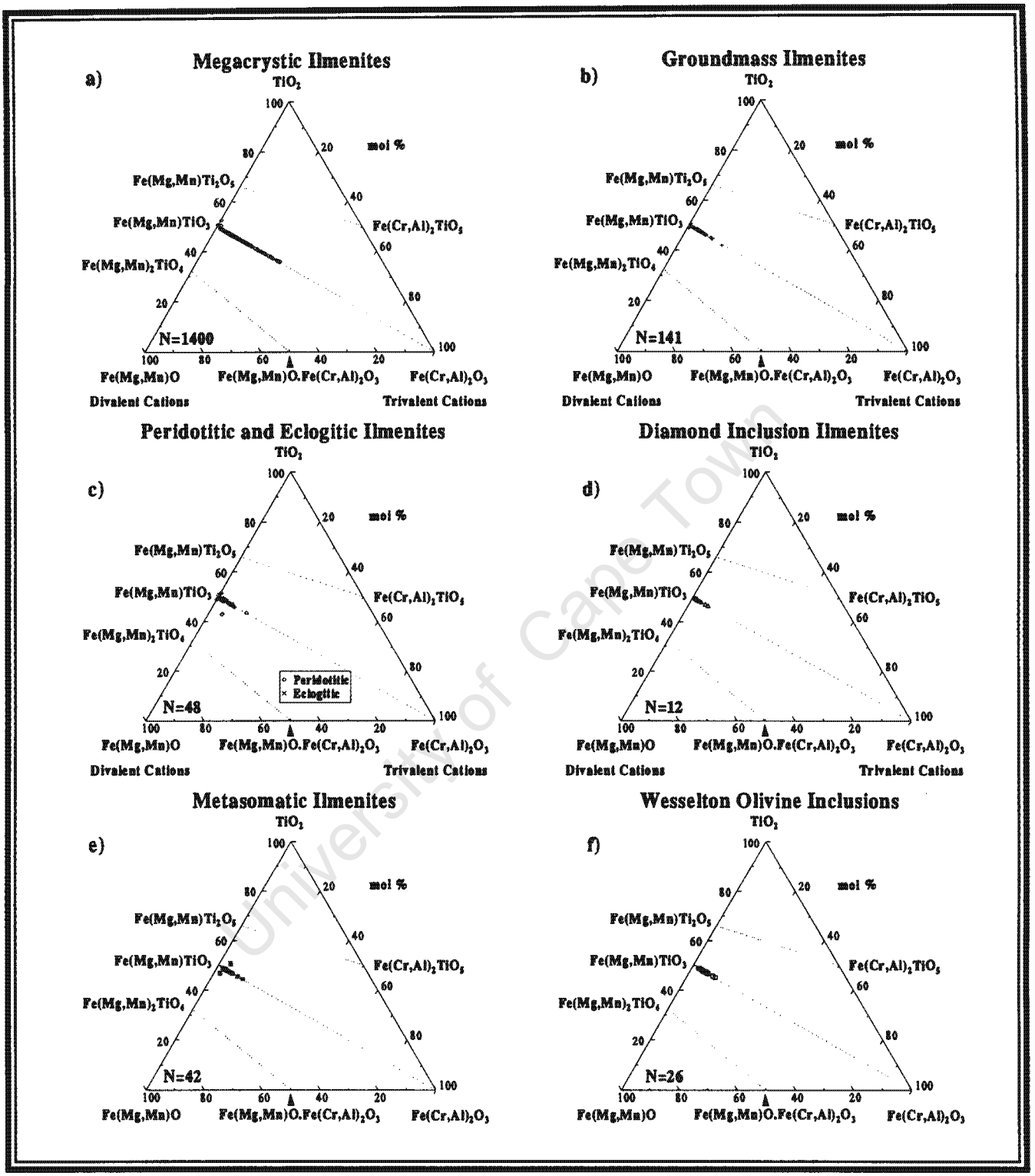

Figure 4.3 $(Fe,Mg,Mn)O\text{-}TiO_2\text{-}(Fe,Cr,Al)_2O_3$ ternary phase diagrams showing compositions of ilmenites from different UMD sources. ***a)*** 1400 megacryst ilmenites analyses from localities around the world. ***b)*** Analyses of 141 ilmenites which have crystallised from kimberlitic magma. ***c)*** Analyses of 48 ilmenites derived from peridotite and eclogite xenoliths. ***d)*** Analyses of 12 rare ilmenite diamond inclusions. ***e)*** Analyses of 42 ilmenites believed to be of metasomatic origin and ***f)*** Analyses of 26 ilmenite inclusions in olivine phenocrysts from the Wesselton kimberlite (Shee, 1985). Most analyses plot along the ilmenite-hematite solid solution.

Trends in Megacrystic Ilmenites

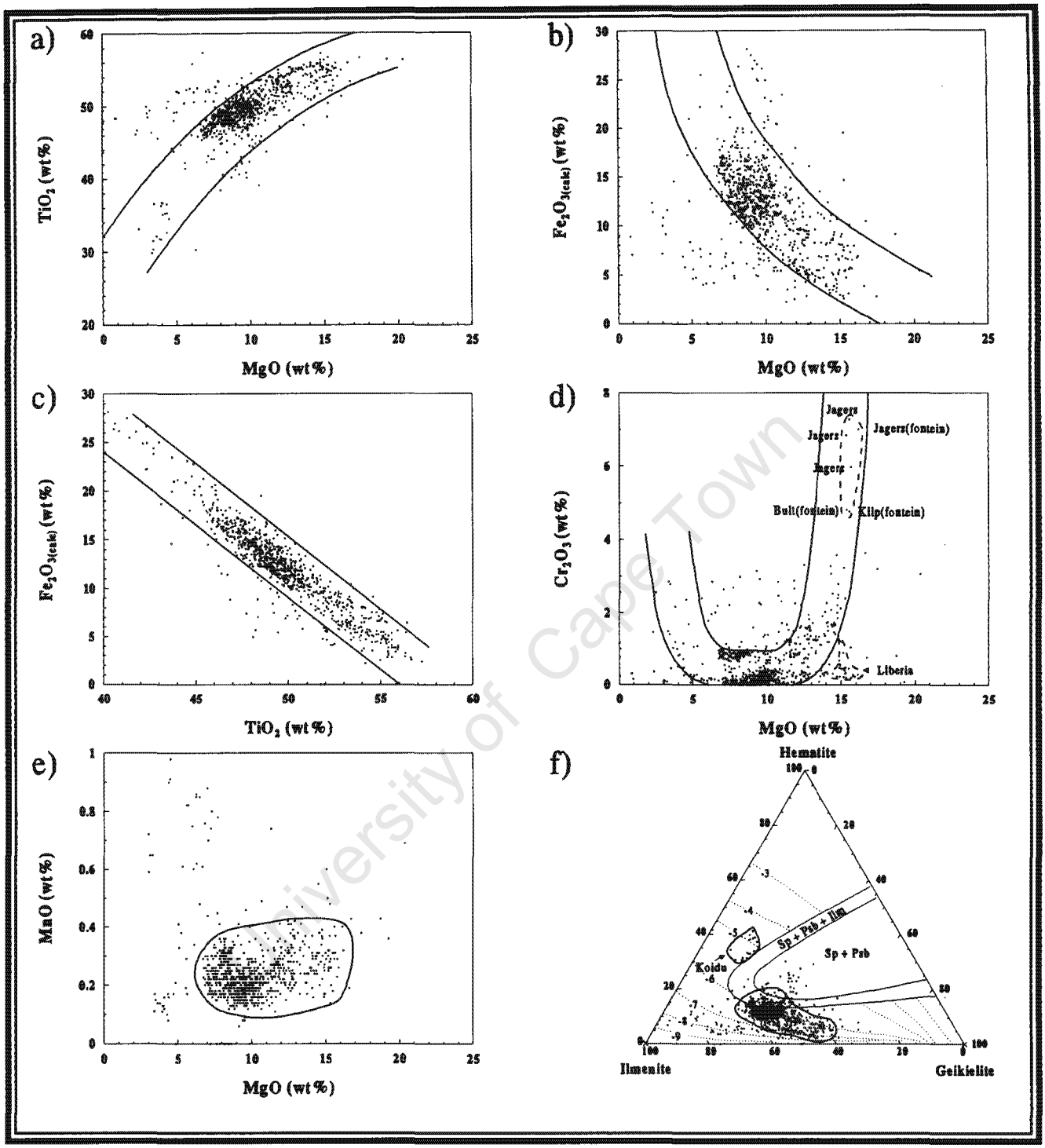

Figure 4.4 Compositional fields and trends based on data from discrete ilmenite nodules and silicate ilmenite intergrowths derived from the megacryst suite, plotted using relationships of important major oxides. Fields are estimated visually and the data has been obtained from the Kimberlite Research Group database (KRGD), University of Cape Town. (Fugacity contours and ternary solvii from Woerman et al, 1969; Haggerty and Tompkins, 1984; Cr-Mg parabola based on Haggerty, 1975)

Trends in Eclogitic Ilmenites

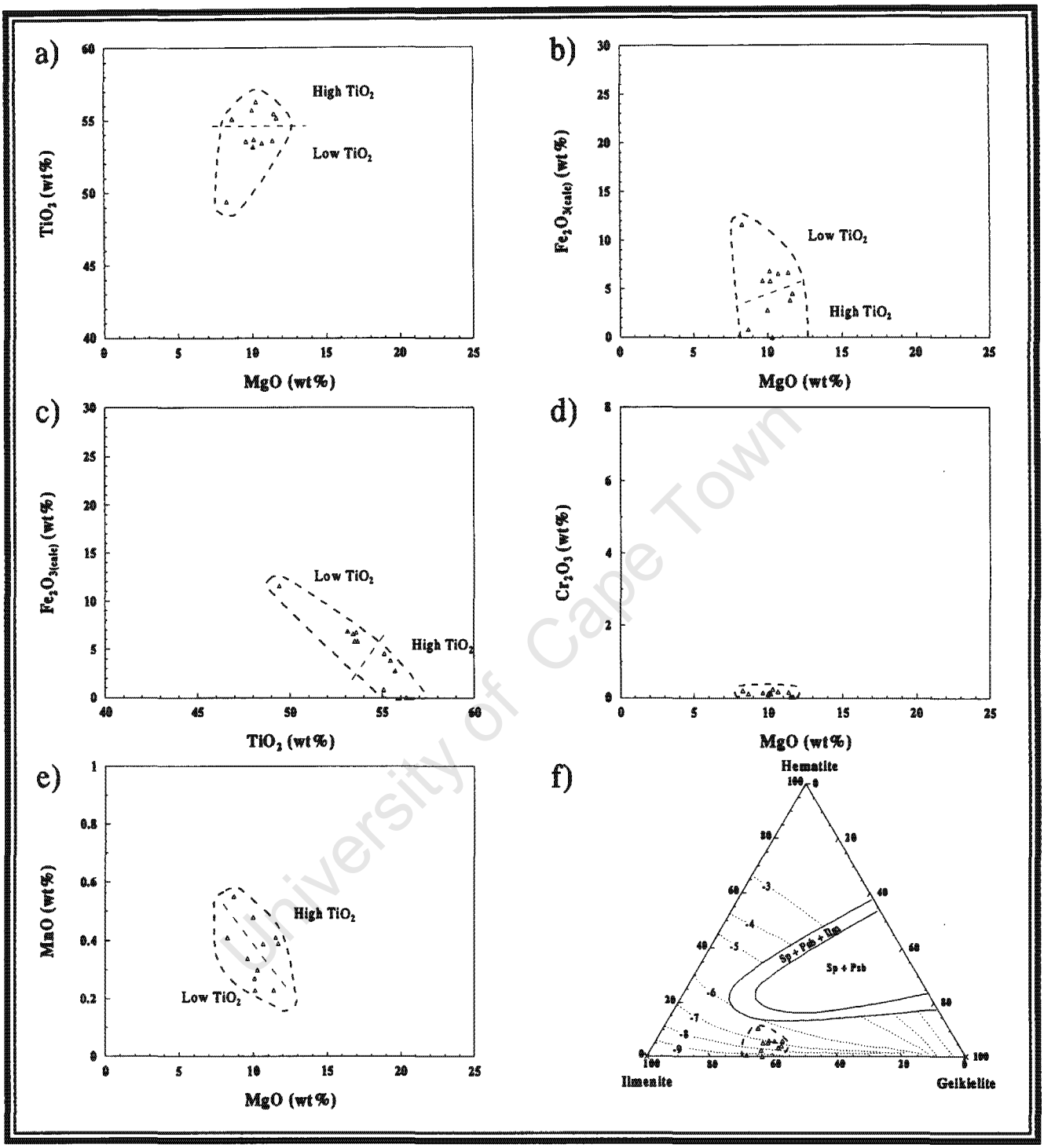

Figure 4.6 Compositional fields and trends based on data for rare ilmenites from eclogite xenoliths, plotted using relationships of important major oxides. Fields are estimated visually and the data has been obtained from the Kimberlite Research Group database (KRGD), university of Cape Town.(Fugacity contours and ternary solvii from Woerman et al, 1969; Haggerty and Tompkins, 1984)

Trends in Peridotitic Ilmenites

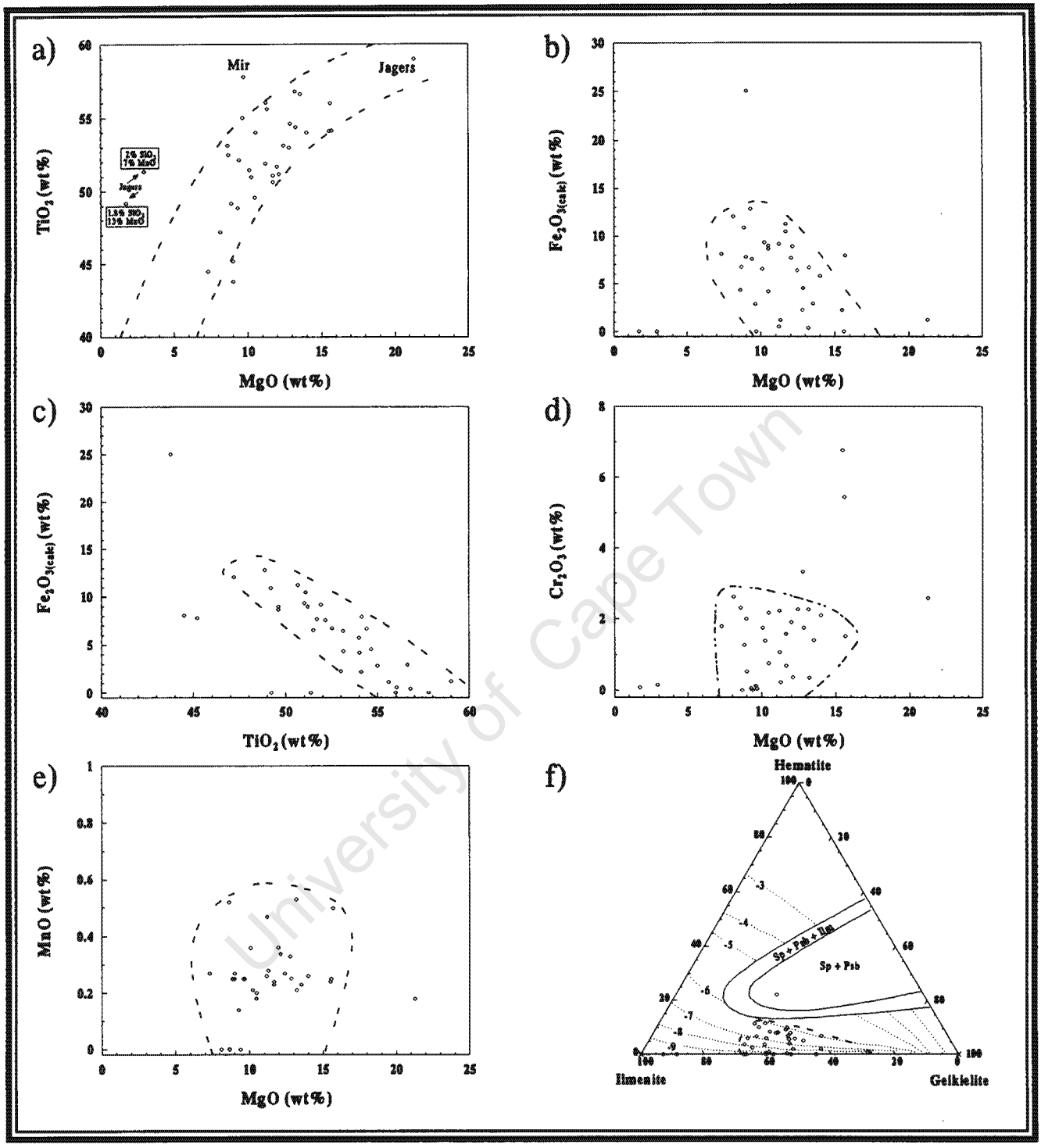

Figure 4.7 Compositional fields and trends based on data for ilmenites from peridotite xenoliths, plotted using relationships of important major oxides. Fields are estimated visually and the data has been obtained from the Kimberlite Research Group database (KRGD), university of Cape Town.(Fugacity contours and ternary solvii from Woerman et al, 1969; Haggerty and Tompkins, 1984)

Trends in Ilmenite Diamond Inclusions

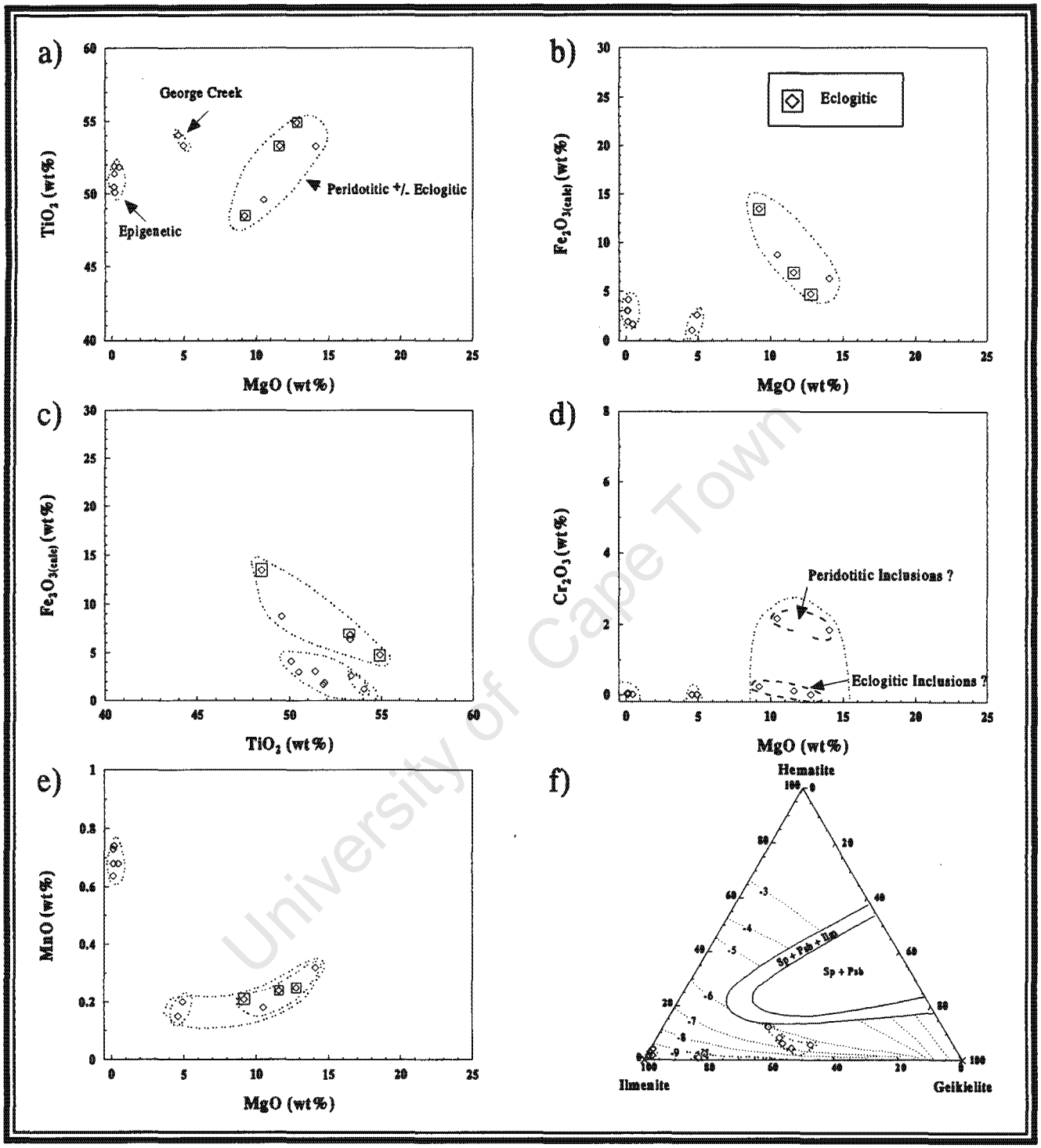

Figure 4.8 Compositional fields and trends based on data for ilmenite diamond inclusions, plotted using relationships of important major oxides. Fields are estimated visually and the data has been obtained from the Kimberlite Research Group database (KRGD), university of Cape Town. (Fugacity contours and ternary solvii from Woerman et al, 1969; Haggerty and Tompkins, 1984)

Trends of Metasomatic Ilmenites

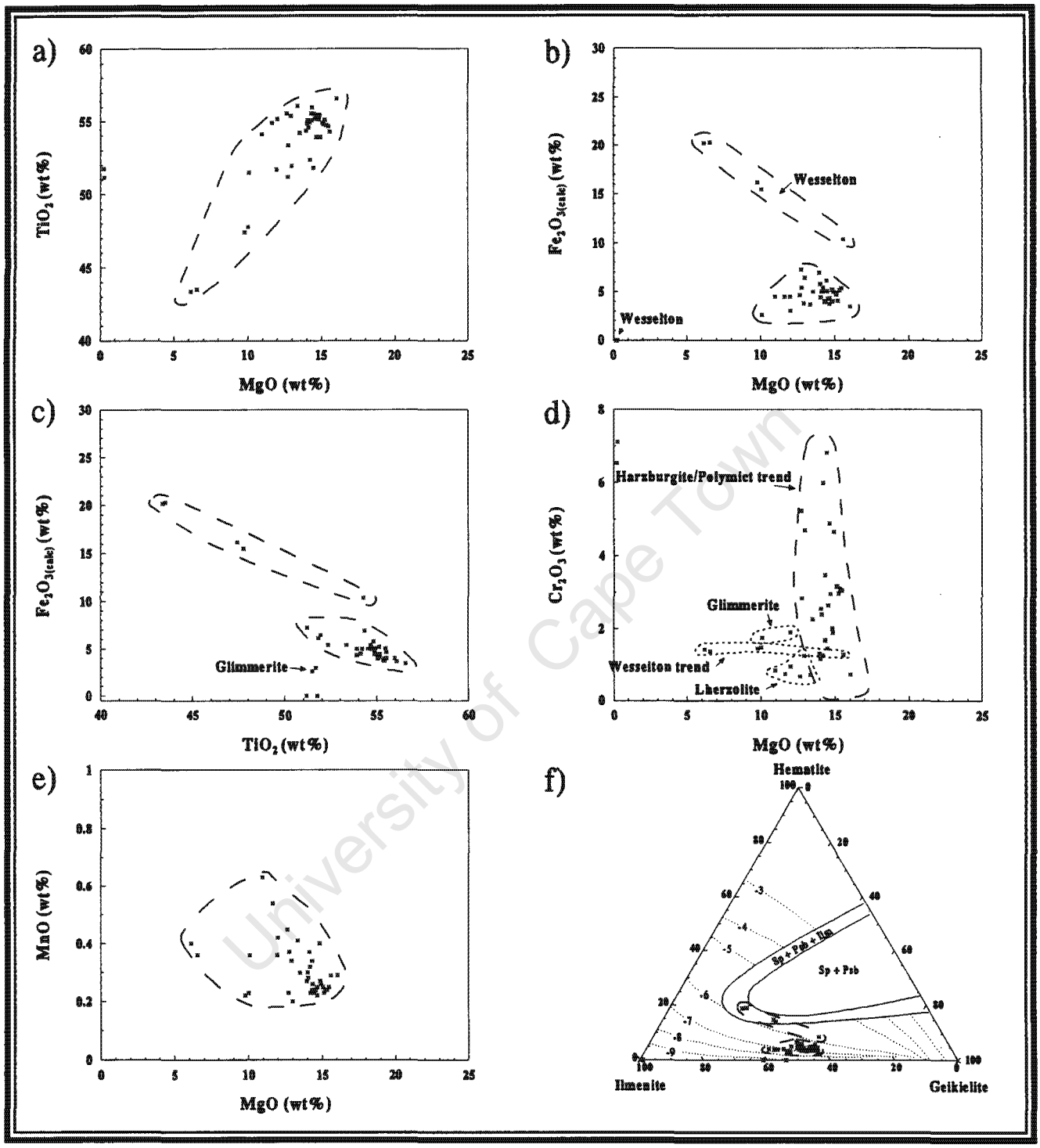

Figure 4.9 Compositional fields and trends based on data for ilmenites from metasomatic xenoliths, plotted using relationships of important major oxides. Fields are estimated visually and the data has been obtained from the Kimberlite Research Group database (KRGD), university of Cape Town.(Fugacity contours and ternary solvii from Woerman et al, 1969; Haggerty and Tompkins, 1984)

Trends of Ilmenite in Olivine Phenocrysts

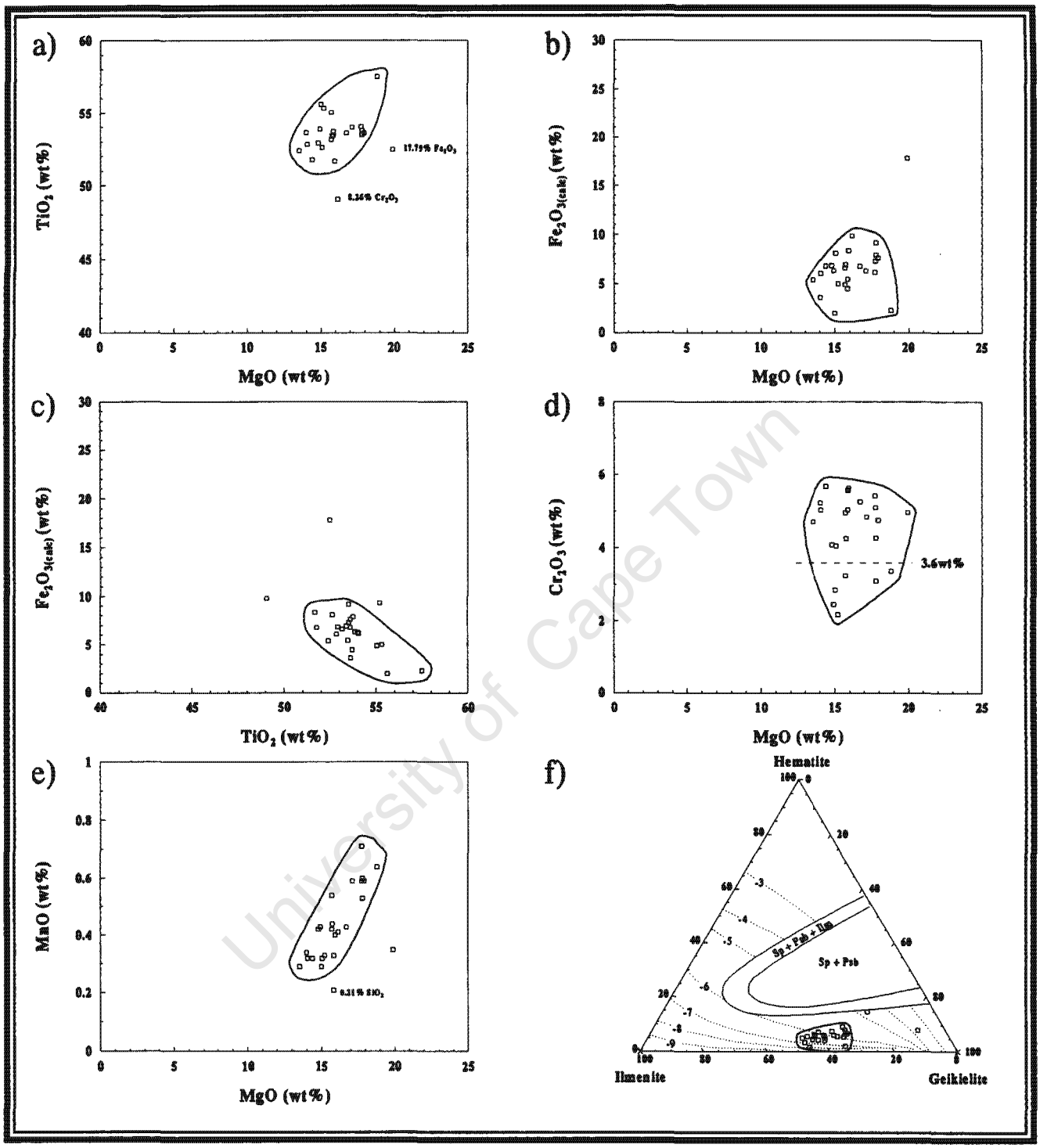

Figure 4.10 Compositional fields and trends based on data for ilmenite inclusions in olivine phenocrysts, plotted using relationships of important major oxides. Fields are estimated visually and the data has been obtained from Shee (1985). (Fugacity contours and ternary solvii from Woerman et al, 1969; Haggerty and Tompkins, 1984)

Trends in UMD Ilmenites

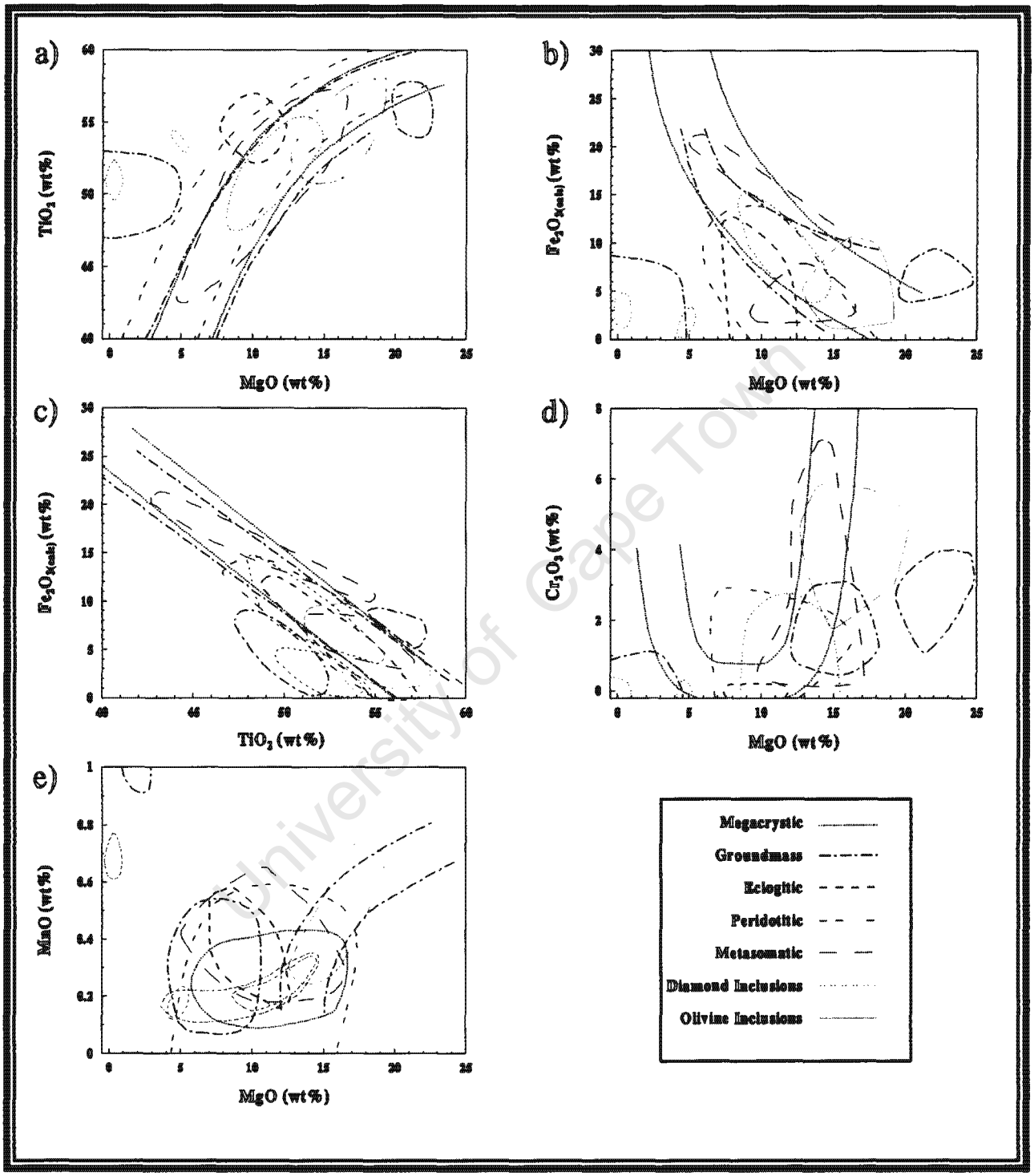

Figure 4.11 Compositional fields and trends for ilmenites from different UMD sources, plotted using relationships of important major oxides. Fields are obtained from data in figures 4.4 to 4.10.

Ilmenite Parageneses - IGH Ternary

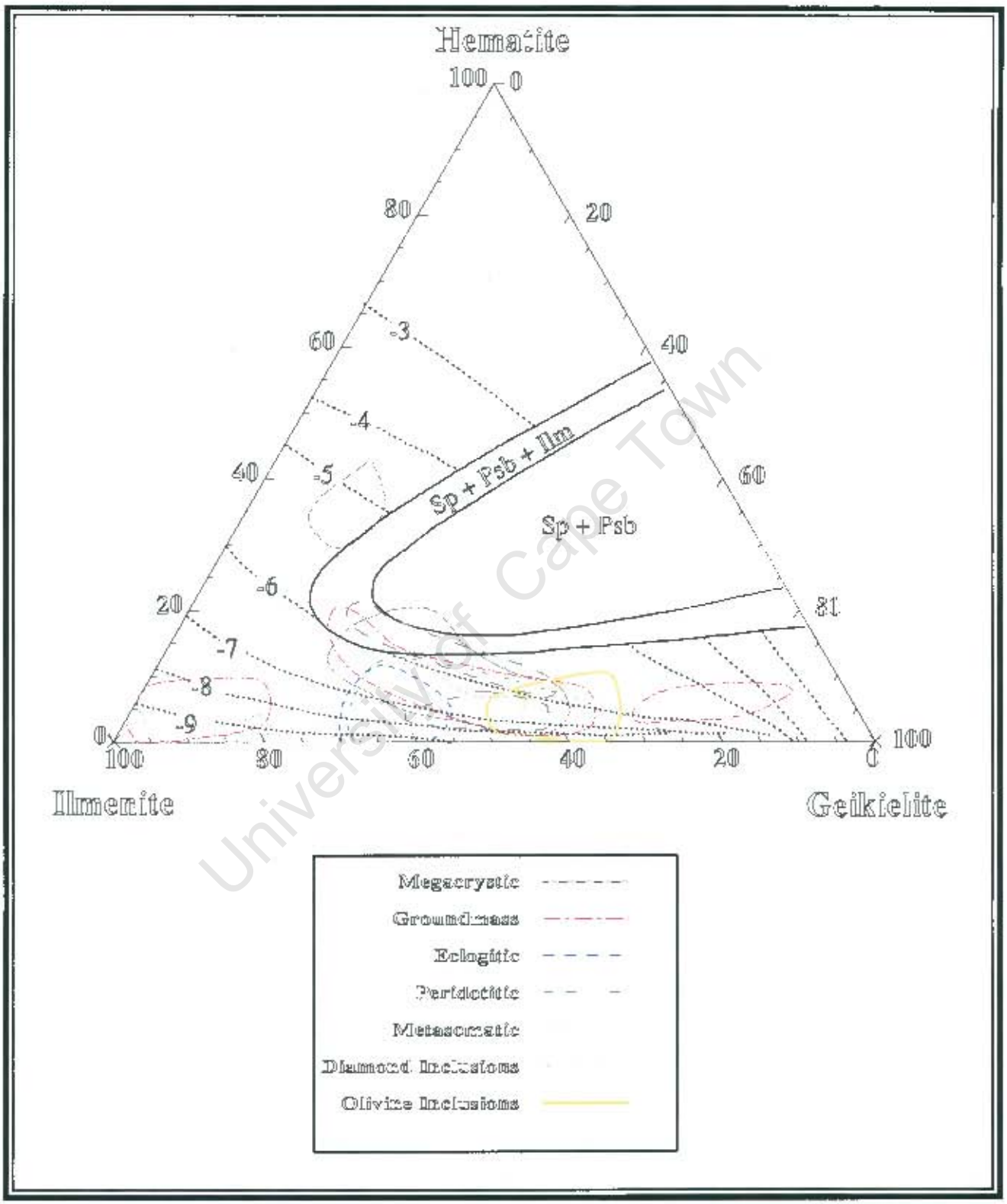

Figure 4.12 Ilmenite-Hematite-Geikielite phase diagram showing compositional fields and trends for UMD ilmenites from different parageneses. (Fugacity contours and ternary solvii from Woerman et al, 1969; Haggerty and Tompkins, 1984)

Ilmenite and Diamond Preservation

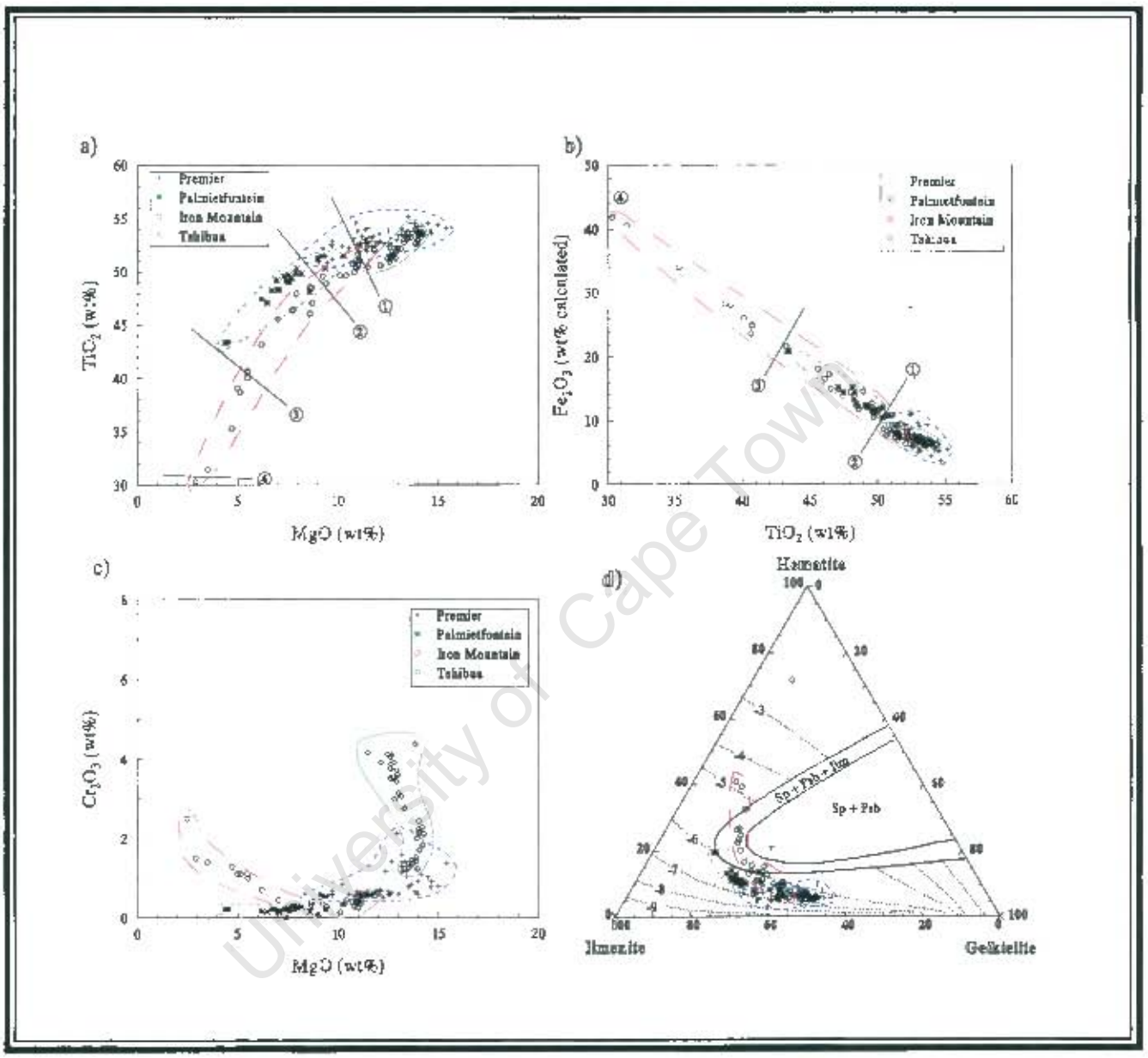

Figure 5.1 Plots of ilmenite analyses from the Tshibua, Premier, Palmietfontein and Iron Mountain kimberlites. The four localities define a trend from less differentiated, high Mg low Fe_2O_3 compositions, to low MgO high Fe_2O_3 more differentiated compositions. The compositions of ilmenites is assumed to correctly predict the preservation of diamonds at these localities, and has been used to establish diamond preservation intervals, which can be applied to other localities and "blind" samples.

Ilmenite and Diamond Preservation

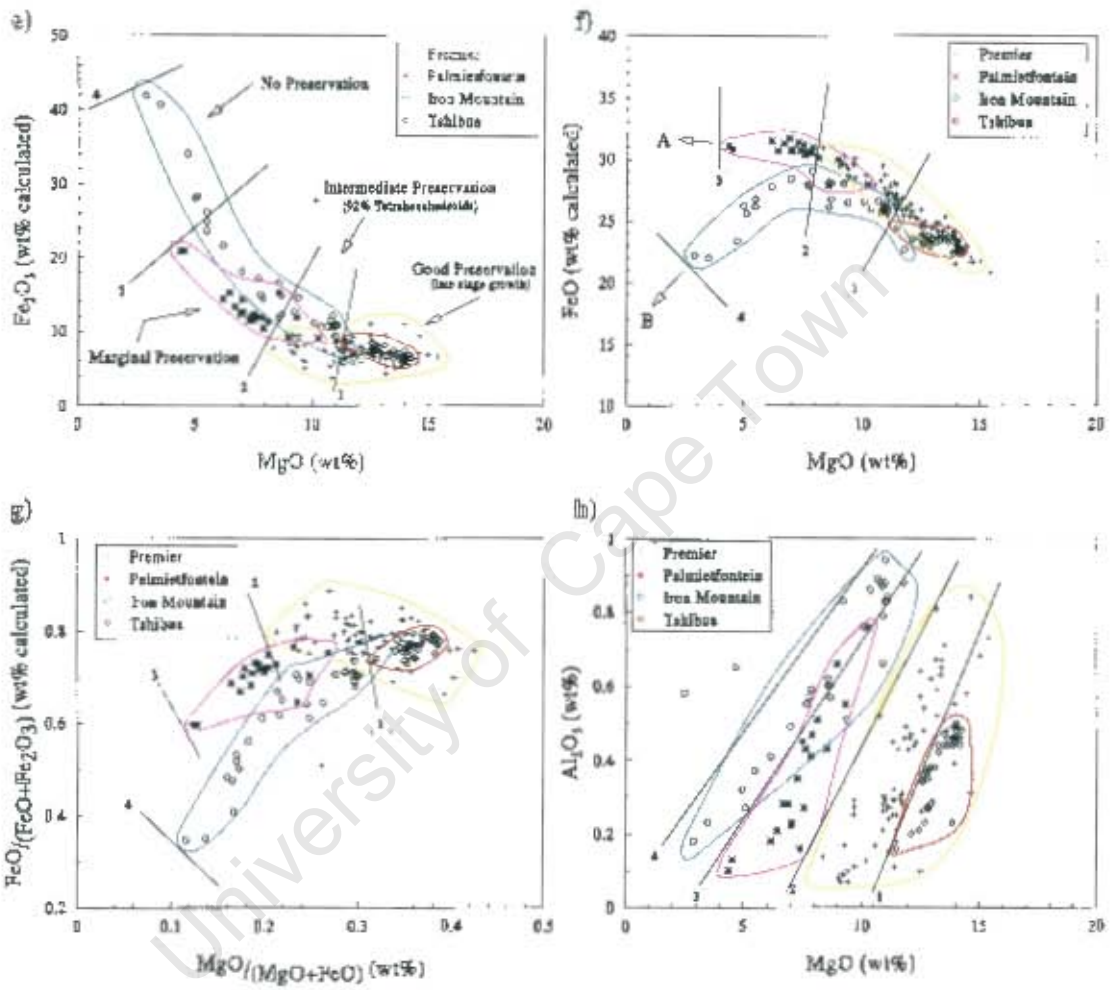

Figure 5.1 continued....

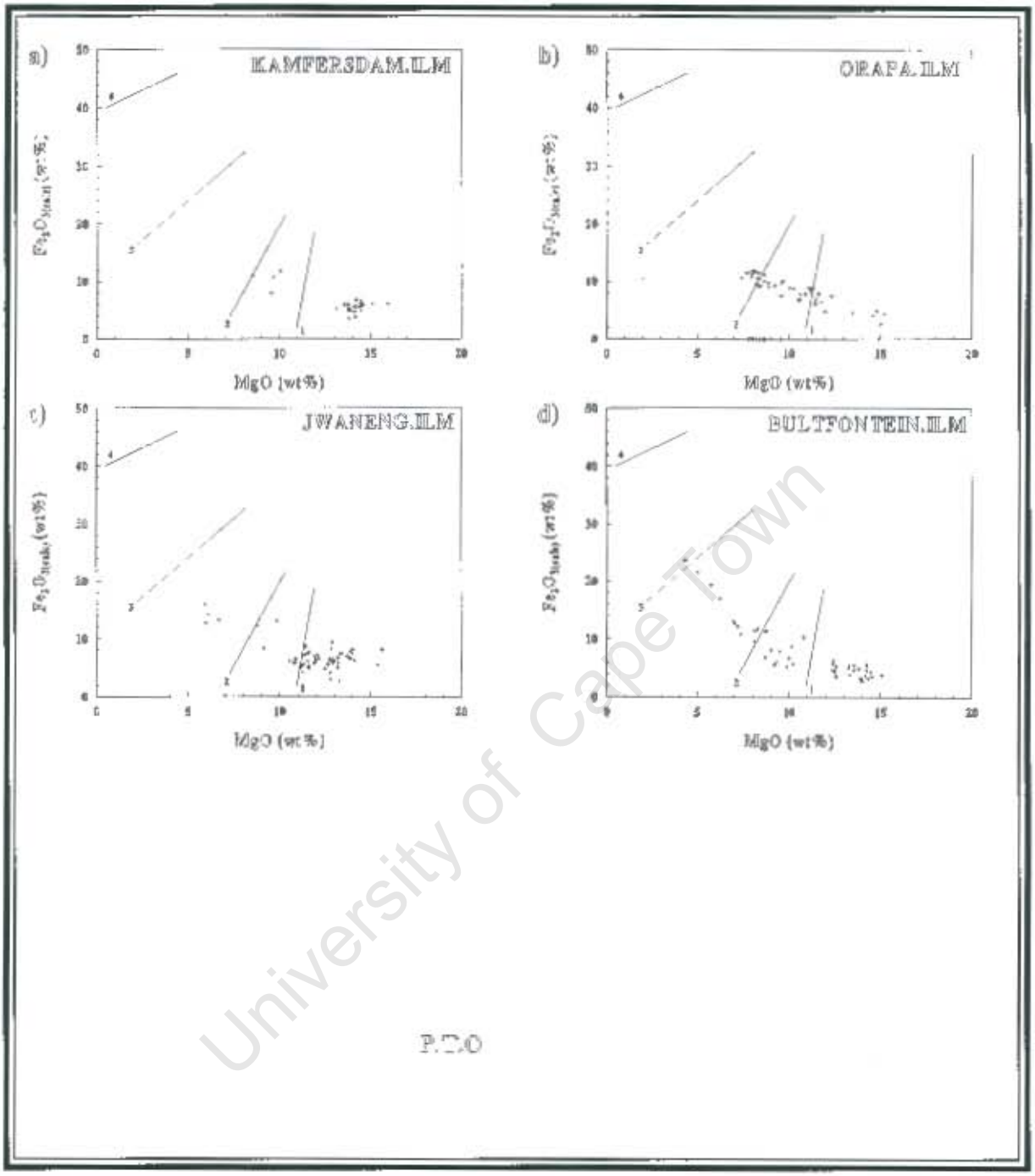

Figure 5.2 Plots of Fe_2O_3 vs MgO for concentrate ilmenites from kimberlites in southern Africa. Trends in the ilmenites are evaluated against categories established using the control datasets from Tshibua, Premier, Palmietfontein and Iron Mountain (figure 5.1), in an attempt to predict the degree of preservation of a parcel of diamonds from these localities.

Ilmenite Concentrate

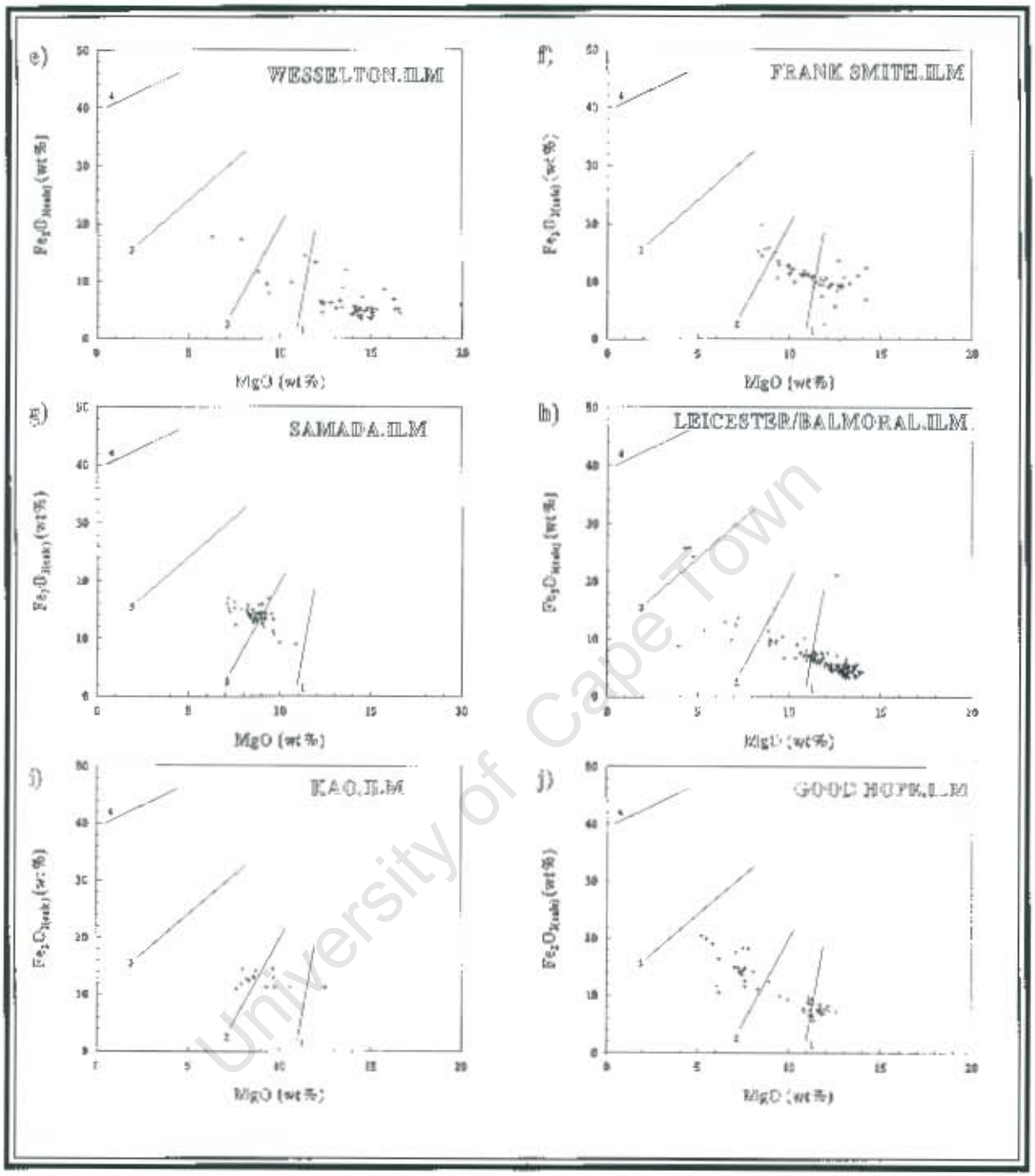

Figure 5.2 continued.....

Ilmenite Concentrate

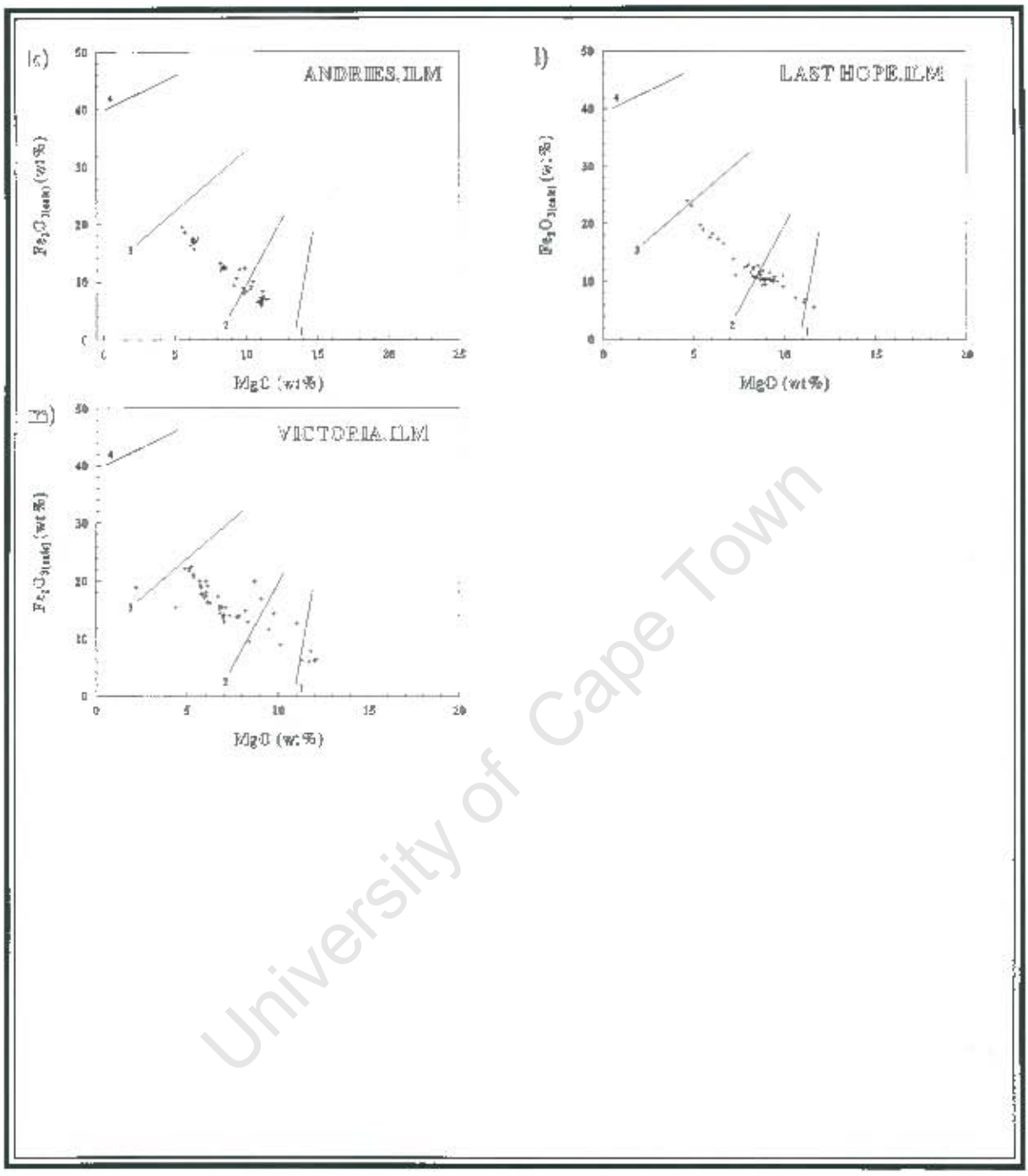

Figure 5.2 continued.....

Kamfersdam Ilmenite Concentrate

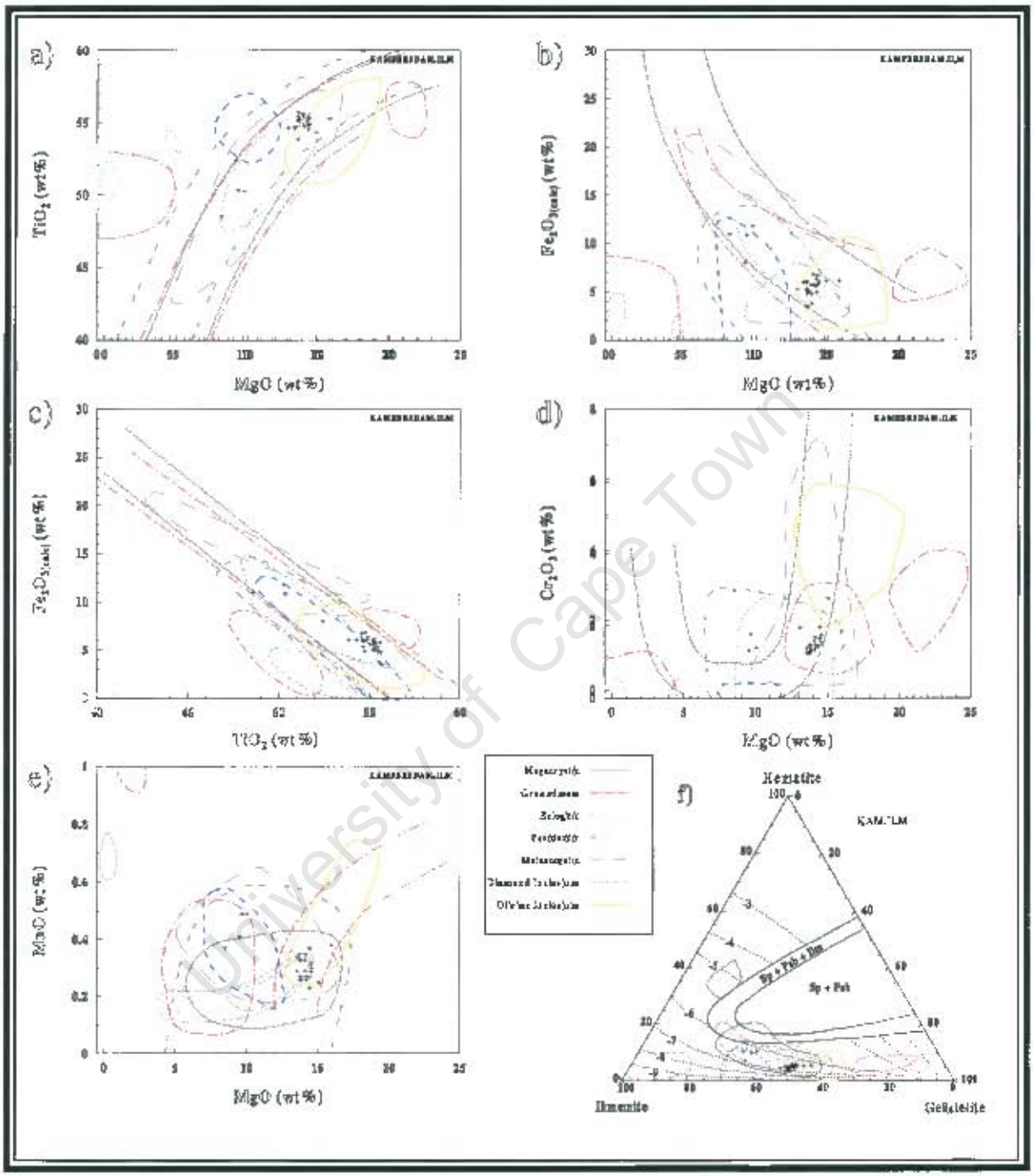

Figure 5.3 Analyses of ilmenite concentrate from Kamfersdam, with superimposed fields for the different parageneses of ilmenite described in chapter 4. The dominant cluster of analyses correspond to the main magmatic trend which was deduced to be a kimberlitic phenocryst phase. Although the analyses overlap with fields for megacrystic ilmenite, the clustering if analyses within the fields is more characteristic of ilmenite phenocrysts in the kimberlite magma. In addition the analyses from Kamfersdam correlate well with the field for ilmenite inclusions in olivine phenocrysts. Kamfersdam concentrate, however also correlate with fields for metasomatic ilmenites, an hence may be of metasomatic origin.

Revised Diamond Preservation Fields

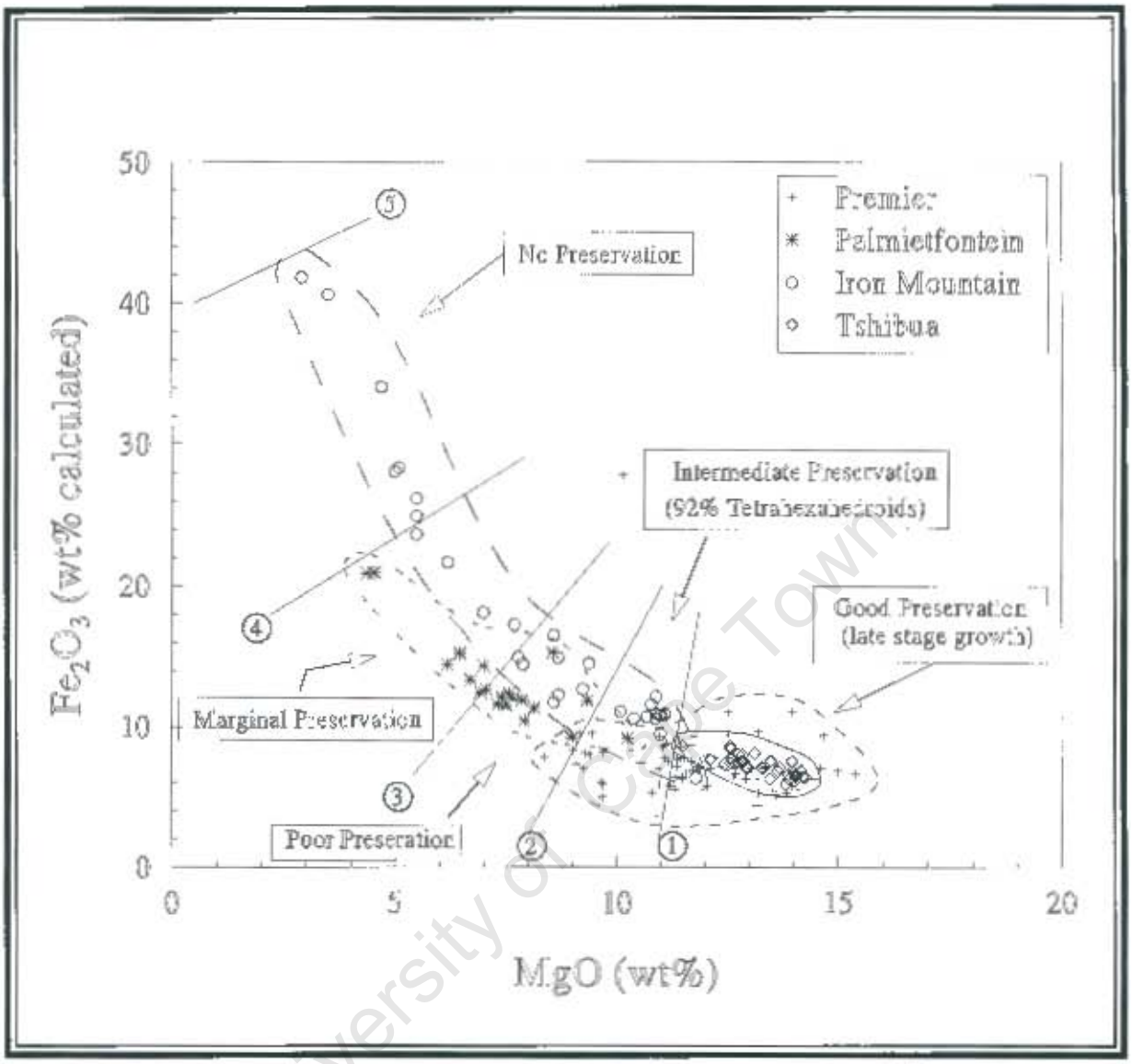

Figure 5.4 Revised plot for Fe_2O_3 vs MgO, based on trends in ilmenites from Tshibua, Premier, Palmietfontein and Iron Mountain (figure 5.1). It was realised while assessing concentrate ilmenite from selected southern African localities, that there was an enormous gap between ilmenite compositions which indicate "intermediate" diamond preservation and the cut-off for "marginal" preservation. Consequently, boundary 2 has been moved to slightly higher MgO concentrations and a new boundary 3 added to indicate "poor" preservation. From an exploration point of view, localities with "intermediate preservation" can be expected to have lost in the vicinity of half the original grade. Localities with "poor" preservation may have lost substantially more, but may still be economic for small operations only. Localities with "marginal" and "no" preservation are likely to be subeconomic. These predictions, however rely on the forecast of grade by pyrope garnets and chromites. A preservation prediction can only detract from a predicted original grade.

APPENDICES

Appendix 2.1

Appendix 2.1 Procedures for the preparation of PDCA(Eluent) and Par.

PDCA (Pyridinedicarboxilic Acid)

2000ml Volumetric Flask
1800ml High quality distilled water in flask
13.6g Sodium Acetate Trihydrate
2g PDCA
5.7ml Acetic Acid

i) Weigh 13.6g of Sodium Acetate Trihydrate ($C_2H_3NaO_2.3H_2O$) and wash this into the volumetric flask.

ii) Weigh out 2g PDCA (Pyridinedicarboxilic acid) 99% accurately and wash into flask. Dissolve fully using a magnetic stirrer.

iii) Add 5.7ml Acetic acid to flask.

iv) Make up flask to 2000ml using distilled water.

.....oooOOooo.....

PAR (4-(2-pyridylaze) resorsinol monosodium salt)

2000ml Volumetric Flask with 1000ml high grade distilled water.
400ml Ammonium Hydroxide 30%
0.2g PAR ($C_{11}H_8N_3NaO_2$)
114ml Ascetic acid

i) Add 400ml Ammonium Hydroxide, 0.2g PAR and 114ml Ascetic acid to flask and make up to 2000ml.

.....oooOOooo.....

Appendix 2.2

Appendix 2.2 Stoichiometric calculation of Fe_2O_3/FeO form electron-microprobe analyses.

1) *Calculate cation proportions as per Deer, Howie and Zussman (Appendix 1).*

2) *Determine Fe^{3+} where*

$$\mathbf{Fe^{3+}}=2X(1-T/S) \quad \text{(Droop, 1987)}$$

X = Theoretical number of oxygens.
T = Theoretical number of cations.
S = Observed cation total.

3) *Determine Fe^{2+} where*

$$\mathbf{Fe^{2+}} = X(Fe_{(at)})-Fe^{3+}$$

$Fe_{(at)}$ = Observed atomic proportion of Fe (from E.M.P)

4) *Determine total weight percent Fe.*

$$\mathbf{Fe_{(wt\%)}} = FeO_{(t)}(0.7773)$$

$\mathbf{FeO_{(t)}}$ = Total iron as oxide FeO from E.M.P

5) *Calculate FeO and Fe_2O_3 where*

$$\mathbf{FeO} = (Fe^{2+}/Fe_{(at)}(X))Fe_{(wt\%)}*1.2865$$

$$\mathbf{Fe_2O_3} =(Fe^{3+}/Fe_{(at)}(X))Fe_{(wt\%)}*1.4298$$

6) *Ferric to Ferrous ratio = Fe_2O_3/FeO*

.....oooOOooo.....

Appendix 3.1

Appendix 3.1 Data input form used during the description of diamond parcels.

DATE:
LOCATION:

SIEVE TYPE:
SIEVE SIZE:
IN (mm) :

NO. of STONES:
PARCEL WEIGHT(g):
(cts):

PAGE:
FILENAME:
MEAN wt/stone:

WEIGHT (g)	WEIGHT (cts)	FORM	COLOUR	COLOUR INTEN.	INCLU SIONS	TYPE of STONE (A)	(B)	RESORB	COMMENTS eg:incl(type and colour), etch, ruts, frost, protrusions, growth laminations, etc.

Appendix 3.2

i) Derivation of the equation for initial grade (IG)
ii) Worked example using Samada diamonds.
(including graph integration)

(i)

$$IG = PG\left(\frac{IM_T}{PM_T}\right) \quad ,where.....$$

$$IM_T = \sum_{r_c=0-11} (IM) \quad ,while.....$$

$$IM = \left(\frac{im}{pm}\right)PM$$

$$\Rightarrow PM = N\left(\frac{PM_T}{N_{TD}}\right)$$

$$\Rightarrow pm = \left(\frac{N}{N_T}\right) PM_T$$

$$\Rightarrow im = \frac{pm(100)}{R}$$

$$\therefore IM = \frac{(N)(PM_T)(100)(N_T)(PM)}{(N_T)(100-R)(PM_T)(N)}$$

$$= \frac{(100)(PM)}{(100-R)}$$

$$= \frac{100(N)(PM_T)}{(100-R)(N_{TD})}$$

Term		*Description*
IG	=	Initial Grade
PG	=	Present (Run-of-Mine) Grade
IM_T	=	Initial Mass of the Total parcel
PM_T	=	Present Mass of the Total parcel
PM	=	Present Mass in a particular resorbtion category
IM	=	Initial Mass calculated from diamonds in a particular resorbtion category
R	=	Percentage diamond lost during resorbtion
r_c	=	Resorbtion Category
pm	=	Normalised Present Mass
im	=	Normalised Initial Mass
N	=	Number of diamonds classified to a particular resorbtion category
N_{TD}	=	Total number of described diamonds
N_T	=	Total Number of diamonds in the parcel

Note: Normalised mass is the mass determined by multiplying the number of stones by the average weight per stone for the parcel. This prevents an individual large diamond from over-influencing the result.

$$\therefore IG = \frac{PG}{PM_T} \sum_{r_c=0-11} \left(\frac{(100(N)(PM_T)}{(100-R)(N_{TD})}\right)$$

(ii) **Worked example of the calculation of initial grade, using the parcel from Samada Mine.**

$$IM = \frac{(100(N)(PM_T)}{(100-R)(N_{TD})} \quad .....(i) \qquad \underline{or} \qquad IM = \frac{(100(N_T)(pm)}{(100-R)(N_{TD})} \quad .....(ii)$$

By using the method outlined in the main text the procedure is broadly as follows:

i) **Determine IM for the described resorbtion categories (0% to 45% loss in mass) using equation (i) above.**

ii) **Determine 'pm' for each resorbtion category and plot 'pm' vs Mass lost due to resorbtion (R). Determine the area under the curve between '35%' and '45%' loss in mass and establish a line from the 'pm' value at '35%' to the 'x-axis' such that the area under this curve equals that between '35%' and '45%'. Determine the exact 'x-intercept', and hence the equation for the line. Finally solve 'y' for all further resorbtion categories.**

iii) **Apply equation (ii) to calculate Initial Mass for all resorbtion categories from 50% to 100% loss in mass.**

PARAMETER	n	*pm*
N_T	2693	
PM_T	468.11	
N_{TD}	353	
PG	10	
r_c=0;R=100	3	0.52
r_c=1;R=95	6	1.04
r_c=2;R=85	46	8.00
r_c=3;R=75	52	9.04
r_c=4;R=65	45	7.82
r_c=5;R=55	201	6.62
r_c=6;R=50		6.02
r_c=7;R=40		4.82
r_c=8;R=30		3.62
r_c=9;R=20		2.42
r_c=10;R=10		1.22
r_c=11;R=0		0.00

i) $$IM_{r_c=0} = \frac{(100(N)(PM_T)}{(100-R)(N_{TD})}$$

$$\therefore = \frac{(100)(3)(468.11)}{(100-0)(353)}$$

$$\therefore = 3.98$$

$$IM_{r_c=1} = 8.38$$
$$IM_{r_c=2} = 71.77$$
$$IM_{r_c=3} = 91.94$$
$$IM_{r_c=4} = 91.81$$

ii) $$pm_{r_c=0} = (\frac{N}{N_T})\ PM_T$$

$$\therefore = \frac{(3)(468.11)}{2693}$$

$$\therefore = 0.52$$

$$pm_{r_c=1} = 1.04$$
$$pm_{r_c=2} = 8.00$$
$$pm_{r_c=3} = 9.04$$
$$pm_{r_c=4} = 7.82$$
$$pm_{r_c=5} = 34.94$$

Plot these 'pm' values against 'R'. Integrate the area under the curve between 'R=35' and 'R=45' ('ABC' + 'ACDE' on figure A). Determine the length of the base 'DF' of triangle 'ADF' such that the area of triangle 'ADF' equals the sum of areas 'ABC' and 'ACDE'. In order to establish 'pm' for 'R>35', it is necessary to establish the equation 'y=mx+c' for line 'AF' and solve 'y' ('pm') for known values of 'x' ('R'). The graph and subsequent calculations follow:

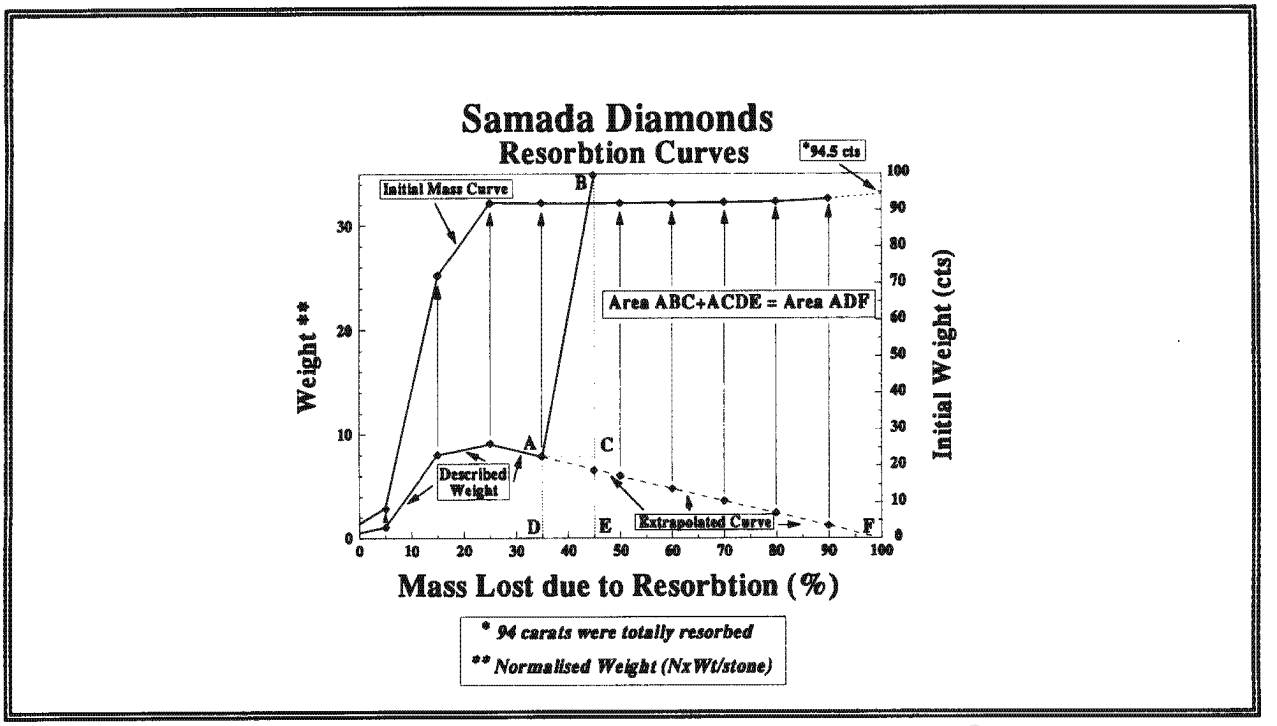

Figure A: Determination of Resorbtion values for R>45 and estimation of Carats totally destroyed.

$$Area ABC + Area ACDE = Area ADF$$

$$\therefore Area ADF = \frac{1}{2}(10)(34.94-7.82)+(7.82)(10)$$

$$\therefore \left(\frac{1}{2}bh\right)_{ADF} = 213.80$$

$$\therefore b = \Delta R = \frac{(213.80)(2)}{7.82} = 54.67$$

$$y = mx + c$$

$$c = 7.82 - \left(\frac{7.82-0}{35-89.67}\right)(35) = 12.8$$

$$y = 12.83 - 0.14x$$

$$\therefore when\ x = 45 \quad ; y = 6.39$$
$$\therefore when\ x = 50 \quad ; y = 5.68$$
$$\therefore when\ x = 60 \quad ; y = 4.24$$
$$\therefore when\ x = 70 \quad ; y = 2.81$$
$$\therefore when\ x = 80 \quad ; y = 1.38$$
$$\therefore when\ x = 89.67; y = 0.00$$

Therefore, using equation (ii) IM can be solved for all resorbtion categories 0-4 and 5-10, totalled and substituted into the equation for initial grade. Resorbtion category 11, which corresponds to diamonds which have been completely resorbed, can be estimated by plotting Initial Mass (IM) against R (see figure A) and extending the curve from R=90% to the right hand y-axis. This intercept value represents the number of carats completely resorbed:

$$IM_{r_c=0} = \frac{(100(N)(PM_T)}{(100-R)(N_{TD})}$$
$$\therefore = \frac{(100)(3)(468.11)}{(100-0)(353)}$$
$$\therefore = 3.98$$

$$IM_{r_c=5} = \frac{(100(N_T)(pm)}{(100-R)(N_{TD})}$$
$$\therefore = \frac{(100)(2693)(6.39)}{(100-45)(353)}$$
$$\therefore = 88.65$$

$IM_{r_c=1}$ = 3.98

$IM_{r_c=1}$ = 8.38

$IM_{r_c=2}$ = 71.77

$IM_{r_c=3}$ = 91.94

$IM_{r_c=4}$ = 91.81

Initial Grade is described by the equation:

$$\therefore IG = \frac{PG}{PM_T}\sum_{r_c=0-11}\left(\frac{(100(N)(PM_T)}{(100-R)(N_{TD})}\right)$$

$$\therefore IG = \frac{10}{468.11}\sum_{r_c=0-11}(IM)$$

$$\therefore IG = \frac{10}{468.11}(648.4) \approx 14$$

$IM_{r_c=5}$ = 88.65

$IM_{r_c=6}$ = 86.60

$IM_{r_c=7}$ = 80.96

$IM_{r_c=8}$ = 71.56

$IM_{r_c=9}$ = 52.76